RESEARCH ARTICLE

A peer-reviewed open-access journal

ZooKeys

Launched to accelerate biodiversity research

The first representatives of the millipede family Glomeridellidae (Diplopoda, Glomerida) recorded from China and Indochina

Weixin Liu[1], Sergei Golovatch[2]

1 *Department of Entomology, College of Agriculture, South China Agricultural University, 483 Wushanlu, Guangzhou 510642, China* **2** *Institute for Problems of Ecology and Evolution, Russian Academy of Sciences, Leninsky pr. 33, Moscow 119071, Russia*

Corresponding author: Weixin Liu (da2000wei@163.com)

Citation: Liu W, Golovatch S (2020) The first representatives of the millipede family Glomeridellidae (Diplopoda, Glomerida) recorded from China and Indochina. ZooKeys 954: 1–15. https://doi.org/10.3897/zookeys.954.54694

Abstract

A new species of glomeridellid millipede is described from Guizhou Province, southern China: *Tonkinomeris huzhengkuni* **sp. nov.** This new epigean species differs very clearly in many structural details, being sufficiently distinct morphologically and disjunct geographically from *T. napoensis* Nguyen, Sierwald & Marek, 2019, the type and sole species of *Tonkinomeris* Nguyen, Sierwald & Marek, 2019, which was described recently from northern Vietnam. The genus *Tonkinomeris* is formally relegated from Glomeridae and assigned to the family Glomeridellidae, which has hitherto been considered strictly Euro-Mediterranean in distribution and is thus new to the diplopod faunas of China and Indochina. *Tonkinomeris* is re-diagnosed and shown to have perhaps the basalmost position in the family Glomeridellidae. Its relationships are discussed, both morphological and zoogeographical, within and outside the Glomeridellidae, which can now be considered as relict and basically Oriental in origin. Because of the still highly limited array of DNA-barcoding sequences of the COI mitochondrial gene available in the GenBank, the first molecular phylogenetic analysis of Glomerida attempted here shows our phylogram to be too deficient to consider meaningful.

Introduction

The chiefly Holarctic millipede order Glomerida (Shelley and Golovatch 2011) is currently known to comprise only three families: Glomeridellidae Cook, 1896, Protoglomeridae Brölemann, 1913, and Glomeridae Leach, 1815 (Enghoff et al. 2015). The family Glomeridellidae presently contains only two accepted genera: *Glomeridella* Brölemann, 1913, with seven or eight species from Spain, France, the eastern Alps, and the northwestern Balkans, and *Typhloglomeris* Verhoeff, 1898 (= *Albanoglomus* Attems, 1926, synonymized by Golovatch (2003)), with ca 15 species, many troglobionts, from the Balkans, Caucasus, and Near East. The family has hitherto been considered strictly Euro-Mediterranean (Enghoff et al. 2015). The ranges of both *Glomeridella* and *Typhloglomeris* overlap only marginally in the northern Dinaric Mountains, Balkans. Makarov et al. (2003) delimited several species groups within *Typhloglomeris* and, based on morphological evidence alone, outlined the main trends of their evolution, both morphological and ecological (= shifts to geo- or cavernicoly).

Continental China, unlike the Nearctic + Southeast Asia + Taiwan which contain several genera of Glomeridae (11) and Protoglomeridae (1) (Enghoff et al. 2015; Nguyen et al. 2019), has heretofore been known to support only numerous (32) species of a single genus, *Hyleoglomeris* Verhoeff, 1910, family Glomeridae (Golovatch and Liu 2020). This genus presently contains 100+ species ranging from the Balkans in the west, through Greece, Anatolia, Caucasus, and Central Asia, to Korea, Japan, and Taiwan in the east and to Indochina, Indonesia (Sumatra, Java, Borneo, and Sulawesi) and the Philippines in the southeast (Golovatch et al. 2006; Enghoff et al. 2015; Nguyen et al. 2019). One species has recently been described from Eocene Baltic amber (Wesener 2019).

All the more interesting is the discovery of a new species of *Tonkinomeris* in southern China. Moreover, this genus appears to actually belong to the family Glomeridellidae, being formally transferred therein from Glomeridae where it was originally placed. This represents the first formal records of glomeridellids not only in China, but also in entire Asia east of Hyrcania (the Republic of Azerbaijan and northeastern Iran near the Caspian Sea coast). The present paper is devoted to a description of our new species and to a discussion of its morphological, molecular and zoogeographical affinities.

Material and methods

Morphological analysis

The underlying material was taken from leaf litter in a protected forest patch and preserved in 95% ethanol. The types are deposited in the Zoological Collection of the South China Agricultural University (SCAU), Guangzhou, Guangdong Province, China. A detailed examination of characters and dissections were performed using a Leica S8 APO stereomicroscope. Line drawings were prepared with a Zeiss Axioskop40 microscope with an attached camera lucida. Photographs of specimens were

taken with a Keyence VHX-5000 digital microscope and edited using Adobe Photoshop CS6. The terminology used here largely follows that of Golovatch and Turbanov (2018), with only a few modifications.

DNA extraction and sequencing

Genomic DNA was extracted from legs and thoracic tissue of the paratype with Qiagen DNeasy Blood and Tissue kit following the manufacturer's extraction protocol. Fragments of the COI gene were amplified using the degenerate primer pair HCO2198-JJ (AWACTTCVGGRTGVCCAAARAATCA) / LCO1490-JJ (CHACWAAYCATAAA-GATATYGG) (Astrin and Stüben 2008). The PCR amplification was performed using a T100™ thermal cycler (BIO-RAD) with a final reaction volume of 25 µL. In addition to the new nucleotide sequence in this study, MT522013, 34 Glomerida and nine non-Glomerida sequences (consisting of four Sphaerotheriida, three Polyxenida and two Polydesmida species) as outgroups were downloaded from the GenBank. All analysed species, Genbank accession numbers and voucher numbers/taxonomy ID were listed in Figure 5.

Phylogenetic analyses

The sequences were aligned using Clustal W and edited in Bioedit (Hall 1999). The final aligned dataset included 44 COI sequences with 656 positions. Bayesian Inference (BI) analysis was implemented through the on-line CIPRES Science Gateway V.3.3 (Miller et al. 2010). The BI analysis was performed by MrBayes 3.2.6 using the Markov chain Monte Carlo technique (MCMC) (Ronquist et al. 2012). The numbers of generations used amounted to 5,000,000 in the parameters for MCMC. The type of a consensus tree was chosen for all compatible groups. Maximum likelihood (ML) analysis was conducted using IQ-TREE web server (Trifinopoulos et al. 2016) with 1,000 bootstrap replications and under the GTR+G+I model (Pende et al. 2014).

Taxonomy

Considering the new species described below, the following amended diagnosis of *Tonkinomeris* can be proposed.

Order Glomerida Leach, 1814
Family Glomeridellidae Cook, 1896

Genus *Tonkinomeris* Nguyen, Sierwald & Marek, 2019

Type species. *Tonkinomeris napoensis* Nguyen, Sierwald & Marek, 2019, from northern Vietnam, by original designation (Nguyen et al. 2019).

Other species included: *T. huzhengkuni* sp. nov., southern China.

New diagnosis. A genus of Glomeridellidae with the caudal margins of several ♂ tergites sometimes modified into small lobes drawn posteriad into small lobes; the caudal margin of the ♂ pygidium is clearly emarginate centrally; the anterior telopods are flattened sagittally, somewhat incrassate, with evident mesal outgrowths on either T3 alone or both T2 and T3; posterior telopods with a trichotele (sometimes rudimentary) on T1, each of T2 and T3 with a caudal process and both forming a rather indistinct apical pincer.

Tonkinomeris huzhengkuni sp. nov.

http://zoobank.org/41BF7A61-D9E7-4B81-9685-4D5AB8B7C071
Figures 1–3

Type material. *Holotype:* ♂ (SCAU TY01), China, Guizhou Province, Tongren City, Jiangkou County, Baishuidong Scenic Area, 27.652873N, 108.795223E, 450 m a.s.l., 25.XI.2019, Zhengkun Hu leg. *Paratype:* 1 ♀ (SCAU TY02), same data as for holotype.

Name. Honours Mr Huzhengkun, the collector and a millipede fan. A noun in genitive case.

Diagnosis. Differs from *T. napoensis* Nguyen, Sierwald & Marek, 2019, the sole other species of the genus (Nguyen et al. 2019), by the larger body size (> 11 mm vs 9.6 mm), the more numerous ommatidia (at least 6+1 vs 5+1), the glabrous, but caudomedially produced posterior margins of ♂ tergites 8–11 (vs unmodified in both sexes), the vivid, peculiar, sexually dimorphic colour pattern (vs even more vivid, but the same in both sexes), and some structural details of the telopods: the much higher central lobe and the much shorter horns of ♂ syncoxite 19 (vs the opposite), the shape and armament of both telopod pairs, the less strongly reduced, 4-segmented ♂ telopodites 17 (vs 2-segmented), etc. (see Discussion below).

Description. Body length of holotype ♂ ca 12.5 mm, width of thoracic shield ca 8.0 mm (broadest), height of thoracic shield ca 4.2 mm (highest). Body length of paratype ♀, 11.2 mm, width of thoracic shield ca 7.1 mm (broadest), height of thoracic shield ca 4.0 mm (highest). Coloration (Fig. 1): body rather uniformly blackish, but with slightly yellowish edges. Dorsal pattern marbled yellow-brownish: collum with a small, rounded, central spot anteriorly and a paramedian pair of larger, transversely ovoid, lateral spots (Fig. 1D); thoracic shield and tergites 3–11 each with a similar, but much larger pair of lateral spots and a yellowish, but slightly purplish, median, narrow, axial stripe. Anal shield (= pygidium) of ♂ without stripe (Figs 1F, 2D), but ♀ with a distinct, yellowish, median, triangular spot near caudal margin (Fig. 1C). Head largely dark brown, only labrum and Tömösváry's organ lighter, grey-yellowish. Antennomeres 3–6 brownish, slightly purplish, remaining antennomeres light yellow-brown. Venter and podomeres 1 and 2 entirely light grey-yellowish, remaining podomeres dark brown, slightly purplish (Fig. 1B, D).
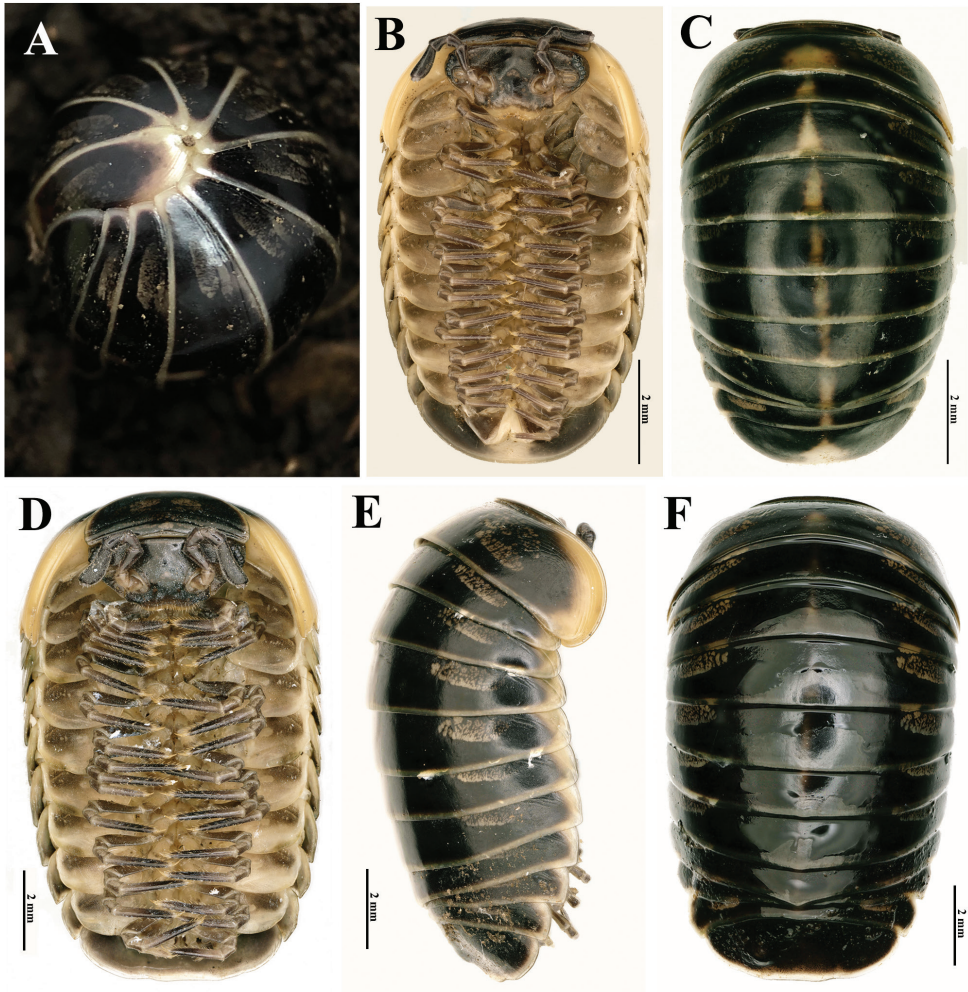
Figure 1. Habitus of *Tonkinomeris huzhengkuni* sp. nov. **A** Live coloration of ♂ holotype **B, C** body of ♀ paratype, ventral and dorsal views, respectively **D–F** body of ♂ holotype, ventral, lateral and dorsal views, respectively.

Head: mandibles (Fig. 3B, C) equal in both sexes, each with a large external tooth and a smaller internal tooth, the latter with four cusps. Molar plate with a long membranous fringe and a groove. At least seven rows of pectinate lamellae and a scaly intermediate area. Gnathochilarium (Fig. 3A) equal in both sexes, unmodified, typical of Glomerida. Left and right eyes asymmetrical, with 9+1/10+1 (♂) (Fig. 2A) or 8+1/6+1 (♀) (Fig. 1B) ommatidia. Tömösváry's organ transversely oval, ca 1.6 times wider than long (Fig. 2A). Lengths of antennomeres: 6>>3>4=5>1=2>7 (Fig. 1B, D). Antennomere 6 ca 2.6 times as long as high. Antennomere 8 with four small, apical, sensory cones.
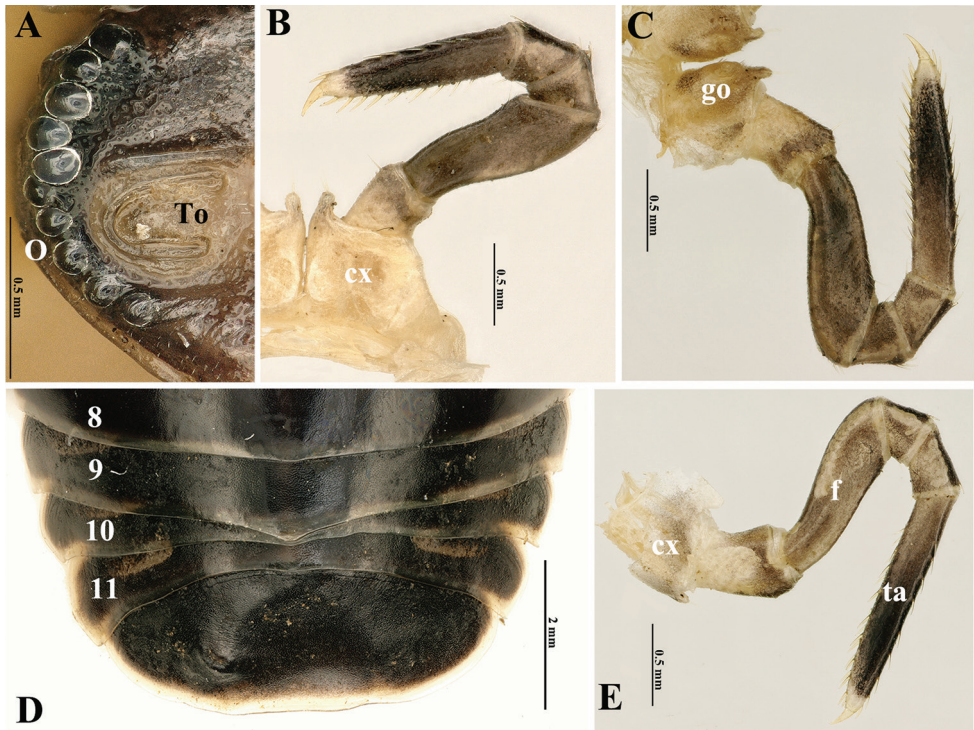
Figure 2. *Tonkinomeris huzhengkuni* sp. nov., ♂ holotype. **A** Right side of head **B** left leg 1 **C** right leg 2 with gonopore **D** posterior part of body, dorsal view **E** left leg 9. Abbreviations: **cx**: coxa, **f**: femur, **go**: gonopore, **O**: ommatidia, **ta**: tarsus, **To**: Tömösváry's organ, **8–11** refer to tergite numbers.

Collum with two complete transverse striae (Fig. 1D). Thoracic shield with a narrow hyposchism extending past caudal tergal margin; about 12 or 13 superficial transverse striae laterally and dorsolaterally, but five or six confusedly arranged and incomplete. One or two starting below, one in front of schism, all others above schism, with three crossing the dorsum; mid-dorsal region with five additional, incomplete, broken, confused, mostly short striolae behind last regular stria (Fig. 1E). Tergites: surface smooth and shining, only paratergites with three or four short, incomplete, and superficial striae (Fig. 1E). Tergite 9 in ♂ drawn posteriad into a small, triangular, glabrous (non-dentate), median lobe (Fig. 2D), this being very week also in tergites 8, 10, and 11. Pygidium in both sexes uneven medially at caudal margin; in ♂ clearly impressed and concave centro-dorsally and with two very small, paramedian, flattened and rounded knobs (Figs 1D–F, 2D), in ♀ only slightly flattened dorsocaudally (Fig. 1C).

Legs long and slender. All podomeres densely setose, setae mostly being short. Coxae 1–16 each with a short, well-rounded, spinigerous, apico-mesal projection, this being especially evident in coxae 1 and 2 (Fig. 2B, C). Coxae 4–21 each with a similar apico-lateral process. Tarsi 1–16 each with two irregular transverse rows of 7–8+7–8 dorsal spines and 9–12+9–12 ventral spines (Fig. 2B, C, E). Femur 9, 2.4 times, tarsus 6.5 times longer than wide (Fig. 2E).
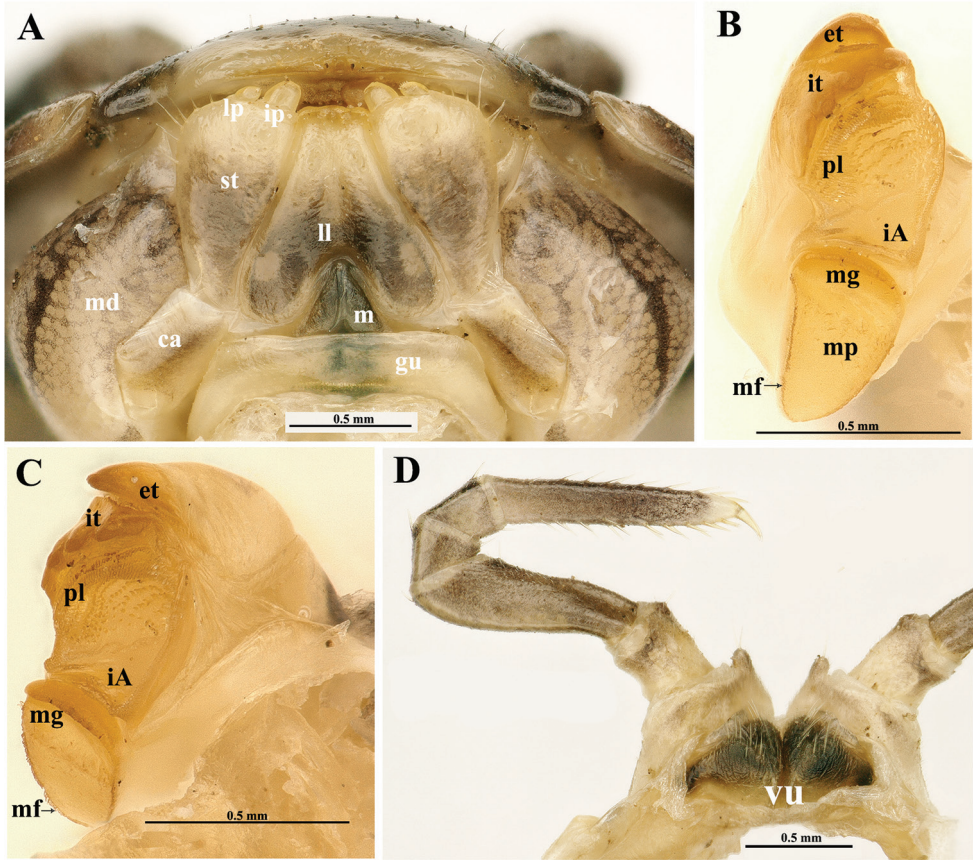
Figure 3. *Tonkinomeris huzhengkuni* sp. nov., ♀ paratype. **A** Gnathochilarium, ventral view, *in situ* **B, C** left mandible, mesal and subfrontal views, respectively **D** coxae 2 with vulvae. Abbreviations: **ca**: cardines of gnathochilarium, **et**: external tooth, **gu**: gula, **iA**: intermediate area, **ip**: inner palpus, **it**: inner tooth, **ll**: lamellae linguales, **lp**: lateral palpus, **m**: mentum, **md**: basal joint of mandible, **mf**: membranous fringe, **mg**: molar groove, **mp**: molar plate, **pl**: pectinate lamellae, **st**: stipites, **vu**: vulvae.

Male sexual characters: gonopore small, oval, with a few short setae around (Fig. 2C). Legs 17 (Fig. 4A) strongly reduced, very densely micropilose throughout. Coxae membranous, contiguous, but clearly separated medially. Each coxa with a very large, rather regularly rounded, outer lobe and a small, rounded, distomedial, setigerous finger. Telopodite 4-segmented, telopoditomere 2 largest, subrectangular, about twice as long as telopoditomere 1 or telopoditomeres 3 and 4 combined. *Anterior telopods* (Fig. 4B, C) also very densely micropilose throughout. Syncoxite (= ?coxosternum) membranous, on either side with a small rounded lobule at base of telopoditomere 1. Telopodite 4-segmented, with a spine apically. Telopoditomere 1 subrectangular, 1.2 times longer than wide. Telopoditomere 2 largest, a little swollen ventro-parabasally, its apico-mesal tooth on caudal face bulged at base, sharp apically and extending to basal 1/4 telopoditomere 3. The latter subtrapezoid, its apico-mesal tooth on cau-
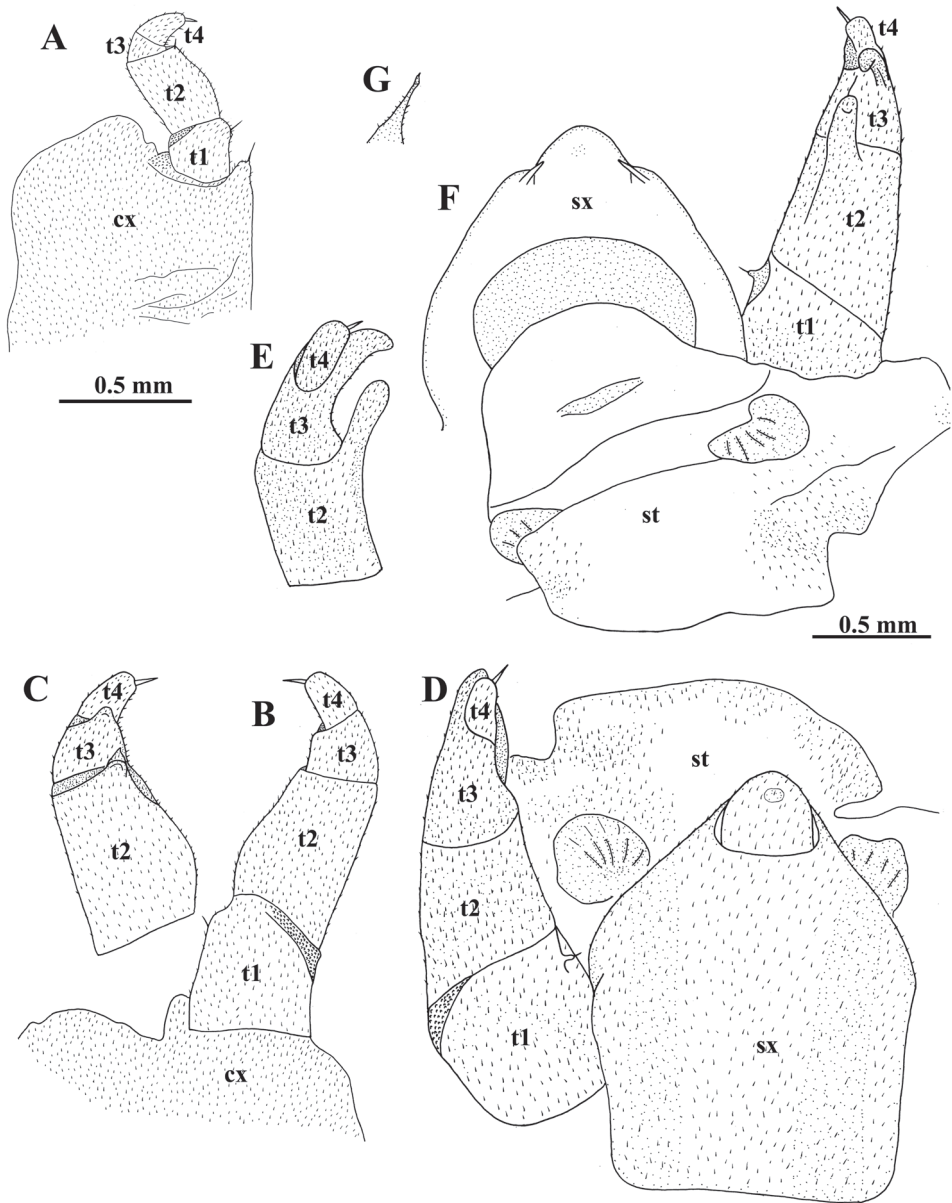
Figure 4. *Tonkinomeris huzhengkuni* sp. nov., ♂ holotype. **A** Left leg17, oral view **B** right anterior telopod, oral view **C** right anterior telopod, caudal view **D–F** left posterior telopod, oral, mesal and caudal views, respectively **G** tip of syncoxital horn, caudal view. Abbreviations: **cx**: coxa, **st**: sternite, **sx**: syncoxite, **t1–t4**: telopoditomeres 1–4. Scale bars: 0.5 mm (**A–C**, left); 0.5 mm (**D–G**, right).

dal face small, rounded, projecting above base of a subcylindrical telopoditomere 4. **Posterior telopods** (Fig. 4D–G) particularly strongly incrassate, likewise very densely micropilose throughout. A large, high, thick, and roundish syncoxite placed on a large membranous sternite, with a high, roundish, median lobe closely flanked by two in-

conspicuous, short, spiniform, obliquely truncate, setose horns (Fig. 3G), each latter being much shorter than syncoxital lobe. Telopodite 4-segmented, with a spine apically. Telopoditomere 1 squarish, with a very small distomesal, setigerous cone (a strongly reduced trichostele). Telopoditomere 2 with a prominent, finger-shaped, distomesal process on caudal face, produced apically to ca 1/3 telopoditomere 3. The latter elongate, gently tapering distad and curved apically basad towards process on telopoditomere 2, with another, much smaller, caudad curved, caudolateral process. Telopoditomere 4 smallest, subcylindrical, erect, clearly shifted anteriad, subtended by and reaching the distal end of telopoditomere 3.

Vulva (Fig. 3D) densely setose, large, covering 1/2 coxa 2.

Comparative morphology and systematics

Originally, *Tonkinomeris* was described in the family Glomeridae Leach, 1815, tentatively assigned to the subfamily Haploglomerinae Mauriès, 1971, and compared to the genus *Peplomeris* Silvestri, 1917, with two species from northern Vietnam (Golovatch 1983; Nguyen et al. 2019). Both *Tonkinomeris napoensis* and *T. huzhengkuni* sp. nov. are very similar and are also sufficiently close geographically. They can easily be distinguished by a good number of morphological characters: both show vivid colour patterns (apparently, because both are epigean and fairly large), the caudal margin of the ♂ pygidium is clearly emarginate centrally (yet with no evident paramedian tubercles), T3 is somewhat incrassate and sagittally flattened, the anterior telopod (♂ leg 18) is supplied with a blunt apico-mesal tooth, there is an elongate, subcylindrical, and suberect posterior telopod (♂ leg 19) which features T1 with a mesal trichostele, each of T2 and T3 have a distinct distocaudal process, etc. Furthermore, the telopodites of the posterior telopods are not only 4-segmented and supplied mesally with a trichostele on T1, but they also show a small caudal process on T3 in addition to a stronger caudal process on T2; thus, T3 is well developed, fully functional, and its apical part forms a kind of underdeveloped pincer together with T2. All this allows us to relegate *Tonkinomeris* from Glomeridae to the family Glomeridellidae. Moreover, as the apical pincer on the posterior telopod seems to be a little better developed in *T. huzhengkuni* sp. nov. than in *T. napoensis*, this pincer in the remaining Glomeridellidae may be considered as being clearly apomorphous. This contradicts the views of Oeyen and Wesener (2015) to regard the Glomeridellidae as the basal family of the order Glomerida, better agreeing instead with their later cladistic analysis (Oeyen and Wesener 2018).

In addition, like most species of *Typhloglomeris*, the caudal margins of a few ♂ tergites in front of the pygidium in *Tonkinomeris huzhengkuni* sp. nov. are modified, each drawn medially posteriad into a small, albeit glabrous, lobe (thus, clearly apomorphous), vs remaining simple and unmodified (plesiomorphous) in *T. napoensis*. In contrast, the particularly strongly reduced, 2- or 3-segmented ♂ telopodites 17 in *T. napoensis* definitely represent an apomorphous condition compared to the usual, 4-segmented ♂ telopodites 17 observed in *T. huzhengkuni* sp. nov. and most other Glom-

erida. The presence of a sharp caudomesal tooth also on T2 of the anterior telopod, vs its absence from *T. napoensis*, is difficult to polarize in terms or apo- or plesiomorphy. However, the particularly strongly developed central syncoxital lobe and the especially small syncoxital horns, as well as the rudimentary trichostele on T1 of the posterior telopods, all observed in *T. huzhengkuni* sp. nov. as opposed to their more usual states in *T. napoensis*, seem to be apomorphous. Therefore, each of the species combines both apo- and plesiomorphies in a number of traits. Most of the characters seem to be more advanced (apomorphous) in *T. huzhengkuni* sp. nov. compared to *T. napoensis*, but a few others vice versa (e.g., the more strongly reduced ♂ legs 17). What appears evident in any case is, that overall *Tonkinomeris* seems to represent the most primitive, perhaps even the basalmost genus of Glomeridellidae. This is primarily because both *T. napoensis* and *T. huzhengkuni* sp. nov. still show very modest modifications of the ♂ tergites and pygidium, while their posterior telopods feature a trichostele on T1 and yet underdeveloped apical pincers formed by T2 and T3.

　　Glomeridae, in contrast to Glomeridellidae, are distinct in the posterior telopods (♂ legs 19) typically being stouter, clearly curved mesad, by themselves forming a strong pincer, some telopoditomeres before last one showing a mesal trichostele or its vestige, while each telopodite is devoid of clear-cut apical pincers. The Protoglomeridae seems to be a polyphyletic group (Oeyen and Wesener 2015), only superficially being similar to Glomeridae; sometimes their tergite 11 is fused to the pygidium (still retaining a suture), while the posterior telopods are even stouter, devoid of trichosteles, both T2 and T4 form a distinct pincer by themselves (T3 being strongly developed), while each telopodite is with an additional apical pincer due to T2 and T4 (e.g., Mauriès 1971). Among the Glomeridellidae, however, the posterior telopods are usually contrasting elongate, slender, suberect, each telopodite forming a more or less distinct pincer due to modified T2 and T4 or T2 and T3 (Attems 1926; Mauriès 1971; Enghoff et al. 2015). Within *Typhloglomeris*, the genus deemed both morphologically and geographically closest to *Tonkinomeris*, the pincers on the posterior telopods in most species are formed by T2 and T3=4, when the real T3 is completely suppressed, or by T2 and T4, when T3 is strongly reduced to a short, rudimentary, non-functional, but still visible, albeit sometimes incomplete, ring. In contrast, the pincers in *Tonkinomeris* tend to be somewhat underdeveloped and peculiar in showing a small caudal process on T3 in addition to a stronger caudal process on T2, with T3 being fully developed and functional. This definitely represents a plesiomorphy, perhaps even the basalmost state whence a gradual reduction of both T3 and a trichostele on T1 is traced within some more advanced Glomeridellidae like *Typhloglomeris* and *Glomeridella* (cf. Attems 1926; Mauriès 1971).

Phylogeny

The phylogeny of Glomerida as recently recovered by Oeyen and Wesener (2018), based on morphological evidence alone, shows that both *Glomeridella* and *Typhloglomeris* cluster together with some Protoglomeridae and thus form no clear-cut family
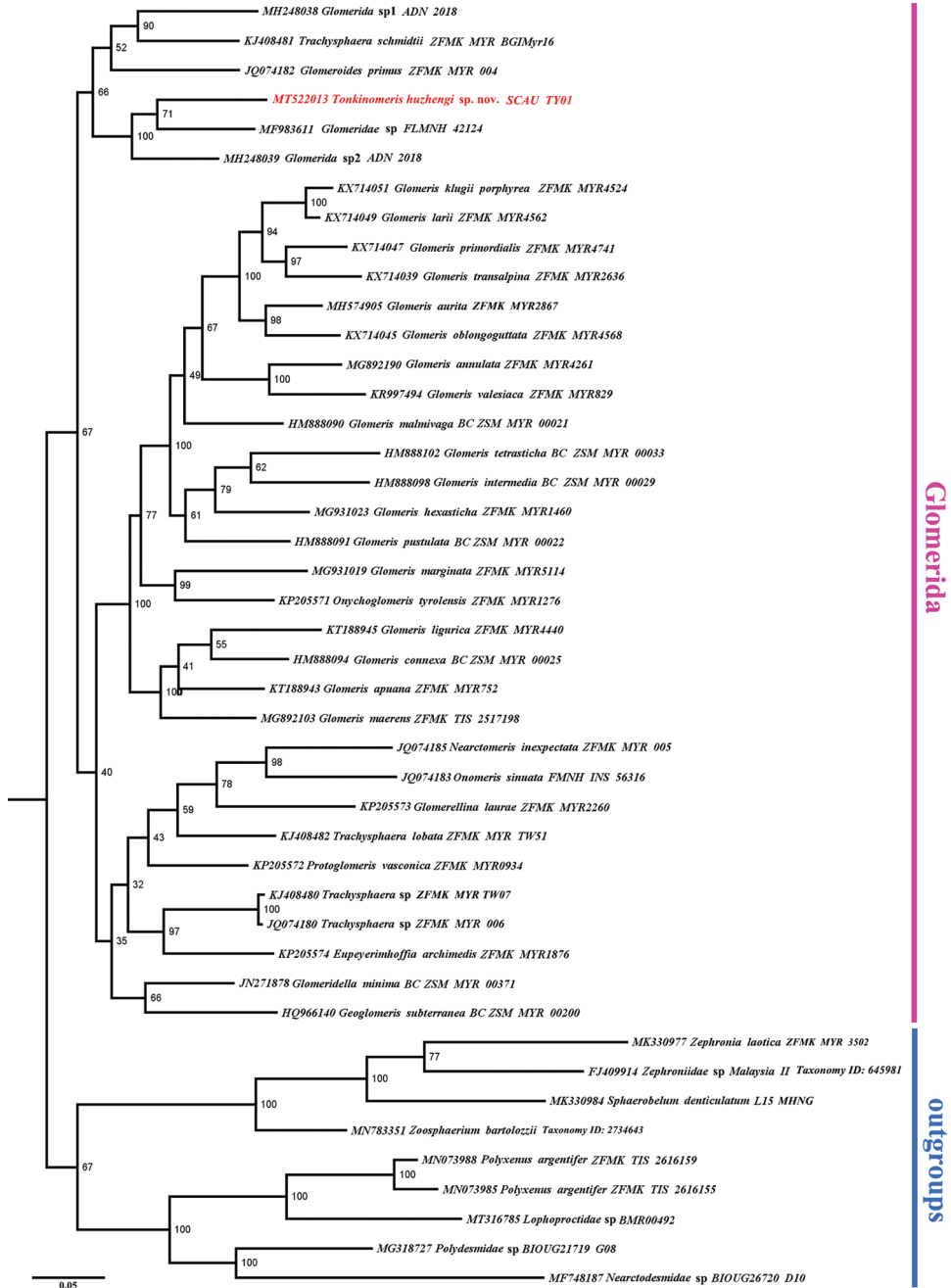
Figure 5. A consensus tree produced from BI analysis. Numbers on branches are estimates of the Bayesian posterior probability of a clade, expressed as percentage.

Glomeridellidae. Moreover, the joint Protoglomeridae + Glomeridellidae clade is not too basal on the tree and, thus, better agrees with our views that the Glomeridellidae is best considered as one of the relatively advanced groups of Glomerida.

The molecular sequences available in the GenBank and used in our phylogenetic analysis, which is apparently the first to be attempted for the entire order Glomerida, have allowed for two phylograms to be obtained. Since both BI and ML trees are similar and neither is congruent with the morphology-based phylogeny recovered by Oeyen and Wesener (2018), we present here only the BI tree (Fig. 5). Because the only genetic data available for Glomeridellidae in the GenBank are for a species of *Glomeridella*, and there is nothing yet for any *Typhloglomeris* sp., *Tonkinomeris* appears to cluster together with or close to two closer unidentified members of Glomeridae, one of which seems to be a *Hyleoglomeris* sp. (Wesener pers. comm.). Thus, there is no hint of a Glomeridellidae cluster. Instead, the whole tree (Fig. 5) is a rather random mixture of mostly genera and species of Glomeridae. This seems to indicate that any molecular analysis is bound to be too deficient and premature at this stage. It would seem especially interesting to compare *Tonkinomeris* to some other representatives of Glomeridellidae, especially the morphologically and geographically closest *Typhloglomeris* spp.

Key to genera of Glomeridellidae

The following key to the accepted genera of Glomeridellidae can be offered:

1   Penultimate (11th) tergite just in front of pygidium strongly reduced, visible only laterally as thin ribbons. Caudal margins both of tergites and pygidium regularly rounded caudally, unmodified. Tergites densely and finely pubescent. Anterior telopods strongly elongate, subcylindrical, T2 and T4 forming a pincer, T3 being small. Syncoxital lobe of 3-segmented posterior telopod telopodites very simple and low, a trichostele on T1 absent, both T2 and T3=4 forming a pincer (apparently, true T3 being totally reduced). Western Europe east to northwestern Balkans..***Glomeridella***

–   No tergites reduced. Caudal margin of tergites and pygidium either unmodified and regularly rounded or (in ♂ only) modified. Tergites bare. Anterior telopods relatively stout, mostly flattened sagittally, each forming no apical pincer. Syncoxital lobe of posterior telopods higher and variously shaped, telopodites 3- (more rarely) or 4-segmented, usually elongate, slender, suberect and each forming a more or less distinct apical pincer **2**

2   Caudal margin of some tergites and pygidium usually modified, several tergites before ♂ pygidium largely crenulate, ♂ pygidium with a paramedian pair of distinct knobs at a centrally emarginate or nearly straight caudal edge. Anterior telopods often flattened sagittally, sometimes also inflated,

but usually devoid of mesal outgrowths. Posterior telopods devoid of trichoteles and each forming a distinct apical pincer (either T2 and T4, when T3 rudimentary, or T2 and T3=4, when true T3 fully suppressed). Eastern Mediterranean ....***Typhloglomeris***

– Caudal margin of some tergites and/or pygidium modified, several tergites before ♂ pygidium glabrous, not crenulate, but sometimes drawn caudad into small central lobes, while ♂ pygidium with a centrally emarginate caudal margin and only sometimes with a paramedian pair of indistinct knobs at rear edge. Anterior telopods flattened sagittally, with evident mesal outgrowths. Posterior telopods with both a trichostele retained on T1 and an indistinct apical pincer (T2 and T3). Southern China and northern Vietnam ....***Tonkinomeris***

Zoogeography

Finding a glomeridellid genus in southern China and northern Vietnam is indeed remarkable, as the geographically closest record belongs to *Typhloglomeris martensi* (Golovatch, 1981), from Hyrcania, southwesternmost Caspian Sea coast within both the Republic of Azerbaijan and northwestern Iran (Golovatch 1981). As the huge gap between Hyrcania and Guizhou Province definitely reflects traces of former extinctions and dispersal events, this allows for the entire family Glomeridellidae to be considered both relict and of Oriental stock. Because on balance *Tonkinomeris* seems to be the most primitive among the glomeridellid genera, this also allows us to suggest some ancient, generally northwestward dispersal events from the Oriental realm to the Mediterranean area via southern China. Interestingly, in certain respects the relatively more advanced *T. huzhengkuni* sp. nov. looks like the remain of a stepping-stone in Guizhou Province, China; this is also quite far west of the overall more primitive *T. napoensis* from Vietnam, near the family's presumed Oriental roots.

The above picture not only so considerably extends the known distribution area of Glomeridellidae to the east, but it also demonstrates the extent to which the millipede fauna of China is still understudied, as well as the possible roles that the Sino-Himalayan (= southern Chinese) and/or Oriental faunogenetic centres could have played in the origins of the Euro-Mediterranean diplopod fauna (Golovatch and Martens 2018; Golovatch and Liu 2020). Such a distribution pattern strongly resembles that of *Hyleoglomeris*, one of the largest, diverse, and widespread genera of Glomeridae and Glomerida (see above).

More information is necessary, especially phylogenetic reconstructions, in order to assess the remarkable disjunction of the Glomeridellidae and both its biological and spatial evolution. Further conclusions must be deferred until more evidence, both morphological and molecular, becomes available. New Glomerida are still being actively found and described from various places in Asia!

Acknowledgements

References

Attems C (1926) Progoneata. In: Krumbach T (Ed.) Handbuch der Zoologie 4(1). Progoneata, Chilopoda, Insecta 1. Walter de Gruyter & Co., Berlin–Leipzig, 7–238.

Astrin JJ, Stüben PE (2008) Phylogeny in cryptic weevils: molecules, morphology and new genera of western Palaearctic Cryptorhynchinae (Coleoptera: Curculionidae). Invertebrate Systematics 22 (5): 503–522. https://doi.org/10.1071/IS07057

Enghoff H, Golovatch SI, Short M, Stoev P, Wesener T (2015) Diplopoda – taxonomic overview. In: Minelli A (Ed.) Treatise on Zoology – Anatomy, Taxonomy, Biology. The Myriapoda 2 (16): 363–453. https://doi.org/10.1163/9789004188273_017

Golovatch SI (1981) Diplopoda from Iran (Glomeridellidae, Glomeridae, Platydesmidae, Polydesmidae). Senckenbergiana biologica 61(5/6): 421–427.

Golovatch SI (1983) On several new Glomeridae (Diplopoda) from Indochina. Annales historico-naturales Musei nationalis hungarici 75: 107–116. http://publication.nhmus.hu/pdf/annHNHM/Annals_HNHM_1983_Vol_75_107.pdf

Golovatch SI (2003) Two new species of Glomeridellidae (Diplopoda: Glomerida) from the Middle East. Arthropoda Selecta 11(4): 255–258. https://kmkjournals.com/upload/PDF/ArthropodaSelecta/11/11_4%20255_258%20Golovatch.pdf

Golovatch SI, Liu WX (2020) Diversity, distribution patterns, and fauno-genesis of the millipedes (Diplopoda) of mainland China. ZooKeys 930: 153–198. https://doi.org/10.3897/zookeys.930.47513

Golovatch SI, Martens J (2018) Distribution, diversity patterns and faunogenesis of the millipedes (Diplopoda) of the Himalayas. ZooKeys 741: 3–34. https://doi.org/10.3897/zookeys.741.20041

Golovatch SI, Turbanov IS (2018) A new cavernicolous species of the millipede genus *Typhloglomeris* Verhoeff, 1898 from western Georgia, Caucasus (Diplopoda: Glomerida: Glomeridellidae). Russian Entomological Journal 27(1): 101–104. https://doi.org/10.15298/rusentj.27.1.14

Golovatch SI, Geoffroy JJ, Mauriès JP (2006) Review of the millipede genus *Hyleoglomeris* Verhoeff, 1910 (Diplopoda, Glomerida, Glomeridae), with descriptions of new species

from caves in Southeast Asia. Zoosystema 28(4): 887–915. https://www.researchgate.net/publication/229005366

Hall TA (1999) BioEdit: a user-friendly biological sequence alignment editor and analysis program for Windows 95/98/NT. Nucleic Acids Symposium Series 41: 95–98.

Makarov SE, Lučić LR, Tomić VT, Karaman IM (2003) Two new glomeridellids (Glomeridellidae, Diplopoda) from Montenegro and Macedonia. Periodicum Biologorum 106(4): 473–477. https://www.researchgate.net/publication/298067881

Mauriès JP (1971) Diplopodes épigés et cavernicoles des Pyrénées espagnoles et des monts Cantabriques. VII. Gloméridés. Essai de classification des Glomeroidea. Bulletin de la Société d'Histoire naturelle de Toulouse 107(3–4): 423–436.

Miller M, Pfeiffer W, Schwartz T (2010) Creating the CIPRES Science Gateway for inference of large phylogenetic trees. Proceedings of the Gateway Computing Environments Workshop (GCE), 14 November 2010, New Orleans, LA, 1–8. https://doi.org/10.1109/GCE.2010.5676129

Nguyen AD, Sierwald P, Marek PE (2019) The pill millipedes of Vietnam: a key to genera and descriptions of five new species (Diplopoda: Glomerida: Glomeridae). Raffles Bulletin of Zoology 67: 260–297. https://lkcnhm.nus.edu.sg/app/uploads/2018/11/RBZ-2019-0020.pdf

Oeyen JP, Wesener T (2015) Steps towards a phylogeny of the pill millipedes: non-monophyly of the family Protoglomeridae, with an integrative redescription of *Eupeyerimhoffia archimedis* (Diplopoda, Glomerida). ZooKeys 510: 49–64. https://doi.org/10.3897/zookeys.510.8675

Oeyen JP, Wesener T (2018) A first phylogenetic analysis of the pill millipedes of the order Glomerida, with a special assessment of mandible characters (Myriapoda, Diplopoda, Pentazonia). Arthropod Structure & Development 47(2): 214–228. https://doi.org/10.1016/j.asd.2018.02.005

Pende N, Leisch N, Gruber-Vodicka H, Heindl N, Ott J, Blaauwen T, Bulgheresi S (2014) Size-independent symmetric division in extraordinarily long cells. Nature Communications 4803(5): 1–10. https://doi.org/10.1038/ncomms5803

Ronquist F, Teslenko M, van der Mark P, Ayres DL, Darling A, Höhna S, Larget B, Liu L, Suchard MA, Huelsenbeck JP (2012) MrBayes 3.2: Efficient Bayesian Phylogenetic Inference and Model Choice Across a Large Model Space. Systematic Biology 61(3): 539–542. https://doi.org/10.1093/sysbio/sys029

Shelley RM, Golovatch SI (2011) Atlas of myriapod biogeography. I. Indigenous ordinal and supra-ordinal distributions in the Diplopoda: Perspectives on taxon origins and ages, and a hypothesis on the origin and early evolution of the class. Insecta Mundi 0158: 1–134. https://journals.flvc.org/mundi/article/view/0158

Trifinopoulos J, Nguyen L-T, von Haeseler A, Minh B (2016) W-IQ-TREE: a fast online phylogenetic tool for maximum likelihood analysis. Nucleic Acids Research 44(W1): W232–W235. https://doi.org/10.1093/nar/gkw256

Wesener T (2019) The oldest pill millipede fossil: a species of the Asiatic pill millipede genus *Hyleoglomeris* in Baltic amber (Diplopoda: Glomerida: Glomeridae). Zoologischer Anzeiger 283: 40–45. https://doi.org/10.1016/j.jcz.2019.08.009

RESEARCH ARTICLE

ZooKeys
A peer-reviewed open-access journal
Launched to accelerate biodiversity research

Taxonomic studies on the genus *Ectatosticta* (Araneae, Hypochilidae) from China, with descriptions of two new species

Yejie Lin¹, Shuqiang Li²

1 *Hebei Key Laboratory of Animal Diversity, College of Life Science, Langfang Normal University, Langfang 065000, China* **2** *Institute of Zoology, Chinese Academy of Sciences, Beijing 100101, China*

Corresponding author: Shuqiang Li (lisq@ioz.ac.cn)

Citation: Lin Y, Li S (2020) Taxonomic studies on the genus *Ectatosticta* (Araneae, Hypochilidae) from China, with descriptions of two new species. ZooKeys 954: 17–29. https://doi.org/10.3897/zookeys.954.52254

Abstract

Species of the spider family Hypochilidae Marx, 1888 from China are studied, including two known species and two new species of the genus *Ectatosticta* Simon, 1892. The new species are *E. wukong* **sp. nov.** (♂♀) from Sichuan and *E. xuanzang* **sp. nov.** (♀) from Tibet.

Keywords

diagnosis, etymology, taxonomy, type, webs

Introduction

Hypochilidae Marx, 1888 is a small family that includes two genera: *Hypochilus* Marx, 1888 and *Ectatosticta* Simon, 1892. *Hypochilus* is endemic to the USA and includes ten species, whereas *Ectatosticta* is endemic to China and until now only included two species: *E. davidi* (Simon, 1889) from Shaanxi and *E. deltshevi* Platnick & Jäger, 2009 from Qinghai (WSC 2020, Li 2020).

Hypochilidae was considered the sister group of all other araneomorph spiders (Platnick 1977), but Wheeler et al. (2017) confirmed that Hypochilidae is the sister group of Filistatidae Simon, 1864. Unlike *Hypochilus*, *Ectatosticta* build simple sheet

webs between soil blocks, huge rocks or in tree trunks. On one side of the web of some species there is a tube-retreat which typically extends into rock crevices, soil or between roots.

In this paper, photographs of two known *Ectatosticta* species are provided, of which *E. davidi* (Simon, 1889) is based on material collected near the type locality and *E. deltshevi* Platnick & Jäger, 2009 is based on the male holotype and females from the same locality as the holotype. In addition, two new species of the genus *Ectatosticta* are described: *E. wukong* sp. nov. (♂♀) from Sichuan and *E. xuanzang* sp. nov. (♀) from Tibet.

Material and methods

All specimens were preserved in 75% ethanol. Female genitalia were cleared in a trypsin enzyme solution to dissolve non-chitinous tissue. Specimens were examined under a LEICA M205C stereomicroscope. Photomicroscope images were taken with an Olympus C7070 zoom digital camera (7.1 megapixels). Photos were stacked with Helicon Focus 6.7.1 (Khmelik et al. 2006) and processed in Adobe Photoshop CC 2018.

All measurements are in millimeters. Eye sizes are measured as the maximum diameter from either the dorsal or frontal view. Leg measurements are given as follows: total length (femur, patella + tibia, metatarsus, tarsus). Distribution maps were generated using ArcMap software 10.2 (ESRI 2002).

Abbreviations:

ALE	anterior lateral eyes	**OS**	outer spermathecae
AME	anterior median eyes	**PLE**	posterior lateral eyes
C	conductor	**PME**	posterior median eyes
E	embolus	**S**	spermathecae
IS	inner spermathecae	**TS**	thickened setae

The material studied in the paper is housed in the Institute of Zoology, Chinese Academy of Sciences (**IZCAS**) in Beijing, China.

Taxonomy

Family Hypochilidae Marx, 1888

Genus *Ectatosticta* Simon, 1892

Type species. *Hypochilus davidi* Simon, 1889 from China.

Diagnosis. *Ectatosticta* can be easily distinguished from *Hypochilus* by the rectangular labium which is almost as long as wide and bears a pair of triangular posterolateral flanges, also by numerous leg spines (Forster et al. 1987) and in the lateral view

of the male palp, the cymbium to bulb length ratio is almost 3:1 (Figs 2, 4) but nearly 1 : 1 in *Hypochilus* (Forster et al. 1987: figs 38, 43, 48, 53, 58, 63, 68, 73).

   Distribution. China.

Key to *Ectatosticta* males

1   Male palp with fewer than 5 thickened setae, the most dorsal setae are dispersed, and the length ratio of the embolus to the embolus base is more than 2 : 1 (Fig. 1) **2**
–   Male palp with 5–7 thickened setae, all closely appressed one another, and the length ratio of the embolus to the embolus base is almost 1 : 1 (Fig. 1) ....***E. davidi***
2   Male palp with 4 thickened setae, the dorsalmost setae are dispersed and the length ratio of the embolus to the embolus base is almost 2 : 1 (Fig. 1)......... .... ***E. deltshevi***
–   Male palp with 2 thickened setae, the length ratio of the embolus to the embolus base is almost 3 : 1 (Fig. 1) ....***E. wukong* sp. nov.**

Key to *Ectatosticta* females

1   Two pairs of spermathecae (Fig. 5A, B, D)..**2**
–   One pair of spermathecae (Fig. 5C) ....***E. wukong* sp. nov.**
2   The ratio of the length of the inner spermathecae to the outer spermathecae is almost 1 : 3 (Fig. 5D) .... ***E. xuanzang* sp. nov.**
–   The ratio of the length of the inner spermathecae to the outer spermathecae is almost 1 : 1 to 1 : 2 (Fig. 5A, B) **3**
3   Spermathecae weakly sclerotized (Fig. 5A) ....***E. davidi***
–   Spermathecae strongly sclerotized (Fig. 5B) .... ***E. deltshevi***

Ectatosticta davidi (Simon, 1889)
Figs 1, 2A, 3A, 4A, 5A, 6F, 8

Hypochilus davidi Simon 1889: 208; Simon 1892: 204, figs 143–146, 148, 149; Gertsch 1958: 13, figs 10, 19, 22–31; Lehtinen, 1967: 431, fig. 15; Platnick and Jäger 2009: 210, figs 1–4; Zhang and Wang 2017: 311, fig. 4f.

Type material. *Syntypes* 1♂ 1♀, Muséum national d'Histoire naturelle, Paris, label reads "Inkiaphou, Chine méridionale", which should be on Mt. Qinling in Shaanxi Province (see Platnick and Jäger 2009: Yinjiapo or Yinjiapu, now known as Yonxingcun in Xi'an City, Huyi District, Laoyu Town, 33.98232N, 108.52079E), not examined.

   Other material examined. 1♂, China, Shaanxi Province, Chang'an, Xiaoyuhecun, Qiaotouchi, 02.V.2020, Jiazhou Lu leg.; 1♀ (IZCAS), China, Shaanxi Province,
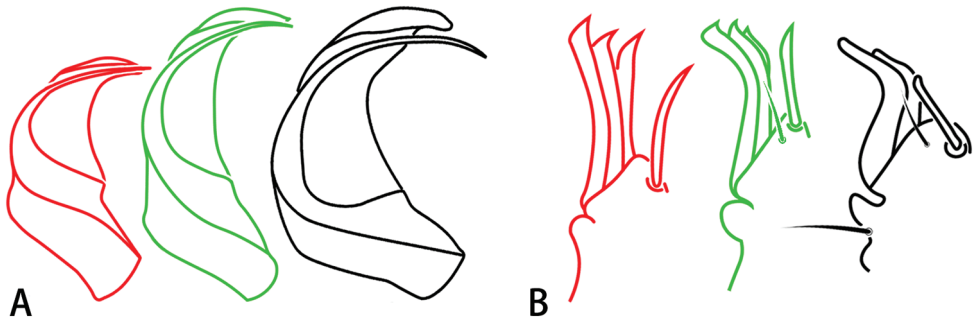
Figure 1. *Ectatosticta* spp., outlines of male bulbs and thickened setae in retrolateral view (Red line, *E. davidi*; green line, *E. deltshevi*, holotype; black line, *E. wukong* sp. nov., holotype) **A** bulbs **B** thickened setae.

Mt. Taibaishan, above Houshenzi, tree line, scattered mixed coniferous/*Rhododendron* forest, 33.9122N, 107.7789E, 12–15.VI.1997, elevation ca. 3050 m, Peter Jäger leg.

Distribution. China (Shaanxi).

Ectatosticta deltshevi **Platnick & Jäger, 2009**
Figs 1, 2B, 3B, 4B, 5B, 6A–C, 7A, B, 8

Ectatosticta davidi Li & Zhu, 1984: 510, figs A–G; Forster et al. 1987: 23, figs 6–16, 18–20, 23, 24, 31–36, 78–82; Song et al. 1999: 41, figs 11D, 17Q–T; Hu 2001: 69, figs 1.1–6; Song et al. 2001: 64, fig. 24A–E. All misidentified.
Ectatosticta deltshevi Platnick & Jäger, 2009: 214.

Type material. *Holotype* ♂ (IZCAS-Ar28579), China, Qinghai Province, Huangyuan County, 15.IX.1984, Zhongshan Li leg., examined.

Other material examined. 2♂2♀ (IZCAS), China, Qinghai Province, Huangyuan County, 15.IX.1984, Zhongshan Li leg.; 2♀ (IZCAS), China, Qinghai Province, Haidong, Huzhutu Autonomous County, Jinchuan County, Jiading, Beishan National Park, 36.9378N, 102.4575E, elevation ca. 2442 m, 30.X.2019, Yejie Lin leg.

Distribution. China (Qinghai).

Natural history. Living in simple sheet webs between soil blocks or tree roots. On one side of the web there is tube-retreat that extends into the soil.

Ectatosticta wukong **sp. nov.**
http://zoobank.org/4BDB5B2E-0307-4B5C-B678-2C45F70762AD
Figs 1, 2C, D, 3C, D, 4C, D, 5C, 6D, 6E, 8

Type material. *Holotype* ♂ (IZCAS-Ar40346), China, Sichuan Province, Hongyuan County, Shuajingsi, Mt. Zhegu to Shuamalukou, 31.9272N, 102.6546E, elevation ca.

Figure 2. *Ectatosticta* spp., prolateral view of left male palps **A** *E. davidi*, male from Shaanxi **B** *E. deltshevi*, holotype **C** *E. wukong* sp. nov., holotype **D** *E. wukong* sp. nov., embolus and conductor of right palp (rotated horizontally), holotype.

3458 m, 23.XI.2019, Zhigang Chen leg. ***Paratypes*** 3♀ (IZCAS-Ar40347–Ar40349), same data as holotype.

Etymology. The species is named after Wukong, a character in the classic Chinese novel *Journey to the West*, noun. *Journey to the West* was written during the Ming Dynas-

Figure 3. *Ectatosticta* spp., ventral view of left male palps **A** *E. davidi*, male from Shaanxi **B** *E. deltshevi*, holotype **C** *E. wukong* sp. nov., holotype **D** *E. wukong* sp. nov., embolus and conductor of right palp (rotated horizontally), holotype.

ty (1368–1644 A.D) and is about the adventures of a priest, Xuanzang, and his three disciples, Wukong, Wuneng, and Wujing, as they travel west in search of the Buddhist Sutra. Their travel begins at what is today Xi'an (near the type locality of *E. davidi*), via

Qinghai (close to the type locality of *E. deltshevi*), to South Xinjiang, Tibet (near the type locality of *E. xuanzang* sp. nov.) and India.

Diagnosis. Males of *E. wukong* sp. nov. can be distinguished by having only two thickened setae retrolaterally on the cymbium and the length ratio of the embolus to the embolus base is almost 3 : 1 (Fig. 3C, D). Females can be distinguished by having one pair of spermathecae (Figs 5C, 6D, E).

Description. Male: Total length 9.29, carapace 5.58 long, 3.14 wide, opisthosoma 4.40 long, 3.14 wide. Eye sizes and interdistances: AME 0.19, ALE 0.26, PME 0.23, PLE 0.24, AME–AME 0.16, AME–ALE 0.21, PME–PME 0.36, PME–PLE 0.10, AME–PME 0.07, ALE–PLE 0.02. Clypeus height 0.30. Chelicerae with seven promarginal and six retromarginal teeth. Leg measurements: leg I: 40.37 (11.60 + 12.88 + 9.42 + 6.47), leg II: 31.79 (9.10 + 10.51 + 7.95 + 4.23), leg III: 24.98 (7.24 + 8.64 + 5.70 + 3.40), leg IV: 32.53 (9.55 + 10.13 + 8.40 + 4.45). Leg formula: 1423.

Male palp (Figs 2C, D, 3C, D, 4C, D) simple, cymbium long, retrolaterally with an apophysis divided into two parts: a small, semicircular lobe with a seta and a large lobe with two strong setae placed closely together. Embolus thin, length ratio of embolus to embolus base 3:1. Conductor sickle-shaped.

Female. Total length 10.77, carapace 4.70 long, 3.28 wide, opisthosoma 6.79 long, 4.87 wide. Eye sizes and interdistances: AME 0.17, ALE 0.26, PME 0.23, PLE 0.29, AME–AME 0.18, AME–ALE 0.28, PME–PME 0.36, PME–PLE 0.27, AME–PME 0.06, ALE–PLE 0.07. Clypeus height 0.36. Chelicerae with seven promarginal and six retromarginal teeth. Leg measurements: Leg I: 29.10 (8.40 + 10.00 + 6.60 + 4.10), leg II: 25.44 (6.99 + 8.91 + 5.90 + 3.64), leg III: 18.73 (5.64 + 6.15 + 4.35 + 2.59), leg IV: 23.92 (7.31 + 7.50 + 5.83 + 3.28). Leg formula: 1243.

Female genitalia (Figs 5C, 6D, E) simple, one pair of spermathecae, spermathecae slightly curved.

Distribution. Known only from the type locality.

Ectatosticta xuanzang sp. nov.

http://zoobank.org/3A050541-598F-4349-8B86-C21E11F5B0CB

Figs 5D, 6G–K, 7C, D, 8

Type material. *Holotype* ♀ (IZCNS-Ar40373), China, Tibet Autonomous Region, Lhoka, Cona County, Marmang, Lebugou, Yelang Valley, 27.8682N, 91.8110E, elevation ca. 3118 m, 12.X.2019, Yejie Lin leg. *Paratypes* 5♀ (IZCNS-Ar40374–Ar40378), same data as holotype.

Etymology. The species is named after Xuanzang, a character in the classic Chinese novel *Journey to the West*, noun.

Diagnosis. Females of *E. xuanzang* sp. nov. can be distinguished by the ratio of the length of the inner spermathecae to the outer spermathecae of almost 1:3 (Figs 5D, 6G–K) (vs. almost 1:1 in *E. davidi* and 1:2 to 1:1 in *E. deltshevi* (Figs 5A, B, 6A–C, F)) and the ratio of leg I length to the carapace length is almost 1:8 (vs. almost 1:6 in *E. wukong* sp. nov. and *E. deltshevi* and 1.7 in *E. davidi*).

Figure 4. *Ectatosticta* spp., retrolateral view of left male palps **A** *E. davidi*, male from Shaanxi **B** *E. delt-shevi*, holotype **C** *E. wukong* sp. nov., holotype **D** *E. wukong* sp. nov., embolus and conductor of right palp (rotated horizontally), holotype.

Description. Female. Total length 12.59, carapace 6.03 long, 3.60 wide, opistho-soma 6.22 long, 4.40 wide. Eye sizes and interdistances: AME 0.15, ALE 0.31, PME 0.29, PLE 0.28, AME–AME 0.19, AME–ALE 0.37, PME–PME 0.42, PME–PLE 0.27, AME–PME 0.07, ALE–PLE 0.06. Clypeus height 0.45. Chelicerae with seven (n = 3) or eight (n = 3) promarginal and 6–9 (6(n = 1), 7(n = 4), 9(n = 1)) retromar-ginal teeth. Leg measurements: Leg I: 51.47 (15.45 + 16.28 + 12.95 + 6.79), leg II:
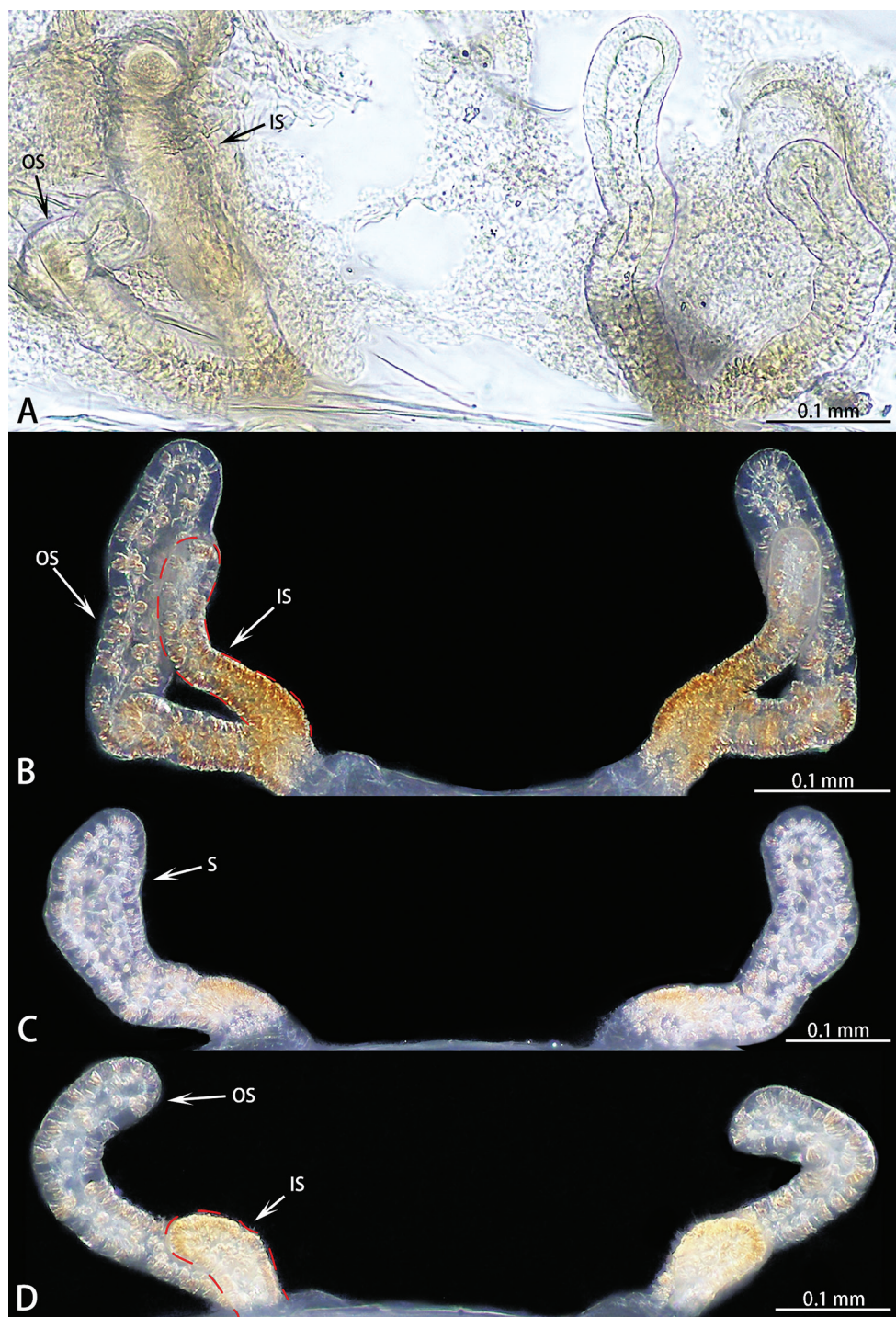
Figure 5. *Ectatosticta* spp., dorsal view of female genitalia **A** *E. davidi*, female from Shaanxi **B** *E. deltshevi*, female from Qinghai (type locality) **C** *E. wukong* sp. nov., paratype **D** *E. xuanzang* sp. nov., holotype.
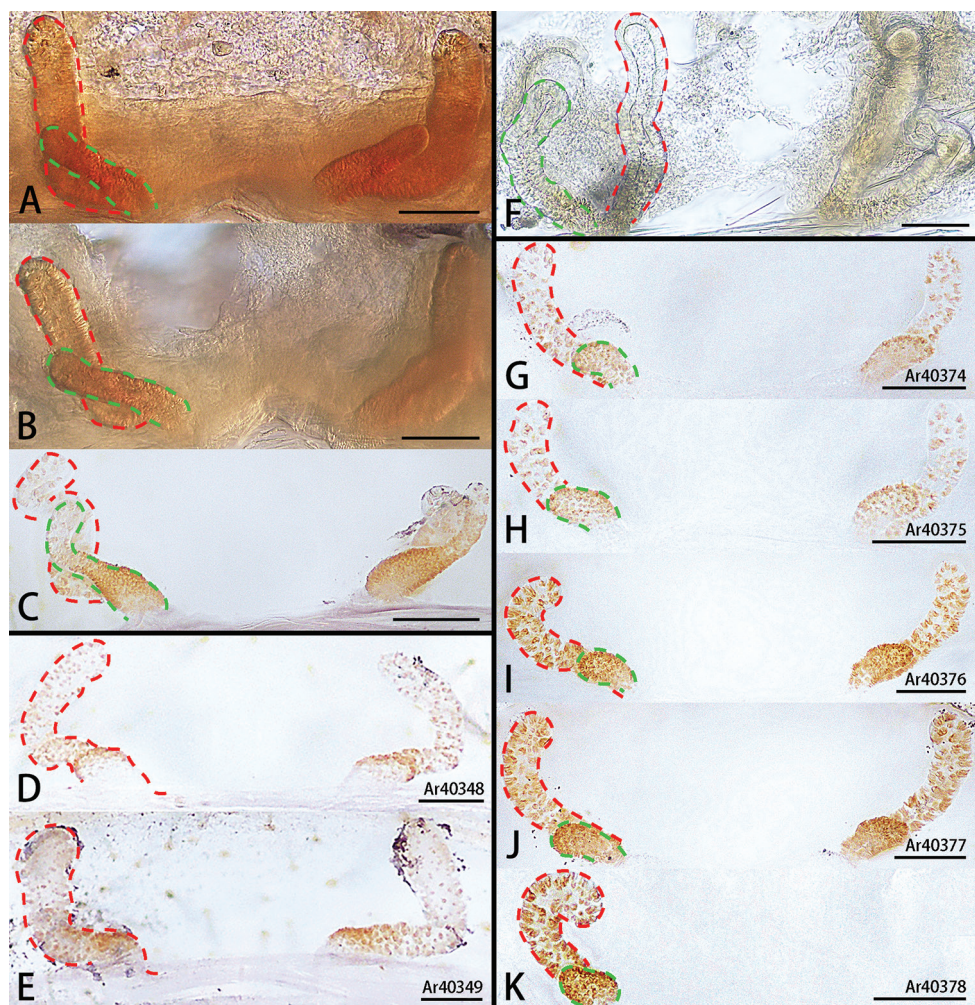
Figure 6. *Ectatosticta* spp., variation of female genitalia (red line, inner spermathecae (**A–C**, **F–K**) or spermathecae (**D, E**); green line, outer spermathecae) **A–C** *E. deltshevi*, females from Qinghai (type locality) **D, E** *E. wukong* sp. nov., paratypes **F** *E. davidi*, females from Shaanxi **G–K** *E. xuanzang* sp. nov., paratypes. Scale bars: 0.1 mm.

47.88 (14.03 + 16.22 + 11.60 + 6.03), leg III: 37.66 (11.67 + 12.50 + 9.04 + 4.45), leg IV: 44.23 (12.31 + 14.49 + 12.11 + 5.32). Leg formula: 1243.

Female genitalia (Figs 5D, 6G–K) simple, with two pairs of slightly curved spermathecae. Inner spermathecae small, outer spermathecae curved, three times the length of inner spermathecae.

Male. Unknown.

Distribution. Known only from the type locality.

National history. In damp rocky areas, hiding between huge stones. They build simple sheet webs without a tube-retreat.
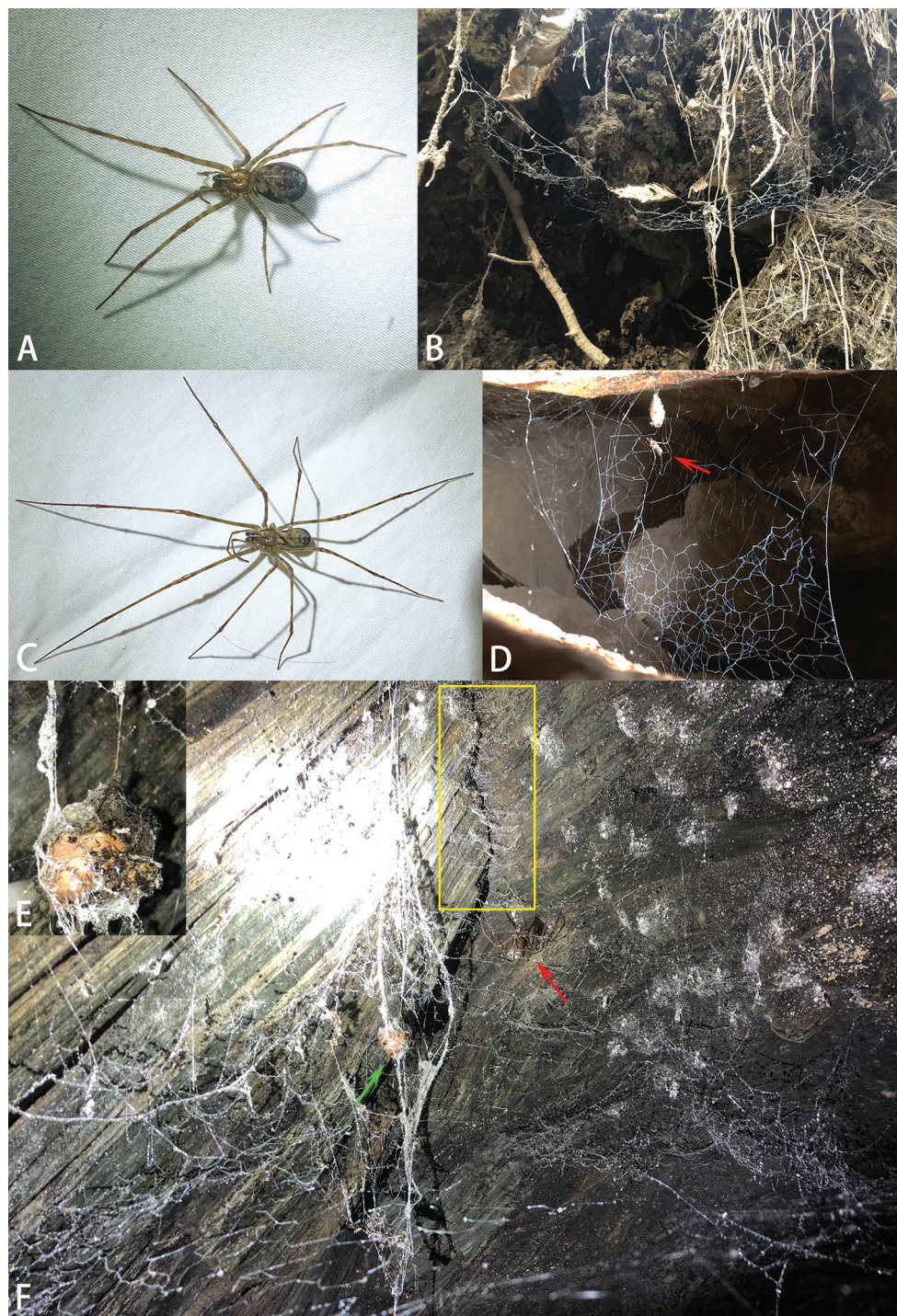
Figure 7. Photos of live *Ectatosticta* spp. **A** *E. deltshevi*, female from Qinghai **B** *E. deltshevi* and web **C** *E. xuanzang* sp. nov., holotype from Tibet **D** *E. xuanzang* and web **E** Egg sac **F** A typical web of *Ectatosticta*. Egg sac marked with green arrow, spider marked with red arrow and assembled nymphs marked with yellow rectangle.
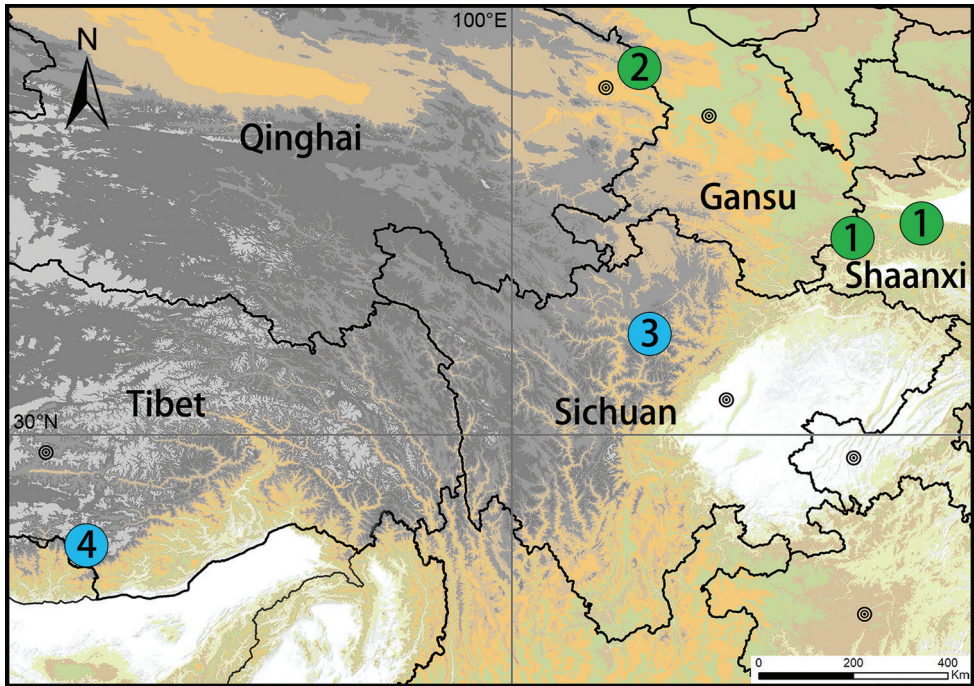
Figure 8. Distribution records of *Ectatosticta* species from China. **1** *E. davidi* **2** *E. deltshevi* **3** *E. wukong* sp. nov. **4** *E. xuanzang* sp. nov.

Discussion

Platnick & Jäger (2009) pointed out that the number of thickened setae in males of *Ectatosticta deltshevi* was four, whereas in *E. davidi* it was five to seven. However, it is necessary to examine more male specimens to learn more about the extent of variation. Based on the examination of all female specimens available, the extent of sclerotization of the spermathecae seems stable within the species. This study is currently being expanded to include molecular data and additional specimens from southwestern China and the Himalayas which will continue to increase our knowledge of *Ectatosticta*.

Acknowledgements

References

ESrI (2002) ArcMap. Version 10.2. Environmental Systems research Institute. redlands, California, USA. Available from: https://desktop.arcgis.com/zh-cn/arcmap/ [accessed 24 May 2020]

Forster RR, Platnick NI, Gray MR (1987) A review of the spider superfamilies Hypochiloidea and Austrochiloidea (Araneae, Araneomorphae). Bulletin of the American Museum of Natural History 185: 1–116.

Gertsch WJ (1958) The spider family Hypochilidae. American Museum Novitates 1912: 1–28.

Hu JL (2001) Spiders in Qinghai-Tibet Plateau of China. Henan Science and Technology Publishing House, 658 pp.

Khmelik VV, Kozub D, Glazunov A (2006) Helicon Focus. Version 6.6.1. http://www.helicon-soft.com/heliconfocus.html [accessed 24 May 2020]

Lehtinen PT (1967) Classification of the cribellate spiders and some allied families, with notes on the evolution of the suborder Araneomorpha. Annales Zoologici Fennici 4: 199–468.

Li S (2020) Spider taxonomy for an advanced China. Zoological Systematics 45(2): 73–77.

Li ZS, Zhu CD (1984) *Ectatosticta davidi* (Simon, 1888) of China (Araneae: Hypochilidae). Journal of the Bethune Medical University 10: 509–510.

Platnick NI (1977) The hypochiloid spiders: a cladistic analysis, with notes on the Atypoidea (Arachnida, Araneae). American Museum Novitates 2627: 1–23.

Platnick NI, Jäger P (2009) A new species of the basal araneomorph spider genus *Ectatosticta* (Araneae, Hypochilidae) from China. ZooKeys 16: 209–215. https://doi.org/10.3897/zookeys.16.231

Simon E (1889) Description de *Hypochilus davidi* sp. nov. Annales de la Société Entomologique de France (6)8(Bull.): 208–209.

Simon E (1892) Histoire naturelle des araignées. Deuxième édition, tome premier. Roret, Paris, 256 pp. https://doi.org/10.5962/bhl.title.51973

Song DX, Zhu MS, Chen J (1999) The Spiders of China. Hebei University of Science and Techology Publishing House, Shijiazhuang, 640 pp.

Song DX, Zhu MS, Chen J (2001) The Fauna of Hebei, China: Araneae. Hebei University of Science and Techology Publishing House, Shijiazhuang, 510 pp.

Wheeler WC, Coddington JA, Crowley LM, Dimitrov D, Goloboff PA, Griswold CE, Hormiga G, Prendini L, Ramírez MJ, Sierwald P, Almeida-Silva LM, Álvarez-Padilla F, Arnedo MA, Benavides LR, Benjamin SP, Bond JE, Grismado CJ, Hasan E, Hedin M, Izquierdo MA, Labarque FM, Ledford J, Lopardo L, Maddison WP, Miller JA, Piacentini LN, Platnick NI, Polotow D, Silva-Dávila D, Scharff N, Szűts T, Ubick D, Vink C, Wood HM, Zhang JX (2017) The spider tree of life: phylogeny of Araneae based on target-gene analyses from an extensive taxon sampling. Cladistics 33(6): 576–616. https://doi.org/10.1111/cla.12182

WSC (2020) World Spider Catalog. Version 21.0. Natural History Museum Bern, http://wsc.nmbe.ch [accessed on 03/19/2020]

Zhang ZS, Wang LY (2017) Chinese Spiders Illustrated. Chongqing University Press, 954 pp.

RESEARCH ARTICLE

Two new species of *Episymploce* Bey-Bienko, 1950 (Blattodea, Ectobiidae, Blattellinae) from China

Ting-Ting Li[1], De-Xing Liu[1], De-Yi Qiu[1], Qiao-Yun Yue[1]

1 *Zhongshan Customs Technology Center, Zhongshan 528400, Guangdong, China*

Corresponding author: Qiao-Yun Yue (779721036@qq.com)

Citation: Li T-T, Liu D-X, Qiu D-Y, Yue Q-Y (2020) Two new species of *Episymploce* Bey-Bienko, 1950 (Blattodea, Ectobiidae, Blattellinae) from China. ZooKeys 954: 31–46. https://doi.org/10.3897/zookeys.954.49738

Abstract

Two new species of *Episymploce* Bey-Bienko from China are described. Nine individuals of *E. sichuanensis* **sp. nov**. were collected from Sichuan Province and four individuals of *E. maxima*, **sp. nov**. were collected from Guangxi Province. Morphology, especially the wings, specialized abdominal tergum and genitalia of adults, are described and illustrated in detail. *Episymploce sichuanensis* **sp. nov.** is similar to *E. kunmingi* (Bey-Bienko, 1969), but can be easily distinguished by the reduced wings, bifurcated two processes at the hind margin of the supra-anal plate, and the unspecialized first abdominal tergum (T1). *Episymploce maxima* **sp. nov.** is similar to *E. taiheizana* Asahina, 1979 but is distinguished by its large size, the latero-medial margins of the subgenital plate without processes, and the unspecialized T1. A key to the recorded *Episymploce* species from China is provided in this paper.

Keywords

Introduction

The genus *Episymploce* was established by Bey-Bienko in 1950, with the type species *E. paradoxura* Bey-Bienko, 1950, who later described three other new species, *E. marginata* Bey-Bienko, 1957, *E. popovi* Bey-Bienko, 1957, and *E. uncinata* Bey-Bienko, 1969. Princis (1969, 1971) recorded six species of *Episymploce*, five of which originated from China. In 1979, Asahina (1979) redescribed the Japanese species *E. amamiensis*

Asahina, 1977, reinterpreted the genus and described another two new species, *E. princisi* Asahina, 1979 and *E. taiheizana* Asahina, 1979. Asahina (1979) considered *Ischnoptera multiramosa* Karny, 1915, recorded by Karny and Shiraki, incompletely documented, while Princis (1969) pointed out a nomenclatural error and changed its name to *E. karnyi* Princis, 1969, but no detailed description was provided. Asahina (1979) renamed *E. karnyi* Princis, 1969 as *E. princisi* Asahina, 1979 and redescribed it. Roth (1985) then renamed *E. princisi* Asahina, 1979 to *E. asahinai* Roth, 1985 and redescribed the species again. Liu et al. (2017) also considered *E. karnyi* Princis, 1969 and *I. multiramosa* Karny, 1915 were synonyms of *E. asahinai* Roth, 1985. *Phyllodromia formosana* Shiraki, 1908 and *I. yoshinoe* Shiraki, 1931 from Taiwan were identified as subspecies of *E. formosana* (Shiraki, 1907) by Asahina (1979). Roth (1987d), Wang (2006) and Liu et al. (2017) considered *E. formosana formosana* (Shiraki, 1907) was a synonym of *E. formosana* (Shiraki, 1907).

Roth (1986) supplemented the genus and reclassified five species of *Symploce* as *Episymploce*. He considered that *E. taiwanica* (Bey-Bienko, 1969) was a synonym of *E. sundaica* (Hebard, 1929). Wang (2006) and Liu et al. (2017) agreed with Roth. Roth (1986) transferred six species of *Symploce* to *Episymploce*, and considered that *E. castanea* (Hanitsch, 1933) was a synonym of *E. ussuensis* Roth, 1985. Roth (1987a, 1987b, 1987c, 1987d) described 41 species of *Episymploce* from six countries, some being new records, of which 27 species and two subspecies were distributed in China, and a key to these Chinese species was provided.

Guo and Feng (1985) established *Asymploce* Guo & Feng, 1985, and recorded two new species, *Asymploce rubroverticis* Guo & Feng, 1985 and *A. hunanensis* Guo & Feng, 1985 from China, but Roth (1991) subsequently revised this genus, placing it as a synonym of *Episymploce*, and placed these two species into *Episymploce.* Roth (1997) transferred 16 species of *Symploce* to *Episymploce* based on the supra-anal plate. In 2003, Roth (2003) transferred *S. guizhouensis* Feng & Woo, 1988 and *S. mamillatus* Feng & Woo, 1988 from *Symploce* to *Episymploce.* Wang at al. (2005) described a new species *E. daozhenana* Wang & Feng, 2005 from Guizhou of China.

By now, there are more than 70 species of *Episymploce* recorded globally, of which 39 species are recorded in China (Beccaloni 2014); a key of the published 39 species and the two new species reported here is provided in this paper.

Materials and methods

On 6 April and 3 May 2014, the second author and another colleague collected specimens in Daheishan, Panzhihua County, Sichuan Province, and Nonggang Village, Longzhou County, Chongzuo City, Guangxi Province. The specimens were brought back to the laboratory for freezing, flattening of wings and limbs with parchment paper, pinning with needles, and drying for preservation. The tergum behind the seventh abdominal tergum (T7) of the male specimen was cut off, placed into a 1.5 ml centrifuge tube with 10% NaOH and digested at 70 °C for 30–45 min. After the digestion, NaOH was removed from the centrifuge tube, and the specimen was rinsed thrice

with water before examination. The specimens were dissected and observed under a ZEISS Discovery V12 stereo microscope. Photographs were taken with a ZEISS/Smart Zoom5 and Canon EOS 5D Mark III, and illustrated with Adobe Photoshop CC 2017 software. After illustration, the genitalia were stored in 0.5 ml centrifuge tubes containing 50% glycerol. The type specimens were deposited in Zhongshan Customs Technology Center.

The terminology used in this paper follows Roth (1977, 1979, 2003).

Taxonomy

Episymploce Bey-Bienko, 1950: 157.

Type species. *Episymploce paradoxura* Bey-Bienko, 1950: 157.

Diagnosis. According to the traits proposed by Bey-Bienko (1950), Asahina (1979) and Roth (1986), this genus can be described as follows: the tegmina and wings are fully developed. Wings cubitus anterior vein has 1–5 complete and 1–6 incomplete branches, and the triangular apical area is small, reduced or absent. The first abdominal tergum can be specialized or unspecialized; the seventh abdominal tergum is always specialized; right and left lateral plates of the ninth abdominal tergum are similar, or the size and shape are obviously different, and the apex can be with or without small spines. The supra-anal plate is asymmetrical, symmetrical, or approximately symmetrical, the apex of the posterior margin is invaginated, or slightly concave; the subgenital plate is asymmetrical. The anteroventral margin of the front femora is of Type A3, rarely Type B, or between Type A and Type B. The male left aedeagus is in the shape of a hook.

Distribution. China; Indonesia (Sumatra, Sulawesi, Java, Flores); Japan; India; Laos; Vietnam; Philippines; Thailand; Borneo Island; Nepal; Burma; Malaysia; Singapore; Australia; Papua New Guinea.

Remarks. We agree with Roth (1987d), Wang (2006) and Liu et al. (2017) that *E. taiwanica* (Bey-Bienko, 1969) is a synonym of *E. sundaica* (Hebard, 1929), and agree with Roth (1987d) and Liu et al. (2017) that *E. karnyi* Princis, 1969 is a synonym of *E. asahinai* Roth, 1985. We also agree with Asahina (1979), Roth (1987d), Wang (2006) and Liu et al. (2017) that *E. formosana formosana* (Shiraki, 1907) is a synonym of *E. formosana* (Shiraki, 1907). So, *E. taiwanica* (Bey-Bienko, 1969), *E. formosana formosana* (Shiraki, 1907) and *E. karnyi* Princis, 1969 were not be included in the key below. Forty-one species in *Episymploce*, including all published 36 species, three subspecies and two newly described species are included in this key, which is adapted from Roth (1987d).

Key to species of *Episymploce* from China (males)

1   Anteroventral margin of front femur Type A3, rarely intermediate between Type A and B..**2**
–   Anteroventral margin of front femur Type B3..**8**

2   Supra-anal plate symmetrical **3**
–   Supra-anal plate weakly asymmetrical or asymmetrical.............................**5**
3   Hind margin of supra-anal plate shallowly concave in middle and without papilla mesad **4**
–   Hind margin of supra-anal plate shallowly concave on the apex and with a minute papilla mesad...***E. asahinai* Roth, 1985**
4   Subgenital plate asymmetrical, styles simple, left and right lateromedial margins with spine-like processes. Left and right lateral plateral of T9 almost same length, ventral margins of both plates with 3 spines near apex............. ....***E. taiheizana* Asahina, 1979**
–   Subgenital plate asymmetrical, styles simple, left and right lateromedial margins without processes. Left and right plate plateral of T9 similar, ventral margins of both plates without spines ....***E. maxima* sp. nov.**
5   Supra-anal plate divided...**6**
–   Supra-anal plate undivided, ligulate ....***E. ligulata* Bey-Bienko, 1957**
6   Hind margin of subgenital plate with a U-or V-shaped excavation.............**7**
–   Hind margin of subgenital plate without a U-or V-shaped excavation.......**11**
7   Left lobe of supra-anal plate wider than right lobe, inner margin of supra-anal plate with a curved incision, inner margin apex with a small papilla ....***E. mamillatus* (Feng & Woo, 1988)**
–   Left lobe of supra-anal plate wider than right lobe, inner margin apex of supra-anal plate without papilla **8**
8   Left and right lateral plateral of T9 almost same length, posteroventral margins without spines ....***E. sundaica* (Hebard, 1929)**
–   Left and right lateral plateral of T9 not similar, posteroventral margins with spines...**9**
9   Basolateral of subgenital plate without spine-like process, right inner ventral margins with a strong spine ....***E. cheni* (Bey-Bienko, 1957)**
–   Basolateral of subgenital plate each with a spine-like processes **10**
10   Left thickened margin of subgenital plate produced transversely truncated, right style long and straight covered with dense hairs ....***E. subvicina* (Bey-Bienko, 1969)**
–   Left thickened margin of subgenital plate produced cylindrical, right style long and straight not covered with dense hairs.. ....***E. vicina* (Bey-Bienko, 1954)**
11   Left and right processes crossed of supra-anal plate hind margin..............**12**
–   Left and right processes uncrossed of supra-anal plate hind margin..........**14**
12   Left and right ventral margins of T9 without serrations **13**
–   Left ventral margins with tines, right ventral margins with or without serrations ....***E. Princisi* (Bey-Bienko, 1969)**
13   Left and right lateral plates of T9 with spines on ventral margin ....***E. malaisei* (Princis, 1950)**
–   Left lateral plate of T9 without spines on posteroventral margin, right lateral plate with or without spines...**15**

14   Ventral margins of T9 with a long spine. Hind margin apex of subgenital plate with a digitiform process ....*E. malaisei externa* **(Bey-Bienko, 1969)**
–   Ventral margins of T9 without spine. Hind margin apex of subgenital plate without process...................................*E. malaisei malaisei* **(Princis, 1950)**
15   Left and right lobes of supra-anal plate with equal width, right apex spine-like, left one round .... *E. dimorpha* **(Bey-Bienko, 1958)**
–   Left and right lobes of supra-anal plate not equal width............................**16**
16   Left and right processes of supra-anal plate joined **20**
–   Left and right processes of supra-anal plate separate.................................**17**
17   Hind margin of both lateral plates of T9 transversely truncated, ventral margins projecting posteriorly with spine-like processes or without processes..**18**
–   Hind margin of left lateral plate of T9 obliquely truncated, posteroventral angles of right plate with slight processes ..... *E. quarta* **(Bey-Bienko, 1969)**
18   Left thickened hind margin of subgenital plate spicular, right margin with an upright or curved hooklike style...**19**
–   Left thickened hind margin of subgenital plate strongly spinulose, right margin without upright style.............................*E. secunda* **(Bey-Bienko, 1957)**
19   Right margin of subgenital plate with a large and upright style .... *E. prima* **(Bey-Bienko, 1957)**
–   Right margin of subgenital plate with a large and curved hooklike style........ .... *E. tertia* **(Bey-Bienko, 1957)**
20   Left and right processes of supra-anal plate curved to the same side of ventral margin **23**
–   Left and right processes of supra-anal plate curved to different sides of ventral margin **21**
21   Middle with fleshy elevation of T7 with a pair of fossae on each side **22**
–   Middle without fleshy elevation of T7 with depressions on each side ....*E. unicolor* **(Bey-Bienko, 1958)**
22   Hind margin of supra-anal plate process on the middle part, chelate. Pronotum with black brown blotch....................... *E. tridens* **(Bey-Bienko, 1957)**
–   Hind margin of supra-anal plate crevice on the middle part, apex of both lobe with curved long spine-like processes, directed along hind margin. Pronotum front margin and disk black brown, lateral and hind margin yellowish-brown .... *E. hunanensis* **(Guo & Feng, 1985)**
23   Right plate of subgenital plate with an irregular lamellar formation ....*E. zagulajevi* **(Bey-Bienko, 1969)**
–   Right plate of subgenital plate without an irregular lamellar formation **24**
24   Left and right ventral margins of T9 apex with small spines **25**
–   Left and right ventral margins of T9 with long spine-like processes..........**27**
25   Hind margin of apex of supra-anal plate with two processes without bifurcate spine ....*E. kryzhanovskii* **(Bey-Bienko, 1957)**
–   Hind margin of apex of supra-anal plate with two processes with bifurcate spine **26**

26	Hind margin apex of supra-anal plate with two bifurcate processes ....
	E. sichuanensis **sp. nov.**
–	Hind margin of supra-anal plate with right process bifurcate, left process spine-like .... *E. kunmingi* **(Bey-Bienko, 1969)**
27	Left and right lateral plates of T7 with a small fossea. Right lobe of apex of supra-anal plate spine-like, left lobe broadly with an adpressed transverse spine ventrally near apex ....
	.... *E. spinosa* **(Bey-Bienko, 1969)**
–	Left and right lateral plates of T7 with a depression. Left and right lobes of supra-anal plate spine-like, left lobe with a long spine ventrally near apex ....
	....*E. longiloba* **(Bey-Bienko, 1969)**
28	Supra-anal plate divided in two.. **31**
–	Supra-anal plate not divided **29**
29	Middle of T7 with two fossea covered in hairs ....
	....*E. marginata* **Bey-Bienko, 1957**
–	Middle of T7 with a pair broad fossea without hair covering.................... **30**
30	Supra-anal plate semitubular, left margin apex with a long style, right margin near apex with a long style, basolateral with a process ....
	....*E. popovi* **Bey-Bienko, 1957**
–	Supra-anal plate weakly asymmetrical, triangular, left margin apex with two long styles, left and right basolateral without processes.................................
	.... *E. forficula* **(Bey-Bienko, 1957)**
31	Hind margin of subgenital plate with V-shaped excavation **32**
–	Hind margin of subgenital plate without V-shaped excavation **36**
32	Right lobe ventrally of supra-anal plate with an adpressed transverse spine...
	E. daozhenana **Wang & Feng, 2005**
–	Right and left lobe of supra-anal plate without spines **33**
33	Left and right lateral plates of T7 with a small fossea............................... **34**
–	Left and right lateral plates of T7 without fossea **35**
34	Left and right lateral plates basolateral of subgenital plate without processes, left plate terminating with a small spine, two styles long spine-like ....
	....*E. paradoxura* **Bey-Bienko, 1950**
–	Left and right lateral plates basolateral of subgenital plate with processes, left plate process is 2.5 times longer than the right plate process, left style curved hooks directed across left side of plate, right style straight spine-like obliquely directed across supra-anal plate ....
	.... *E. potanini* **(Bey-Bienko, 1950)**
35	Left and right lateral plates basolateral of subgenital plate with process, left plate thickened, terminating with a small spine, styles dissimilar, their bases widely separated..*E. hassenzana* **Roth, 1987**
–	Left and right lateral plates basolateral of subgenital plate with processes, left plate thickened, terminating without a small spine, both styles nearly touch-

ing basally, left style long spine-like, right style directed across right rear.......
....***E. paravicina* (Bey-Bienko, 1969)**

36   Left and right ventral margins of apex of T9 with spines..........................**37**
–   Left and right ventral margins of T9 directed to long spine-like processes....**39**
37   Hind margin near left corner of supra-anal plate with a larger deflexed spine-
      like process, left margin apex thickened, hind margin medially with a pair of
      minute filamentous processes...................***E. splendens* (Bey-Bienko, 1957)**
–   Hind margin of supra-anal plate each terminating with a spine-like deflexed
      process, left margin apex not thickened, hind margin medially without fila-
      mentous processes..**38**
38   Right and left lateral plates of T9 similar, hind margin transversely truncated,
      each with ventral margin terminating in a small spine..................................
      ....***E. formosana* (Shiraki, 1907)**
–   Left ventral margin of T9 with a small spine, right ventral margin without
      spine ....***E. formosana yoshinoe* (Shiraki, 1931)**
39   Upper base of both sides of supra-anal plate black brown. A red inverted pen-
      tagram marking is formed on vertex, ocular and antennal areas.....................
      .... ***E. rubroverticis* (Guo & Feng, 1985)**
–   Upper base of both sides of supra-anal plate not black brown. No red inverted
      pentagram marking present on the face..**40**
40   Left lateral plate of T9 with a narrow, apex spine-like, right plate short with
      a long, curved spine, not inserted in genital cavity. Pronotum with a pair of
      rust-chestnut spots.......................................***E. uncinata* Bey-Bienko, 1969**
–   Left lateral plate of T9 with a short spine-like, right plate with a long spine,
      inserted in genital cavity. Pronotum yellowish-brown ....
   .... ***E. guizhouensis* (Feng & Woo, 1988)**

Episymploce sichuanensis sp. nov.

http://zoobank.org/290ECF9F-4DA0-4EEF-9086-4AB258357B65
Figures 1–14

Specimens examined. *Holotype:* 1 male, 26°38.48'N, 101°41.62'E, Daheishan, Pan-zhihua City, Sichuan Province, 6 April 2 014, coll. Ke-Liang Wu et De-Xing Liu. *Allotype:* 1 female, *paratype*: 7 males, allotype and paratype were collected together with holotype.

    Diagnosis. This species is similar to *E. kunmingi* (Bey-Bienko, 1969), but can be distinguished as follows: 1) tegmina and wings reduced, only reaching the second abdominal tergum (T2), while in *E. kunmingi* (Bey-Bienko, 1969) tegmina and wings reach the apex of abdomen; 2) T1 is unspecialized, whereas T1 is specialized in *E. kunmingi* (Bey-Bienko, 1969); 3) two inwardly curved bifurcate processes on the hind margin of the supra-anal plate, while in *E. kunmingi* (Bey-Bienko, 1969) right process bifurcate and left process spine-like.
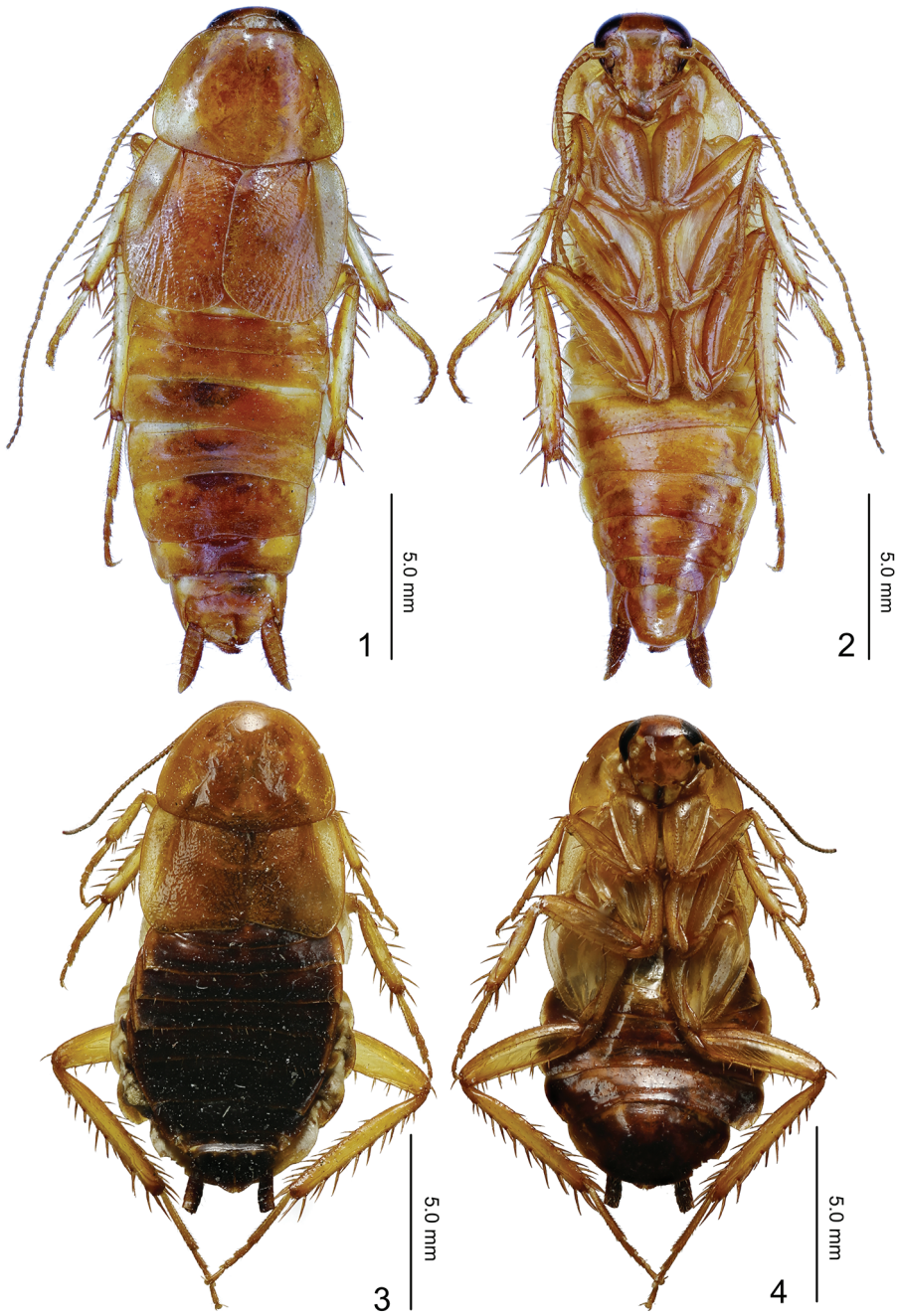
Figures 1–4. *Episymploce sichuanensis* sp. nov. **1** male, dorsal view **2** male, ventral view **3** female, dorsal view **4** female, ventral view.
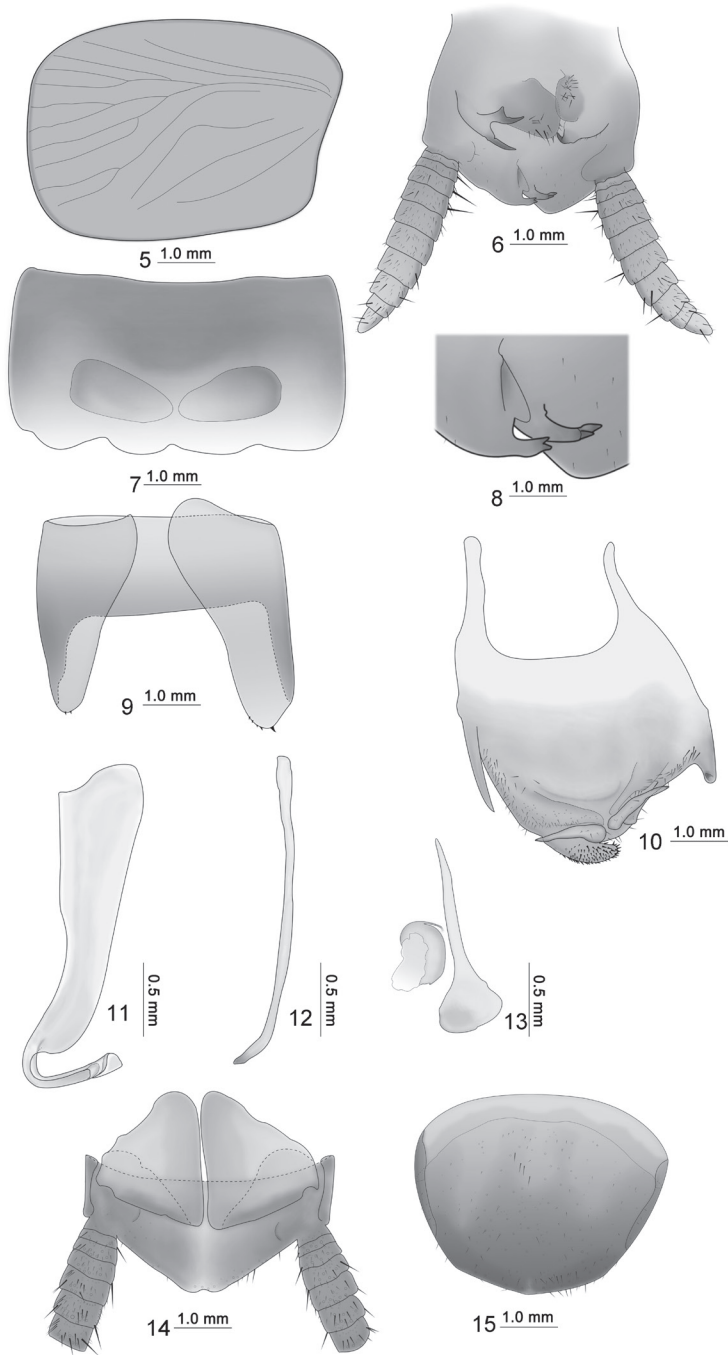
Figures 5–15. *Episymploce sichuanensis* sp. nov. **5** tegmen **6** male, supra-anal plate and paraprocts, ventral view **7** male, T7, dorsal view **8** male, bifurcate process of the supra-anal plate **9** male, T9, ventral view **10** male, subgenital plate, dorsal view **11** male, left aedeagus **12** male, median aedeagus **13** male, right aedeagus **14** female, supra-anal plate and paraprocts, ventral view **15** female, subgenital plate, ventral view.

Description. Male, pronotum: length × width: 2.8–3.0 × 3.8–4.4 mm; tegmen: 3.5–4.0 mm; overall length (including tegmen): 16.2–17.9 mm. Female, pronotum: length × width: 3.2 × 5.0 mm; tegmen: 3.8 mm; overall length (including tegmen): 14.4 mm.

Small size. Body yellowish orange, head extending somewhat beyond pronotum, ocellus white, interocular space almost equivalent to ocellus space. Pronotum approximate ladder-like, hind margin wide. Tegmina and wings reduced, veins inconspicuous, reaching of T2. Anteroventral margin of front femur Type A3; the first tarsus of the hind leg longer than the sum of the remaining tarsi; tarsal claws symmetrical and unspecialized, arolium and pulvillus present. The T1 unspecialized; T7 specialized with a pair of approximately triangular depressions (Fig. 7); T9 asymmetrical with left side longer than right, apex margin with some small spines (Fig. 9). Male supra-anal plate asymmetrical, hind margin of lamina bilobed, left hind margin has two inwardly curved processes, apex process of which is bifurcate (Figs 6, 8); left side paraproct with three processes and right side with single process. Subgenital plate asymmetrical, basolateral with two processes, left process longer, and apex of right process curved; left of hind margin apparently thicker and covered strongly spinulose, middle hind margin with two spine-like processes reversed and outwardly with long styles (Fig. 10); left aedeagus hook-shaped (Fig. 11). Female is similar to male; abdominal tergum suffused with dark brown, supra-anal plate symmetrical, approximately triangular, apex concave (Fig. 14). Subgenital plate simple and hind margin rounded (Fig. 15).

Etymology. Species name *sichuanensis* refers to the type locality.

Distribution. China (Sichuan).

Episymploce maxima sp. nov.

http://zoobank.org/4C780B62-095A-48CD-9765-C7BD7EEAA95C

Figures 16–30

Specimens examined. *Holotype:* 1 male, 22°28.26'N, 106°57.43'E, Nonggang Village, Longzhou County, Chongzuo City, Guangxi Province, 3 May 2014, coll. Ke-Liang Wu et De-Xing Liu. *Allotype:* 1 female, *paratype:* 1 male, 1 female, all speciemens were collected at the same place at the same time.

Diagnosis. This species is similar to *E. taiheizana* Asahina, 1979, but can be distinguished as follows: 1) lateromedial margins of subgenital plate without processes, while with processes in *E. taiheizana* Asahina, 1979; 2) T1 was unspecialized, but T1 was specialized in *E. taiheizana* Asahina, 1979; 3) ventral margins of T9 without spines, but with 3 spines in *E. taiheizana* Asahina, 1979.

Description. Male, pronotum: length × width: 5.2–6.0 × 6.0–6.5 mm; tegmen: 23.5 mm; overall length (including tegmen): 27.8–28.5 mm. Female, pronotum: length × width: 5.5–6.6 × 6.0–6.6 mm; tegmen: 23.4 mm; overall length (including tegmen): 27.8–29.5 mm.
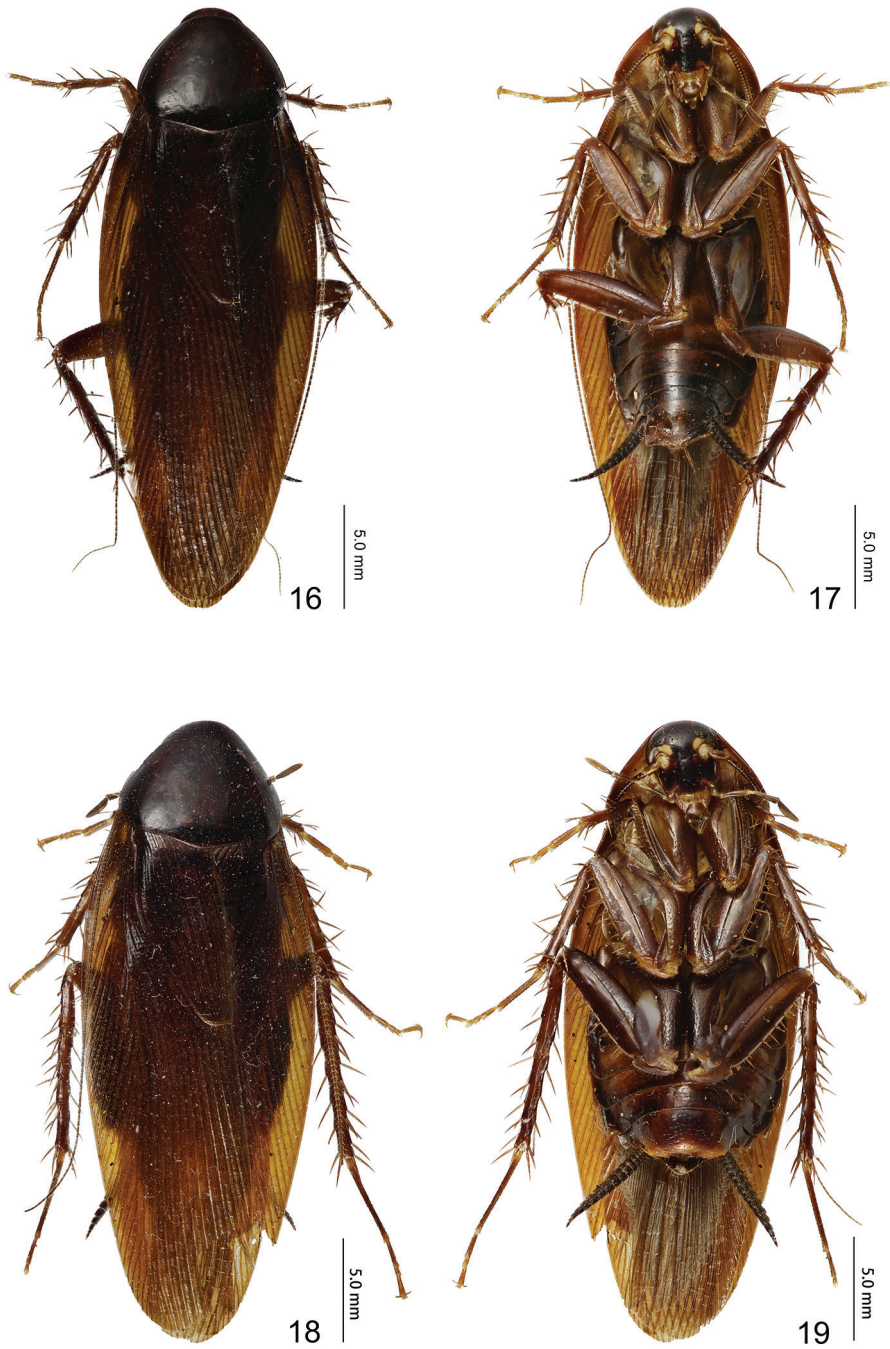
Figures 16–19. *Episymploce maxima* sp. nov. **16** male, dorsal view **17** male, ventral view **18** female, dorsal view **19** female, ventral view.
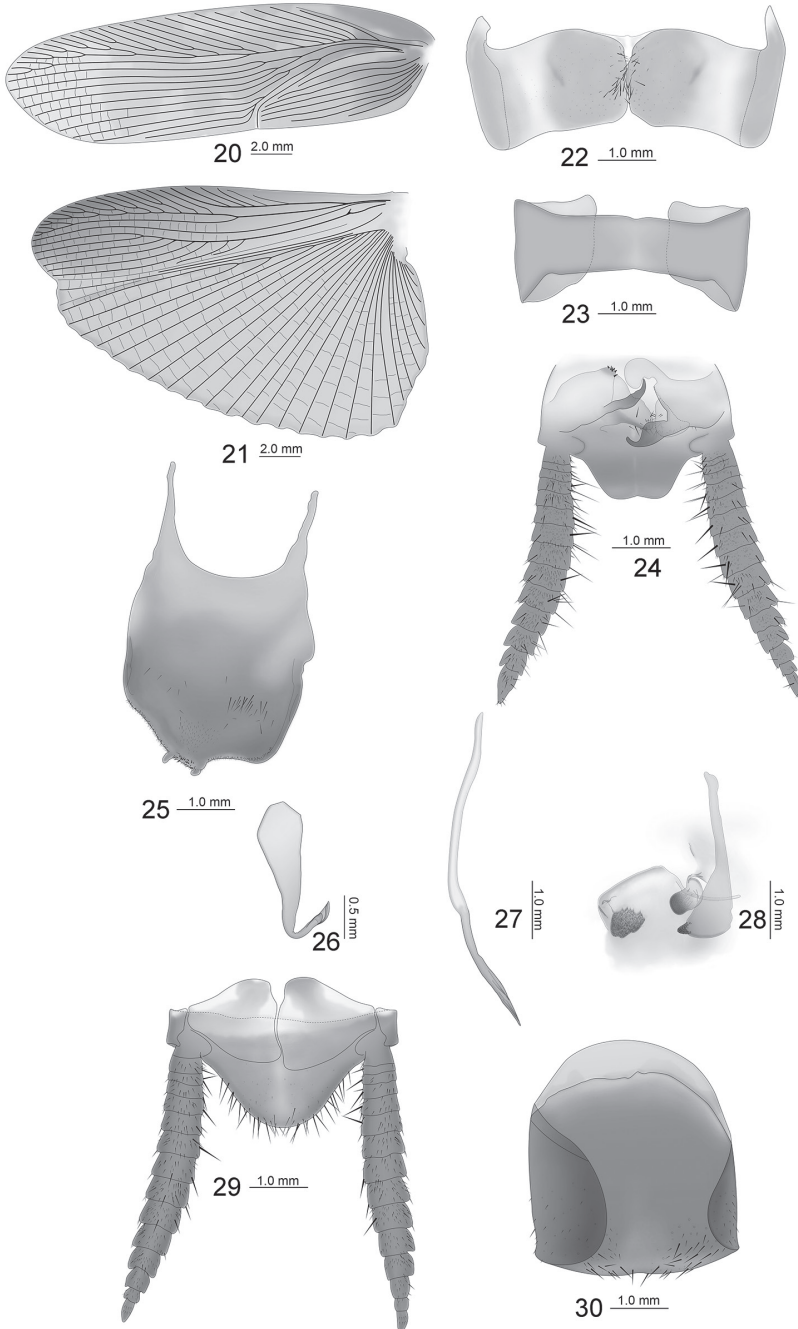
Figures 20–30. *Episymploce maxima*, sp. nov. **20** tegmen **21** hind wing **22** male, T7, dorsal view **23** male, T9, dorsal view **24** male, supra-anal plate and paraprocts, ventral view **25** male, subgenital plate, dorsal view **26** male, left aedeagus **27** median aedeagus **28** male, right aedeagus **29** female, supra-anal plate and paraprocts, ventral view **30** female, subgenital plate, ventral view.

Large size. Body dark brown, head extending beyond the pronotum, vertex tawny, ocellus yellow, face dark brown, interocular space is 3/4 of ocellus space, antenna base dark brown, a pair of symmetrical reddish-brown dots next to the antenna sockets, antenna sockets slightly wider than ocellus width. Pronotum approximate triangular, hind margin wide, dark brown. Tegmina and wings fully developed, tegmina extending beyond the end of abdomen; hind wing with radius vein branched near middle; medial vein simple; cubitus anterior vein with five complete and two incomplete branches, triangular apical area small. Anteroventral margin of front femur Type A3; the first tarsus of the hind leg longer than the sum of the rest tarsi; tarsal claws symmetrical and unspecialized, arolium and pulvillus present. The T1 unspecialized; T7 specialized with numerous hairs in the intermediate region (Fig. 22); right and left lateral plates of the T9 are similar, hind margins truncate, posterior corners rounder (Fig. 23). Male supra-anal plate symmetrical, middle of the hind margin concave (Fig. 24); subgenital plate asymmetrical, two styles on the left side of the hind margin, with some spines in the interstylar margin (Fig. 25); left aedeagus hook-shaped (Fig. 26); median aedeagus exposed, extending beyond the supra-anal plate, spicular (Fig. 27). Female similar to male; supra-anal plate and subgenital plate symmetrical, hind margin round, apex with small concavity (Figs 29, 30).

Etymology. Species name *maxima* refers to its large size, currently the largest species in *Episymploce*.

Distribution. China (Guangxi).

Discussion

The genus *Symploce* was established before the genus *Episymploce*, but it turned out that many species from other genera of cockroaches were included (Roth 1984). In 1950, Bey-Bienko (1950) established the genus *Episymploce*, and pointed out the difference between *Episymploce* and *Symploce* in the hind wings, the irregularly branched radial of the tegmina, and the conversion of the hind lateral processes of the T9 into spines. Subsequently, Asahina (1979) redefined *Episymploce* and dissected the male genitalia in detail, providing more reliable features for distinguishing *Symploce* from *Episymploce*. Roth (1986) considered that Bey-Bienko put too much emphasis on wing venation when distinguishing *Episymploce* from *Symploce*. He considered that the wing venation could not be used to distinguish *Episymploce* from *Symploce*, and suggested the symmetry of the supra-anal plate should be considered. He transferred *E. marginata* Bey-Bienko, 1957, *E. popovi* Bey-Bienko, 1957 and *E. ligulata* Bey-Bienko, 1957 to *Symploce*. In 1984 and 1986, Roth (1984, 1986) respectively collated and supplemented the characteristics of the abdominal tergum, wing venation, anteroventral margin of front femur, and supra-anal plate to distinguish *Symploce* from *Episymploce*. More specializations of the male abdominal tergum were observed in *Symploce* than in *Episymploce*. In 1997, Roth rejected that symmetry of the supra-anal plate distinguished between *Episymploce* and *Symploce*, and returned *E. marginata* Bey-Bienko, 1957, *E. popovi*

Bey-Bienko, 1957 and *E. ligulata* Bey-Bienko, 1957 to *Episymploce*. We do not think it is appropriate to distinguish one genus from another only by a single feature as there are many similarities between the characteristics of *Episymploce* and *Symploce*.

In 1985, Roth (1985) compared the characteristics of *Blattella*, *Symploce*, *Parasymploce* and *Episymploce*. He considered that the difference between *Parasymploce* and the other three is that the supra-anal plate is symmetrical and the T7 was always specialized. Roth (1995) considered *Aristiger* and *Parasymploce* were synonyms of *Hemithyrsocera*. The supra-anal plate of *E. sichuanensis* sp. nov. is asymmetrical, which is obviously different from *Hemithyrsocera*. *Episymploce maxima* sp. nov. has similar features to *Hemithyrsocera* on the supra-anal plate and T7, but *E. maxima* sp. nov. has 5 complete and 2 incomplete branches in the cubitus anterior vein of the hind wing, while the cubitus anterior vein of the hind wings of *Hemithyrsocera* have no branches or 1–3 complete branches, and no incomplete branches. The supra-anal plate of *E. sichuanensis* sp. nov. is asymmetrical and T1 unspecialized, T7 and T9 are specialized. In the diagnosis of *Symploce* (Roth, 1984), the supra-anal plate was described as symmetrical, rarely asymmetrical, and T7 and T9 without specialization at the same time. *Episymploce maxima* sp. nov. was similar to the genus *Symploce* in regard to the supra-anal plate, but the subgenital plate of *Symploce* has a highly specialized style, while the subgenital plate of *E. maxima* sp. nov. has a simple style and T1 is unspecialized, T7 specialized, and the left and right plate of T9 are similar. We think that these two new species do not agree with the characteristics of *Symploce* and *Hemithyrsocera*, whereas they do agree with the characteristics of the genus *Episymploce*.

Acknowledgements

References

Asahina S (1979) Taxonomic notes on Japanese Blattaria. XII. the species of the tribe Ischnopterites, II (ind. Taiwanese species). Japanese Journal Sanitary Zoology 30(4): 335–353. https://doi.org/10.7601/mez.30.335

Beccaloni G (2014) Cockroach Species File Online. Version 5.0/5.0. https://Cockroach.SpeciesFile.org/ [accessed 11 July 2014]

Bey-Bienko GY (1950) Fauna of the USSR. Insects. Blattodea. Trudy Zoologicheskogo Instituta Akademiya Nauk SSSR 40: 1–344.

Bey-Bienko GY (1957) Blattodea of Szechuan and Yunnan. Communication I. The results of the Chinese-Soviet zoologico-botanical expeditions to southwestern China 1955–1956. Entomologicheskoe Obozrenie 36(4): 895–915.

Bey-Bienko GY (1969) New genera and species of cockroaches (Blattoptera) from tropical and subtropical Asia. Entomologicheskoe Obozrenie 48(4): 831–862.

Feng PZ, Woo FZ (1988) Three New Species and Two New Records of Blattaria From Yunnan and Guizhou, China. Entomotaxonomia 10(3–4): 305–312.

Guo YY, Feng PZ (1985) Descriptions of one new genus and two new species of Blattellidae (Blattodea). Entomotaxonomia 7(4): 333–336.

Hebard M (1929) Studies in Malayan Blattidae (Orthoptera). Proceedings of the Academy of Natural Sciences of Philadelphia 81: 1–109.

Liu XW, Zhu WB, Dai L, Wang HQ (2017) Cockroaches of southeastern China. Henan Science and Technology Press, Zhengzhou, 118–135.

Princis K (1969) Blattariae: Subordo Epilamproidea. Fam. Blattellidae. In: Beier M (Ed.) Orthopterprum Catalogus part 13: 713–1038.

Princis K (1971) Blattariae, Subordo Epilamproidea. Fam. Blattellidae. In: Beier M (Ed.) Orthopterprum Catalogus part 14: 1039–1224.

Roth LM (1977) A taxonomic revision of the Panesthiinae of the world I. The Panesthiinae of Australia (Dictyoptera: Blattaria: Blaberidae). Australian Journal of Zoology Supplementary Series 25(48): 1–122. https://doi.org/10.1071/AJZS048

Roth LM (1979) A taxonomic revision of the Panesthiinae of the world II. The genera *Salganea* Stål, *Microdina* Kirby, and *Caeparia* Stål (Dictyoptera: Blattaria: Blaberidae). Australian Journal of Zoology Supplementary Series 27(69): 1–201. https://doi.org/10.1071/AJZS069

Roth LM (1984) The genus *Symploce* Hebard. I. Species from the West Indies. (Dictyoptera: Blattaria: Blattellidae). Entomologica Scandinavica 15(1): 25–63. https://doi.org/10.1163/187631284X00046

Roth LM (1985) A taxonomic revision of the genus *Blattella* Caudell (Dictyoptera, Blattaria: Blattellidae). Entomologica Scandinavica Supplement 22(1): 1–221.

Roth LM (1986) The genus *Episymploce* Bey-Bienko. I. Species chiefly from Java, Sumatra and Borneo (Kalimantan, Sabah, Sarawak). (Dictyoptera, Blattaria, Blattellidae). Entomologica Scandinavica 16(4): 355–374. https://doi.org/10.1163/187631285X00333

Roth LM (1987a) The genus *Episymploce* Bey-Bienko. III. Species from Laos, North and South Vietnam and Thailand. (Dictyoptera: Blattaria, Blattellidae). Entomologica Scandinavica 17(4): 455–474. https://doi.org/10.1163/187631286X00044

Roth LM (1987b) The genus *Episymploce* Bey-Bienko. IV. Species from India. (Dictyoptera: Blattaria, Blattellidae). Entomologica Scandinavica 18(2): 111–123. https://doi.org/10.1163/187631286X00378

Roth LM (1987c) The genus *Episymploce* Bey-Bienko. V. Species from China. (Dictyoptera: Blattaria, Blattellidae). Entomologica Scandinavica 18(2): 125–141. https://doi.org/10.1163/187631286X00378

Roth LM (1987d) The genus *Episymploce* Bey-Bienko. VI. Species from Taiwan and the Japanese Islands. (Dictyoptera: Blattaria, Blattellidae). Entomologica Scandinavica 18(2): 143–153. https://doi.org/10.1163/187631286X00378

Roth LM (1991) New combinations, synonymies, redescriptions, and new species of cockroaches, mostly Indo-Australian Blattellidae. Invertebrate Taxonomy 5(5): 953–1021. https://doi.org/10.1071/IT9910953

Roth LM (1995) The cockroach genera *Hemithyrsocera* Saussure, and *Symplocodes* Hebard (Dictyoptera: Blattellidae: Blattellinae). Invertebrate Taxonomy 9(5): 959–1003. https://doi.org/10.1071/IT9950959

Roth LM (1997) The cockroach genera *Pseudothyrsocera* Shelford, *Haplosymploce* Hanitsch, and *Episymploce* Bey-Bienko (Blattaria: Blattellidae, Blattellinae). Tijdschrift Voor Entomologie 140: 67–110.

Roth LM (2003) Systematics and Phylogeny of cockroaches (Dicty: Blattaria). Oriental Insects 37: 1–186. https://doi.org/10.1080/00305316.2003.10417344

Shiraki T (1908) Neue Blattiden und Forficuliden Japans. Trans. Sapporo. Nat. Hist. Soc., 2: 103–111.

Shiraki T (1931) Orthoptera of the Japanese Empire II. Blattidae. Insecta Mattsumrana 5(4): 171–209.

Wang ZQ, Song QZ, Feng PZ (2005) Blattodea: Blattidae, Blattellidae. In: Yang MF, Jin DC (Eds) Insects from Dashahe Nature Reserve of Guizhou. Guizhou People Press, Guiyang, Guizhou, 47–50.

Wang ZQ (2006) The Taxonomic study and Phylogeny of Blattellidae from China. PhD Dissertation, Beijing, Chinese Academy of Agricultural Sciences.

RESEARCH ARTICLE

Description of *Neoperla mindoroensis* sp. nov., the first record of a stonefly from Mindoro, Philippines (Plecoptera, Perlidae), and identification of its life stages using COI barcodes

Arthien Lovell Pelingen[1], Hendrik Freitag[1]

1 *Department of Biology, School of Science and Engineering, Ateneo de Manila University, Quezon City, Philippines*

Corresponding author: *Arthien Lovell Pelingen* (arthien.pelingen@obf.ateneo.edu)

Citation: Pelingen AL, Freitag H (2020) Description of *Neoperla mindoroensis* sp. nov., the first record of a stonefly from Mindoro, Philippines (Plecoptera, Perlidae), and identification of its life stages using COI barcodes. ZooKeys 954: 47–63. https://doi.org/10.3897/zookeys.954.53746

Abstract

The new stonefly species, *Neoperla mindoroensis* **sp. nov.** (Perlidae), from Mindoro island is described. The new species is assigned to the *N. recta* species complex of the *N. montivaga* group on account of its obvious T7 and T8 with pointed processes and the presence of basolateral lobes in the everted aedeagal sac. The male adult is distinguishable by its aedeagus with a slightly raised mediodorsal lobe, fully covered with fine spinules, while the female adult has comparably small eggs (240 × 220 μm) with a punctate, chorionic surface with punctae arranged in polygonal FCIs. The life stages and sexes were assigned using COI mtDNA barcodes (2.2% maximum intraspecific genetic distance), which were compared with available barcodes of congeners, which had interspecific genetic distances varying by at least 23.5%. Biogeographic aspects, ecological habitat requirements, and suitability as potential bioindicator of the species are also briefly discussed.

Keywords

DNA barcode, integrative taxonomy, Mt Hinundungan key biodiversity area, new species

Introduction

Plecoptera (stoneflies) is a basal, aquatic order of Neopteran insects known for their intolerance to organic pollution (Fochetti and Tierno de Figueroa 2008). Their presence and abundance are important in rapid assessments of water quality in freshwater ecosystems, especially rivers and streams, as the order occurs worldwide, except in Antarctica (DeWalt and Ower 2019).

One of the most diverse stonefly genera in the Oriental Realm and Southeast Asia is *Neoperla* Needham, 1905. In fact, in the Philippines alone, there are already 23 recorded *Neoperla* species even if these are only known from few major islands (Jewett 1958; Kawai 1969; Sivec 1984; Zwick 1986; Sivec and Stark 2011; Dela Cruz et al. 2018) and have not been comprehensively sampled yet. Interestingly, some closely related species occur syntopically (Sivec 1984).

Usually, only the male adult stages of stoneflies were formally described from the Philippines (Zwick 1982, 1986; Sivec 1984; Sivec and Stark 2011). Conspecificity with female adults and nymphs were ambiguous due to a lack of material or suitable matching tools, which made it difficult to use them as bioindicators in freshwater assessments. In recent decades, DNA barcoding has increasingly been used in associating life stages of aquatic insects with their adults (Freitag 2013; Dela Cruz et al. 2016; Garces et al. 2018). For the first time, a new set of modified primers is applied here to Philippine Plecoptera.

This study focuses in the Baroc River Catchment, which is in the Key Biodiversity Area "69 Hinunduang Mt." (*sensu* Ong et al. 2002) on Mindoro island. Here, several interesting aquatic insects have been discovered during the comprehensive assessment of the Ateneo Biodiversity Laboratory (Freitag 2013; Mey and Freitag 2013; Komarek and Freitag 2014; Vidal et al. 2017; Garces et al. 2018). This study also aims to address the lack of taxonomic studies of stoneflies from this biogeographically interesting island, where no stonefly records have been known until now, and specifically to describe one new *Neoperla* species based on male and female adults along with the associated nymphs identified by COI mtDNA barcodes.

Methods

As part of a freshwater biodiversity assessment project, the stonefly fauna of the Baroc River Catchment, Roxas, Oriental Mindoro, was sampled in 2018–2019. Nymphs were collected by manual collection from rock surfaces, submerged wood, and trapped leaf packs in riffle sections of the Baroc River and its tributaries, while the adults were collected by the use of black-light traps and emergence traps as described by Freitag (2004). The collections were preserved in 95% ethanol and stored at –20 °C at the Biodiversity Laboratory, Ateneo de Manila University until scientific treatment. The following codes were used to identify the sampling sites (all belong to the Baroc River System and are within the area of Barangay San Vicente, Roxas Municipality, Oriental

Mindoro, the Philippines); maps indicating collections sites and notes are provided by Mey and Freitag (2013: 301) and Vidal et al. (2017: 2–5):

HBT: Quirao Buhay Creek tributary Tagugoy Creek, disturbed secondary forest; ca 12°36'30"N, 121°22'38"E, 200 m a.s.l.

HOC: Hinundungan River tributary Quianao Creek, secondary forest; ca 12°35'20"N, 121°21'40"E, 280 m a.s.l.

HR3:   upper Hinundungan River, secondary forest; ca 12°35'10"N, 121°21'36"E, 280 m a.s.l.

TBC: Taugad Daka River tributary Batuwayang Creek, secondary forest; ca 12°38'09"N, 121°19'45"E, 490 m a.s.l.

TDR1:   Taugad Daka River near Sitio Taugad Diit, rural extensive farmland and secondary vegetation; ca 12°37'33"N, 121°21'18"E, 180 m a.s.l.

TDR3:   upper Taugad Daka River, secondary forest; ca 12°38'05"N, 121°19'33"E, 530 m a.s.l.

THC: Taugad River tributary Hiyong Creek, rural extensive farmland and secondary vegetation; ca 12°37'27"N, 121°22'48"E, 147 m a.s.l.

TIR: Taugad Diit River near Sitio Taugad Diit, rural extensive farmland and secondary vegetation; ca 12°37'32"N, 121°22'17"E, 180 m a.s.l.

TR2:   Taugad River downstream Sitio Taugad Diit, secondary vegetation; ca 12°37'18"N, 121°22'58"E, 140 m a.s.l.

The external morphology of the specimens was studied under a Leica EZ4 stereomicroscope. The cold maceration technique (Zwick 1982) was employed to properly observe the aedeagus. The aedeagus, aedeagal sac, female inner genitalia, and the nymphal mouthparts were examined as wet mounts on microscopic slides under an Olympus CX21 compound microscope. Digital imaging of dissected parts was done using these microscopes with a DinoEye Eyepiece camera, then stacked using CombineZP software (Hadley 2010). The female inner genitalia were drawn in Adobe Illustrator 2020. The images of habitus and male terminalia were produced using a Canon EOS 650D and a Canon EOS 6D, respectively, with macro lens and a stack rack operated by Helicon Remote, and then stacked using Helicon Focus. Stacked images were enhanced with Adobe Lightroom and Adobe Photoshop 2020. Preparation of eggs was done following the procedure of Sivec et al. (1988) and examined and photographed using a Hitachi TM-1000 Table Top Scanning Electron Microscope (SEM) at the Materials Physics Laboratory, Ateneo de Manila University. Terminologies follow Murányi et al. (2015).

All type material is stored in alcohol and has been deposited at the Museum of Natural History of the National Museum of the Philippines, Manila, Philippines (**NMP**); Biodiversity Laboratory, Ateneo de Manila University, Quezon City, Philippines (**AdMU**); Collection Arthien Pelingen, Philippines (**CAP**), currently deposited in AdMU; Museum für Naturkunde Berlin, Germany (**ZMB**).

DNA was extracted from the legs using Qiagen DNeasy kit (Qiagen, Hilden, Germany) following the protocol for animal tissues (Qiagen 2002). The 5'-end of the

Table 1. GenBank accession numbers of DNA sequences, geographical origins, collection sites, and sample references of specimens. External data are indicated by superscript numbers: [1]Dela Cruz et al. 2018; [2]Pilgrim et al. 2011.

Species	Locality	Stage	Voucher	Genbank accession number	GenSeq nomenclature
Neoperla mindoroensis sp. nov.	Mindoro	nymph	PL21	MT547994	genseq-2 COI
	Mindoro	♀ adult	PL22	MT547995	genseq-2 COI
	Mindoro	♂ adult	PL50	MT547996	genseq-1 COI
Neoperla obliqua	Mindanao	♂ adult		KT307712[1]	
	Mindanao	♀ adult		KT307713[1]	
Neoperla clymene	USA			JN200655[2]	

cytochrome c oxidase subunit I (COI) region was then amplified using the primers LCO1490_mod (5'-TTTCAACAAACCATAAGGATATTGG-3') and HCO2198_mod (5'-TAAACTTCAGGATGRCCAAAAAATCA-3') (Garces et al. 2018). In a 25 µl Polymerase Chain Reaction (PCR) mix, it includes 17.8 µl ddH$_2$O, 2.5 µl 10× buffer, 1 µl Mg (25 mM), 0.5 µl dNTP mix (10 mM), 0.5 µl of each primer (10 mM), 0.2 µl Taq Polymerase (NEB), and 2 µl template DNA of unknown concentration. The PCR program was set as follows: 180 s at 94 °C; 30 s at 94 °C, 30 s at 47 °C, 60 s at 72 °C (× 35 cycles); 300 s at 72 °C. The amplification success was then checked in a 1.5% agarose gel using gel electrophoresis. The successfully amplified PCR products were sent to MACROGEN for cleaning and sequencing. The forward and reverse sequences were then manually traced and aligned (CLUSTALW) using BIOEDIT v. 7.2.5 (Hall 1999) along with the corresponding partial COI sequences of *Neoperla clymene* (Newman, 1839) and *Neoperla obliqua* Banks, 1913 retrieved from GenBank as seen in Table 1 (Pilgrim et al. 2011; Dela Cruz et al. 2018). A statistical parsimony analysis was conducted with TCS (Clement et al. 2002), and the haplotype network was visualized using POPART v. 1.7 (Leigh and Bryant 2015) and edited in Adobe Illustrator 2020.

The pairwise genetic distance analysis was performed in MEGA 7 (Kumar et al. 2016) using Kimura-2-parameter (K2P) model with bootstrap method in 1000 replicates.

Taxonomy

Neoperla mindoroensis sp. nov.
http://zoobank.org/22178DC3-B257-48B3-BDED-3193FFDF7F4F

Type locality. Philippines • Oriental Mindoro, Municipality of Roxas, Barangay San Vicente: Quirao Buhay Creek tributary Tagugoy Creek; secondary forest, ca 12°36'30"N, 121°22'38"E, ca 200 m asl.

Material. *Holotype*: 1 ♂ adult (NMP), labelled "PHIL: Or[iental]. Mindoro, Roxas, Brgy. San Vicente, Quirao \ Buhay tributary, Tagugoy Creek; secondary forest; \ 12°36'30"N, 121°22'38"E 200 m a.s.l.; leg. AL Pelingen, \ C Pangantihon, H Freitag 05 Feb. 2018 (HBT)L", preserved in a cryovial with 95% ethanol, right hindleg and

all left legs missing as used for DNA extraction (PL50), both cerci partially broken, tips of wings partially broken, dissected aedeagus stored inside the same vial. **Paratypes:** Philippines • 1 ♂ adult; HBT E; 12 Aug.–21 Sept. 2018; leg. Freitag & Pangantihon; NMP; left midleg and hindleg missing, both cerci partially broken, dissected aedeagus stored inside the same vial • 1 ♂ adult; HR3 E; 15 Jan.–17 Feb. 2019; leg. Pangantihon; ZMB; both cerci partially broken, dissected aedeagus stored inside the same vial • 1 ♀ adult; TDR1 L; 08 May 2018; leg. Freitag and Pangantihon; NMP; right legs used for DNA extraction (PL22), both cerci partially broken, eggs used for SEM • 1 ♂ nymph; TDR1f; 22 Sept. 2019; submerged wood in run; leg. Freitag and Pangantihon; AdMU; dissected mouth parts stored in the same vial • 1 ♀ nymph; TDR3f; 08 Feb. 2018; submerged wood in run; leg. Freitag; NMP; left midleg and hindleg used for DNA extraction (PL21); left foreleg broken but stored in the same vial, both cerci partially broken • 1 ♂ adult; TDR3/TBC L; 08 May 2018; leg. Freitag & Pangantihon; CAP-AdMU; right and left midlegs broken but stored inside the same vial, both cerci partially broken, dissected aedeagus stored inside the same vial • 1 ♀ adult; TDR3/TBC L; 08 May 2018; leg. Freitag & Pangantihon; AdMU; left hindleg missing, both cerci partially broken, right forewing broken but stored in the same vial • 1 ♀ adult; THC E; 19 Nov.–02 Dec. 2018; leg. Freitag; ZMB; both cerci broken • 1 ♂ adult; TIR E; 24 Jan.–16 Feb. 2018; leg. Pangantihon; ZMB; right cercus partially broken, dissected aedeagus stored inside the same vial • 1 ♂ adult; TIR E; 24 Jan.–16 Feb. 2018; leg. Freitag; AdMU; left hindleg missing, both cerci partially broken, tips of wings partially broken, dissected aedeagus stored inside the same vial • 1 ♀ adult; TR2 L; 11 Aug. 2019; leg. Freitag; ZMB; both cerci partially broken • 1 ♀ adult; TR2 L; 11 Aug. 2019; leg. Freitag & Pangantihon; NMP; left midleg missing, both cerci partially broken • 1 ♂ adult; TR2 E; 22 Dec. 2018–15 Jan. 2019; leg. Freitag & Pangantihon; AdMU; right midleg broken but stored in the same vial, both cerci partially broken, wings damaged, dissected aedeagus stored inside the same vial. **Other Material:** Philippines • 1 ♂ larva; HOCg; 16 Jan. 2019; rock surface in riffle, leg. Freitag; AdMU; right hindleg missing, both cerci partially broken • 1 ♀ larva; TIRd; 22 Sept. 2019; leaf pack in riffle; leg. Freitag and Pangantihon; AdMU; both cerci partially broken • 1 ♂ larva; TIRd; 22 Sept. 2019; leaf pack in riffle; leg. Freitag and Pangantihon; CAP-AdMU; segments IX and X including cerci missing • 4 ♀ adults; TR2 E; 19 Nov.–02 Dec. 2018 leg. Freitag; AdMU; some legs missing and all cerci partially broken • 3 ♀ adults; TR2 E; 22 Dec. 2018–15 Jan. 2019; leg. Freitag & Pangantihon; AdMU; some legs missing and all cerci partially broken.

Description. *Imago:* Medium-sized species (Fig. 1). Forewing length of holotype male: 14 mm, paratype males: 14–18 mm, paratype females: 16–18 mm. General color pale with dark patterns. Ocelli relatively of the same size in both male and female; distance between ocelli more than its diameter in male, less than its diameter in female. Head predominantly pale; dark mottling present posterior of ocelli; with two triangular, dark-brown patches anterior of ocelli and another patch near anterior of head delimiting a pale but distinct M-line. Antenna and palpi slightly darker than head. Pronotum trapezoidal, narrower than head with eyes; anterior edges slightly angled; ground color brown

Figure 1. Paratype male adult habitus of *Neoperla mindoroensis* sp. nov. Scale bar: 2.00 mm.

with distinct yellow rugosities and with medial, longitudinal, brown stripe and dark, transverse anterior and posterior lines. Meso- and metanotum pale brownish. Legs yellow; tibia darker than the rest of the legs. Wings hyaline, nearly transparent; veins brown.

Male terminalia (Fig. 2A): Sterna and terga 2–6 simple. Posterior process of tergum 7 with large, median hump associated with sparsely arranged and long setae, and sensilla basiconica on its hump. Tergum 8 with distinct medial process, strongly curved anteriorly like a hook, bearing dense sensilla basiconica. Tergum 9 simple, with irregular, sparse
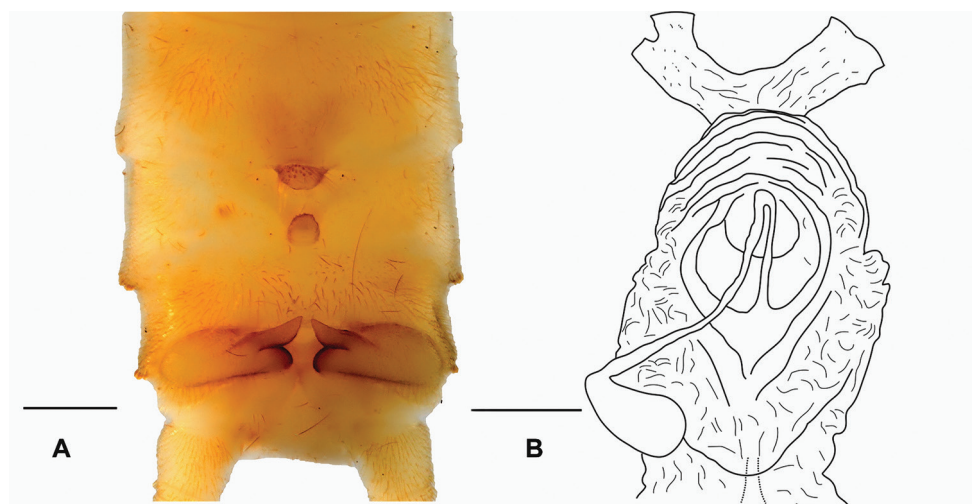
Figure 2. A male terminalia of *Neoperla mindoroensis* sp. nov. **B** female inner genitalia. Scale bars: 0.5 mm (**A**); 0.1 mm (**B**).

Figure 3. Aedeagus of *Neoperla mindoroensis* sp. nov. **A** dorsal **B** lateral **C** ventral. Scale bar: 0.1 mm.

setation throughout. Posterolateral margin of segments 7–9 with rows of moderately densely arranged, stout, brown setae. Hemitergal lobe covered with fine setae. Hemitergal processes short, not raised in lateral view, slightly bent anteriad subparallel to midline.

Female terminalia. Terga and sterna simple; subgenital plate with slightly bilobed posterior edge of S8, half as wide as segment's width; inner genitalia (Fig. 2B) unsclerotized and transparent, with distinct lamellae attached to the receptacle stalk; concentric and lateral folds discernable around and apically of the seminal receptacle's attachment, respectively.

Aedeagus (Fig. 3A–C): Aedeagal tube slightly bulky, with dorsobasal and short elongate, ventrobasal sclerites; basoventral surface of tube with hump. Dorsal surface of entire aedeagal tube with wrinkles, but entirely without any spines. Everted aedeagal sac bent slightly ventrad, shorter than aedeagal tube; basolateral lobes with strong apical spines and smaller spinules basally, posterobasal area almost glabrous; mediodorsal lobe slightly raised, fully covered with fine spinules; subapical portion with strong spines, basad increasingly with fine spinules on ventral surface; lateral and dorsal areas around the mediodorsal lobe almost glabrous.

Egg: Color dark brown, oval, nearly spherical, length ca 240 μm, width ca 220 μm, hatching line visible. Chorionic surface regularly punctate throughout, with punctae arranged in polygonal FCIs. Micropyles without any grouped rims near the hatching line (Fig. 4A–D).
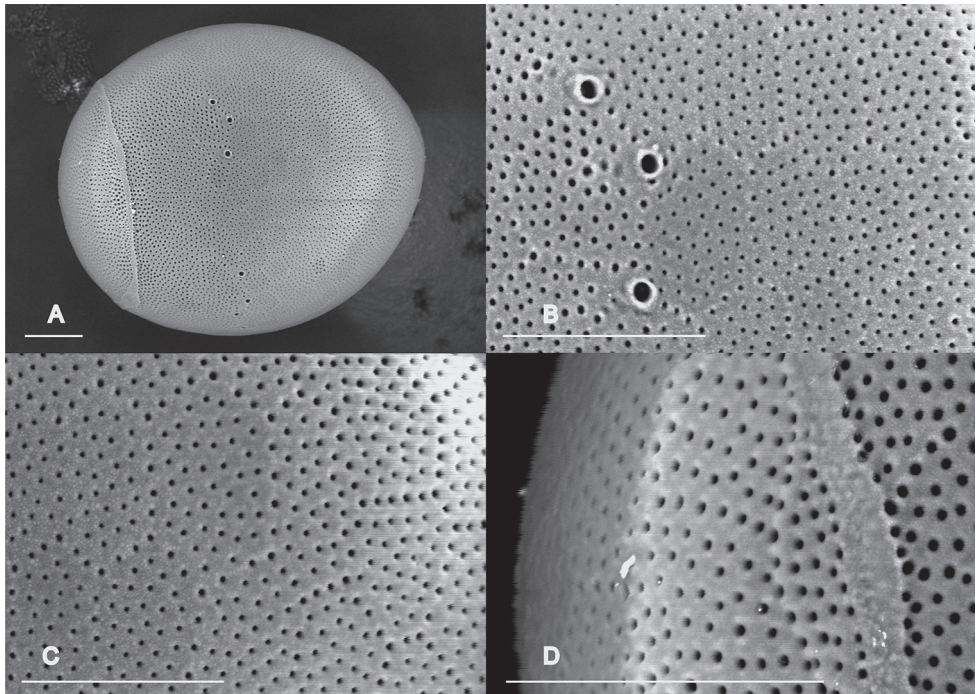

Figure 4. SEM micrographs of the egg of *Neoperla mindoroensis* sp. nov. **A** full egg **B** micropyles **C** chorion surface **D** hatching line. Scale bars: 20 μm.

Figure 5. Female larval habitus of *Neoperla mindoroensis* sp. nov. Scale bar: 4.0 mm.

*Nymph***:** General color pale brown, abdomen darker brown (Fig. 5, larva with identical pattern). Venter pale brown. Female total length 16–18 mm. Male total length 12–13 mm.

Head. Pale, predominantly brownish, slightly wider than pronotum, margins with black outline. M-line pale and tentorial callosities indistinct; stem of ecdysial suture forms a white line which opens in a white spot in the middle of the dark markings anterior of occipital area. Frons simple, with bands of mottlings. Distance in between ocelli slightly greater than their diameter. Antennae longer than combined pro-and mesothorax, yellow. Labium, labial palp, paraglossae, glossae (Fig. 6A), mandible (Fig. 6B), maxilla (Fig. 6C) family-typical. Mandible (Fig. 6B) with deeply curved molar and five uneven incisors. Maxilla (Fig. 6C): lacinia scythe blade-like with broad basal half, subapical tooth a third shorter of the apical tooth, four large setae and few smaller setae in the marginal fringe, galea almost as long as lacinia with thin apical seta.

Thorax. Pronotum with yellow middorsal stripe and dark margins. Meso- and meta-notum with yellow mid-dorsal stripe; dark bands extending from mid-length to anterior corners lining borders of wingpads; additional dark markings evident on all thoracic segments. Legs yellow, proportion 1.0:1.3:1.5; proleg: 6.0–6.5 mm, midleg: 7.0–8.0 mm, hindleg: 9.0–10.0 mm long; posterior of all legs entirely lined with very fine, dense setae; setae ca 0.5 mm long. Thoracic gills very dense, length up to 1.0 mm.

Abdomen. Posterior margins of abdominal segments with distinct dark bands. Terga sparsely covered with short, very fine, dark hairs; terga II–X with thin and sharp intercalary setae. Cerci yellow, about half as long as body; cercal hairs short and blunt. Segment X with one pair of anal gills, of approximately 20 filaments in each cluster, ca 0.5 mm long.

Differential diagnosis. *Neoperla mindoroensis* sp. nov. imagines are similar to *Neoperla nishidai* Sivec, 1984 from Greater Palawan in having pointed processes in terga 7 and 8 and in the two large, finger-shaped basolateral lobes at the aedeagal sac. However, *N. nishidai* has smaller T8 process, and its basolateral lobes and the aedeagal sac are dorsally covered by spines and bare ventrally, while in *N. mindoroensis* sp. nov. the
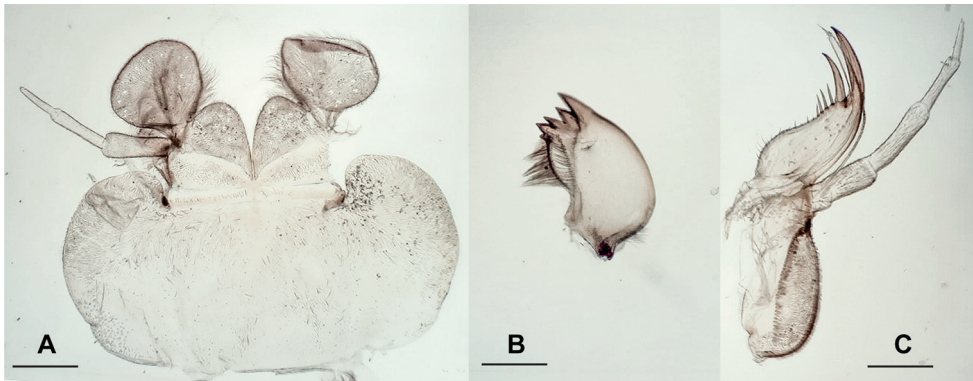
Figure 6. Nymphal mouthparts of *Neoperla mindoroensis* sp. nov. **A** labium, ventral **B** left mandible **C** left maxilla Scale bars: 0.1 mm.

basolateral lobes are densely armed with spinules, and possess a fully spinulose, slightly raised mediodorsal lobe on the sac. The aedeagal sac of *N. nishidai* was also described as strongly bent ventrally, while *N. mindoroensis* sp. nov. is only slightly bent ventrally. Additionally, the egg of *N. mindoroensis* sp. nov. is significantly smaller (240 × 220 μm) and has less pronounced FCIs than that of the supposedly conspecific female of *N. nishidai* (340 × 300 μm) (Sivec 1984). *Neoperla* PA-9 (Sivec and Stark 2011: 272, 273), which was claimed to be the putative true female of *N. nishidai*, also has larger eggs (271 × 256 μm) and an entirely different morphology from *N. mindoroensis* sp. nov. In addition, *Neoperla* PA-9 egg has a thin and obscure opercular line, but bearing a series of small, raised spine-like processes, while *N. mindoroensis* sp. nov. does not have any spine-like structure. The aedeagus of *N. palawan* Sivec & Stark, 2011 also resembles that of *N. mindoroensis* sp. nov., but its basolateral lobes are distinctly smaller, rounded, and not elongate, with a low, rounded medioventral lobe. In addition, it does not have a prominent T8 process on the dorsal abdomen. From all other male adult Philippine *Neoperla*, the new species can easily be distinguished externally by the distinct, complex pattern in its pronotum, structure of its hemitergites, and its genitalia, as described above. The female adult bears the same pronotum pattern.

Etymology. The toponym refers to the Philippine island of Mindoro, where the type locality is situated.

Distribution. This species is known so far only from the Baroc River Catchment, Roxas, Oriental Mindoro, Philippines.

Ecology. In the Baroc River Catchment, the specimens were found in altitudes of 140–530 m a.s.l. from Hinundungan River and Tauga River tributaries (Fig. 7). These collection sites were surrounded by either secondary forest or rural extensive farmland, if not secondary vegetation. Along these small to medium-sized (0.4–12 m wide) streams, the nymphs were found on submerged leaf packs, woods, and rock surfaces in riffle sections. In these microhabitats, the following physico-chemical variables were measured or estimated: water current 0.01–0.93 m/s, water temperature 21.5–26.8 °C,

Figure 7. Type locality and an additional sampling site of *Neoperla mindoroensis* sp. nov. **A** HBT **B** TIR (Photos by Mr. Clister Pangantihon).
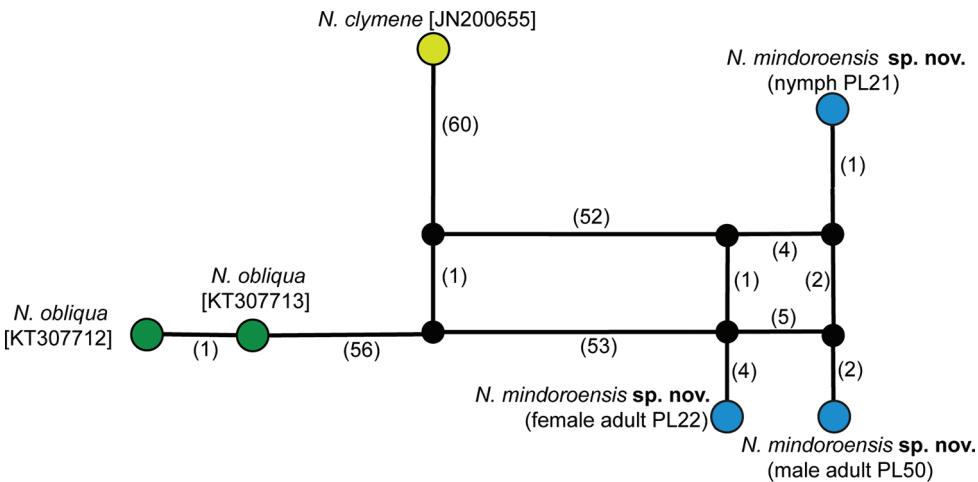

Figure 8. Statistical parsimony haplotype network of *Neoperla* samples and Genbank records from aligned sequences of 567 bp.

pH 7.5–8.5, dissolved oxygen 6.7–8.75 mg/L (mostly, but not always near 100% saturation), biochemical oxygen demand (BOD_5) 0.1–1.18 mg/L. The maximum values for dissolved nutrients were 0.5 mg/L phosphate and 1.0 mg/L nitrate.

Updated checklist of *Neoperla* Needham, 1905 from the Philippines

N. agtouganon Sivec & Stark, 2011 (Mindanao)
N. agusani Sivec, 1984 (Mindanao)
N. andreas Sivec & Stark, 2011 (Palawan)
N. atripennis Banks, 1924 (Leyte, Mindanao)
N. connectens Zwick, 1986 (Borneo, Mindanao)
N. dentata Sivec, 1984 (Borneo, Busuanga, Palawan)
N. flinti Sivec, 1984 (Luzon, Mindanao)
N. hermosa Banks, 1924 (Mindanao)
N. jewetti Sivec, 1984 (Luzon)
N. mindoroensis sp. nov. (Mindoro)
N. nigra Sivec, 1984 (Luzon)
N. nishidai Sivec, 1984 (Busuanga, Palawan)
N. obliqua Banks, 1913 (Luzon, Mindanao)
N. oculata Banks, 1924 (Biliran, Leyte, Luzon, Mindanao)
N. palawan Sivec & Stark, 2011 (Palawan)
N. pallescens Banks, 1924 (Mindanao)
N. pallicornis Banks, 1937 (Leyte, Luzon, Samar)
N. philippina Sivec, 1984 (Busuanga)
N. pseudorecta Sivec, 1984 (Busuanga, Cebu, Luzon, Negros, Palawan)
N. recta Banks, 1913 (Luzon, Negros, Mindanao)
N. sabang Sivec & Stark, 2011 (Palawan)
N. salakot Sivec & Stark, 2011 (Palawan)
N. wagneri Sivec, 1984 (Mindanao)
N. zwicki Sivec, 1984 (Luzon, Mindanao, Samar)

Discussion

Among the four stonefly genera which are known from the Philippines, *Neoperla* is the best documented genus in the country, with currently 24 species as listed above. For the first time, an integrative taxonomic approach was applied to describe a new Philippine *Neoperla* species using a newly designed primer. The same primer has proved to be efficient in generating DNA barcodes of Ephemeroptera species (Garces et al. 2018, 2020). In a preliminary analysis of a comprehensive assessment of Swiss stoneflies (Gattolliat et al. 2016), one of the factors pointed out is the need to explore more specific primers other than the standard COI primers (Folmer et al. 1994) for better output. In this study, the barcodes have been instrumental to associate the different stages of the new species and differentiate them from congeners of which mtDNA sequences are available. As a result, the female adult and the nymph were also properly described.

In biodiversity surveys of aquatic insects and ecological assessments of rivers (e.g. Junqueira et al. 2010), the nymphs, which are usually difficult to be identified to

species level, are commonly collected and not the adult forms. Among all Oriental *Neoperla* recorded, the only nymphal stage described from the Philippines is *Neoperla obliqua* Banks, 1913 (Dela Cruz et al. 2018). Because of the very limited material and literature, the distinctive features of the nymphs are still unclear. In addition, when adults are collected, the females, which were not given proper taxonomic identification aside from its ootaxonomy, are also hard to identify. Describing the nymphs and female adults together with conspecific males using barcoding would somehow aid in overcoming the impediments to species identification in macroinvertebrate assessments. With the rise in popularity of eDNA technology in biodiversity surveys nowadays, the need of barcode references has never been more important than now (Balke et al. 2013; Lim et al. 2016; Fernández et al. 2018).

In this study, the 3.5% intraspecific divergence threshold was followed as observed in several EPT sequence divergence analyses (Zhou et al. 2010; Gattolliat et al. 2016). The maximum intraspecific divergence of 2.2% (Table 2) clearly contrasts from the minimum interspecific distance of 23.5%. The haplotype network association (Fig. 8) of the specimens does also support the morphological species concept. Barcoding of stonefly species in the Philippines has just started recently (Dela Cruz et al. 2016, 2018). Clearly, additional efforts must be done in collection and identification of stoneflies using integrative taxonomy to further advance the building of a comprehensive reference library which would aid studies on Plecoptera systematics and zoogeography.

Neoperla mindoroensis sp. nov. is a member of the *N. recta* Banks, 1913 species complex within the *N. montivaga* Zwick, 1977 species group (*sensu* Zwick 1983), which is recognized for its T7 and T8 with pointed processes, presence of basolateral lobes in the everted aedeagal sac, concentric and lateral folds visible around and in front of the receptacle attachment, and punctate, chorionic egg surface (Zwick 1983; Sivec 1984). With closest similarity to *N. nishidai* Sivec, 1984, this species complex now has six members, including *N. andreas* Sivec & Stark, 2011, *N. pseudorecta* Sivec, 1984, *N. recta* Banks, 1913, and *N. zwicki* Sivec, 1984 (Sivec and Stark 2011). The *N. recta* species complex has been proposed to have taken the "Formosa-Luzon migratory track" instead of the "Sumatra track" due to low species similarity with Borneo, Java, and Sumatra (Zwick 1986). The presence of *N. mindoroensis* sp. nov. on Mindoro Island, a large land mass between Luzon and Palawan, helps now to hypothesize how the species complex reached down to Palawan as well as to the oceanic islands of the

Table 2. Intraspecific and interspecific pairwise distances of COI sequences based on Kimura-2-parameter (K2P) model.

		1	2	3	4	5	6
1	*N. mindoroensis* sp. nov. nymph PL21						
2	*N. mindoroensis* sp. nov. female adult PL22	0.022					
3	*N. mindoroensis* sp. nov. male adult PL50	0.009	0.020				
4	*N. obliqua* KT307712	0.243	0.237	0.245			
5	*N. obliqua* KT307713	0.245	0.235	0.243	0.002		
6	*N. clymene* JN200655	0.245	0.245	0.253	0.248	0.246	

eastern Philippines as some of its representatives have also been recorded in Cebu, Negros, Samar, and Mindanao (Sivec 1984; Sivec and Stark 2011).

The material treated here was exclusively retrieved from the Baroc River catchment as the main field research locality of the work group. During the long-term sampling program, the disturbed lower river reaches as well as various major and minor tributaries were accessed repeatedly. The new species was only found in rather undisturbed, clean tributaries (see Ecology), which suggests it has value as bioindicator for such habitats. However, to further assess its suitability and potential, an intensive ecological assessment is recommended.

Acknowledgements

References

Balke M, Hendrich L, Toussaint EFA, Zhou X, von Rintelen T, de Bruyn M (2013) Suggestions for a molecular biodiversity assessment of South East Asian freshwater invertebrates. Lessons from the megadiverse beetles (Coleoptera). Journal of Limnology 72: 61–68. https://doi.org/10.4081/jlimnol.2013.s2.e4

Banks N (1913) On a collection of neuropteroid insects from the Philippine Islands. Proceedings of the Entomological Society of Washington 15: 170–180. http://www.biodiversitylibrary.org/bibliography/2510

Banks N (1924) Descriptions of new neuropteroid insects. Bulletin of the Museum Comparative Zoology 65: 419–455. https://archive.org/details/TLD-BANKS_1924_71/page/n1/

Banks N (1937) Philippine Neuropteroid Insects. The Philippine Journal of Science 63: 126–174. https://archive.org/details/TLD-BANKS_1937_83/

Clement M, Snell Q, Walker P, Posada D, Crandall K (2002) TCS: estimating gene genealogies. In: Proceedings 16th International Parallel and Distributed Processing Symposium. IEEE, 7 pp. https://doi.org/10.1109/IPDPS.2002.1016585

Dela Cruz INB, Nuñeza OM, Lin C-P (2016) Description of a new Oriental stonefly species, *Phanoperla constanspina* (Plecoptera: Perlidae) from Mindanao, Philippines and association of life stages using DNA barcoding. Zootaxa 4193: 102–116. https://doi.org/10.11646/zootaxa.4193.1.4

Dela Cruz INB, Nuñeza OM, Lin C-P (2018) A new record of *Neoperla obliqua* Banks, 1930 [sic] (Plecoptera: Perlidae) from Mt. Malindang, Mindanao, Philippines and association of life stages using DNA barcodes. Zootaxa 4514: 145–150. https://doi.org/10.11646/zootaxa.4514.1.12

DeWalt RE, Ower GD (2019) Ecosystem services, global diversity, and rate of stonefly species descriptions (Insecta: Plecoptera). Insects 10: 1–99. https://doi.org/10.3390/insects10040099

Fernández S, Rodríguez S, Martínez JL, Borrell YJ, Ardura A, García-Vázquez E (2018) Evaluating freshwater macroinvertebrates from eDNA metabarcoding: a river Nalón case study. PLoS ONE 13: e0201741. https://doi.org/10.1371/journal.pone.0201741

Fochetti R, Tierno de Figueroa JM (2008) Global diversity of stoneflies (Plecoptera: Insecta) in freshwater. In: Balian EV, Lévêque C, Segers H, Martens K (Eds) Freshwater Animal Diversity Assessment. Hydrobiologia, Dordrecht, 365–377. https://doi.org/10.1007/s10750-007-9031-3

Folmer O, Black M, Hoeh W, Lutz R, Vrijenhoek R (1994) DNA primers for amplification of mitochondrial cytochrome *c* oxidase subunit I from diverse metazoan invertebrates. Molecular Marine Biology and Biotechnology 3: 294–299. https://www.ncbi.nlm.nih.gov/pubmed/7881515

Freitag H (2004) Adaptations of an emergence trap for use in tropical streams. International Review of Hydrobiology 89: 363–374. https://doi.org/10.1002/iroh.200310709

Freitag H (2013) *Ancyronyx* Erichson, 1847 (Coleoptera, Elmidae) from Mindoro, Philippines, with description of the larvae and two new species using DNA sequences for the assignment of the developmental stages. ZooKeys 321: 35–64. https://doi.org/10.3897/zookeys.321.5395

Garces JM, Bauernfeind E, Freitag H (2018) *Sparsorythus sescarorum*, new species from Mindoro, Philippines (Ephemeroptera, Tricorythidae). ZooKeys 795: 13–30. https://doi.org/10.3897/zookeys.795.28412

Garces JM, Sartori M, Freitag H (2020) Integrative taxonomy of the genus *Dudgeodes* Sartori, 2008 (Insecta, Ephemeroptera, Teloganodidae) from the Philippines with description of

new species and supplementary descriptions of Southeast Asian species. ZooKeys 910: 93–129. https://doi.org/10.3897/zookeys.910.48659

Gattolliat J-L, Vinçon G, Wyler S, Pawlowski J, Sartori M (2016) Toward a comprehensive COI DNA barcode library for Swiss Stoneflies (Insecta: Plecoptera) with special emphasis on the genus *Leuctra*. Zoosymposia 11: 135–155. https://doi.org/10.11646/zoosymposia.11.1.15

Hadley A (2010) CombineZP. http://www.hadleyweb.pwp.blueyonder.co.uk/CZP/News.htm [Accessed on: 2010-6-6]

Hall TA (1999) BioEdit: a user-friendly biological sequence alignment editor and analysis program for Windows 95/98/NT. Nucleic Acids Symposium 41: 95–98.

Jewett SGJ (1958) Stoneflies from the Philippines. Fieldiana Zoology 42: 77–87. https://archive.org/details/stonefliesfromph426jewe/page/n5/

Junqueira MV, Friedrich G, Pereira De Araujo PR (2010) A saprobic index for biological assessment of river water quality in Brazil (Minas Gerais and Rio de Janeiro states). Environmental Monitoring and Assessment 163: 545–554. https://doi.org/10.1007/s10661-009-0857-1

Kawai T (1969) Stoneflies (Plecoptera) from Southeast Asia. Pacific Insects 11: 613–625. https://archive.org/details/pacific-insects-11-613/

Komarek A, Freitag H (2014) Revision of *Anacaena* Thomson, 1859 XI. Republic of the Philippines (Coleoptera: Hydrophilidae). Koleopterologische Rundschau 84: 235–276.

Kumar S, Stecher G, Tamura K (2016) MEGA7: Molecular Evolutionary Genetics Analysis version 7.0 for bigger datasets. Molecular Biology and Evolution 33: 1870–1874. https://doi.org/10.1093/molbev/msw054

Leigh JW, Bryant D (2015) POPART: full-feature software for haplotype network construction. Methods in Ecology and Evolution 6: 1110–1116. https://doi.org/10.1111/2041-210X.12410

Lim NKM, Tay YC, Srivathsan A, Tan JWT, Kwik JTB, Baloğlu B, Meier R, Yeo DCJ (2016) Next-generation freshwater bioassessment: eDNA metabarcoding with a conserved metazoan primer reveals species-rich and reservoir-specific communities. Royal Society Open Science 3: 160635. https://doi.org/10.1098/rsos.160635

Mey W, Freitag H (2013) Trichoptera of Mindoro, the Philippines I. New species and records from the Baroc River Catchment, Roxas, Oriental Mindoro (Insecta, Trichoptera). Esperiana Band 18: 259–269. https://www.researchgate.net/publication/260086326

Murányi D, Li W, Jeon MJ, Hwang JM, Seo HY (2015) Korean species of the genus *Neoperla* Needham, 1905 (Plecoptera: Perlidae). Zootaxa 3918: 113–127. https://doi.org/10.11646/zootaxa.3918.1.5

Needham JG (1905) New genera and species of Perlidae. Proceedings of the Biological Society of Washington 18: 107–110. https://archive.org/details/3908801205153818biolrich/page/n6/

Newman E (1839) On the Synonymy of the *Perlites*, together with brief charaters of the old and of a few new species. Art. IV. Magazine of Natural History, New Series 3 (25): 32–37. [84–90.] https://archive.org/details/magazineofnatura13loud/page/n6/

Ong PS, Afuang LE, Rosell-Ambal RG [Eds] (2002) Philippine Biodiversity Conservation Priorities: a second iteration of the National Biodiversity Strategy and Action Plan Final Report. Department of Environment and Natural Rescources-Protected Areas and Wildlife Bureau, Conservation International Philippines, Biodiversity Conservation Program-

University of the Philippines Center for Integrative and Development Studies, Foundation for the Philippine Environment, Quezon City, 113 pp.

Pilgrim EM, Jackson SA, Swenson S, Turcsanyi I, Friedman E, Weigt L, Bagley MJ (2011) Incorporation of DNA barcoding into a large-scale biomonitoring program: opportunities and pitfalls. Journal of the North American Benthological Society 30: 217–231. https://doi.org/10.1899/10-012.1

Qiagen (2002) DNeasy Tissue Kit Handbook 05/2002. Hilden, Germany, 43 pp.

Sivec I (1984) Study of the genus *Neoperla* (Plecoptera: Perlidae) from the Philippines. Scopolia 7: 1–44. https://www.zobodat.at/pdf/Scopolia_7_0001-0044.pdf

Sivec I, Stark BP (2011) New species of *Neoperla* Needham and *Phanoperla* Banks (Plecoptera: Perlidae) from the Philippine Islands. Illiesia 7: 264–279. http://illiesia.speciesfile.org/papers/Illiesia07-24.pdf

Sivec I, Stark BP, Uchida S (1988) Synopsis of the world genera of Perlinae (Plecoptera: Perlidae). Scopolia 16: 1–66. http://bionames.org/references/b03a0eced7dcde94d-b948e9e48db642b

Vidal AR, Go KCTS, Freitag H (2017) Hydraenidae (Insecta: Coleoptera) of Mindoro, Philippines. I: *Hydraena* Kugelann, 1794 of the Baroc River basin, Roxas, Oriental Mindoro with description of three new species. Aquatic Insects 38: 1–20. https://doi.org/10.1080/01650424.2017.1303517

Zhou X, Jacobus LM, DeWalt RE, Adamowicz SJ, Hebert PDN (2010) Ephemeroptera, Plecoptera, and Trichoptera fauna of Churchill (Manitoba, Canada): insights into biodiversity patterns from DNA barcoding. Journal of the North American Benthological Society 29: 814–837. https://doi.org/10.1899/09-121.1

Zwick P (1982) A revision of the Oriental stonefly genus *Phanoperla* (Plecoptera: Perlidae). Systematic Entomology 7: 87–126. https://doi.org/10.1111/j.1365-3113.1982.tb00128.x

Zwick P (1983) The *Neoperla* of Sumatra and Java (Indonesia). Spixiana 6: 167–204. https://www.biodiversitylibrary.org/page/28257608#page/179/

Zwick P (1986) The Bornean species of the stonefly genus *Neoperla* (Plecoptera: Perlidae). Aquatic Insects 8: 1–53. https://doi.org/10.1080/01650428609361227

RESEARCH ARTICLE

A world key to the genera of Elcanidae (Insecta, Orthoptera), with a Jurassic new genus and species of Archelcaninae from China

Jun-Jie Gu[1,3], He Tian[2], Junyou Wang[4], Wenzhe Zhang[1], Dong Ren[2], Yanli Yue[1]

1 *College of Agronomy, Sichuan Agricultural University, Chengdu, Sichuan, 611130, China* **2** *College of Life Sciences, Capital Normal University, 105 Xisanhuanbeilu, Haidian District, Beijing, 100048, China* **3** *Institute of Ecological Agriculture, College of Agronomy, Sichuan Agricultural University, Chengdu, Sichuan, 611130, China* **4** *Inner Mongolia Museum of Natural History, No.13, South 2nd Ring Road, Saihan District, Hohhot City, Inner Mongolia, 010010, China*

Corresponding author: *Yanli Yue* (yueyanli2010@qq.com)

Citation: Gu J-J, Tian H, Wang J, Zhang W, Ren D, Yue Y (2020) A world key to the genera of Elcanidae (Insecta, Orthoptera), with a Jurassic new genus and species of Archelcaninae from China. ZooKeys 954: 65–74. https://doi.org/10.3897/zookeys.954.52088

Abstract

A new fossil genus and species is described from the Middle Jurassic of China. The type of *Sinoelcana minuta* **gen. et sp. nov.** has body and legs preserved. It is distinguished from all other elcanids by the unique combination of wing venation and stout ovipositor. The sickle-shaped ovipositor suggests that the new species had a preference for oviposition on plant material. A world key to the genera of Elcanidae is provided based on the wing venation.

Keywords

Jiulongshan Formation, Middle Jurassic, ovipostion, *Sinoelcana*, wing venation, Yanliao biota

Introduction

Elcanidae Handlirsch, 1906 is the most diverse family of the enigmatic group Elcanidea. In the history of taxonomic study of elcanids, over a hundred species names were proposed, mostly based on the structure of their wings (Germar 1842; Giebel 1856;

Handlirsch 1906–1908, 1939). After a critical investigation of wing venation, 104 species names in Elcanidae were considered to be invalid and were discarded from use (Zessin 1987). To date, Elcanidae consists of two subfamilies: Elcaninae Handlirsch, 1906 and Archelcaninae Gorochov, Jarzembowski & Coram, 2006 (Gorochov et al. 2006). Elcaninae, which are characterized by presence of a distal fusion among CuPaß, CuPb, and 1A, contains the genera *Probaisselcana* Gorochov, 1989; *Panorpidium* Westwood, 1854; *Eubaisselcana* Gorochov, 1986; *Cratoelcana* Martins-Neto, 1991; and *Minelcana* Gorochov, Jarzembowski & Coram, 2006. Archelcaninae are characterized by free distal part of CuPaß, CuPb, and 1A, and contains the genera *Parelcana* Handlirsch, 1906; *Synelcana* Zessin, 1988; *Archelcana* Sharov, 1968; *Sibelcana* Gorochov, 1990; *Hispanelcana* Penalver & Grimaldi, 2010; *Cascadelcana* Fang, Muscente, Heads, Wang, and Xiao 2018; and *Jeholelcana* Fang, Heads, Wang, Zhang, & Wang, 2018.

Northeastern China is rich and diverse in fossil insects (Zhang et al. 2010; Gu et al. 2012; Wang et al. 2012; Ren 2019). More than 60 species of Orthoptera have been reported from Yanliao and Jehol biota; however, only four are elcanids (Fang et al. 2015, 2018; Tian et al. 2019a, 2019b). Nevertheless, based on the compression fossil and amber collections of Elcanidae, this group exhibits a potentially higher diversity than expected (pers. obs.). Here, we describe a new genus with a new species of Elcanidae collected from Daohugou, Ningcheng, Inner Mongolia of China. This new finding enriches the diversity of Elcanidae and increases our knowledge of the wing morphology and reproduction behavior of this group. Furthermore, a world key to genera of Elcanidae, including this new genus and species, is provided based on wing venation characters.

Method and materials

The specimens were examined with a Nikon SMZ 25 microscope and photographed with a Nikon DS-Ri 2 digital camera system. Line drawings were prepared using Adobe Illustrator CC 17.0.0 and Adobe Photoshop CC 14.0 graphics software. The measurements were taken using Adobe Illustrator. The specimens are housed at the Inner Mongolia Museum of Natural History, Hohhot, China.

Wing-venation analyses follow the interpretation proposed by Béthoux and Nel (2002). Notably, another venation system is also used to interpret the wing of Orthoptera (Sharov 1968; Gorochov 1995). The main difference is the interpretation between media and cubitus area. To make the wing constructions clear and unambiguous for readers, we list the other venation system used for Orthopera in brackets. Corresponding abbreviations used in taxonomical descriptions are as follows: CP (not covered), posterior costa; ScA (C), anterior subcosta; ScP (Sc), posterior subcosta; RA (RA), RP (Rs), anterior and posterior radius, respectively; MA (MA1), MP (MA2), anterior, posterior media, respectively; CuA (MP), CuP, anterior, posterior cubitus, respectively; CuPα (CuA1), the anterior branch of first posterior cubitus; CuPaβ (CuA2), the posterior branch of first posterior cubitus; CuPb (CuP), the second posterior cubitus; AA1 (1A), first branch of anterior anal vein.

Systematic palaeontology

Class Insecta Linnaeus, 1758
Order Orthoptera Olivier, 1789
Superfamily Elcanoidea Handlirsch, 1906
Family Elcanidae Handlirsch, 1906
Subfamily Archelcaninae Gorochov, Jarzembowski & Coram, 2006

Sinoelcana **Gu, Tian, Wang & Yue, gen. nov.**
http://zoobank.org/9E558599-9AFF-4FB6-A3A5-55E5E253893E

Type species. *Sinoelcana minuta* Gu, Tian, Wang & Yue, sp. nov.

Etymology. The generic name is a combination of the Greek prefix "sin-" (China) and *Elcana*. Gender: feminine.

Diagnosis. Sickle-shaped ovipositor; meta-tibiae has leaf-like spurs; presence of two longitudinal veins between stem of RP and CuA+CuPaα; free CuPaα short, fused with M+CuA immediately after diverging from CuPa; CuPaα fused with M+CuA for a long distance.

Comments. Based on the forewing venation, *Sinoelcana* gen. nov. can be assigned to Archelcaninae owing to its free distal parts of CuPaβ, CuPb, and AA1. The new genus is similar to *Sibelcana* Gorochov, 1990 and *Synelcana* Zessin 1988 by presence of two longitudinal veins between CuA+CuPaα and stem of RP, but it differs from *Sibelcana* in having a very short, free CuPaα and having CuA+CuPaα reaching the posterior wing margin, far beyond of the end of ScP; it differs from *Synelcana* in having a short, free CuPa, M, CuA, and CuPaα fused for a long distance, and narrow anals. *Parelcana* Handlirsch 1906 and *Cascadelcana* Fang, Muscente, Heads, Wang & Xiao, 2018 have the free CuA fused with CuPaα, which is much different from the new genus. Furthermore, the less numerous and spaced branches of the subcosta and radius, short CP, and more basal end of CuA+ CuPaα of *Cascadelcana* are quite different from the new genus. *Sinoelcana* differs from *Archelcana* Sharov, 1968 in that the latter only has one longitudinal vein between CuA+CuPaα and stem of RP. The type of *Sinoelcana* has leaf-like subapical spurs of meta-tibiae; the first three pairs are rather large. This kind of spurs is also present in another Chinese elcanid genus *Jeholelcana* Fang, Heads, Wang, Zhang & Wang, 2018, but differs from *Hispanelcana* Penalver & Grimaldi, 2010. *Sinoelcana* can be distinguished from *Jeholelcana* by its three branches of M and short CuPa.

Sinoelcana minuta **Gu, Tian, Wang & Yue, sp. nov.**
http://zoobank.org/874D154C-777D-4254-8972-7622A13A2413

Diagnosis. As for genus.

Materials. *Holotype:* IMMNH-PI11334 (Part), IMMNH-PI11335 (Counterpart), Female.
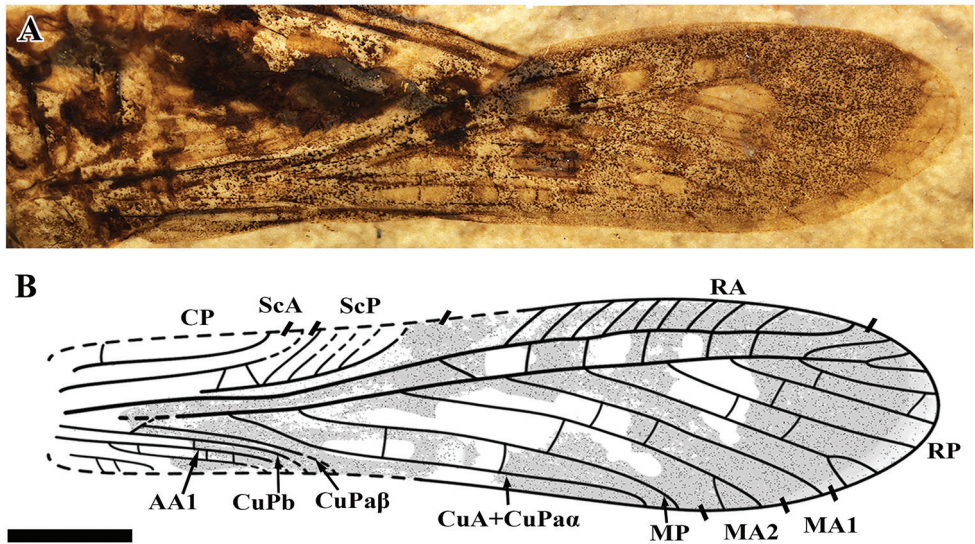
Figure 1. Holotype of *Sinoelcana minuta* sp. nov., IMMNH-PI11334, forewing. **A** Photograph **B** reconstruction drawing. Scale bar: 2 mm.

Locality and age. Daohugou Village, Wuhua Township, Ningcheng County, Inner Mongolia, China; Jiulongshan Formation, Bathonian–Callovian boundary interval (Xu et al. 2016; Yang et al. 2020), Middle Jurassic.

Description. Head: head hypognathous, with large, oval eyes; scape cylindrical, much wider than pedicel and the flagellum; compound eyes rather large, 1.1 mm long, oval; Thorax (Fig. 2A, B): pronotum saddle-shaped, 2.4 mm long, lateral lobe 2.6 mm high. Legs: meta-femur 8.1 mm long, 1.9 mm wide; meta-tibiae has three pairs of large, leaf-like spurs, and one basal and small spur, ds3 1.86 mm long, ds2 1.86 mm long, ds1 1.25 mm, ds4 0.85 mm long (Fig. 2C, D). Forewing (Fig. 1): 14.3 mm long, 3.4 mm wide (maximum width recorded); CP distally curved and reaching anterior wing margin beyond the origin of CuA+CuPaα; ScA simple, ending in anterior margin nearly 1/4 of the wing length; ScP reaching anterior margin basal of the origin of stem RP and giving off 5 long and oblique branches ending in anterior margin; stem R long and strong, branched into RA and RP close to the middle of wing length; area between ScP and R basally narrow, getting wider after ScP reaching wing margin; RA has numerous oblique branches reaching anterior margin; RP fused with MA1 distal to the end of ScP; RP has 6 main pectinate branches and 8 terminals; M forking into MA and MP at the level of the end of ScA; MA forking into MA1 and MA2 at the level of the end of ScP; the fusion of RP and MA1 distant to the origin of MA1, MA2 distally branch; MP simple, originates at the level of the end of ScP; area between branches of RA and RP covered with simple and straight crossveins; CuA+CuPaα simple, slightly undulate, originating basal of the end of CP; CuPa short, forking into CuPaα and CuPaβ close to the wing base; CuPaα fused with M+CuA immediately and running for a long distance; CuPaβ and CuPb simple; AA1 strong, reaching posterior wing margin distal of the end
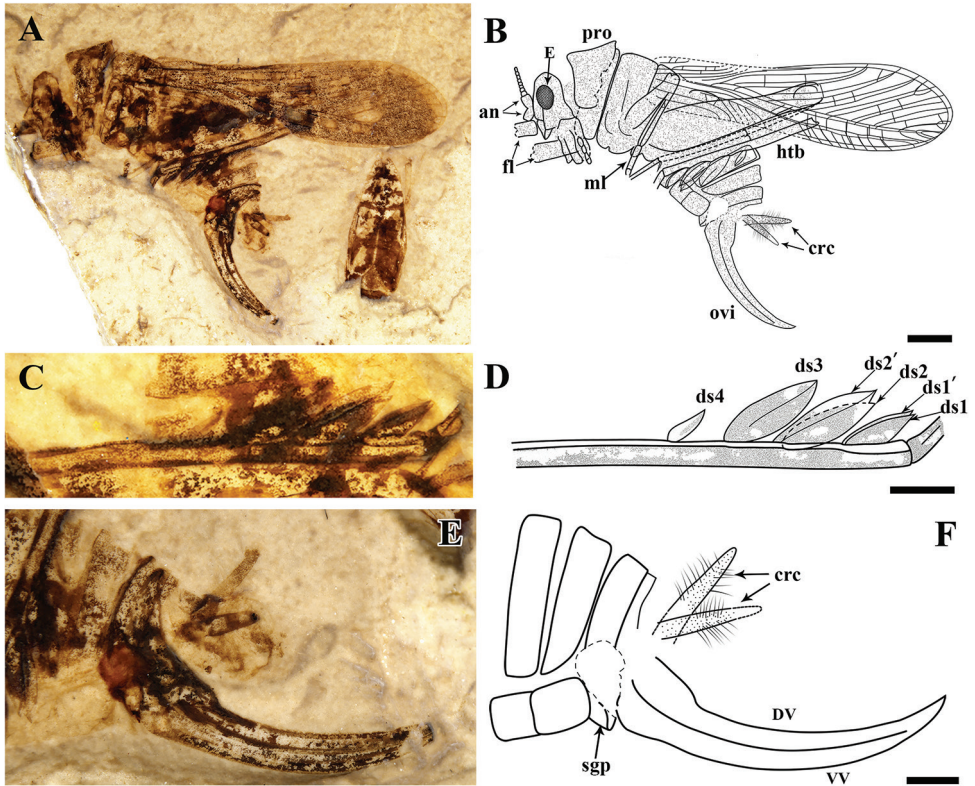
Figure 2. Holotype of *Sinoelcana minuta* sp. nov., IMMNH-PI11334. **A, B** Habitus, photograph (**A**) and reconstruction drawing (**B**). **C, D** meta-tibiae, photograph (**C**) and reconstruction drawing (**D**). **E, F** ovipositor, photograph (**E**) and reconstruction drawing (**F**). Scale bars: 2 mm (**A, B**); 1 mm (**C–F**).

of ScA; without distinct coloration spots on the wing. Abdomen: cerci short and conical, unsegmented, 2.3 mm long, with numerous hairs; ovipositor sickle like, 6.4 mm long (measured from the tip to the base), more than twice as long as the pronotum.

Discussion

The ovipositors of ensiferans are always specially modified related to the site and pattern of oviposition (Gwynne 2001; Rentz 2010). Currently, only a few fossil elcanid species have ovipositors preserved, which exhibit a straight, elongated, and sharply pointed shape (Zessin 1987; Martins-Neto 1991; Tian et al. 2019a). Although the ovipositors of these insects are quite different in their measurements, their shapes are similar and sword-like. These similarities to extant Ensifera imply that laying eggs in the ground/soil was a common behavior of Mesozoic elcanids. In contrast with the ovipositor structural design above, *S. minuta* Gu, Tian, Wang & Yue sp. nov. has a comparatively short and stout ovipositor. The ovipositor is slightly curved and its apical portion of dorsal valvulae is smooth

and without any serrations (Fig. 2E, F). This kind of sickle-shaped ovipositor indicates that the species oviposits on plant material, either dead wood or stems (Rentz 2010).

Currently, 11 genera are attributed to Elcaninae and Archelcaninae (Gorochov et al. 2006). Among them, *Cratoelcana* were described with two new species including females and males from Crato, Brazil. These specimens are exquisite and almost completely preserved, but with greatly overlapped wings. Based on the reconstructions of the wing, it is worth examining the area of the cubitus and anal veins, which is not common in general for fossil elcanid species. From the drawing of specimen CV-1098 of *Cratoelcana zessin* (Martins-Neto 1991), the reconstruction brings a unique fusion with CuPb and AA1, but the interpretation might need a more thorough examination of the specimen. Hence, the present subfamily assignment should be regarded with caution.

Jeholelcana yixianensis was described from the Jehol biota and presented with a very unique character: specifically a long and oblique free CuA vein fused to the CuPa vein, which was treated as a diagnostic character for the species and genus (Fang et al. 2018). This condition is very peculiar in Elcanidae and even among orthoperans in general. Fang et al. (2018) followed the nomenclature proposed by Béthoux and Nel (2002); however, they made an incorrect interpretation regarding the venation. Based on the reconstruction of the wing, the cubitus part exhibits a typical pattern of Elcanidae where CuPa basally forks into CuPaα and CuPaβ, and then CuPaα fuses with M+CuA. In other words, the vein CuA+CuPa interpreted by Fang et al. should be CuA+CuPaα. Furthermore, the forewing shows an unusual condition in that CuPaβ fuses with CuA+CuPaα for short distance. It is not common in orthoperans, if we treat it as a stable character state, but some similar conditions were documented in several relatives of orthoperan species. *Longzhua loculata* exhibits an unusual condition in which a branch of CuA fuses with the posterior branch of M (Gu et al. 2011). Based on more than 60 samples of forewings, and with only two specimens have a branch of CuA fusing to the posterior branch of M, and this condition is reasonable to interpret as a translocation of a vein or a consequence of fusion, rather than a unique character state (Gu et al. 2011). The same situation occurs in another Carboniferous archaeorthopteran species, *Miamia maimai* (Béthoux et al. 2012). Regardless, for extant orthopterans, this condition is also present among winged caeliferans and ensiferans. To verify this assumption, we examined six wing pairs of *Calliptamus abbreviates* and found that one of them exhibited a CuPaβ distally fused with CuA+CuPaα, whereas the CuPaβ of the remainder of the specimens examined were distant to CuPaα (unpublished data). Therefore, CuPaβ fused with CuA+CuPaα is not a suitable diagnostic character for *Jeholelcana*.

Due to the rare occurrence of complete wingsets of Elcanidae and the typical requirements for a large sample of species to establish wing venation characters, taxonomy and further phylogenetic work in the Elcanidae are challenging. As more new materials are discovered, a comprehensive rechecking of the classification of known species worldwide is needed. Presently, there are six amber-embedded species attributed to Elcanidae (Poinar et al. 2007; Peñalver and Grimaldi 2010; Heads et al. 2018). Lack of wing preservation has made establishment of their subfamily positions hard to confirm. From the current database of Orthotpera species (Cigliano et al. 2020),

Elcanopsis sydneiensis Tillyard, 1918 and *Macrelcana ungeri* (Heer, 1849) are presently included within the Elcanidae. However, *Elcanopsis sydneiensis* is only known for a fragment, which is probably the distal part of the forewing of an elcanid-like insect (Tillyard 1918). *Macrelcana ungeri* (Heer, 1849) is lacking the diagnostic characters of Elcanidae based on the reconstruction of the wing (Karny 1932). In conclusion, we propose a key to the genera of Elcanidae based on forewing venation characters where the amber-embedded taxa and *Cratoelcana* are not considered.

Key to the genera of fossil Elcanidae based on wing venation

1	Area between RA and RP widened; CuPaβ, CuPb, and AA1 without fusion ...**2**	
–	Area between RA and RP not widened; CuPaβ, CuPb, and AA1 distally fused or just CuPaβ fused with CuPb..**8**	
2	CuPaα fused with free CuA..**3**	
–	CuPaα fused with M+CuA..**4**	
3	Presence of three longitudinal veins between CuA+CuPaα and stem of RP ... .***Parelcana***	
–	Presence of two longitudinal veins between CuA+CuPaα and stem of RP ....***Cascadelcana***	
4	M has two branches, forming MA and MP................................***Archelcana***	
–	M has more than two branches, MA branched **5**	
5	MA has three main branches...***Jeholelcana***	
–	MA has two main branches..**6**	
6	Free CuPa long, slightly arched to the anterior wing margin ....***Synelcana***	
–	Free CuPa short, directed towards the anterior wing margin **7**	
7	CuPa vertically diverges from CuP; CuPaα fused with M+CuA and separated from the fusion with CuA immediately..***Sibelcana***	
–	CuPa obliquely diverges from CuP; CuPaα fused with M+CuA for a long distance...***Sinoelcana* gen. nov.**	
8	CuPaβ, CuPb, and AA1 distally fused..**9**	
–	CuPaβ distally fused with CuPb...***Eubaisselcana***	
9	Area between MP and posterior wing margin broad and covered by oblique, regular, long cross-veins ....***Minelcana***	
–	Area between MP and posterior wing margin narrow, without long, oblique cross-veins...**10**	
10	M with three branches ....***Probaisselcana***	
–	M with more than three branches...***Panorpidium***	

References

Béthoux O, Gu J-J, Yue Y, Dong R (2012) *Miamia maimai* n. sp., a new Pennsylvanian stem-orthopteran insect, and a case study on the application of cladotypic nomenclature. Fossil Record 15: 103–113. https://doi.org/10.1002/mmng.201200008

Béthoux O, Nel A (2002) Venation pattern and revision of Orthoptera sensu nov. and sister groups. Phylogeny of Palaeozoic and Mesozoic Orthoptera sensu nov. Zootaxa 96: 1–88. https://doi.org/10.11646/zootaxa.96.1.1

Cigliano MM, Braun H, Eades DC, Otte D (2020) Orthoptera Species File. Version 5.0/5.0. http://Orthoptera.SpeciesFile.org [Accessed on: 2020-01-21]

Fang Y, Heads S, Wang H, Zhang H, Wang B (2018) The first Archelcaninae (Orthoptera, Elcanidae) from the Cretaceous Jehol Biota of Liaoning, China. Cretaceous Research 86: 129–134. https://doi.org/10.1016/j.cretres.2018.02.008

Fang Y, Wang B, Zhang H, Wang H, Jarzembowski EA, Zheng D, Zhang Q, Li S,Liu Q (2015) New Cretaceous Elcanidae from China and Myanmar (Insecta, Orthoptera). Cretaceous Research 52: 323–328. https://doi.org/10.1016/j.cretres.2014.05.004

Germar EF (1842) Beschreibung einiger neuen fossilen Insecten (i.). In: Münster G (Ed.) Muenster Beiträge zur Petrefaktenkunde, Bayreuth. Beiträge zur Petrefactenkunde, Münster, 79–94.

Giebel CG (1856) Fauna der Vorwelt mit steter Breucksichtigung der lebenden Thiere. Brockhaus F.A., Leipzig, 551 pp.

Gorochov AV, Jarzembowski EA, Coram RA (2006) Grasshoppers and crickets (Insecta: Orthoptera) from the Lower Cretaceous of southern England. Cretaceous Research 27: 641–662. https://doi.org/10.1016/j.cretres.2006.03.007

Gorochov AV (1995) System and evolution of the suborder Ensifera (Orthoptera) Part I. Proceedings of the Zoological Institute-Russian Academy of Sciences 260: 1–223.

Gu J-J, Béthoux O, Ren D (2011) *Longzhua loculata* n. gen. and n. sp., one of the most completely documented Pennsylvanian Archaeorthoptera (Insecta; Ningxia, China). Journal of Paleontology 85: 303–314. https://doi.org/10.1666/10-085.1

Gu J-J, Montealegre-Z F, Robert D, Engel MS, Qiao G-X, Ren D (2012) Wing stridulation in a Jurassic katydid (Insecta, Orthoptera) produced low-pitched musical calls to attract females. Proceedings of the National Academy of Sciences 109: 3868–3873. https://doi.org/10.1073/pnas.1118372109

Gwynne DT (2001) Katydids and Bush-Crickets: Reproductive Behavior and Evolution of the Tettigoniidae. Cornell University Press, Ithaca and London, 317pp.

Handlirsch A (1906–1908) Die fossilen Insekten und die Phylogenie der rezenten Formen. Ein Handbuch für Paläontologen und Zoologen. Wilhelm Engelmann, Berlin, 1430 pp.

Handlirsch A (1939) Neue Untersuchungen über die fossilen Insekten, part 2. Annalen des Naturhistorischen Museums in Wien 49: 1–240.

Heads S, Thomas M, Wang Y (2018) A new genus and species of Elcanidae (Insecta: Orthoptera) from Cretaceous Burmese amber. Zootaxa 4527: 575–580. https://doi.org/10.11646/zootaxa.4527.4.8

Karny HH (1932) Über zwei angebliche *Gryllacris*-Arten aus dem Miocän von Radoboj. Jahrbuch der Geologischen Bundesanstalt 82: 65–70.

Martins-Neto RG (1991) Sistemática dos Ensifera (Insecta, Orthopteroida) da Formação Santana, Cretáceo inferior do Nordeste do Brasil. Acta Geologica Leopoldensia 14: 3–162.

Peñalver E, Grimaldi DA (2010) Latest occurrences of the Mesozoic family Elcanidae (Insecta: Orthoptera), in Cretaceous amber from Myanmar and Spain. Annales de la Société Entomologique de France (N.S.) 46: 88–99. https://doi.org/10.1080/00379271.2010.10697641

Poinar G, Gorochov AV, Buckley R (2007) *Longioculus burmensis* n. gen., n. sp. (Orthoptera, Elcanidae) in Burmese amber. Proceedings of the Entomological Society of Washington 109: 649–655.

Ren D (2019) Jurassic–Cretaceous non-marine stratigraphy and entomofaunas in Northern China. In: Ren D, Shih C, Gao T, Yao Y and Y. Wang (Eds) Rhythms of Insect Evolution-Evidence from the Jurassic and Cretaceous in Northern China. Wiley Blackwell, Hoboken, USA, 1–16. https://doi.org/10.1002/9781119427957.ch1

Rentz D (2010) A Guide to the Katydids of Australia. CSIRO Publishing, Collingwood, 224pp. https://doi.org/10.1071/9780643100183

Sharov AG (1968) Filogeniya orthopteroidnykh nasekomykh. Trudy Paleontologicheskogo Instituta, Akademiya Nauk SSSR 118: 1–216.

Tian H, Gu J-J, Yin XC, Ren D (2019b) The first Elcanidae (Orthoptera, Elcanoidea) from the Daohugou fossil bed of northeastern China. Zookeys 897: 19–28. https://doi.org/10.3897/zookeys.897.37608

Tian H, Gu J-J, Huang F, Zhang H, Ren D (2019a) A new species of Elcaninae (Orthoptera, Elcanidae) from the Lower Cretaceous Yixian Formation at Liutiaogou, Inner Mongolia, NE China, and its morphological implications. Cretaceous Research 99: 275–280. https://doi.org/10.1016/j.cretres.2019.03.010

Tillyard RJ (1918) A fossil Insect-wing from the roof of the coal-seam on the Sidney Harbour Colliery. Proceedings of the Linnean Society of New South Wales 43: 260–264.

Wang Y, Labandeira CC, Shih CK, Ding Q, Wang C, Zhao YY, Ren D (2012) Jurassic mimicry between a hangingfly and a ginkgo from China. Proceedings of the National Academy of Sciences of the United States of America 109: 20514–20519. https://doi.org/10.1073/pnas.1205517109

Xu X, Zhou Z, Corwin S, Wang Y, Ren D (2016) An updated review of the Middle–Late Jurassic Yanliao biota: chronology, taphonomy, paleontology and paleoecology. Acta Geologica Sinica 90: 2229–2243. https://doi.org/10.1111/1755-6724.13033

Yang H, Shi C, Engel SM, Zhao Z, Ren D, Gao T (2020) Early specializations for mimicry and defense in a Jurassic stick insect. National Science Review. https://doi.org/10.1093/nsr/nwaa056

Zessin W (1987) Variabilität, Merkmalswandel und Phylogenie der Elcanidae im Jungpaläozoikum und Mesozoikum und die Phylogenie der Ensifera (Orthopteroidea, Ensifera). Deutsche Entomologische Zeitschrift (N.F.) 34: 1–76. https://doi.org/10.1002/mmnd.4800340102

Zhang H, Wang B, Fang Y (2010) Evolution of insect diversity in the Jehol biota. Science China-Earth Sciences 53: 1908–1917. https://doi.org/10.1007/s11430-010-4098-5

RESEARCH ARTICLE

A peer-reviewed open-access journal

ZooKeys

Launched to accelerate biodiversity research

Tauritermes bandeirai: A new drywood termite (Isoptera, Kalotermitidae) from the Caatinga and Atlantic Forest of Brazil

Rudolf H. Scheffrahn[1], Alexandre Vasconcellos[2]

1 *Fort Lauderdale Research and Education Center, University of Florida, 3205 College Avenue Davie, Florida 33314, USA* **2** *Universidade Federal da Paraíba, Departamento de Sistemática e Ecologia, Laboratório de Termitologia, CEP: 58051-900, João Pessoa, Paraíba, Brazil*

Corresponding author: Rudolf H. Scheffrahn (rhsc@ufl.edu)

Abstract

The imago and soldier castes of a new *Tauritermes* Krishna, 1961 species, *Tauritermes bandeirai* **sp. nov.** are described. It is the fourth species of *Tauritermes* and occurs from the Caatinga and Atlantic Forest of Brazil. Unlike its congeners, the soldier of *T. bandeirai* has prominent frontal horns.

Keywords

Imago, new species, soldier, South America

Introduction

In South America, six kalotermitid genera have soldiers with partial to robust head capsule phragmosis: *Calcaritermes*, *Cryptotermes*, *Eucryptotermes*, *Glyptotermes*, *Proneotermes*, and *Tauritermes* (Scheffrahn 2019a). According to Krishna et al. (2013), *Tauritermes* Krishna, 1961 was known only from southern Brazil and northern Argentina. Actually, Mélo and Bandeira (2004) and Vasconcellos et al. (2005) reported an unidentified species from the semiarid Caatinga and Atlantic Forest of northeastern Brazil, respectively. This was followed by additional *Tauritermes* records from the same region (Vasconcellos et al. 2010; Souza et al. 2012; Cancello et al. 2014). Dambros

et al. (2013) expanded the range of *Tauritermes* to include Amazonas (Manaus). Most recently, Scheffrahn (2019a) reported *Tauritermes* from Bolivia and Paraguay.

Tauritermes, as other kalotermitid genera, is best characterized by venation of the winged imago and soldier head capsule morphology. For Kalotermitidae, most diagnostic characters at the intrageneric level are attributed to head capsule characters. Noirot (1995) reported some consistent differences in the gut anatomy of kalotermitids compared to other lower termite families. Furthermore, Gonçalvez (1979), Myles (1997), and Godoy (2004) described parts of the gut of *Rugitermes*, *Marginitermes*, and *Tauritermes*, respectively. They found that differentiation of the gut morphology of kalotermitids remains elusive at both the generic and specific levels.

Herein, we report on a new *Tauritermes* species, *T. bandeirai* sp. nov. from samples collected by Vasconcellos et al. (2005) and additional specimens from the Brazilian Caatinga and Atlantic Forest. This is the fourth species of *Tauritermes* to be described based on external imago and soldier characters.

Material and methods

Photomicrographs were taken as multi-layer montages using a Leica M205C stereomicroscope controlled by the Leica Application Suite version 3 software. Preserved specimens were taken from 85% ethanol and suspended in a pool of Purell Hand Sanitizer to position the specimens on a transparent Petri dish background. All University of Florida Termite Collection (UFTC) records are available online (Scheffrahn 2019b).

Taxonomy

Tauritermes bandeirai sp. nov.
http://zoobank.org/3C739327-4FB8-4B77-8AD0-862A82237292
Figures 1, 2

Diagnosis. The soldier of *T. bandeirai* differs from soldiers of the other three *Tauritermes* species by having a distinct and robust frontal horn and a roundly protruding dorsal horn (Fig. 2C). The dorsal and frontal horns of *T. triceromegas* (Silvestri, 1901) are more angular but much smaller, barely elevated above the frons in oblique view (Fig. 3C). In *T. vitulus* Araujo & Fontes, 1979, the dorsal horn is similar to that of *T. bandeirai* sp. nov., while the fronal horn is absent (Araujo and Fontes 1979, fig. 10). In *T. taurocephalus* (Silvestri, 1901), the dorsal horn is more elevated and angular, while the frontal horn is also absent (Fig. 4C).

The *T. bandeirai* soldier differs from its congeners in that its frons and horns are more rugose, the basal mandible humps are broader and more angular, and the third antennal article is more club-shaped. Only *T. taurocephalus* has a similarly shaped postmentum (Figs 2D, 4D). In *T. triceromegas*, the postmentum is posteriorly elongated (Fig. 3D) and in *T. vitulus* it is posteriorly widened (Araujo and Fontes 1979, fig. 15).

The imago head and pronotum of *T. bandeirai* are mostly unremarkable, except for a relatively large ocellus in comparison with the rather small compound eye. Among kalotermitid genera, the forewing venation is closest to *Incisitermes* Krishna with one diagnostic exception. In *Incisitermes*, the median vein is not sclerotized and its terminus does not closely approach the radial sector (Scheffrahn 2014, fig. 5). In *T. bandeirai*, the distal third of the median vein is sclerotized and closely paralells the radial sector (Fig. 1C). The wing venation of *T. vitulus* is similar to that of *T. bandeirai*, but no sclerotization is reported (Araujo and Fontes 1979, fig. 1).

Description. ***Imago*** (Fig. 1A–C, Table 1). Head capsule and pronotum light brown. Compound eye obtusely triangular; ocellus a shade lighter than vertex, very large, and roundly ellipsoid; nearly touching eye margin. Vertex covered with about one dozen short setae. Pronotum about as wide as head capsule; anterior margin weakly emarginate in middle. Pronotum covered with a few dozen setae in middle, lateral margins with about one dozen setae each. Antennae with 15 articles, basal article relative lengths 1>2<3>4. Fore wing with subcosta joining costal margin at about one-eighth of wing length from suture. Radius joining costal margin at one-third wing length; radial sector with about four anterior branches. Median vein becoming lightly sclerotized at distal third as it encroaches near the radial sector. Wing membrane and first 4–5 branches of cubitus lightly pigmented, concolorous with apical radial sector and median veins. Arolium present.

Soldier (Fig. 2A–D, Table 2). Head capsule, in dorsal view (Fig. 2A), dark castaneous brown from postclypeus to antennal carinae, grading to orange at occiput. Head capsule narrowing toward antennal carinae; antennal carinae rugose and visible from above. Frontal ridge V-shaped with deep median cleft. About a dozen fine setae on vertex and genae. Eye spots hyaline, narrowly elliptical. In lateral view (Fig. 2B), dorsal horns (or protuberances) forming a rounded shelf near right angle; frontal horns projecting above base of mandibles. Genal horns slightly posterior to frontal horns, anterior to dorsal horns. Pronotum shield-shaped, wider than head; anterior margin rugose, incised in middle with rounded anterior lobes. In oblique view (Fig. 2C), dorsal and frontal horns rising prominently from frons; horns and frons coarsely rugose. Postclypeus (Fig. 2D) forming elongated, nearly symmetrical hexagon. Third antennal article slightly club-shaped, relative article length 2<3>4=5. Mandibles two-fifths length of head capsule; basal humps robust, rugose; lateral margin of humps parallel.

Table 1. Measurements (mm) of the *Tauritermes bandeirai* sp. nov. imago.

Character	Females, four colonies (n = 7)		Males, one colony (n = 4)	
	Mean	Range	Mean	Range
Head width, maximum (w/out eyes)	0.8	0.63–0.88	0.81	0.79–0.86
Head width, maximum (with eyes)	0.93	0.70–1.04	0.93	0.91–0.98
Pronotum, maximum width	0.98	0.90–1.08	0.85	0.83–0.90
Eye diameter, maximum	0.33	0.30–0.35	0.29	0.26–0.30
Body length	5.54	4.56–6.32	5.08	4.88–5.36
Right fore wing length	7.7	7.62–7.78	6.56	6.51–6.67
Body length with wings	9.92	9.84–10.00	8.47	8.25–8.73
Number of antennal articles	15	15	–	–
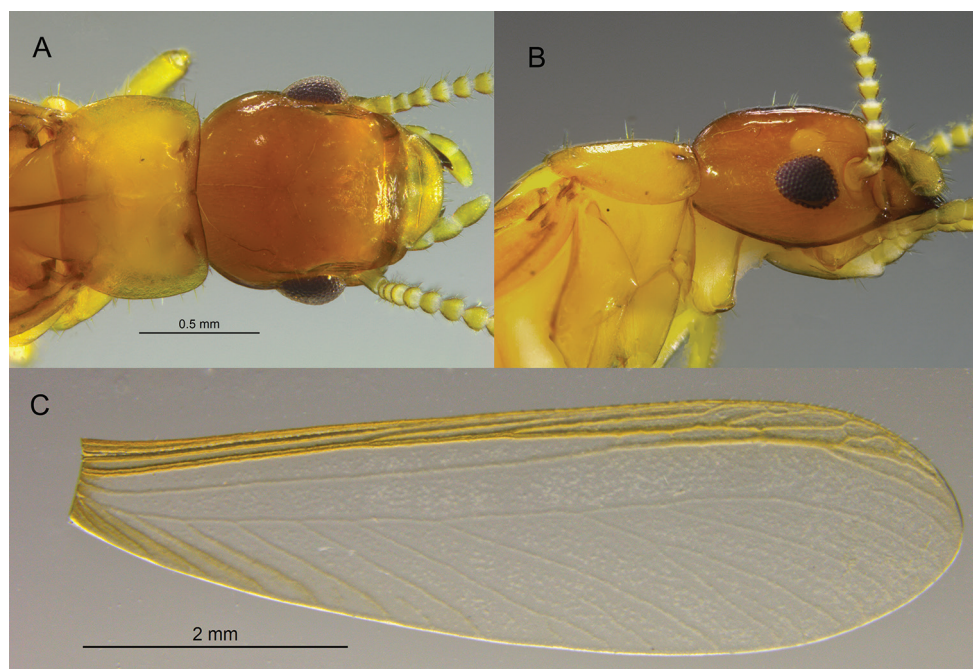
Figure 1. Imago of *Tauritermes bandeirai* sp. nov. (SA502) **A** dorsal and **B** lateral views of head and pronotum **C** right forewing.

Table 2. Measurements of *Tauritermes bandeirai* sp. nov. soldiers (n = 21) from nine colonies.

Character	Mean	Range
Head length to tip of mandibles	2.12	1.95–2.25
Head length to postclypeus	1.42	1.30–1.50
Head width, maximum	1.11	0.95–1.20
Antennal carinae, outside span	1.08	0.98–1.18
Span of dorsal horns	0.82	0.72–0.95
Span of frontal horns	0.89	0.82–0.98
Labrum, maximum width	0.25	0.21–0.32
Pronotum, maximum width	1.11	0.98–1.19
Pronotum, maximum length	0.82	0.70–0.93
Left mandible length to ventral condyle	1.00	0.88–1.10
Postmentum, maximum width	0.37	0.33–0.40
Postmentum, minimum width	0.22	0.18–0.26
Postmentum, length in middle	0.57	0.50–0.68
Head height, excluding postmentum	0.88	0.77–0.96
Third antennal article length	0.13	0.09–0.18
Number of antennal articles	10.58	9–12

Outside margin of blade nearly straight from above, then curving at right angle at one-fifth from apex; apical tooth thick, marginal dentition weak. Mandibles curve evenly by about 15° in lateral view.

Figure 2. Soldier of *Tauritermes bandeirai* sp. nov. (SA499) **A** dorsal **B** lateral **C** oblique, and **D** ventral views of head and pronotum. AC = antennal carina, DH = dorsal horn, FH = frontal horn, and GH = genal horn.

Type material examined. *Holotype* **soldier,** Brazil: Paraíba, São José da Mata (7.1829, -35.9767); 659 meters A.S.L., 17AUG2000, A. Vasconcellos (AV); one soldier (labelled as holotype, Fig. 2), one soldier and pseudergates (paratypes); University of Florida Termite Collection (UFTC) no. SA499, subsample from Universidade Federal da Paraíba Termite Collection (UPTC) no. 3160.

Other material examined. Brazil: Bahia, Itagiba, Fa. Conjunto S. Luis (-14.2840, -39.8428), 194 m, 18MAR1994, Jan Křeček; one soldier, pseudergates; UFTC SA444. Bahia, Morro do Chapéu (-11.6474, -41.2694), 974 m, 5NOV2015, AV; four soldiers, four imagos, pseudergates; SA504, 7309 (UFTC and UPTC accession numbers respectively). Bahia, Milagres (-11.6473, -39.8333), 700 m, 16MAR2012, AV; four soldiers, pseudergates; 4362. Paraíba, Maturéia (-7.2669, -37.3514); 700 m, 20MAY2000, AV; three soldiers, pseudergates; SA497, 1255. Paraíba, Mamanguape (-6.8386, -35.1261); 33 m, 24JUN2000, AV; two soldiers, pseudergates; SA498, 1799. Paraíba, João Pessoa (-7.1554, -34.8731); 53 m, 20DEC2012, AV; three soldiers, five imagos; SA502, 4747. Paraíba, São José dos Cordeiros, RPPN Faz. Almas (-7.3905, -36.8083), 523 m, 07MAR2003, AV; three soldiers, pseudergates; 4746. Pernambuco, Buíque (-8.5333, -37.2333); 705 m, 16APR2009, AV; two soldiers, one imago, pseudergates; SA500, 3307. Pernambuco, Floresta Tacaratu (-8.6500, -38.0167); 924 m, 29JUN2010, A. A. V. O. Couto; one soldier, two imagos, pseudergates; SA503, 5014.

Figure 3. Soldier of *Tauritermes triceromegas* (PA942) **A** dorsal **B** lateral **C** oblique, and **D** ventral views of head and pronotum. DH = dorsal horn and FH = frontal horn.

Pernambuco, Igarassu (-7.8371, -35.0006); 129 m, 10MAR2016, A. A. V. O. Couto; two soldiers, pseudergates; SA505, 8512.

Distribution. (Fig. 5) Northeastern Brazil, Caatinga and Atlantic Forest biomes. *Tauritermes* localities taken from the literature are given in Table 3.

Etymology. Named for Dr. Adelmar Gomes Bandeira, the graduate and post-graduate advisor of AV who died in 2019. Dr. Bandeira was one of the first termitologists to work on termite ecology in the New World.

Biology. The colonies of *T. bandeirai* were collected inside dry trunks in the beginning stages of decomposition (diameter > 3cm) and in dead terminal branches still attached to the trunks, both in areas of Caatinga and Atlantic Forest. In the Caatinga, colonies of *T. bandeirai* were relatively easy to extract from dead terminal branches of *Commiphora leptophloeos* (Mart.) J.B. Gillett (Burseraceae). This tree is also a "hot spot" for collecting other kalotermitids, such as *Cryptotermes*, *Neotermes*, and *Rugitermes*.

Using light traps over a year (December 2017 to November 2018) in a Caatinga area located in the municipality of São José dos Cordeiros, Paraíba-Brazil, the alates of *T. bandeirai* were collected five times; once in December, thrice in January, and once in February. This period represents a transition between the dry and rainy season in the area. For the Atlantic Forest, alates were recorded in wood in March, June, and December.
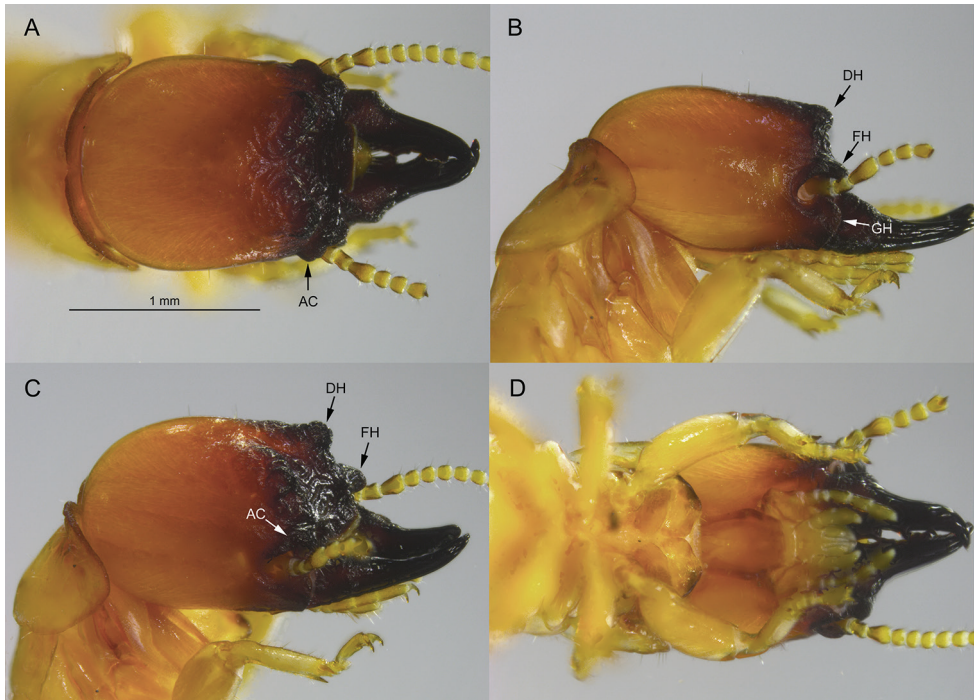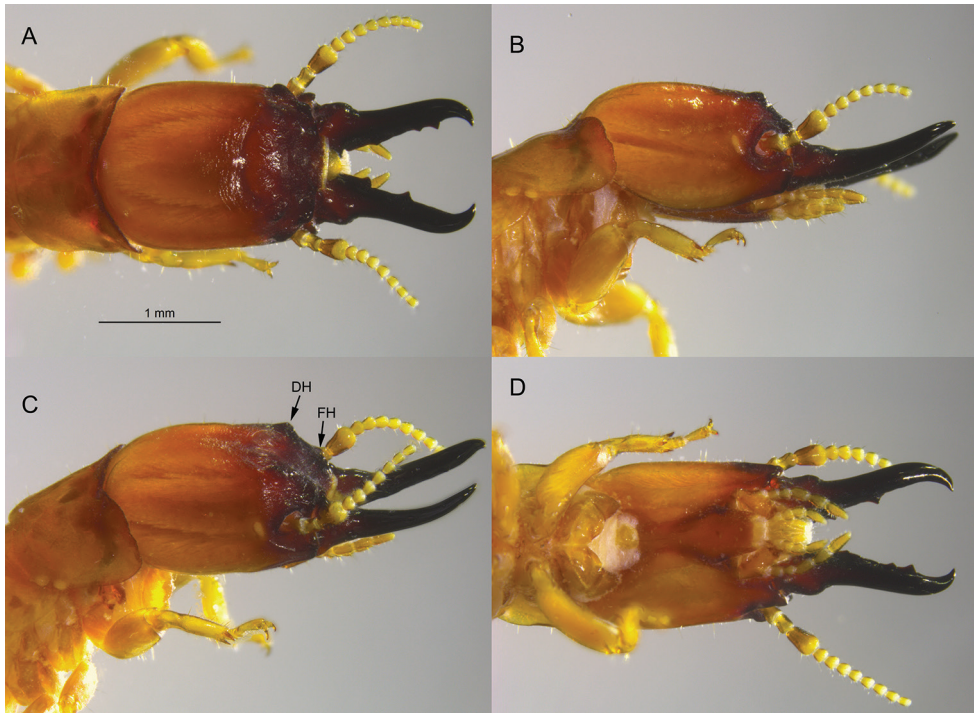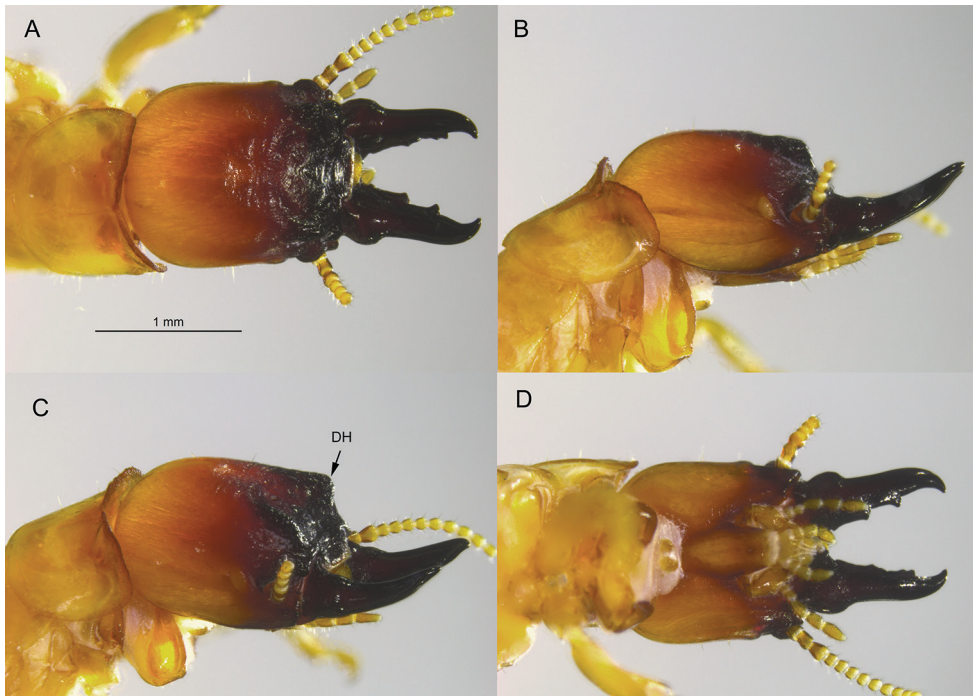
Figure 4. Soldier of *Tauritermes taurocephalus* (BO722) **A** dorsal **B** lateral **C** oblique, and **D** ventral views of head and pronotum. DH = dorsal horn.

Table 3. Localities of *Tauritermes* spp. Taken from the literature and mapped in Fig. 5.

Tauritermes sp.	Location	Latitude / Longitude	Reference
T. sp.	Brazil: Paraíba	-7.47, -36.87	Vasconcellos et al. (2010)
T. sp.	Brazil: Mataraca	-6.48, -34.93	Vasconcellos et al. (2005)
T. sp.	Brazil:Amazonas, Manaus	-3.1, -59.97	Dambros et al. (2013)
T. sp.	Brazil: "Atlantic forest"	-5.93, -35.18	Souza et al. (2012)
T. sp.	Brazil: Bahia, Mata de S. João	-12.97, -38.51	Cancello et al. (2014)
T. sp.	Argentina: Picomayo P. Nat.	-25.109, -58.144	Roisin and Leponce (2004)
T. taurocephalus	Argentina: Corrientes	-27.49, -58.8	Torales et al. (1997)
T. taurocephalus	Brazil: Mato Grosso, Corumbá	-19.02, -57.65	Silvestri (1901)
T. taurocephalus	Argentina: Chaco, Captain Solari	-26.8, -59.56	Godoy (2004)
T. taurocephalus	Artentina: Formosa, Pres. Irigoyen Dept.	-26.18, -58.85	Godoy (2004)
T. taurocephalus	Argentina: Formosa, P. N. Picomayo	-25.066, -58.089	Roisin and Leponce (2004)
T. taurocephalus	Argentina: Formosa, P. N. Picomayo	-25.026, -58.097	Roisin and Leponce (2004)
T. taurocephalus	Argentina: Salta, Urundel	-23.56, -64.4	Fontes (1998)
T. taurocephalus	Argentina: Salta, Urundel	-23.56, -64.4	Fontes (1998)
T. triceromegas	Argentina: Cordoba, Cosquin	-31.24, -64.47	Silvestri (1901)
T. triceromegas	Argentina: Corrientes, Concepcion	-27.48, -57.3	Torales et al. (1997)
T. triceromegas	Argentina: Salta, La Estrella	-23.82, -64.07	Fontes (1998)
T. vitulus	Brazil: Santa Catarina, Blumenau	-26.9, -49.1	Araujo and Fontes (1979)
T. vitulus	Brazil: Santa Catarina, Itapema	-27.1, -48.6	Araujo and Fontes (1979)

There are no records of *Tauritermes bandeirai* infestations in buildings, either in urban or agricultural environments. Other *Tauritermes* species infest sound, dry wood (RHS, unpubl.) and are even structural pests (Araujo and Fontes 1979).
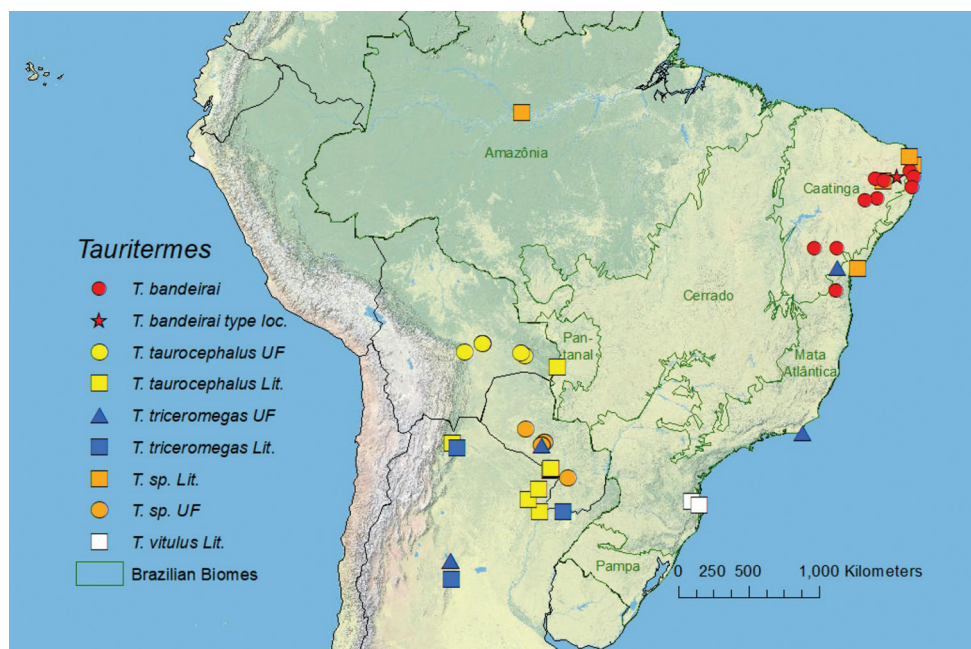
Figure 5. Map of *Tauritermes* from the literature and UFTC. Biomes are shown for Brazil. See Scheffrahn (2019b) for UFTC data and Table 3 for literature references.

Discussion

The Caatinga and the Atlantic Forest are neighboring domains (Fig. 5), but drastically different in terms of age and environmental conditions. The Caatinga is a semi-arid region of northeastern Brazil and is part of the "Seasonally Dry Tropical Forests" (Silva et al. 2017). On the other hand, the Atlantic Forest is distributed along the east coast of South America and is part of the "Tropical Rain Forests" (Morellato and Haddad 2000). Even with such different physiognomies and ecological dynamics, several species of termites, in addition to *T. bandeirai* sp. nov, are found in both domains such as *Heterotermes longiceps* (Snyder, 1924), *Ruptitermes reconditus* (Silvestri, 1901), *Nasutitermes macrocephalus* (Silvestri, 1903), *Microcerotemes indistinctus* Mathews, 1977, among others.

Acknowledgments

References

Araujo RL, Fontes LR (1979) Notes on the Neotropical genus *Tauritermes*, with a new species from Brasil (Isoptera, Kalotermitidae). Revista Brasileira de Entomologia 23(1): 29–34.

Cancello EM, Silva RR, Vasconcellos A, Reis YT, Oliveira LM (2014) Latitudinal variation in termite species richness and abundance along the Brazilian Atlantic Forest hotspot. Biotropica 46: 441–450. https://doi.org/10.1111/btp.12120

Dambros CS, Silva VNV, Azevedo R, Morais JW (2013) Road-associated edge effects in Amazonia change termite community composition by modifying environmental conditions. Journal for Nature Conservation 21: 279–285. https://doi.org/10.1016/j.jnc.2013.02.003

Fontes LR (1998) Novos aditamentos ao "Catálogo dos Isoptera do Novo Mundo", e uma filogenia para os gêneros neotropicais de Nasutitermitinae. In: Fontes LR, Vulcano M (Eds) Cupins: o Desafio do Conhecimento. Fundação de Estudos Agrários Luiz de Queiroz, São Paulo, 309–412.

Godoy MC (2004) Gut structure of two species of the Neotropical genus *Tauritermes* Krishna (Isoptera: Kalotermitidae). Neotropical Entomology 33(2): 163–167. https://doi.org/10.1590/S1519-566X2004000200006

Gonçalvez IS (1979) Anatomia do tubo digestivo de *Rugitermes niger* Oliveira, 1979 (Isoptera, Kalotermitidae). Revista Brasileira de Entomologia 23: 229–243.

Krishna K (1961) A generic revision and phylogenetic study of the family Kalotermitidae (Isoptera). Bulletin of the American Museum of Natural History 122(4): 303–408.

Krishna K, Grimaldi DA, Krishna V, Engel MS (2013) Treatise on the Isoptera of the world. Vol. 2 Basal Families. American Museum of Natural History Bulletin 377: 201–623. https://doi.org/10.1206/377.2

Mélo ACS, Bandeira AG (2004) A qualitative and quantitative survey of termites (Isoptera) in an open shrubby Caatinga in northeast Brazil. Sociobiology 44(3): 707–716.

Morellato LPC, Haddad CFB (2000) Introduction: The Brazilian Atlantic Forest. Biotropica 32(4b): 786–792. https://doi.org/10.1111/j.1744-7429.2000.tb00618.x

Myles TG (1997) A second species of the drywood termite genus *Marginitermes* (Isoptera: Kalotermitidae). The Canadian Entomologist 129(4): 757–768. https://doi.org/10.4039/Ent129757-4

Noirot C (1995) The gut of termites (Isoptera). Comparative anatomy, systematics, phylogeny. I. Lower termites. Annales de la Société entomologique de France 31: 197–226.

Roisin Y, Leponce M (2004). Characterizing termite assemblages in fragmented forests: A test case in the Argentinian Chaco. Austral Ecology 29(6): 637–646. https://doi.org/10.1111/j.1442-9993.2004.01403.x

Scheffrahn RH (2014) *Incisitermes nishimurai*, a new drywood termite species (Isoptera: Kalotermitidae) from the highlands of Central America. Zootaxa 3878(5): 471–478. https://doi.org/10.11646/zootaxa.3878.5.5

Scheffrahn RH (2019a) Expanded New World distributions of genera in the termite family Kalotermitidae. Sociobiology 66(1): 136–153. https://doi.org/10.13102/sociobiology.v66i1.3492

Scheffrahn RH (2019b) UF Termite database. University of Florida termite collection. https://www.termitediversity.org/ [Accessed on: 2020-3-10]

Silva JMC, Leal I, Tabarelli M [Ed]) (2017) Caatinga: The largest tropical dry forest region in South America. Springer International Publishing, New York. https://doi.org/10.1007/978-3-319-68339-3

Silvestri F (1901) Nota preliminare sui Termitidi sud-americani. Bollettino dei Musei di Zoologia ed Anatomia Comparata della Reale Università di Torino 16 (389): 1–8. https://doi.org/10.5962/bhl.part.26628

Souza HBDA, Alves WDF, Vasconcellos A (2012) Termite assemblages in five semideciduous Atlantic Forest fragments in the northern coastland limit of the biome. Revista Brasileira de Entomologia 56: 67–72. https://doi.org/10.1590/S0085-56262012005000013

Torales GJ, Laffont ER, Arbino MO, Godoy MC (1997) Primera lista faunística de los isópteros de la Argentina. Revista de la Sociedad Entomológica Argentina 56: 47–53.

Vasconcellos A, Mélo ACS, Segundo EDMV, Bandeira AG (2005) Termites from two Restinga forests of Northeastern Brazil. Iheringia Série Zoologia, 95: 127–131. https://doi.org/10.1590/S0073-47212005000200003

Vasconcellos A, Bandeira AG, Moura FMS, Araújo VFP, Gusmão MAB, Constantino R (2010) Termite assemblages in three habitats under different disturbance regimes in the semiarid Caatinga of NE Brazil. Journal of Arid Environments 74: 298–302. https://doi.org/10.1016/j.jaridenv.2009.07.007

RESEARCH ARTICLE

A new species of the genus *Lycodon* (Serpentes, Colubridae) from Guangxi, China

Jian Wang[1*], Shuo Qi[1*], Zhi-Tong Lyu[1,2], Zhao-Chi Zeng[1], Ying-Yong Wang[1]

1 *State Key Laboratory of Biocontrol/The Museum of Biology, School of Life Sciences, Sun Yat-sen University, Guangzhou 510275, China* **2** *School of Ecology, Sun Yat-sen University, Guangzhou 510006, China*

Corresponding author: *Ying-Yong Wang* (wangyy@mail.sysu.edu.cn)

Citation: Wang J, Qi S, Lyu Z-T, Zeng Z-C, Wang Y-Y (2020) A new species of the genus *Lycodon* (Serpentes, Colubridae) from Guangxi, China. ZooKeys 954: 85–108. https://doi.org/10.3897/zookeys.954.53432

Abstract

A new species of colubrid snake, *Lycodon cathaya* **sp. nov.**, is described based on two adult male specimens collected from Huaping Nature Reserve, Guangxi, southern China. In a phylogenetic analyses, the new species is shown to be a sister taxon to the clade composed of *L. futsingensis* and *L. namdongensis* with low statistical support, and can be distinguished from all known congeners by the significant genetic divergence in the mitochondrial cytochrome *b* gene fragment (*p*-distance ≥ 7.9%), and morphologically by the following combination of characters: (1) dorsal scales in 17–17–15 rows, smooth throughout; (2) supralabials eight, third to fifth in contact with eye, infralabials nine; (3) ventral scales 199–200 (plus two preventral scales), subcaudals 78; (4) loreal single, elongated, in contact with eye or not, not in contact with internasals; (5) a single preocular not in contact with frontal, supraocular in contact with prefrontal, two postoculars; (6) maxillary teeth 10 (4+2+2+2); (7) two anterior temporals, three posterior temporals; (8) precloacal plate entire; (9) ground color from head to tail brownish black, with 31–35 dusty rose bands on body trunk, 13–16 on tail; (10) bands in 1–2 vertebral scales broad in minimum width; (11) bands separate ground color into brownish black ellipse patches arranged in a row along the top of body and tail; (12) elliptical patches in 3–6 scales of the vertebral row in maximum width; (13) ventral surface of body with wide brownish black strip, margined with a pair of continuous narrow greyish white ventrolateral lines. With the description of the new species, 64 congeners are currently known in the genus *Lycodon*, with 16 species occurring in China.

Keywords

---

* Contributed equally as the first authors.

Introduction

The colubrid genus *Lycodon* Boie, 1827 currently comprises 63 known species, and is distributed widely throughout the Middle East to Southeast Asia, as well as to the Indo-Australian Archipelago (Lanza 1999; Siler et al. 2013; Neang et al. 2014; Uetz et al. 2020). Fifteen species have so far been recorded from China, i.e. *L. aulicus* (Linnaeus, 1758), *L. fasciatus* (Anderson, 1879), *L. flavozonatus* (Pope, 1928a), *L. futsingensis* (Pope, 1928b), *L. gongshan* Vogel & Luo, 2011, *L. laoensis* Günther, 1864, *L. liuchengchaoi* Zhang, Jiang, Vogel & Rao, 2011, *L. meridionalis* Bourret, 1935, *L. multizonatus* (Zhao & Jiang, 1981), *L. rosozonatus* (Hu & Zhao, 1972), *L. rufozonatus* Cantor, 1842, *L. ruhstrati* (Fischer, 1886), *L. septentrionalis* (Günther, 1875), *L. subcinctus* Boie, 1827 and *L. synaptor* Vogel & David, 2010 (Zhao. 1981; Zhao et al. 1998; Luo et al. 2010; Vogel and David 2010; Vogel and Luo 2011; Zhang et al. 2011).

During recent herpetological surveys in Guangxi, southern China, two colubrid snake specimens were collected from Huaping Nature Reserve (Fig. 1). Detailed morphological examinations and further molecular analyses revealed that these specimens represented a separately evolving lineage within the genus *Lycodon* and can be distinguished from all recognized congeners. We herein describe this overlooked *Lycodon* population as a new species, based on an integrative taxonomic approach.
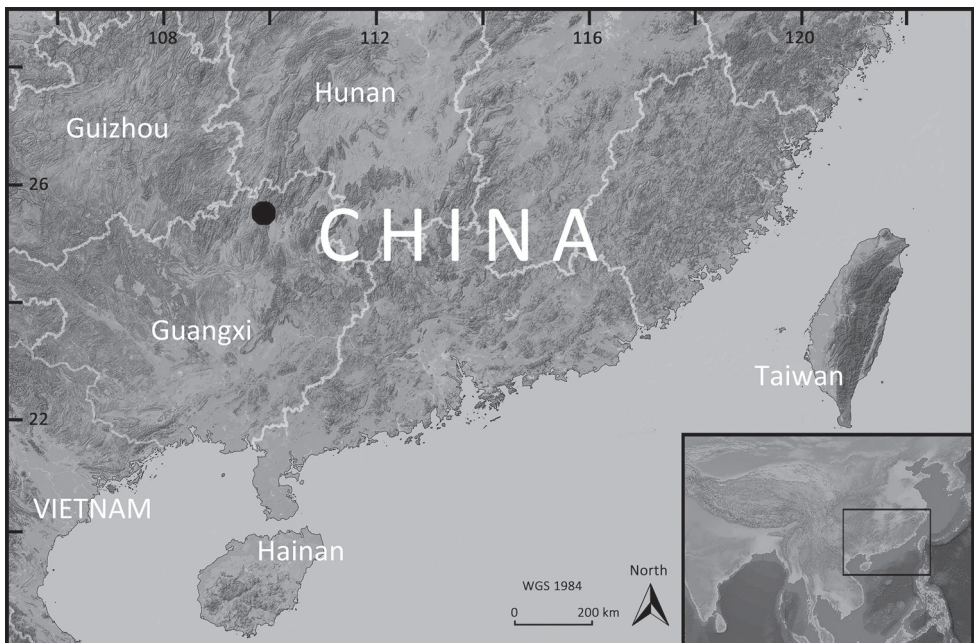
Figure 1. The type locality of *Lycodon cathaya* sp. nov., Huaping Nature Reserve, Guangxi, China.

Materials and methods

Morphometrics

Morphological examinations were performed based on two specimens collected from Huaping Nature Reserve, Guangxi, China. All specimens were fixed in 10 % buffered formalin and later transferred to 70 % ethanol for permanent preservation, and deposited in the Museum of Biology, Sun Yat-sen University (**SYS**).

Morphological descriptions followed Dowling (1951), Vogel (2009), Vogel and David (2010), and Janssen et al. (2019). Measurements were taken with digital calipers to the nearest 0.1 mm. These measurements were as follows:

ED   eye horizontal diameter;
HL   head length (from tip of snout to posterior margin of the mandible);
HW   maximum head width;
SVL   snout-vent length (from tip of snout to posterior margin of cloacal plate);
TaL   tail length (from posterior margin of cloacal plate to tip of tail);
TL   total length (from tip of snout to tip of tail).

Scalation features and their abbreviations are as follows: dorsal scale rows (**DSR**) counted at one head length behind head, at midbody, and at one head length before vent, respectively; supralabials (**SPL**); numbers of supralabials in contact with the eye (**SPL-E**); infralabials (**IFL**); chin shields (**CS**); numbers of infralabials in contact with the anterior chin shield (**IFL-aCS**); number of infralabials in contact with the posterior chin shield (**IFL-pCS**); preoculars (**PrO**); postoculars (**PtO**); loreal (**LoR**); loreal in contact with the eye or not (**L-E**); anterior temporals (**aTMP**); posterior temporals (**pTMP**); preventral scales (**PrV**); ventral scales (**V**); precloacal plate (**PrC**); subcaudals (**SC**); and body scale surface (**BSC**). Sex was determined by dissection or by the presence/absence of everted hemipenis. The number of maxillary teeth (**MT**) were counted by carefully dissecting the gums of the right maxilla under the stereo microscope. The light bands on the body and tail were counted on one side; hardly visible or incomplete bands were counted as one band; obviously fused bands were counted as two bands. The collar band on the neck was not included in counts and bands covering the cloacal plate were regarded as body bands.

Morphological characters of recognized *Lycodon* species were obtained from examination of museum specimens (see Appendix 1) and from the following references: Günther (1864), Günther (1875), Blanford (1878), Boulenger (1893), Boulenger (1900), Wall (1906), Stejneger (1907), Griffin (1909), Taylor (1922), Pope (1928a, b), Smith (1943), Taylor (1950), Leviton (1965), Hu et al. (1975), Zhao (1981), Ota and Ross (1994), Manthey and Grossman (1997), Captain (1999), Lanza (1999), Slowinski et al. (2001), Daltry and Wüster (2002), Gaulke (2002), Gaulke et al.

(2003), Jackson and Fritts (2004), Vijayakumar and David (2005), Zhao (2006), Mukherjee and Bhupathy (2007), Mistry et al. (2007), Vogel et al. (2009), Bahuguna and Bhuta (2010), Vogel and David (2010), Vogel and Luo (2011), Zhang et al. (2011), Vogel et al. (2012), Guo et al. (2013), Vogel and Harikrishnan (2013), Grismer et al. (2014), Lei et al. (2014), Neang et al. (2014), Zhang et al. (2015), Gawor et al. (2016), Do et al. (2017), Wostl et al. (2017), Ganesh and Vogel (2018), Luu et al. (2018), Melvinselvan et al. (2018), Janssen et al. (2019), Luu et al. (2019), and Vogel and David (2019). Data shown in Table 1 was modified based on Janssen et al. (2019), with distinguishing characters marked in bold.

Phylogenetic analyses

For molecular analysis, a total of 20 samples was used, encompassing 18 samples from eight known *Lycodon* species (one sample of *L. fasciatus*, two samples of *L. flavozonatus*, four samples of *L. futsingensis*, two samples of *L. liuchengchaoi*, one sample of *L. multizonatus*, two samples of *L. rufozonatus*, four samples of *L. ruhstrati*, and two samples of *L. subcinctus*) and two samples of the unnamed species. Tissue samples were taken prior to fixation, and preserved in 99 % alcohol and stored at -40 °C.

Genomic DNA was extracted from muscle or liver tissue samples, using a DNA extraction kit from Tiangen Biotech (Beijing) Co., Ltd. A fragment of the mitochondrial cytochrome *b* (CYTB) gene was amplified using the primer pair L14910 (5'–GACCT-GTGATMTGAAAACCAYCGTTGT-3') and H16064 (5'– CTTTGGTTTACAA-GAACAATGCTTTA-3') following Burbrink et al. (2000). PCR amplification was run using the following cycling conditions: initial denaturing step at 94 °C for 5 min; followed by 35 cycles of 94 °C for 30 s, 48 °C for 1 min and 72 °C for 70 s; and final extension step at 72 °C for 10 min. PCR products were purified with spin columns and then sequenced with forward primers using BigDye Terminator Cycle Sequencing Kit as per the guidelines on an ABI Prism 3730 automated DNA sequencer by Guangzhou Tianyi Huiyuan Bio-tech Co., Ltd.

Twenty sequences from 12 known *Lycodon* species and two out-group sequences *Boiga cynodon* (Boie, 1872) and *Dasypeltis atra* Sternfeld, 1912, following Janssen et al. (2019) were obtained from GenBank and incorporated into our dataset (Table 2). DNA sequences were aligned by the Clustal W algorithm with default parameters (Thompson et al. 1997) and trimmed with gaps partially deleted in MEGA 6 (Tamura et al. 2013). The aligned dataset was tested in jmodeltest v2.1.2 (Darriba et al. 2012) with Akaike and Bayesian information criteria, all resulting the best-fitting nucleotide substitution models of GTR+I+G. Sequence data was analyzed using Bayesian inference (BI) in MrBayes 3.2.4 (Ronquist et al. 2012), and maximum likelihood (ML) in RaxmlGUI 1.3 (Silvestro and Michalak 2012). In the BI analysis, three independent runs were conducted, each being run for 2 million generations and sampled every 1000 generations with the first 25% samples were discarded as burn-in. In the ML analysis, the bootstrap consensus tree was inferred from 1000 replicates. Pairwise distances (*p*-distance) were calculated in MEGA6 using the uncorrected *p*-distance model.

Table 1. Selected morphological characters of *Lycodon* species for comparison (after Janssen et al. 2019, see Materials and methods). Bold font indicates distinguishing characteristics.

Lycodon species	*cathaya* sp. nov.	*albofuscus*	*alcalai*	*anamallensis*	*aulicus*	*banksi*	*bibonius*	*butleri*	*capucinus*	*cardamomensis*	*carinatus*
DSR	17-17-15	?-17-?	**19-17-15**	17-17-15	17-17-15	17-17-15	**19-17-15**	**?-17/19-?**	17-17-15	**19-17-15**	17/19-**19**-17
MT	10	**12**	**11-13**	?	?	?	**11-14**	?	**15**	10-12	?
SPL	8	8	**9**	**9**	8-10	8	7-9	8-9	**9-10**	**9-10**	8-9
SPL-E	3rd–5th	3rd–5th	**4th–5th**	3rd–5th	3rd–5th	3rd–5th	3rd/4th–5th	3rd–5th	3rd–5th	3rd–5th	3rd–5th
IFL	9	?	**10**	**10-11**	**10-11**	**10**	9-10	9-10	9-10	9-10	?
PrO	1	1	**2**	2-3	1	1	**2**	1	1	1	1
PoO	2	2	**3**	1-2	2	2	2-3	2	2	2-3	2
Loreal	1	1	1	1-2	1	1	1	1	1	1	1
L-E	yes/no	no	no	?	no	no	no	yes	no	no	no
aTMP	2	2	2	2	2	2	2+3	2	2	2	2
pTMP	3	**2**	3	**3-4**	3	3	**2+3+3**	**2**	3	2-3	2-3
V	199–200	241	203–207	174–204	180–215	241	204–212	220–227	182–211	215–228	185–202
SC	78	155–208	108–126	60–74	57–78	26 (broken tail)	110–120	81–96	59–74	87–93	51–64
PrC	entire	**divided**	entire	entire/divided	**divided**	entire	entire	entire	**divided**	entire	entire
BSC	smooth	keeled	smooth	smooth	smooth and glossy	smooth (**six central DSR of posterior 1/3 feebly keeled**)	smooth	keeled	weakly keeled	weakly keeled	strongly keeled

Lycodon species	*cavernicolus*	*chrysopateros*	*davidi*	*davisonii*	*dumerilii*	*effraenis*	*fasciatus*	*fuasti*	*ferroni*	*flaviocollis*	*flavomaculatus*
DSR	17-17-15	**19-17-15**	17-17-15	**?-13-?**	**19-17-15**	?-17-?	17-17-15	**19-17-15**	**19-17-15**	17-17-15	17-17-15
MT	?	**11-13**	**11**	?	**13-15**	?	**11**	**13**	**12**	?	?
SPL	**9-10**	**9**	8	7	**11-13**	**9**	8	**9**	**10**	**9**	**9**
SPL-E	**4th–6th**	3rd–5th	3rd–5th	**3rd–4th**	**4th–5th**	3rd–5th	3rd–5th	**4th–5th**	**4th–6th**	3rd–5th	3rd–5th
IFL	**10-11**	**10**	**10**	8	9-10	**10-11**	8-10	9-10	**10**	**11**	**10**
PrO	1	**2**	1	1	1-2	1	1	**2**	**2**	1	1
PoO	2	2-3	2	2-3	2	2-3	2	**3**	2	2	2
Loreal	1	1	1	1	1	**0**	1	1	1	1	1
L-E	yes	no	no	yes	yes/no	**no LoR**	yes	?	no	no	no
aTMP	2-3	2-3+4	2	1-2	2	2	2	2	2	2-3	1-2
pTMP	**3-4**	2-3-4	2-3	**2**	3	2-3	**2**	2-3	**3-4**	3 (rarely 2)	3 (rarely 2)
V	232–245	186–194	224	233–265	195–221	215–228	182–225	207–215	203	210–224	165–183
SC	92–113	111–117	99	90–108	111–120	72–99	65–94	135–148	109	65–72	53–63
PrC	entire	entire	entire	entire	entire	entire	entire	**divided**	entire	**divided**	**divided**
BSC	**the 8 medial rows weakly keeled**	smooth	middorsal scale rows slightly **keeled**	smooth	?	smooth	**keeled**	smooth	smooth	smooth with single apical pit	smooth

Table 1. Continued.

Lycodon species	flavozonatus	futsingensis	gammiei	gibsonae	gongshan	gracilis	hypsirhinoides	jara	kundui	laoensis	liuchengchaoi
DSR	17–17–15	17–16/17–15	17–17/19–15	17–17–15	17–17–15	?–15–?	17–17–15	17–17–15	15–15–15	17–17–15	17–17–15
MT	13	12–15	?	13	?	9	9	?	?	?	8–9
SPL	8	7–8	7–9	8	8	8	9	8–9	7	9–10	7–8
SPL-E	3rd–5th	2–4; 3/4–5; 4–6	3rd–4th/5th	3rd–4th/5th	3rd–5th	3rd–4th	3rd–5th	3rd–5th	3rd–4th	3rd–5th	3rd–5th
IFL	10	9–11	?	10	8	?	10	1	?	10	7–9
PrO	1	1	1	1	1	2	1	1	?	1	1
PrO	2	2–3	1–2	2	2	2	2	2	2	2–3	2
Loreal	1	1	1	1	1	1	1	1	1	1	1
LoR-E	no	no	no	yes	yes	yes	no	no	no	no	yes
aTMP	2	1–2	2 or irregular	2	2	2	2	1–2	1	2	1–3
pTMP	2–3	2–3	2 or irregular	3	2–3	3	3	2–3	2	3	1–3
V	211–221	193–208	205–220	223–226	210–216	234	188–210	167–188	186	163–192	190–228
SC	80–88	72–87	98–111	91–92	92–96	81–83	61–75	52–74	70	60–76	68–75
PrC	entire /divided	entire	entire	entire	entire	entire	divided	divided	entire /divided	divided	divided
BSC	the 7 medial rows feebly keeled	smooth	the 9 medial rows keeled	upper 3 or 4 rows keeled	the 7–13 medial rows keeled	keeled	smooth	smooth	smooth	smooth	feebly keeled in median rows

Lycodon species	mackinnoni	meridionalis	muelleri	multifasciatus	multizonatus	namdongensis	nympha	ophiophagus	orientalis	paucifasciatus	philippinus
DSR	17–17–15	17–17–15	19–17–15	17–17–?	17–17–15	17–17–15	13–13–13	17–17–15	?–17–?	19–17/19–15	?–15–?
MT	?	11	14–15	?	10–11	12	8–10	11–13	10–11	11–12	8
SPL	7–8	8	9	?	7–8	8	6–8	8	8	8	7
SPL-E	3rd–5th	3rd–5th	4th–5th	?	3rd–5th	3rd–5th	3rd–4th	3rd–5th	3rd–5th	3rd–5th	3rd–4th
IFL	8	10	10	?	7–8	10	?	10	8	10	7
PrO	1	1	1–2	?	0–1	1–2	1–2	1	0	1	0–1
PrO	2	2	2–3	?	2	3	2	2	2	2	2–3
Loreal	0–1	1	1	?	1	1	1	1	1	1	1
L-E	no	no	no	no	yes	no	yes	no	yes	no	yes
aTMP	1–2	2	2	?	1–2	2	2	2	2	2	2
pTMP	2–3	3	3+4	?	2–3	2	2–3	3	3	3	3
V	163–187	227–240	205–213	229–237	190–195	218	200–243	211–212	200–208	219–222	216–225
SC	48–56	96–106	112–117	106–119	68–75	85	65–88	87–90	68–74	90–92	87–99
PrC	divided	divided	entire	?	divided	entire	divided	entire	divided	entire	entire
BSC	smooth	the 10–12 medial rows feebly keeled	?	keeled	smooth	smooth	keeled	smooth	scales with a very faint keel along their anterior half	the 3–5 medial rows distinctly keeled	smooth

Table 1. Continued.

Lycodon species	*pictus*	*rosozonatus*	*rufozonatus*	*rubstrati rubstrati*	*rubstrati abditus*	*sealei*	*semicarinatus*	*septentrionalis*	*sidiki*	*soliuvagus*	*stormi*
DSR	17–17–15	19–19–15/17	17/19–17–15	17–17–15		?–17–?	?–17–?	17–17–15	17–17–15	19–17–15	?–19–?
MT	13–14	12–13	11–13	?	11–13	?	?	7	7	11–13	?
SPL	8	8	8	8		?	8	8	8	9	8
SPL-E	3rd–5th	?	3rd–5th	3rd–5th		?	3rd–5th	3rd–5th	3rd–5th	4th–5th	3rd–4th
IFL	10	?	9–10	9–10	9–11	?	?	7–8	9–10	10	?
PrO	1	1	1	1	1	0	1	1	0	2	1
PtO	2	2	2	1–2	2	?	2	2	2	2–3	2
Loreal	1	1	1	1	1	1	1	1	1	1	1
L-E	yes	no	no	no		yes	no	no	yes	no	no
aTMP	2 (rarely 1)	2	2	1–2		1	2	2	2	2	1
pTMP	3 (rarely 2)	3	3	2–3		?	3	3	2	3	3
V	212–218	221–234	184–225	212–228	197–229	?	211–234	202–224	195	198–203	217
SC	90–91	?	53–98	97–114	90–103	?	65–105	83–104	85	112–115	75
PrC	entire	entire	entire	entire		divided	entire	entire	divided	entire	entire
BSC	smooth	weakly keeled	feebly keeled in the posterior body part	the 7–13 medial rows distinctly keeled	the 5 medial rows distinctly keeled	?	keeled along anterior half (4 outer rows smooth)	the 7/9 medial rows feebly keeled	keeled	smooth	smooth

Lycodon species	*striatus*	*subannulatus*	*subcinctus*	*striatus*	*submamulatus*	*subcinctus*	*synaptor*	*tessellatus*	*tiwarii*	*travancoricus*	*tristrigatus*
DSR	17–17–15	15–15–15	17–17–15	17–17–15	15–15–15	17–17–15	15/17–17–15	17–17–15	?–17–15	17–17–15	?–15–?
MT	?	8–10	8–14	?	8–10	8–14	10	?	?	?	8–10
SPL	9	7	8	9	7	8	8	8–9	?	9	7
SPL-E	3rd–5th	3rd–4th	3rd–5th/6th	3rd–5th	3rd–4th	3rd–5th/6th	3rd–5th	4th–5th	?	3rd–5th	3rd–4th
IFL	11	8	7–8	11	8	7–8	8	?	?	?	?
PrO	1	1	0	1	1	0	1	1	?	1	0
PtO	2	2	2–3	2	2	2–3	2	2	?	2	2
Loreal	1	1	1	1	1	1	1	1	?	1	1
L-E	no	yes	yes	no	yes	yes	no	no	?	no	yes
aTMP	2 (rarely 1)	2	1	2 (rarely 1)	2	1	2	2	?	2–3	2
pTMP	3 (rarely 2)	2	2	3 (rarely 2)	2	2	2	2–3	?	3	2–3
V	153–178	225–244	190–230	153–178	225–244	190–230	201–203	222–232	218–237	176–206	224
SC	42–66	93–111	60–91	42–66	93–111	60–91	68–69	56	61–102	64–76	86
PrC	divided	entire	entire/divided	divided	entire	entire/divided	entire	divided	divided	entire	entire
BSC	smooth	keeled	feebly keeled	smooth	keeled	feebly keeled	the 6–7 medial rows keeled	smooth	?	smooth	keeled

Table 1. Continued.

Lycodon species	striatus	subannulatus	subcinctus	synaptor	tessellatus	tiwarii	travancoricus	tristrigatus	zawi	zoosvictoriae
DSR	17–17–15	15–15–15	17–17–15	15/17–17–15	17–17–15	?–17–15	17–17–15	?–15–?	17–17–15	17–17–15
MT	?	8–10	8–14	10	?	?	?	8–10	12	9
SPL	9	7	8	8	8–9	?	9	7	8–9	8
SPL-E	3rd–5th	3rd–4th	3rd–5th/6th	3rd–5th	4th–5th	?	3rd–5th	3rd–4th	3rd–5th	3rd/4th–5th
IFL	11	8	7–8	8	?	?	?	?	9–10	10
PrO	1	1	0	1	1	?	1	0	1	1–2
PtO	2	2	2–3	2	2	?	2	2	1–2	2
Loreal	1	1	1	1	1	?	1	1	1	1
L-E	no	yes	yes	no	no	?	no	yes	no	no
aTMP	2 (rarely 1)	2	1	2	2	?	2–3	2	2–3	2
pTMP	3 (rarely 2)	2	2	2	2–3	?	3	2–3	3–4	2
V	153–178	225–244	190–230	201–203	222–232	218–237	176–206	224	179–207	213
SC	42–66	93–111	60–91	68–69	56	61–102	64–76	86	45–75	85
PrC	divided	entire	entire/divided	entire	divided	divided	entire	entire	divided	entire
BSC	smooth	keeled	feebly keeled	the 6–7 medial rows keeled	smooth	?	smooth	keeled	smooth	weakly keeled

Table 2. Localities, voucher information, and GenBank numbers for all samples used in this study.

Lycodon species	Voucher No.	Collection locality	GenBank No.	References
(1) *Lycodon cathaya* sp. nov.	SYS r001542	**China:** Huaping National NR, Longsheng County, Guangxi	MT602075	This study
(2) *Lycodon cathaya* sp. nov.	SYS r001630	**China:** Huaping National NR, Longsheng County, Guangxi	MT602076	This study
(3) *L. banksi*	VNUF R.2015.20	**Laos:** Khammouane Province	MH669272	Luu et al. 2018
(4) *L. butleri*	LSUHC:8365	**Malaysia:** Bukit Larut, Perak	KJ607892	Grismer et al. 2014
(5) *L. butleri*	LSUHC:9137	**Malaysia:** Bukit Larut, Perak	KJ607891	Grismer et al. 2014
(6) *L. cavernicolus*	LSUHC 9985	**Malaysia:** Perlis	KJ607889	Grismer et al. 2014
(7) *L. cavernicolus*	LSUHC 10500	**Malaysia:** Perlis	KJ607890	Grismer et al. 2014
(8) *L. fasciatus*	CAS 234875	**Myanmar:** Chin State	KC010365	Siler et al. 2013
(9) *L. fasciatus*	CAS 234957	**Myanmar:** Chin State	KC010366	Siler et al. 2013
(10) *L. fasciatus*	SYS r002401	**China:** Ruili City, Yunnan	MT625862	This study
(11) *L. flavozonatus*	SYS r001357	**China:** Bamianshan National NR, Guidong County, Hunan	MT625850	This study
(12) *L. flavozonatus*	SYS r001358	**China:** Bamianshan National NR, Guidong County, Hunan	MT625851	This study
(13) *L. futsingensis*	SYS r001250	**China:** Mt. Nankun, Huizhou City, Guangdong	MT625847	This study
(14) *L. futsingensis*	SYS r001494	**China:** Shimentai National NR, Yingde City, Guangdong	MT625853	This study
(15) *L. futsingensis*	SYS r001667	**China:** Gaoping Provincial NR, Renhua County, Guangdong	MT625857	This study
(16) *L. futsingensis*	SYS r002123	**China:** Gaoping Provincial NR, Renhua County, Guangdong	MT625861	This study
(17) *L. gongshan*	GP 3516	**China:** Lincang City, Yunnan	KP901022	Guo et al. 2015
(18) *L. gongshan*	GP 3546	**China:** Lincang City, Yunnan	KP901024	Guo et al. 2015
(19) *L. laoensis*	FMNH 258659	**Laos:** Salavan Province	KC010368	Siler et al. 2013
(20) *L. laoensis*	LSUHC 8481	**Cambodia:** Pursat Province	KC010370	Siler et al. 2013
(21) *L. liuchengchaoi*	SYS r001654	**China:** Shennongjia National NR, Hubei	MT625855	This study
(22) *L. liuchengchaoi*	SYS r001655	**China:** Shennongjia National NR, Hubei	MT625856	This study
(23) *L. namdongensis*	VNUF R.2017.23	**Vietnam:** Nam Dong Nature Reserve, Thanh Hoa	MK585007	Luu et al. 2019
(24) *L. meridionalis*	VNUF R.2017.54	**Vietnam:** Ninh Binh	MH669268	Luu et al. 2018
(25) *L. meridionalis*	VNUF R.2017.88	**Vietnam:** Ninh Binh	MH669269	Luu et al. 2018
(26) *L. multizonatus*	KIZ01623	**China:** Luding County, Sichuan	KF732926	Lei et al. 2014
(27) *L. multizonatus*	SYS r002411	**China:** Baishuijiang National NR, Longnan City, Gansu	MT625863	This study
(28) *L. pictus*	ZFMK93746	**Vietnam:** Ha Lang District, Cao Bang	MN395829	Janssen et al. 2019
(29) *L. pictus*	ZFMK93747	**Vietnam:** Ha Lang District, Cao Bang	MN395830	Janssen et al. 2019
(30) *L. rufozonatus*	SYS r001770	**China:** Mt. Tiantai, Zhejiang	MT625858	This study
(31) *L. rufozonatus*	SYS r002061	**China:** Yangjifeng National NR, Guixi City, Jiangxi	MT625860	This study
(32) *L. ruhstrati*	SYS r001275	**China:** Shaowu Jiangshi Provincial NR, Nanping City, Fujian	MT625848	This study
(33) *L. ruhstrati*	SYS r001309	**China:** Jiulianshan National NR, Longnan County, Jiangxi	MT625849	This study
(34) *L. ruhstrati*	SYS r001362	**China:** Bamianshan National NR, Guidong County, Hunan	MT625852	This study
(35) *L. ruhstrati*	SYS r001631	**China:** Huaping National NR, Longsheng County, Guangxi	MT625854	This study
(36) *L. semicarinatus*	N/A	**Japan:** Ryukyu Archipelago	AB008539	Kumazawa et al. 1996
(37) *L. subcinctus*	SYS r001155	**China:** Neilingding Island, Shenzhen City, Guangdong	MT625846	This study
(38) *L. subcinctus*	SYS r001943	**China:** Shimentai National NR, Yingde City, Guangdong	MT625859	This study
(39) *L. synaptor*	GP 3515	**China:** Lincang City, Yunnan	KP901021	Guo et al. 2015
(40) *L. synaptor*	GP 3545	**China:** Lincang City, Yunnan	KP901023	Guo et al. 2015
Outgroups				
(41) *Boiga cynodon*	KU 324614	**Philippines:** Negros Occidental	KC010340	Siler et al. 2013
(42) *Dasypeltis atra*	CAS 201641	**Uganda:** Kabale district	AF 471065	Lawson et al. 2005

Results

The CYTB nucleotide sequence matrix contained 1050 characters without insertion deletions. The MP and BI analyses produced essentially identical topologies, which were integrated in Fig. 2. Major nodes of the tree were supported with the Bayesian posterior probabilities (BPP) > 0.95 and the bootstrap supports (BS) for Maximum Likelihood analysis > 75. Uncorrected *p*-distances among *Lycodon* species based on the CYTB gene are shown in Table 3.

The phylogenetic topologies are very similar to those recovered by previous study (Janssen et al. 2019). The unnamed *Lycodon* samples from Guangxi, southern China clustered in a monophyletic lineage with high nodal supports (BPP = 1.00 and = BS 100). This lineage are genetically differentiated from all congeners with the uncorrected *p*-distance ≥ 7.9%, which is significant when compared with that between other recognized species (e.g., *p*-distance = 2.7 % between *L. flavozonatus* and *L. meridionalis*, *p*-distance 6.8 % between *L. futsingensis* and *L. namdongensis*, and *p*-distance = 6.7–7.1 % between *L. liuchengchaoi* and *L. multizonatus*). The phylogenetic placement of the new lineage is largely unresolved, even though it forms the sister taxon to the clade composed of *L. futsingensis* and *L. namdongensis* while the nodal support is insignificant.

Figure 2. Bayesian Inference and Maximum Likelihood phylogenies.

Table 3. Uncorrected *p*-distances among *Lycodon* species based on partial mitochondrial CYTB gene.

ID	*Lycodon* species	1–2	3	4–5	6–7	8–10	11–12	13–16	17–18	19–20	21–22	23	24–25	26–27	28–29	30–31	32–35	36	37–38	39–40
1–2	*Lycodon cathaya* sp. nov.	0																		
3	*L. banksi*	9.6	–																	
4–5	*L. butleri*	17.3	20.2	0																
6–7	*L. cavernicolus*	17	18.7	9.6	0															
8–10	*L. fasciatus*	12–13.7	14.6–16.3	10.4–11.5	9.8–10.7	0.7–1.8														
11–12	*L. flavozonatus*	9.3	10.1	18	17.4	14.2–14.6	0													
13–16	*L. futsingensis*	8.9	9.5	16.9	17.1	14.8–15.4	9.2	0												
17–18	*L. gongshan*	14.5–14.7	14.9–15.1	8.9–9.1	7.6–7.7	7.1–8.5	14.1–14.3	14.1–14.3	0.1											
19–20	*L. laoensis*	16.6–17.4	17–17.2	20.1–21.3	17.6–19.2	16.3–17.9	16.6–17.2	17.8–18.8	15.4–17	0.2										
21–22	*L. liuchengchaoi*	16.3–16.5	17–17.2	13.7–13.8	13.4–13.5	12.3–13	16.3–16.5	14.6–14.8	10.1–10.5	18.7–20.1	0.1									
23	*L. namdongensis*	7.9	8.8	17.1	16.5	14.2–15.2	8	6.8	14.3–14.5	17.2–18.2	15.7–15.9	–								
24–25	*L. meridionalis*	7.9	9.6	17.2	17.4	13.1–13.6	2.7	8.5	13.7–13.9	15.9–16.5	15.3–15.5	8.1	0							
26–27	*L. multizonatus*	14.8–15.1	16–16.7	14.2–14.5	14.5–15.8	15.6–15.8	12.7–13	14.6–15.4	11.9–12.1	18–19.4	6.7–7.1	15.2–15.9	15.3	1.6						
28–29	*L. pictus*	14.3–14.7	15.7–15.9	14.2–14.8	15.3–16	12.8–13.6	13.8–14.2	14.9	11.2–12.5	17.6–18.6	9.5–9.7	14.1–14.5	14	10–10.4	0.6					
30–31	*L. rufozonatus*	10.7–11.2	12.2–12.7	17.1	17.9–18.6	15.2–15.9	8.9–9.4	10.1–11	14.5–14.8	17.7–18.7	15.9–16.7	10.4–10.6	9.4–9.6	15.2–15.7	14–15.1	2				
32–35	*L. ruhstrati*	14–14.4	15.9–16.3	13.4–13.6	12.9–13.1	12.2–13.2	13.8–14	15.1–15.3	9.7–10.3	16–17.6	11.5–11.9	14.9–15.3	13.4–13.6	10.6–11.1	10.8–11.4	14–14.6	0–0.3			
36	*L. semicarinatus*	11.2	12.2	17.7	18.9	15.2–15.5	11.8	12.8	15.1–15.3	18.1–18.3	16.4–16.6	12.3	11.2	15.6	15.9–16.1	10.5–10.9	15–15.4	–		
37–38	*L. subcinctus*	15.8	17.3	18.4	16.5	16.2–16.8	15.5	16.2	16.1–16.3	15.7–16.5	17.9–18.1	16.1	15.9	17.9–18.1	16.1–17.1	16.4–17	13.6–13.8	17.9	0–0.3	
39–40	*L. synaptor*	16.6	18	15.4	13	12.8–13	15.3	15.4	11.5–11.6	18.9–19.5	14–14.2	15.4	15.1	14.3–14.7	12.2–12.4	14.1–14.5	11.1–11.2	17.1–17.6	17.6	0

Moreover, it is noteworthy that the unnamed *Lycodon* possesses significant morphological differences that can be easily distinguished from all other congeners (see below). Therefore, based on the combination of molecular and morphological data, we describe the unnamed population from Huaping Nature Reserve, Guangxi, southern China as a new species, *Lycodon cathaya* sp. nov.

Taxonomic account

Lycodon cathaya sp. nov.
http://zoobank.org/BA36B7DE-36BD-4B3C-A317-BF4B8E451A26
Figures 3A, 4, 5A, B

Holotype. SYS r001542, adult male, collected on 20 July 2016 by Jian Wang from Huaping Nature Reserve (25.62521N, 109.91376E (DD); ca 1000 m a.s.l.), Longsheng County, Guilin City, Guangxi Zhuang Autonomous Region, China.

Paratypes. SYS r001630, adult male, collected on 2 September 2016 by Jian Wang from Huaping Nature Reserve (25.62667N, 109.91351E (DD); ca 850 m a.s.l.).

Etymology. The specific name *cathaya* is a noun referring to the monotypic botanic genus *Cathaya* Chun & Kuang, 1958. The single species *C. argyrophylla* Chun & Kuang, 1958 is an endangered relict plant, and was firstly discovered from Huaping Nature Reserve by the investigation team of Sun Yat-sen University. In memory of the predecessors and their contributions on the taxonomy of Chinese flora and fauna, we denominate this new snake species from Huaping Nature Reserve as *Lycodon cathaya* sp. nov. Its common name is suggested as "Huaping wolf snake" in English and "Hua Ping Bai Huan She (花坪白环蛇)" in Chinese.

Diagnosis. *Lycodon cathaya* sp. nov. can be differentiated from its congeners by the combination of the following morphological characters: (1) dorsal scales in 17–17–15 rows, smooth throughout; (2) supralabials eight, third to fifth in contact with eye, infralabials 9; (3) ventral scales 199–200 (plus two preventral scales), subcaudals 78; (4) loreal single, elongated, in contact with eye or not, not in contact with internasals; (5) a single preocular not in contact with frontal, supraocular in contact with prefrontal, two postoculars; (6) maxillary teeth 10 (4+2+2+2); (7) two anterior temporals, three posterior temporals; (8) precloacal plate entire; (9) ground color from head to tail brownish black, with 31–35 dusty rose bands on body trunk, 13–16 on tail; (10) bands in 1–2 vertebral scales broad in minimum width; (11) bands separate ground color into brownish black ellipse patches, similar arrangement in a row along the top of body and tail; (12) elliptical patches in 3–6 scales of the vertebral row in maximum width; (13) ventral surface of body with a wide brownish black strip, margined with a pair of continuous narrow greyish white ventrolateral lines.

Comparisons. The detailed comparisons among all *Lycodon* congeners are given in Table 1, with distinguishing characters marked in bold.

In our phylogenetic tree (Fig. 2), *Lycodon cathaya* sp. nov. (Figs 3A, 4, 5A, B) is relatively close to *L. futsingensis* (Figs 3B, 5C) and *L. namdongensis*. However, the new species possesses significant morphological differences: (1) 10 maxillary teeth (vs. MT 12–15 in *L. futsingensis*), bands on dorsal body and tail link with each other and separate ground color into ellipse patches (vs. bands on dorsal body and tail separate with each other in *L. futsingensis*), venter line on ventral body margined with a pair of continuous ventrolateral line (vs. ventrolateral lines discontinuous, interrupted by black patches in *L. futsingensis*); (2) ten maxillary teeth (vs. MT 12 in *L. namdongensis*), nine infralabials (vs. IFL ten in *L. namdongensis*), two postocular (vs. PtO 3 in *L. namdongensis*), three posterior temporals (vs. pTMP 3 in *L. namdongensis*), ventral scales 199–200 (vs. V 218 in *L. namdongensis*), dorsal body with 31–35 dusty rose bands (vs. dorsal body with 23 greyish cream bands in *L. namdongensis*).

Lycodon cathaya sp. nov. can be further distinguished from *L. ruhstrati* (Figs 3C, 5D), which used to be confused with *L. futsingensis*, to which it is morphologically similar (Pope 1935; Vogel et al. 2009), by the following morphological characters: (1) dorsal scales smooth throughout (vs. dorsum with keeled scales); (2) subcaudals 78 (vs. subcaudals ≥ 90); (3) bands on dorsal body and tail link with each other and separate ground color into ellipse patches (vs. bands on dorsal body and tail separate with each other); (4) ventral with a brownish black venter strip margined with a pair

Figure 3. General aspects in life and close-ups of body scales of **A** *Lycodon cathaya* sp. nov. (SYS r001542, holotype) from Huaping Nature Reserve, Guangxi, China **B** *L. futsingensis* (SYS r002123) from Gaoping Nature Reserve, Shaoguan City, Guangdong, China, and **C** *L. ruhstrati* (SYS r001631) from Huaping Nature Reserve, Guangxi, China.

of continuous greyish white ventrolateral lines (vs. brownish black venter strip absent, and ventrolateral lines discontinuous, interrupted by black patches).

Lycodon cathaya sp. nov. can be significantly distinguished from *L. albofuscus*, *L. banksi*, *L. butleri*, *L. capucinus*, *L. cardamomensis*, *L. carinatus*, *L. cavernicolus*,

Figure 4. General aspect of *Lycodon cathaya* sp. nov. (SYS r001542, holotype) in life when observed.

L. davidi, *L. fasciatus*, *L. flavozonatus*, *L. gammiei*, *L. gibsonae*, *L. gongshan*, *L. gracilis*, *L. liuchengchaoi*, *L. meridionalis*, *L. multifasciatus*, *L. nympha*, *L. orientalis*, *L. paucifasciatus*, *L. rosozonatus*, *L. semicarinatus*, *L. septentrionalis*, *L. sidiki*, *L. subannulatus*, *L. subcinctus*, *L. synaptor*, *L. tristrigatus* and *L. zoosvictoriae* by its smooth dorsal scales (vs. dorsal body with keeled scales). By having dorsal scales in 17–17–15 rows, *Lycodon cathaya* sp. nov. can be easily distinguished from *L. alcalai* (DSR 19–17–15), *L. bibonius* (DSR 19–17–15), *L. chrysoprateros* (DSR 19–17–15), *L. davisonii* (DSR ?–13–?), *L. dumerilii* (DSR 19–17–15), *L. fausti* (DSR 19–17–15), *L. ferroni* (DSR ?–13–?), *L. kundui* (DSR 15–15–15), *L. muelleri* (DSR 19–17–15), *L. philippinus* (DSR ?–15–?), *L. solivagus* (DSR 19–17–15) and *L. stormi* (DSR ?–19–?). From the remaining 18 congeners, *Lycodon cathaya* sp. nov. can be easily distinguished from *L. ophiophagus*, *L. pictus*, and *L. zawi* by having fewer maxillary teeth; from *L. anamallensis*, *L. effraenis*, *L. flavicollis*, *L. flavomaculatus*, *L. hypsirhinoides*, *L. laoensis*,
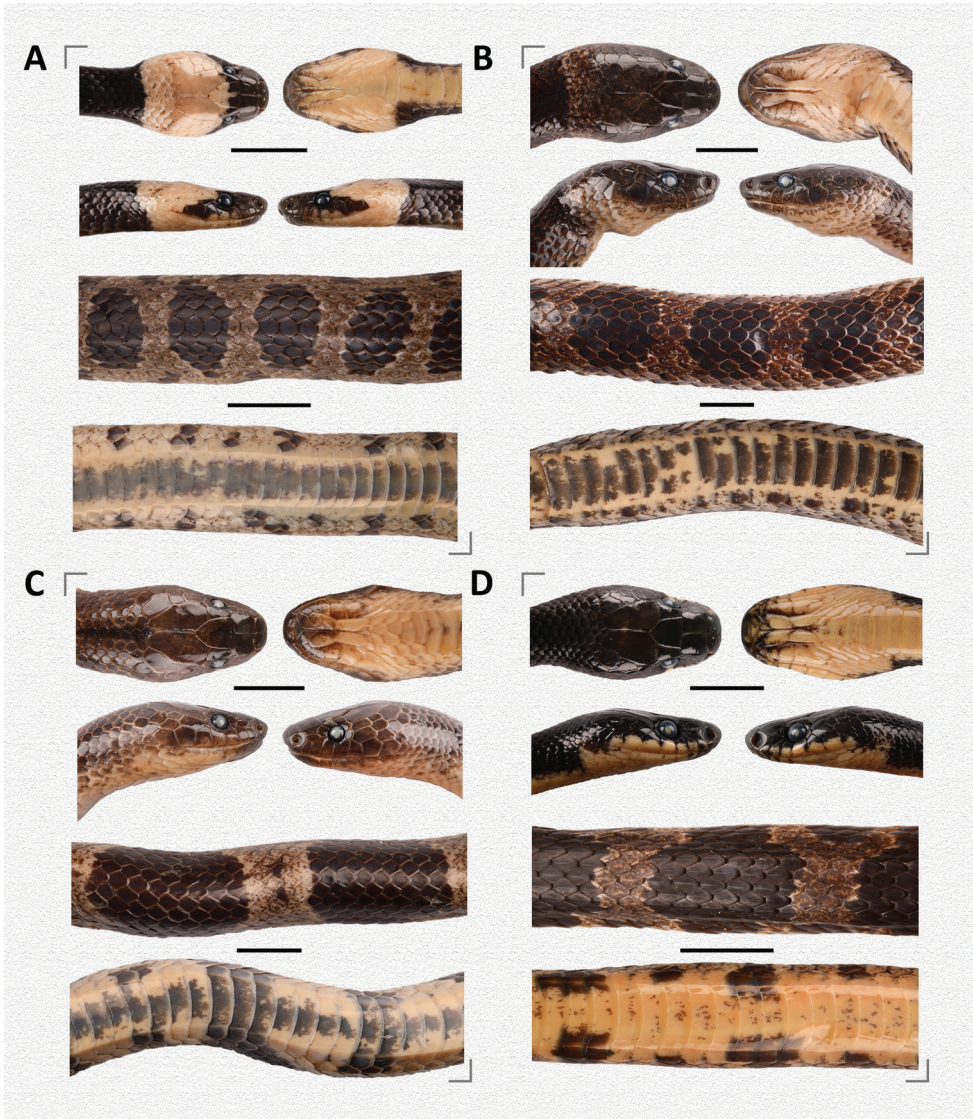
Figure 5. Comparative characters of head scalation and color patterns (in preservative) of **A** *Lycodon cathaya* sp. nov. (SYS r001542, holotype) **B** *Lycodon cathaya* sp. nov. (SYS r001630, paratype) **C** *L. futsingensis* (SYS r002123), and **D** *L. ruhstrati* (SYS r001631). Scale bars: 10 mm.

L. striatus, and *L. travancoricus* by having fewer supralabials; from *L. anamallensis*, *L. aulicus*, *L. effraenis*, *L. flavicollis*, *L. flavomaculatus*, *L. hypsirhinoides*, *L. laoensis*, *L. multizonatus*, *L. ophiophagus*, *L. pictus,* and *L. striatus* by having fewer infralabials and from *L. mackinnoni* by having more infralabials; from *L. aulicus*, *L. flavicollis*, *L. flavomaculatus*, *L. hypsirhinoides*, *L. jara*, *L. laoensis*, *L. mackinnoni*, *L. multizonatus*, *L. sealei*, *L. striatus*, *L. tessellatus,* and *L. tiwarii* by having an entire precloacal plate (vs. precloacal plate divided); from *L. jara*, *L. mackinnoni,* and *L. striatus* by having more

ventrals and from *L. pictus*, *L. tessellatus,* and *L. tiwarii* by having fewer ventrals; from *L. anamallensis*, *L. flavicollis*, *L. hypsirhinoides*, *L. jara*, *L. laoensis*, *L. flavomaculatus*, *L. mackinnoni*, *L. multizonatus*, *L. striatus*, *L. tessellatus* and *L. zawi* by having more subcaudals and from *L. ophiophagus* and *L. pictus* by having fewer subcaudals; from *L. effraenis* and *L. sealei* by the presence of a single loreal (vs. loreal absent).

Description of holotype. Adult male. Body slender, TL 562.5 mm (SVL 451.4 mm, TaL 111.1 mm, TaL/TL ratio 0.198); dorsal scales in 17–17–15 rows, smooth throughout, the vertebral scales not enlarged; head elongate, moderately distinct from neck, rather flattened, longer than wide, and narrow anteriorly, HL 17.2 mm, HW 11.1 mm (HW/HL ratio 0.643); eye large, ED 2.2 mm, pupil vertically elliptic; rostral triangular, much broader than high, barely visible from above; nostril lateral, located in the middle of nasal; nasal divided into two scales by nostril; two internasals, anteriorly rounded, almost as wide as high, bordered by two large, pentagonal prefrontals posteriorly; a single enlarged hexagonal frontal, narrowed posteriorly; parietals paired, longer than wide, in contact with each other medially, with upper anterior and posterior temporals, paraparietal laterally and four nuchal scales posteriorly; paraparietal slightly elongate, nearly rectangular; one elongated loreal on each side, in contact with eye, not in contact with internasals; one preocular located above loreal, in contact with eye and supraocular posteriorly, with prefrontal anteriorly, and not in contact with frontal; two postoculars, almost equal in length, upper one in contact with eye anteriorly, with supraocular and parietal, and with upper temporal posteriorly, lower one in contact with eye anteriorly, with anterior temporals posteriorly, and with fifth and sixth supralabials below; eight supralabials on each side, first and second in contact with nasal, third to fifth entering orbit; nine infralabials on each side, first pair in broad contact with each other, first to fourth in contact with anterior pair of chin shields, fourth to fifth in contact with posterior chin shields; two pairs of chin shields, elongate, anterior pair larger, second pair meeting in midline; two anterior temporals, almost equal in size, three posterior temporals, upper one smallest, lower one largest; 199 ventrals plus two preventrals; 78 pairs of subcaudals, excluding tail tip; precloacal plate entire.

Dentition. 10 (4+2+2+2) maxillary teeth on both sides, four small anterior teeth, enlarged posteriorly; two noticeably enlarged snag shaped teeth (second largest); two moderately enlarged teeth; two moderately enlarged kukri liked teeth (the anterior one larger, both with posterior cutting edges). Diastemas present between the above-mentioned maxillary teeth groups.

Hemipenis. Hemipenis elongated, apex not fully everted after injection of formalin. Truncus bulbous, lower 1/3 smooth without spines, spine ornamentation starting at upper part with somewhat enlarged, medium sized spines. Apex with dense microspines. Sulcus spermaticus stretches to base of apex. Apex not fully everted, ending somewhat widened with an oblique opening, with microspines inside.

Coloration of holotype. In life (Figs 3A, 4), dorsal surface of head brownish black, a distinctly dusty rose collar band that crosses over the head and nape of the neck; ventral surface of head almost white, mental, the 1st–3rd supralabials and the anterior pair of chin shields with brownish black patches, the 4th and 5th and the posterior pair of chin shields with brownish black mottles. Ground color of dorsal surface

Table 4. Measurements, scale counts, and body proportions of *Lycodon cathaya* sp. nov.

	Voucher number	
Character	1542	1630
Age	adult	adult
Sex	male	male
SVL	451.4	730.1
TaL	111.1	180.5
TL	562.5	910.6
TaL/TL	0.198	0.198
HL	17.2	23.3
HW	11.1	14.6
HW/HL	0.643	0.627
ED	2.2	3.0
DSR	17–17–15	17–17–15
SpL	8	8
IfL	9	9
IFL-1CS	1st–4th	1st–4th
IFL-2CS	4th–5th	4th–5th
CS	2	2
V	199	200
Sc	78	78
S-V Bands	35	31
TaL Bands	16	13
MT	10	10

brownish black, with 35 transverse dusty rose bands on body trunk and 16 similarly colored bands on tail, including two incomplete bands between collar band and the first complete transverse band; each band in 1–2 scales of the vertebral row in minimum width and widen laterally to a width of 3–4 scales; bands link with each other in ventrolateral body and tail, and separate the ground color into brownish black ellipse patches: such patches in 3–6 scales of the vertebral row in maximum width, and arranged in a row along the top of body and tail; a brownish black ventrolateral blotch on each ventrolateral side of bands. Middle of each ventral with irregular brownish black blotches forming a relatively continuous venter strip, and greyish white on both sides, forming a pair of continuous ventrolateral lines, which run in parallel along the venter strip. Subcaudals almost entirely light brown. In preservative (Fig. 5A), the collar band faded to beige, bands become darker, and the ventral surface faded to beige.

Variations. Measurements, body proportions and scale counts of the two specimens are listed in Table 4. The paratype has a relatively small and faint collar band, just crossing over the nape of the neck; dorsal bands are faint and there are more dark brown speckles than in the holotype. It appears that this specimen represents an older age group than the holotype, and differences in coloration may indicate an ontogenetic development. The loreal is in contact with eye in the holotype, while the loreal is separated from the eye by the preocular and the third supralabial.

Distribution and habits. Currently, *Lycodon cathaya* sp. nov. is only known from its type locality, Huaping Nature Reserve (Fig. 1; ca 850–1000 m a.s.l.), and is sympatric with *L. meridionalis* and *L. ruhstrati*. All of them are nocturnal species. The holotype was observed climbing on a wilted bush by the roadside, approximately half a meter above the ground (Fig. 4). The paratype and an individual of its sympatric species *L. ruhstrati*

is (Fig. 3C) were found on the ground on the same night. The surrounding environment consisted of well-preserved montane evergreen broad-leaved forest or mixed forest.

Discussion

The description of *Lycodon cathaya* brings the total species number of this genus to 64, 16 of which occur in China. The new discovery further emphasizes the very high diversity level of the genus *Lycodon* (Zhao 1981; Zhao et al. 1998; Zhao 2006; Luo et al. 2010).

The Huaping Nature Reserve is located in the hilly region among Guangxi, Hunan, and Guizhou. Thus, the new species is expected to occur in southwestern Hunan and southeastern Guizhou. The area within the jurisdiction of Huaping Nature Reserve has been well valued and protected by relevant local departments, with a considerable amount of research and investigation efforts having been conducted. However, further research on the true distribution, population sizes and trends, habitat conditions and conservation actions are urgently needed in the potential distribution areas outside the jurisdiction of Huaping Nature Reserve. Moreover, since the rapid and notable developments on the knowledge about the Chinese herpetofauna, the hilly regions in southern China have received more attention and a number of new species have been discovered in the recent years (Chen et al. 2018; Li et al. 2018; Lyu et al. 2018; Peng et al. 2018; Sung et al. 2018; Wang et al. 2018ab; Chen et al. 2019; Lyu et al. 2019ab; Wang et al. 2019abc; Wang et al. 2020ab); this in turn strengthens appeals for more powerful and targeted conservation actions in these regions.

Acknowledgements

References

Anderson J (1879) Reptilia and amphibia. Anatomical and Zoological Researches: Comprising an Account of the Zoological Results of the Two Expeditions to Western Yunnan in 1868

and 1875. Bernard Quarich, London 1: 705–860, 969–975. https://doi.org/10.5962/bhl. title.55401 [index 1878]

Bahuguna B, Bhuta PT (2010) Extension of the range and redescription of *Lycodon jara* (Shaw) (Reptilia: Serpentes: Colubridae). Records of the Zoological Survey of India 110(4): 3739.

Burbrink FT, Lawson R, Slowinski JB (2000) Mitochondrial DNA phylogeography of the polytypic North American rat snake (*Elaphe obsoleta*): a critique of the subspecies concept. Evolution 54(6): 2017–2018. https://doi.org/10.1554/0014-3820(2000)054[2107:MDP OTP]2.0.CO;2

Blanford WT (1878) Notes on some Reptilia from the Himalayas and Burma. Journal of the Asiatic Society of Bengal (2)47: 125–131.

Boie F (1827) Bemerkungen über Merrem's Versuch eines Systems der Amphibien, 1. Lieferung: Ophidier. Isis van Oken 20: 508–566.

Boulenger GA (1893) Catalogue of the Snakes in the British Museum (Natural History). Vol I. Trustees of the British Museum, London, 448 pp. [28 pls.]

Boulenger GA (1900) Description of a new snake from the Perak Hills. Journal of the Bombay Natural History Society 13: 336.

Captain A (1999) On the identification of *Lycodon flavomaculatus* Wall 1907. Journal of the Bombay Natural History Society 96: 323–327.

Chen WC, Bei YJ, Liao XW, Zhou SC, Mo YM (2018) A new species of *Gracixalus* (Anura: Rhacophoridae) from West Guangxi, China. Asian Herpetological Research 9: 74–84.

Chen WC, Liao X, Zhou SC, Mo YM (2019) A new species of *Leptobrachella* (Anura: Megophryidae) from southern Guangxi, China. Zootaxa 4563: 67–82. https://doi.org/10.11646/ zootaxa.4563.1.3

Daltry JC, Wüster W (2002) A new species of wolf snake (Serpentes: Colubridae: *Lycodon*) from the Cardamom Mountains, southwestern Cambodia. Herpetologica 58(4): 498–504. https://doi.org/10.1655/0018-0831(2002)058[0498:ANSOWS]2.0.CO;2

Darriba D, Taboada GL, Doallo R, Posada D (2012) JModelTest 2: more models, new heuristics and parallel computing. Nature Methods 9: 772. https://doi.org/10.1038/ nmeth.2109

Do DT, Ngo CD, Ziegler T, Nguyen TQ (2017) First record of *Lycodon cardamomensis* Daltry & Wüster, 2002, (Squamata: Colubridae) from Vietnam. Russian Journal of Herpetology 24(2): 167–170. https://doi.org/10.30906/1026-2296-2019-24-2-167-170

Dowling HG (1951) A proposed standard system of counting ventral in snakes. Journal of Herpetology 1: 97–99. https://doi.org/10.2307/1437542

Ganesh SR, Vogel G (2018) Taxonomic reassessment of the Common Indian Wolf Snakes *Lycodon aulicus* (Linnaeus, 1758) complex (Squamata: Serpentes: Colubridae). Bonn Zoological Bulletin 67(1): 25–36.

Gawor A, Pham CT, Nguyen TQ, Nguyen TT, Schmitz A, Ziegler T (2016) The herpetofauna of the Bai Tu Long National Park, northeastern Vietnam. Salamandra 52(1): 23–41.

Gaulke M (2002) A new species of *Lycodon* from Panay Island, Philippines (Reptilia, Serpentes, Colubridae). Spixiana 25: 85–92.

Gaulke M, Demegillo A, Reiter J, Tacud B (2003) Additions to the Herpetofauna of Panay Island, Philippines. Salamandra 39(2): 111–122.

Griffin LE (1909) A list of snakes found in Palawan. Philippine Journal of Science 4: 595–601.

Grismer LL, Quah ESH, Anuar S, Muin MA, Wood Jr PL, Aziza S (2014) A diminutive new species of cave-dwelling Wolf Snake (Colubridae: *Lycodon* Boie, 1826) from Peninsular Malaysia. Zootaxa 3815: 51–67. https://doi.org/10.11646/zootaxa.3815.1.3

Guo P, Zhang L, Liu Q, Li C, Pyron RA, Jiang K, Burbrink FT (2013) *Lycodon* and *Dinodon*: one genus or two? Evidence from molecular phylogenetics and morphological comparisons. Molecular Phylogenetics and Evolution 68: 144–149. https://doi.org/10.1016/j.ympev.2013.03.008

Günther ACLG (1864) The reptiles of British India. Ray Society, London, 452 pp. [pls 1–26]

Günther ACLG (1875) Second report on collection of Indian reptiles obtained by the British Museum. Proceedings of the Zoological Society of London 1875 (March): 224–234. [pls 30–34]

Hu SC, Djao EM, Huang CC (1975) Three new species of reptiles from Hainan Island, Guangdong Province (in Chinese with English abstract). Acta Zoologica Sinica, Peking 21(4): 379–384. [English translation by Koshikawa A (1982) Smithsonian Herpetological Information Service, Washington 53: 1–9.] https://doi.org/10.5479/si.23317515.53.1

Jackson K, Fritts TH (2004) Dentitional specialisations for durophagy in the Common Wolf snake, *Lycodon aulicus capucinus*. Amphibia-Reptilia 25: 247–254. https://doi.org/10.1163/1568538041975134

Janssen HY, Pham CT, Ngo HT, Le MD, Nguyen TQ, Ziegler T (2019) A new species of *Lycodon* Boie, 1826 (Serpentes, Colubridae) from northern Vietnam. ZooKeys 875: 1–29. https://doi.org/10.3897/zookeys.875.35933

Kumazawa Y, Ota H, Nishida M, Ozawa T (1998) The complete nucleotide sequence of a snake (*Dinodon semicarinatus*) mitochondrial genome with two identical control regions. Genetics 150: 313–329.

Lanza B (1999) A new species of *Lycodon* from the Philippines, with a key to the genus (Reptilia Serpentes Colubridae). Tropical Zoology 12: 89–104. https://doi.org/10.1080/03946975.1999.10539380

Lei J, Sun XY, Jiang K, Vogel G, Booth DT, Ding L (2014) Multilocus Phylogeny of *Lycodon* and the Taxonomic Revision of *Oligodon multizonatum*. Asian Herpetological Research 5: 26–37. https://doi.org/10.3724/SP.J.1245.2014.00026

Leviton AE (1965) Contributions to a review of Philippine snakes, VIII The snakes of the genus *Lycodon* H. Boie. The Philippine Journal of Science 94(1): 117–140.

Luo J, Ryabov SA, Luo Y, Gao HY, Luo ZR, Hu XC (2010) Classification and distribution of the genus *Dinodon*. Sichuan Journal of Zoology 29(4): 579–582. [in Chinese with English abstract]

Li C, Yuan ZY, Li HB, Wu YK (2018) The tenth member of Stout Newt (Amphibia: Salamandridae: *Pachytriton*): Description of a new species from Guangdong, southern China. Zootaxa 4399: 207–219. https://doi.org/10.11646/zootaxa.4399.2.5

Luu VQ, Bonkowski M, Nguyen TQ, Le MD, Calame T, Ziegler T (2018) A new species of *Lycodon* Boie, 1826 (Serpentes: Colubridae) from central Laos. Revue suisse de Zoologie 125(2): 263–276. https://doi.org/10.11646/zootaxa.4586.2.3

Luu VQ, Ziegler T, Ha NV, Le MD, Hoang TT (2019) A new species of *Lycodon* Boie, 1826 (Serpentes: Colubridae) from Thanh Hoa Province, Vietnam. Zootaxa 4586(2): 261–277. https://doi.org/10.11646/zootaxa.4586.2.3

Lyu ZT, Wu J, Wang J, Sung YH, Liu ZY, Zeng ZC, Wang X, Li YY, Wang YY (2018) A new species of *Amolops* (Anura: Ranidae) from southwestern Guangdong, China. Zootaxa 4418(6): 562–576. https://doi.org/10.11646/zootaxa.4418.6.4

Lyu ZT, Huang LS, Wang J, Li YQ, Chen HH, Qi S, Wang YY (2019a) Description of two cryptic species of the *Amolops ricketti* group (Anura, Ranidae) from southeastern China. ZooKeys 812: 133–156. https://doi.org/10.3897/zookeys.812.29956

Lyu ZT, Mo YM, Wan H, Li YL, Pang H, Wang YY (2019b) Description of a new species of Music frogs (Anura, Ranidae, *Nidirana*) from Mt. Dayao, southern China. ZooKeys 858: 109–126. https://doi.org/10.3897/zookeys.858.34363

Manthey U, Grossman W (1997) Amphibien & Reptilien Südostasiens. Natur und Tier-Verlag, Münster, 512 pp.

Melvinselvan G, Nibedita D, Murali G (2018) Observations on the reproduction and feeding habit of a rare colubrid, Indian bridal Snake *Lycodon nympha* Daudin 1803 (Serpentes: Colubridae) from Southern India. Captive & Field Herpetology 2(1): 16–22.

Mistry V, Vogel G, Tillack F (2007) Rediscovery of *Dinodon gammiei* (Blanford 1878) (Serpentes, Colubridae), with discussion of its validity. Hamadryad 31(2): 265–273.

Mukherjee D, Bhupathy S (2007) A new species of wolf snake (Serpentes: Colubridae: *Lycodon*) from Anaikatti Hills, Western Ghats, Tamil Nadu, India. Russian Journal of Herpetology 14(1): 21–26.

Neang T, Hartmann T, Hun S, Souter NJ, Furey NM (2014) A new species of wolf snake (Colubridae: *Lycodon* Fitzinger, 1826) from Phnom Samkos Wildlife Sanctuary, Cardamom Mountains, southwest Cambodia. Zootaxa 3814(1): 068–080. https://doi.org/10.11646/zootaxa.3814.1.3

Ota H, Ross CA (1994) Four new species of *Lycodon* (Serpentes: Colubridae) from the northern Philippines. Copeia 1994(1): 159–174. https://doi.org/10.2307/1446682

Pope CH (1928a) Four new snakes and a new lizard from South China. American Museum Novitates 325: 1–4.

Pope CH (1928b) Seven new reptiles from Fukien Province, China. American Museum Novitates 320: 1–6.

Pope CH (1935) The Reptiles of China. Turtles, Crocodilians, Snakes, Lizards. American Museum of Natural History, New York, Natural History. Central Asia 10: lii, 1–604.

Peng LF, Wang LJ, Ding L, Zhu YW, Luo J, Yang DC, Huang RY, Lu SQ, Huang S (2018) A new species of the genus *Sinomicrurus* Slowinski, Boundy and Lawson, 2001 (Squamata: Elapidae) from Hainan Province, China. Asian Herpetological Research 9: 65–73.

Siler CD, Oliveros CH, Santanen A, Brown RM (2013) Multilocus phylogeny reveals unexpected diversification patterns in Asian Wolf Snakes (Genus *Lycodon*). Zoologica Scripta 42: 262–277. https://doi.org/10.1111/zsc.12007

Slowinski JB, Pawar SS, Win H, Thin T, Gyi SW, Oo SL, Tun H (2001) A new *Lycodon* (Serpentes: Colubridae) from Northeast India and Myanmar (Burma). Proceedings of the California Academy of Science 52: 397–405. https://www.mapress.com/j/zt/article/view/zootaxa.4276.4.6

Smith MA (1943) The fauna of British India, Ceylon and Burma, including the whole of the Indo-chinese subregion. Reptilia and Amphibia. Vol. III. Serpentes. Taylor & Francis, London, 583 pp.

Stejneger L (1907) Herpetology of Japan and adjacent territory. Bulletin of the United States National Museum 58: 1–577. https://doi.org/10.5479/si.03629236.58.i

Sung YH, Lee WH, Ng HN, Zhang YJ, Yang JH (2018) A new species of *Hemiphyllodactylus* (Squamata: Gekkonidae) from Hong Kong. Zootaxa 4392: 361–373. https://doi.org/10.11646/zootaxa.4392.2.8

Taylor EH (1922) The snakes of the Philippine Islands. Manila (Bureau of Printing or Science), Monograph 16: 1–312. https://doi.org/10.5962/bhl.title.55346

Taylor EH (1950) The snakes of Ceylon. University of Kansas Science Bulletin 33(14): 519–603. https://doi.org/10.5962/bhl.part.16131

Tamura K, Stecher G, Peterson D, Filipski A, Kumar S (2013) MEGA6: molecular evolutionary genetics analysis, version 6.0. Molecular Biology and Evolution 30: 2725–2729. https://doi.org/10.1093/molbev/mst197

Thompson JD, Gibson TJ, Plewniak F, Jeanmougin F, Higgins DG (1997) The CLUSTAL_X windows interface: flexible strategies for multiple sequence alignment aided by quality analysis tools. Nucleic Acids Research 25: 4876–4882. https://doi.org/10.1093/nar/25.24.4876

Ronquist F, Teslenko M, Van Der Mark P, Ayres DL, Darling A, Höhna S, Larget B, Liu L, Suchard MA, Huelsenbeck JP (2012) MrBayes 3.2: efficient Bayesian phylogenetic inference and model choice across a large model space. Systematic Biology 61: 539–542. https://doi.org/10.1093/sysbio/sys029

Silvestro D, Michalak I (2012) RaxmlGUI: a graphical front-end for RAxML. Organisms Diversity and Evolution 12: 335–337. https://doi.org/10.1007/s13127-011-0056-0

Uetz P, Freed P, Hošek J (2020) The Reptile Database, http://www.reptile-database.org [accessed 6 June 2020]

Vijayakumar SP, David P (2005) Taxonomy, natural history, and distribution of the snakes of the Nicobar Islands (India), based on new materials and with an emphasis on endemic species. Russian Journal of Herpetology 13(1): 11–40.

Vogel G, David P, Pauwels OSG, Sumontha M, Norval G, Hendrix R, Vu NT, Ziegler T (2009) A revision of *Lycodon ruhstrati* (Fischer 1886) auctorum (Squamata Colubridae), with the description of a new species from Thailand and a new subspecies from the Asian mainland. Tropical Zoology 22: 131–182.

Vogel G, David P (2010) A new species of the genus *Lycodon* (Boie, 1826) from Yunnan Province, China (Serpentes: Colubridae). Bonn Zoological Bulletin 57(2): 289–296.

Vogel G, David P (2019) A new species of the *Lycodon fasciatus* complex from the Khorat Plateau, eastern Thailand (Reptiles, Squamata, Colubridae). Zootaxa 4577(3): 515–528. https://doi.org/10.11646/zootaxa.4577.3.6

Vogel G, David P, Pauwels OSG, Sumontha M, Norval G, Hendrix R, Vu NT, Ziegler T (2009) A revision of *Lycodon ruhstrati* (Fischer 1886) auctorum (Squamata Colubridae), with the description of a new species from Thailand and a new subspecies from the Asian mainland. Tropical Zoology 22: 131–182.

Vogel G, Harikrishnan S (2013) Revalidation of *Lycodon hypsirhinoides* (Theobald, 1868) from Andamanislands (Squamata: Serpentes: Colubridae). Taprobanica 5(1): 19–31. https://doi.org/10.4038/tapro.v5i1.5657

Vogel G, Luo J (2011) A new species of the genus *Lycodon* (Boie, 1826) from the southwestern mountains of China (Squamata: Colubridae). Zootaxa 2807: 29–40. https://doi.org/10.11646/zootaxa.2807.1.2

Vogel G, Nguyen TQ, Kingsada P, Ziegler T (2012) A new species of the genus *Lycodon* (Boie, 1826) from Laos (Squamata: Serpentes: Colubridae). North-Western Journal of Zoology 8(2): 344–352. http://biozoojournals.3x.ro/nwjz/index.html

Wall F (1906) A new Himalayan snake (*Lycodon mackinnoni*). Journal of the Bombay Natural History Society 17: 29–30.

Wostl E, Hamidy A, Kurniawan N, Smith EN (2017) A new species of Wolf Snake of the genus *Lycodon* H. Boie in Fitzinger (Squamata: Colubridae) from the Aceh Province of northern Sumatra, Indonesia. Zootaxa 4276(4): 539–553. https://doi.org/10.11646/zootaxa.4276.4.6

Wang J, Yang JH, Li Yao, Lyu ZT, Zeng ZC, Liu ZY, Ye YH, Wang YY (2018a) Morphology and molecular genetics reveal two new *Leptobrachella* species in southern China (Anura, Megophryidae). ZooKeys 776: 105–137. https://doi.org/10.3897/zookeys.776.22925

Wang J, Zeng ZC, Lyu ZT, Liu ZY, Wang YY (2018b) Description of a new species of *Gracixalus* (Amphibia: Anura: Rhacophoridae) from Guangdong Province, southeastern China. Zootaxa 4420(2): 251–269. https://doi.org/10.11646/zootaxa.4420.2.7

Wang J, Lyu ZT, Yang CY, Li YL, Wang YY (2019a) A new species of the genus *Takydromus* (Squamata, Lacertidae) from southwestern Guangdong, China. ZooKeys 871: 119–139. https://doi.org/10.3897/zookeys.871.35947

Wang J, Lyu ZT, Liu ZY, Liao CK, Zeng ZC, Zhao J, Li YL, Wang YY (2019c) Description of six new species of the subgenus *Panophrys* within the genus *Megophrys* (Anura, Megophryidae) from southeastern China based on molecular and morphological data. ZooKeys 851: 113–164. https://doi.org/10.3897/zookeys.851.29107

Wang J, Li Y, Zeng ZC, Lyu ZT, Sung YH, Li YY, Lin CY, Wang YY (2019c) A new species of the genus *Achalinus* from southwestern Guangdong Province, China (Squamata: Xenodermatidae). Zootaxa 4674(4): 471–481. https://doi.org/10.11646/zootaxa.4674.4.6

Wang J, Lyu ZT, Zeng ZC, Lin CY, Yang JH, Nguyen TQ, Le MD, Ziegler T, Wang YY (2020a) Re-examination of the Chinese record of *Opisthotropis maculosa* (Squamata, Natricidae), resulting in the first national record of *O. haihaensis* and description of a new species. ZooKeys 913: 141–159. https://doi.org/10.3897/zookeys.913.48622

Wang K, Ren JL, Chen HM, Lyu ZT, Guo XG, Jiang K, Chen JM, Li JT, Guo P, Wang YY, Che J (2020b) The updated checklists of amphibians and reptiles of China. Biodiversity Science 28(2): 189–218.

Zhang J, Jiang K, Vogel G, Rao D (2011) A new species of the genus *Lycodon* (Squamata, Colubridae) from Sichuan Province, China. Zootaxa 2982: 59–68.

Zhang L, Peng LF, Yu L, Wang ZP, Huang LQ, Huang S (2015) New Record of *Lycodon liuchengchaoi* in Anhui. Zoological Research 36(1): 178–180.

Zhao EM (2006) Snakes of China. I. Anhui Science and Technology Publishing House, Hefei, 372 pp. [in Chinese]

Zhao EM (1981) Studies on amphibians and reptiles of Mt. Gongga Shan, Sichuan, China. I. A new species and a new subspecies of snake from Sichuan (in Chinese). Acta Herpetologica Sinica, Chengdu, [old ser.] 5(7): 53–58.

Zhao EM, Huang MH, Zong Y (1998) Fauna Sinica: Reptilia. Vol. 3. Squamata, Serpentes. Science Press, Beijing, 522 pp. [in Chinese]

Appendix I

Examined specimens

Lycodon flavozonatus (N = 11): Nanling Nature Reserve, Guangdong, China: SYS r000819; Mt. Jinggang, Jiangxi, China: SYS r000317, 001956, 001972; Mt. Huanggang, Jiangxi, China: SYS r000640; Mt. Bamian, Hunan, China: SYS r001357, 001358, 001360, 001778; Mt. Wuyi, Fujian, China: SYS r001722; Mt. Dongbai, Zhejiang, China: SYS r001772.

Lycodon futsingensis (N = 9): Nanling Nature Reserve, Guangdong, China: SYS r000051, 000054; Mt. Wutong, Shenzhen, Guangdong, China: SYS r000617, 001016; Gaoping Nature Reserve, Shaoguan, China: SYS r001542, 001630, 001667, 002123; Shimentai Nature Reserve, Guangdong, China: SYS r001494.

Lycodon liuchengchaoi (N = 1): Shimentai Nature Reserve, Guangdong, China: SYS r002114.

Lycodon meridionalis (N = 5): Heishiding Nature Reserve, Guangdong, China: SYS r001355, 002053; Mt. Jiuwan, Guangxi, China: SYS r001812; Mt. Dayao, Guangxi, China: SYS r002326, 002327.

Lycodon rosozonatus (N = 2): Jianfengling, Hainan, China: SYS r001617; Bawangling, Hainan, China: SYS r002164.

Lycodon rufozonatus (N = 3): Mt. Jinggang, Jiangxi, China: SYS r000318; Mt. Bamian, Hunan, China: SYS r001361; Mt. Tiantai, Zhejiang, China: SYS r001770.

Lycodon ruhstrati (N = 7): Mt. Jiulian, Jiangxi, China: SYS r001309; Jiangshi Nature Reserve, Fujian, China: SYS r001275; Mt. Jinggang, Jiangxi, China: SYS r001256; Mt. Qiyun, Jiangxi, China: SYS r000882; Mt. Bamian, Hunan, China: SYS r001362; Huaping Nature Reserve, Guangxi, China: SYS r001631, 001633.

Lycodon subcinctus (N = 13): Sun Yet-sen University, Zhuhai, Guangdong, China: SYS r001013; Heishiding Nature Reserve, Guangdong, China: SYS r001523, 001757; Neilingding Island, Shenzhen, Guangdong, China: SYS r001155, 001511; Tiegang Reservoir, Shenzhen, Guangdong, China: SYS r001430; Maluanshan Country Park, Shenzhen, Guangdong, China: SYS r002146; Shimentai Nature Reserve, Guangdong, China: SYS r001943, 002021; Mt. Diaoluo, Hainan, China: SYS r001621; Xishuangbanna, Yunnan, China: SYS r000689, 000690.

RESEARCH ARTICLE

Systematics of *Pholidobolus* lizards (Squamata, Gymnophthalmidae) from southern Ecuador, with descriptions of four new species

Vanessa Parra[1], Pedro M. Sales Nunes[2], Omar Torres-Carvajal[1]

1 *Museo de Zoología, Escuela de Ciencias Biológicas, Pontificia Universidad Católica del Ecuador, Avenida 12 de Octubre 1076 y Roca, Quito, Ecuador* **2** *Departamento de Zoologia, Centro de Biociências, Universidade Federal de Pernambuco, Avenida Professor Moraes Rego, s/n. Cidade Universitária CEP 50670-901, Recife, PE, Brazil*

Corresponding author: Omar Torres-Carvajal (omartorcar@gmail.com)

Abstract

Four new species of *Pholidobolus* lizards are described from poorly explored areas in the Andes of southern Ecuador based on morphological and genetic evidence. Among other morphological characters, *Pholidobolus samek* **sp. nov.** and *P. condor* **sp. nov.** differ from their congeners in having green dorsolateral stripes on head. Males of *P. condor* **sp. nov.** differ from those of *P. samek* **sp. nov.** in having reddish flanks and venter. *P. dolichoderes* **sp. nov.** is distinguished by having a long neck, with more scales between orbit and tympanum, whereas *P. fascinatus* **sp. nov.** is distinguished by lacking enlarged medial scales on collar and a conspicuous vertebral stripe. In addition, the phylogenetic position of the new species is inferred using DNA sequences of mitochondrial and nuclear genes. The phylogeny supports strongly monophyly of each of the new species and renders *P. macbrydei* paraphyletic and split into six subclades. Available data suggest that the new species have restricted distribution ranges (< 100 km² each), and it is proposed that their classification be as Data Deficient or Critically Endangered species. The results reveal unexpected levels of diversity within *Pholidobolus* in the Andes of southern Ecuador and highlight the importance of improving scientific collections and conservation efforts in this area.

Keywords

Andes, Cordillera del Cóndor, diversity, phylogeny, taxonomy

Introduction

The uplift of the Andes mountains was one of the most influential geological events for the evolution and diversification of the South American biota during the Cenozoic. For example, it created many habitats and microclimates that became important centers of biodiversity and endemism (Pérez-Escobar et al. 2017). Therefore, the evolution of diverse Andean taxa is a complex research topic that has attracted the attention of many scientists (Castoe et al. 2004, Torres-Carvajal et al. 2015, Betancourt et al. 2018, Moravec et al. 2018, Lehr et al. 2019). With more than 250 species, Gymnophthalmidae is one of the most diverse lizard clades in the Neotropics. The uplift of the Andes had a strong influence on the radiation of gymnophthalmid lizards, resulting in high levels of diversity and endemism along the Tropical Andes (Torres-Carvajal et al. 2016; Moravec et al. 2018).

Pholidobolus lizards are among the most prominent gymnophthalmids in the northern Andes. They are small (SVL ≤ 60 mm), terrestrial, oviparous, and restricted to the Andes of Colombia, Ecuador, and northern Peru at elevations between 1800 and 4100 m (Hurtado-Gómez et al. 2018; Torres-Carvajal et al. 2014; Venegas et al. 2016). *Pholidobolus* is currently known to include ten species: *P. affinis*, *P. anomalus*, *P. dicrus*, *P. hillisi*, *P. macbrydei*, *P. montium*, *P. paramuno*, *P. prefrontalis*, *P. ulisesi*, and *P. vertebralis*, of which three were described in recent years. Remarkably, *P. anomalus* is the only species in the genus that occurs in southern Peru (Cusco), but its generic identity remains questionable (Torres-Carvajal and Mafla-Endara 2013).

The study of *Pholidobolus* and other gymnophthalmid taxa has been often hampered by the paucity of specimens in collections. For example, the recent description of *P. paramuno* reveals the importance of increased sampling effort in the Paramo ecosystem in the northern Andes of Colombia. Similarly, recent collections in poorly explored areas of the southern Andes of Ecuador yielded new specimens of *Pholidobolus* lizards, which we were unable to assign to any of the currently recognized species. Based on these specimens, here we combine evidence from morphology and DNA sequences to describe four new species of *Pholidobolus* and infer their phylogenetic affinities.

Materials and methods

Genetic data

Total genomic DNA was digested and extracted from liver or muscle tissue using a guanidinium isothiocyanate extraction protocol. Tissue samples were first mixed with Proteinase K and a lysis buffer and digested overnight prior to extraction. DNA samples were quantified using a Nanodrop ND-1000 (NanoDrop Technologies, Inc.), resuspended and diluted to 25 ng/µl in ddH2O prior to amplification.

Using primers and amplification protocols from the literature (Pellegrino et al. 2001; Torres-Carvajal and Mafla-Endara 2013), we obtained 1,493 aligned nucleotides (nt) encompassing three mitochondrial genes, 12S (339 nt), 16S (533 nt), and ND4 (621 nt) from 16 individuals of the four new species herein described, as well as 21 individuals of

Pholidobolus macbrydei. In addition, we obtained 411 nucleotides of the Dynein Axonemal Heavy Chain 3 (DNAH3) nuclear gene from 65 individuals of *Anadia rhombifera*, *Macropholidus annectens*, *M. huancabambae*, *M. labiopunctatus*, *M. ruthveni*, *Pholidobolus affinis*, *P. dicrus*, *P. hillisi*, *P. macbrydei*, *P. montium*, *P. prefrontalis*, *P. ulisesi*, *P. vertebralis*, and the four new species. DNAH3 was amplified using the primers DNAH3_f1 (GG-TAAAATGATAGAAGAYTACTG) and DNAH3_r6 (CTKGAGTTRGAHACAAT-KATGCCAT). The amplification protocol consisted of 1 cycle of initial denaturation for 5 min at 95 °C, 40 cycles of denaturation for 35s at 94 °C, annealing for 1 min at 72 °C, and extension for 1 min at 72 °C, as well as a final extension for 10 min at 72 °C (Townsend et al. 2008). Positive PCR products were visualized in agarose electrophoretic gels and treated with ExoSAP-IT to remove unincorporated primers and dNTPs. Cycle sequencing reactions were carried out by Macrogen Inc. GenBank accession numbers of sequences generated in this study are shown in Table 1. After incorporating GenBank sequences, our data matrix for phylogenetic analyses contained 74 taxa and 1904 characters.

Phylogenetic analyses

Data were assembled and aligned in Geneious v5.4.6. (Kearse et al. 2012) under default settings for MAFFT Multiple Alignment (Katoh and Toh 2010). ND4 and DNAH3 sequences were translated into amino acids for confirmation of alignment. The best-fit nucleotide substitution models and partitioning scheme were chosen simultaneously using PartitionFinder v2.1.1 (Lanfear et al. 2012) under the Bayesian Information Criterion (BIC). Genes were combined into a single dataset with four partitions: (i) 1st codon position of ND4 and 12S [GTR + I + G]; (ii) 2nd codon position of ND4, 1st codon and 2nd codon positions of DNAH3 [HKY + I + G]; (iii) 3rd codon position of ND4 [GTR + G]; (iv) 16S and 3rd codon position of DNAH3 [SYM + I + G]. Both maximum likelihood (ML) and Bayesian inference (BI) methods were used to obtain the optimal tree topology of the combined, partitioned dataset using the programs RAxML v.8.2.12 (Stamatakis 2014) and MrBayes v3.2.6 (Ronquist et al. 2012), respectively. The ML analysis was performed under the GTRGAMMA model for all partitions. Nodal support (BS) was assessed with the rapid bootstrapping algorithm under the MRE-based Boot-stopping criterion (252 replicates). For BI analysis, all parameters were unlinked between partitions (except topology and branch lengths), and rate variation (prset ratepr = variable) was invoked. Four independent runs, each with four MCMC chains, were set for ten million generations, sampling every 10,000 generations. All analyses were performed using the CIPRES platform (Miller et al. 2010). Results were analyzed in Tracer 1.6 (Rambaut and Drummond 2007) to assess convergence and effective sample sizes (ESS) for all parameters, based on which the first 10% of trees were removed from each run. The remaining trees were used to calculate posterior probabilities (PP) for each bipartition in a Maximum Clade Credibility Tree. The phylogenetic trees were visualized and edited using FigTree v1.4.2 (Rambaut 2014). In order to address interspecific genetic differentiation, uncorrected genetic distances were calculated in MEGA 7 (Kumar et al. 2016) after removing ambiguous positions for each sequence pair (pairwise deletion option).

Table 1. Vouchers, locality data, and GenBank accession numbers of taxa included in this study. Sequences added in this study are in bold.

Taxon	Voucher	Locality	GenBank number				GenSeq Nomenclature
			12S	16S	ND4	DNAH3	
Anadia rhombifera	QCAZ 11862	QCAZ 11862; Ecuador: Cotopaxi: San Francisco de Las Pampas	KU902135	KU902216	KU902291	**MN849427**	genseq-4
Macropholidus annectens	QCAZ 11120	Ecuador: Loja: 15 km E Loja	KC894341	KC894355	KC894369	**MN849430**	genseq-4
	QCAZ 11121	Ecuador: Loja: 15 km E Loja	KC894342	KC894356	KC894370	**MN849431**	genseq-4
Macropholidus huancabambae	CORBIDI 10492	Peru: Piura: Huancabamba: Las Pozas	KC894343	KC894357	KC894371	**MN849428**	genseq-4
	CORBIDI 10493	Peru: Piura: Huancabamba: Las Pozas	KC894344	KC894358	KC894372	–	genseq-4
	CORBIDI 10496	Peru: Piura: Huancabamba: Las Pozas	KC894345	KC894359	KC894373	**MN849429**	genseq-4
Macropholidus labiopunctatus	CORBIDI 12932	Peru: Piura: Ayabaca	KP874774	KP874826	KP874936	**MN849432**	genseq-4
Macropholidus ruthveni	CORBIDI 4281	Peru: Lambayeque: El Totora	KC894354	C894368	C894382	**MN849433**	genseq-4
Pholidobolus affinis	QCAZ 9641	Ecuador: Cotopaxi: San Miguel de Salcedo, Cutuchi River	KC894348	C894362	C894376	**MN849435**	genseq-4
	QCAZ 9900	Ecuador: Chimborazo: Colta	KC894349	KC894363	KC894377	–	genseq-4
Pholidobolus condor sp. nov.	QCAZ 16788	Ecuador: Morona-Santiago: el Quimi	**MN724005**	**MN720239**	**MN717135**	**MN849464**	genseq-2
	QCAZ 16789	Ecuador: Morona-Santiago: el Quimi	**MN724006**	**MN720240**	**MN717134**	**MN849465**	genseq-2
	QCAZ 16790	Ecuador: Morona-Santiago: el Quimi	**MN724007**	**MN720241**	**MN717136**	**MN849466**	genseq-2
	QCAZ 15844	Ecuador: Morona-Santiago: el Quimi	**MN723996**	**MN720230**	**MN717125**	**MN849434**	genseq-1
Pholidobolus dicrus	QCAZ 5304	Ecuador: Morona-Santiago: Guarumales	KP874776	KP874828	KP874938	**MN849436**	genseq-4
	QCAZ 6936	Ecuador: Tungurahua: Río Blanco	–	KP874829	KP874939	**MN849437**	genseq-4
Pholidobolus dolichoderes sp. nov.	QCAZ 16349	Ecuador: Cañar: Oña	**MN724000**	**MN720234**	**MN717129**	**MN849459**	genseq-2
	QCAZ 16350	Ecuador: Cañar: Oña	**MN724001**	**MN720235**	**MN717130**	**MN849460**	genseq-2
	QCAZ 16351	Ecuador: Cañar: Oña	**MN724002**	**MN720236**	**MN717131**	**MN849461**	genseq-2
	QCAZ 16352	Ecuador: Cañar: Oña	**MN724003**	**MN720237**	**MN717132**	**MN849462**	genseq-2
	QCAZ 16353	Ecuador: Cañar: Oña	**MN724004**	**MN720238**	**MN717133**	**MN849463**	genseq-1
Pholidobolus fascinatus sp. nov.	QCAZ 15118	Ecuador: El Oro: Chillacocha	**MN724017**	**MN720251**	**MN717146**	**MN849476**	genseq-2
	QCAZ 15120	Ecuador: El Oro: Chillacocha	**MN724018**	**MN720252**	**MN717147**	**MN849477**	genseq-1
	QCAZ 15122	Ecuador: El Oro: Chillacocha	**MN724019**	**MN720253**	–	**MN849478**	genseq-2
	QCAZ 15170	Ecuador: El Oro: Chillacocha	**MN724020**	**MN720254**	**MN717148**	**MN849479**	genseq-2

Taxon	Voucher	Locality	GenBank number				GenSeq Nomenclature
			12S	16S	ND4	DNAH3	
Pholidobolus hillisi	QCAZ 4998	Ecuador: Zamora-Chinchipe: near San Francisco Research Station	KP090167	KP090170	KP090173	**MN849438**	genseq-4
	QCAZ 4999	Ecuador: Zamora-Chinchipe: near San Francisco Research Station	KP090169	KP090172	KP090175	**MN849439**	genseq-4
	QCAZ 5000	Ecuador: Zamora-Chinchipe: near San Francisco Research Station	KP090168	KP090171	KP090174	**MN849440**	genseq-4
"Pholidobolus macbrydei"	KU 218406	Ecuador: Azuay: Cuenca	AY507848	AY507867	AY507886	–	genseq-4
	QCAZ 9914	Ecuador: Azuay: Guablid	KC894352	KC894366	KC894380	**MN849441**	genseq-4
	QCAZ 9932	Ecuador: Azuay: 20 km on road Cuenca-El Cajas	KC894353	KC894367	KC894381	**MN849442**	genseq-4
	QCAZ 9947	Ecuadro: Cañar: Cañar	**MN724012**	**MN720246**	**MN717141**	**MN849474**	genseq-4
	QCAZ 10051	Ecuador: Cañar: Río Guallicanga, quebrada Juncal	**MN724014**	**MN720248**	**MN717143**	**MN849472**	genseq-4
	QCAZ 10052	Ecuador: Cañar: Río Guallicanga, quebrada Juncal	**MN724015**	**MN720249**	**MN717144**	**MN849473**	genseq-4
	QCAZ 10050	Ecuador: Cañar: A 1000 m de la Panamericana Juncal	**MN724013**	**MN720247**	**MN717142**	**MN849471**	genseq-4
	QCAZ 15811	Ecuador: Cañar: Mazar	**MN724021**	**MN720255**	**MN717149**	**MN849480**	genseq-4
	QCAZ 15812	Ecuador: Cañar: Mazar	**MN724022**	**MN720256**	**MN717150**	**MN849481**	genseq-4
	QCAZ 15813	Ecuador: Cañar: Mazar	**MN724023**	**MN720257**	**MN717151**	**MN849482**	genseq-4
	QCAZ 15814	Ecuador: Cañar: Mazar	**MN724024**	**MN720258**	**MN717152**	–	genseq-4
	QCAZ 15815	Ecuador: Cañar: Mazar	**MN724025**	**MN520259**	**MN717153**	–	genseq-4
	QCAZ 15816	Ecuador: Cañar: Mazar	**MN724026**	**MN720260**	**MN717154**	**MN849483**	genseq-4
	QCAZ 15817	Ecuador: Cañar: Mazar	**MN724027**	**MN720261**	**MN717155**	**MN849484**	genseq-4
	QCAZ 15818	Ecuador: Cañar: Mazar	**MN724028**	**MN720262**	**MN717156**	**MN849485**	genseq-4
	QCAZ 15819	Ecuador: Cañar: Mazar	**MN724029**	**MN720263**	**MN717157**	**MN849486**	genseq-4
	QCAZ 15820	Ecuador: Cañar: Mazar	**MN724030**	**MN720264**	**MN717158**	**MN849487**	genseq-4
	QCAZ 15823	Ecuador: Cañar: Mazar	**MN724031**	**MN720265**	**MN717159**	**MN849488**	genseq-4
	QCAZ 15824	Ecuador: Cañar: Mazar	**MN724032**	**MN720266**	**MN717160**	**MN849489**	genseq-4
	QCAZ 6945	Ecuador: Loja: Jimbura	**MN724008**	**MN720242**	**MN717137**	**MN849467**	genseq-4
	QCAZ 6946	Ecuador: Loja: Jimbura	**MN724009**	**MN720243**	**MN717138**	**MN849468**	genseq-4

Taxon	Voucher	Locality	GenBank number				GenSeq Nomenclature
			12S	16S	ND4	DNAH3	
"*Pholidobolus macbrydei*"	QCAZ 10054	Ecuadro: Loja: Colombo Yacuri Forest	**MN724016**	**MN720250**	**MN717145**	**MN849475**	genseq-4
	QCAZ 7894	Ecuador: El Oro: Guanazán	**MN724011**	**MN720245**	**MN717140**	**MN849470**	genseq-4
	QCAZ 7891	Ecuador: El Oro: Guanazán	**MN724010**	**MN720244**	**MN717139**	**MN849469**	genseq-4
Pholidobolus montium	QCAZ 4051	Ecuador: Pichincha: Quito	KC894346	KC894360	KC894374	**MN849443**	genseq-4
	QCAZ 9044	Ecuador: Pichincha: Tababela	KC894347	KC894361	KC894375	**MN849444**	genseq-4
Pholidobolus paramuno	MHUAR 12451	Colombia: Antoquia	MK215018	MK215032	MK215046	–	genseq-4
	MHUAR 12480	Colombia: Antoquia	MK215019	MK215033	MK215047	–	genseq-4
	MHUAR 12481	Colombia: Antoquia	MK215020	MK215034	MK215048	–	genseq-4
Pholidobolus prefrontalis	QCAZ 9908	Ecuador: Chimborazo: Alausí	KC894350	KC894364	KC894378	–	genseq-4
	QCAZ 9951	Ecuador: Chimborazo: Tixán	KC894351	KC894365	KC894379	**MN849448**	genseq-4
Pholidobolus samek sp. nov.	QCAZ 14954	Ecuador: Zamora Chinchipe: Cerro Plateado	**MN723997**	**MN720231**	**MN717126**	**MN849445**	genseq-2
	QCAZ 14955	Ecuador: Zamora Chinchipe: Cerro Plateado	**MN723998**	**MN720332**	**MN717127**	**MN849446**	genseq-1
	QCAZ 14956	Ecuador: Zamora Chinchipe: Cerro Plateado	**MN723999**	**MN720233**	**MN717128**	**MN849447**	genseq-2
Pholidobolus ulisesi	CORBIDI 12735	Peru: Cajamarca: Jaen: Huamantanga Forest	KP874787	KP874839	KP874948	**MN849449**	genseq-4
	CORBIDI 12737	Peru: Cajamarca: Jaen: Huamantanga Forest	KP874788	KP874840	KP874949	–	genseq-4
	CORBIDI 1679	Perú: Chota: La Granja	KP874786	KP874838	KP874947	**MN849450**	genseq-4
Pholidobolus vertebralis	QCAZ 10667	Ecuador: Pichincha: Santa Lucía de Nanegal	KP874784	KP874836	KP874946	**MN849455**	genseq-4
	QCAZ 10750	Ecuador: Pichincha: Santa Lucía de Nanegal	KP874785	KP874837	KP874947	**MN849458**	genseq-4
	QCAZ 5057	Ecuador: Carchi: Chilma Bajo	KP874778	KP874830	KP874940	**MN849451**	genseq-4
	QCAZ 8687	Ecuador: Carchi: Chilma Bajo	KP874779	KP874831	KP874941	**MN849452**	genseq-4
	QCAZ 8688	Ecuador: Carchi: Chilma Bajo	KP874780	KP874832	KP874942	**MN849453**	genseq-4
	QCAZ 8689	Ecuador: Carchi: Chilma Bajo	KP874781	KP874833	KP874943	**MN849454**	genseq-4
	QCAZ 8717	Ecuador: Carchi: next to Chilma Bajo	KP874782	KP874834	KP874944	**MN849456**	genseq-4
	QCAZ 8724	Ecuador: Carchi: next to Chilma Bajo	KP874783	KP874835	KP874945	**MN849457**	genseq-4

Specimens and morphological data

We examined 98 specimens of *Pholidobolus macbrydei* (Appendix I) and 41 of the new species described herein (see corresponding type series). All specimens are deposited in the herpetological collection at Museo de Zoología, Pontificia Universidad Católica del Ecuador, Quito (**QCAZ**). The following measurements were taken with a digital caliper (to the nearest 0.1 mm):

AGD	axilla-groin distance;	**ShL**	shank length;
HL	head length;	**SVL**	and snout-vent length.
HW	head width;		

Tail length (**TL**) was measured with a ruler. Sex was determined by dissection or by noting the presence of everted hemipenes. We followed the terminology of Montanucci (1973) and Kizirian (1996) for morphological characters.

Because the new species are similar in morphology to *Pholidobolus macbrydei*, we assessed the degree of differentiation among them with a Principal Components Analysis (PCA) in R (R Core Team 2018). The PCA was based on 16 quantitative morphological characters: (1) number of supraoculars (NSO), (2) number of scales along margin of upper jaw (SUJ), (3) number of scales along margin of lower jaw (SLJ), (4) number of gular and jaw scales (SGJ), (5) number of ventrals (SGV), (6) number of dorsals (DEL), (7) number of temporals (NTS), (8) number of scales around body (SAB), (9) number of scales around tail (SAT), (10) number of supradigital scales of third finger (SF3), (11) number of supradigital scales of fifth finger (SF5), (12) number of supradigital scales of third toe (ST3), (13) number of supradigital scales of fourth toe (ST4), (14) number of supradigital scales of fifth toe (ST5), (15) lower eyelid scales (LES), and (16) collar scales (i.e., posterior transverse row of gulars; SGC) (Peters 1964, Montanucci 1973).

Hemipenes were prepared following the procedures described by Manzani and Abe (1988), as modified by Pesantes (1994) and Zaher (1999). Organs were everted after immersion in a potassium hydroxide solution, the retractor muscles were manually separated, and the everted organs filled with blue-stained petroleum jelly. Hemipenes were then immersed in an alcoholic solution of Alizarin Red for 24 hours in order to stain eventual calcified structures (e.g., spines or spicules), in an adaptation proposed by Nunes et al. (2012) on the procedures described by Uzzell (1973) and Harvey and Embert (2008). The terminology of hemipenial structures follows previous literature (Dowling and Savage 1960; Hurtado-Gómez et al. 2018; Nunes et al. 2012; Sánchez-Pacheco et al. 2017; Savage 1997; Venegas et al. 2016).

Systematics

The taxonomic conclusions of this study are based on the observation of morphological features and color pattern, as well as inferred phylogenetic relationships. We

consider this information as species delimitation criteria following a general lineage or unified species concept (de Queiroz 1998; 2007).

The new species share with all known species of *Pholidobolus* the presence of a ventrolateral fold between fore and hind limbs and the absence of a single transparent palpebral disc (Montanucci 1973).

Results

Phylogenetic relationships and genetic distances

Tree topologies under ML and BI approaches were generally similar; here we describe the maximum clade credibility tree (Fig. 1). Our hypothesis supports the monophyly of *Pholidobolus* (BS= 60, PP = 0.99) and is congruent with previous molecular phylogenies in that *P. ulisesi* and *P. hillisi* form a clade (BS = 62, PP = 0.92) sister to all other congeners (Torres-Carvajal et al. 2015, 2016; Hurtado-Gómez et al. 2018). Following branching order, the strongly supported species pair *P. affinis*, *P. montium* is sister to all remaining species, which form a clade where (*P. prefrontalis* (*P. paramuno* (*P. dicrus*, *P. vertebralis*))) is sister to a subclade containing the new species described in this paper and a paraphyletic *P. macbrydei*. Hereafter we refer to the latter subclade as the "*P. macbrydei*" species complex.

The "*P. macbrydei*" species complex (BS = 81, PP = 1) is divided into two allopatric and strongly supported clades (Fig. 1) that include four new species described below and a paraphyletic "*P. macbrydei*" divided in six subclades (Clades A–F). A southeastern clade (BS = 99, PP = 1) contains *P. condor* sp. nov. as sister to (*P. samek* sp. nov., "*P. macbrydei*" Clade A [Loja province]). The ML tree recovered *P. condor* as sister to "*P. macbrydei*" Clade A with low support (BS = 58). A northwestern clade (BS = 85, PP = 0.96) is composed of "*P. macbrydei*" Clade B from Cañar province as sister to a clade that includes all remaining samples, in which *P. fascinatus* sp. nov. is nested along with "*P. macbrydei*" Clades C, D, and E (Azuay and Cañar provinces) in a strongly supported subclade (BS = 71, PP = 1) sister to the maximally supported (*P. dolichoderes*, "*P. macbrydei*" Clade F [El Oro province]). All new species are strongly supported as monophyletic (BS ≥ 98, PP = 1).

Uncorrected *p*-genetic distances for 16S, 12S, and ND4 are presented in Tables 2, 3, and 4, respectively. Distance values among all recognized species of *Pholidobolus*, the four new species described in this paper, and the six "*P. macbrydei*" clades range between 1 (e.g., *P. condor* sp. nov. vs. *P. samek* sp. nov., Clade C vs. Clade D)–10% (e.g., *P. paramuno* vs. *P. dicrus*) for 12S (average = 5% ± 0.01 SD); 1 (*P. dolichoderes* sp. nov. vs. Clade F)–6% (e.g., *P. dicrus* vs. *P. ulisesi*) for 16S (average = 4% ± 0.01 SD); and 4 (*P. dolichoderes* sp. nov. vs. Clade F)–19% (e.g., *P. dicrus* vs. *P. vertebralis*) for ND4 (average = 14% ± 0.03 SD). Maximum distance values within the "*P. macbrydei*" complex are 5% (Clade A vs. Clade F) for 12S, 4% (*P. condor* sp. nov. vs. Clade F) for 16S, and 14% (Clade A vs. Clade F) for ND4. The genetic distances for the nuclear gene NDH3 are generally low (0–3%, average = 1% ± 0.01 SD).
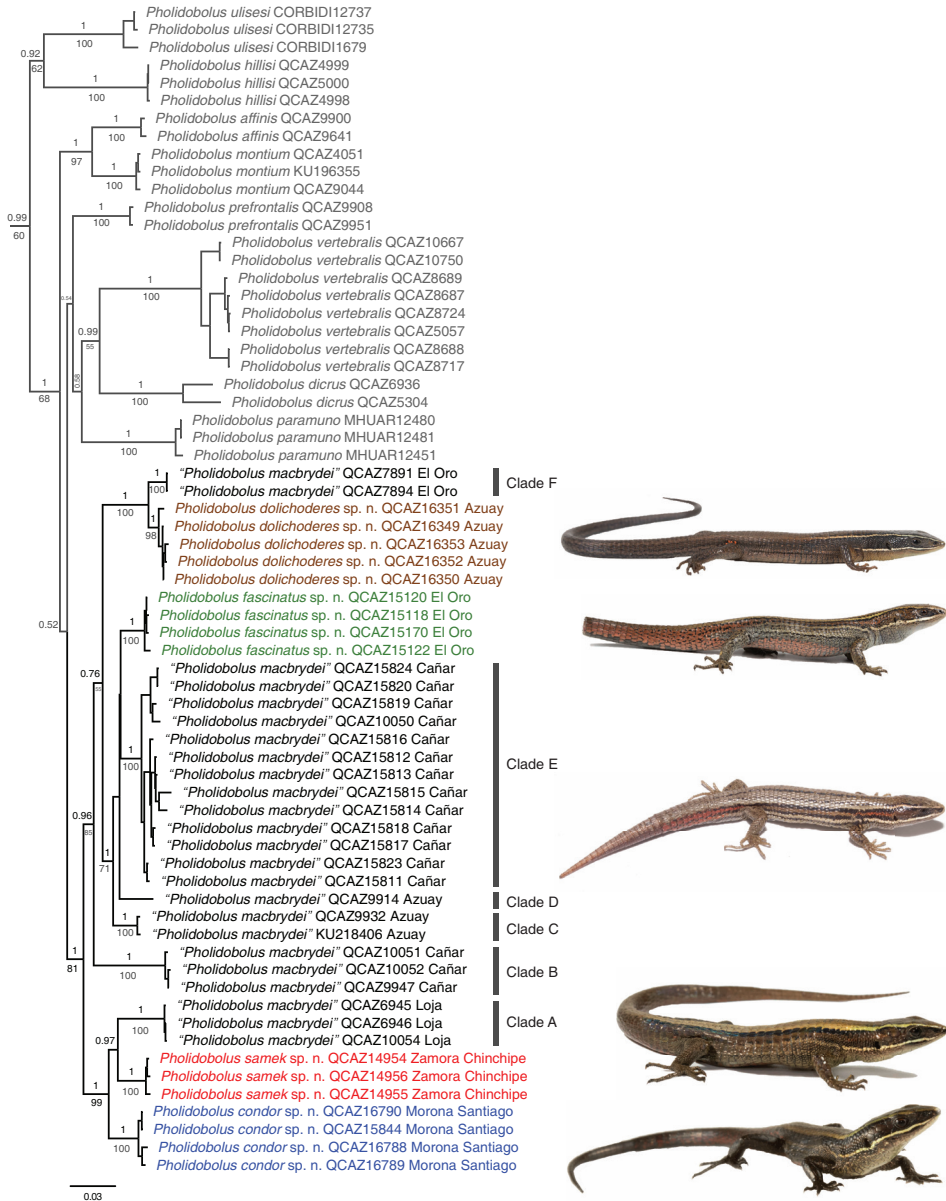
Figure 1. Phylogeny of *Pholidobolus*. Maximum clade credibility tree derived from a partitioned analysis of 1904 bp of mitochondrial and nuclear DNA. Bayesian posterior probabilities are shown above branches and bootstrap values (RAxML analysis) below branches; values ≤ 0.5 and 50, respectively, are not shown. For clarity, outgroup taxa and values on short branches are not shown. Species outside the "*P. macbrydei*" complex are in grey; new species described in this paper are in color matching the distribution records of the map in Figure 7. The species name followed by voucher number and province ("*P. macbrydei*" complex only) are provided for each terminal. Photographs from top to bottom: *P. dolichoderes* sp. nov. holotype, *P. fascinatus* sp. nov. holotype, "*P. macbrydei*" (Clade B) QCAZ 15824, *P. samek* sp. nov. holotype, *P. condor* sp. nov. holotype.

Table 2. Pairwise genetic distances (uncorrected *p*) of 16S DNA sequences among species and clades of *Pholidobolus* included in this study. This analysis involved 66 nucleotide sequences and 533 positions.

	Taxon	1	2	3	4	5	6	7	8	9	10	11	12	13	14	15	16	17
1	*Pholidobolus condor* sp. nov.																	
2	*Pholidobolus samek* sp. nov.	0.03																
3	*Pholidobolus dolichoderes* sp. nov.	0.04	0.03															
4	*Pholidobolus fascinatus* sp. nov.	0.03	0.03	0.03														
5	Clade A	0.03	0.02	0.04	0.03													
6	Clade B	0.03	0.03	0.03	0.03	0.02												
7	Clade C	0.02	0.02	0.03	0.02	0.03	0.03											
8	Clade D	0.03	0.02	0.03	0.03	0.03	0.03	0.02										
9	Clade E	0.03	0.03	0.04	0.02	0.04	0.03	0.02	0.03									
10	Clade F	0.04	0.03	0.01	0.04	0.04	0.02	0.03	0.03	0.04								
11	*Pholidobolus affinis*	0.04	0.03	0.03	0.03	0.04	0.03	0.03	0.02	0.03	0.03							
12	*Pholidobolus dicrus*	0.04	0.04	0.04	0.04	0.04	0.04	0.04	0.03	0.05	0.04	0.05						
13	*Pholidobolus hillisi*	0.05	0.05	0.05	0.05	0.04	0.04	0.04	0.03	0.05	0.04	0.04	0.05					
14	*Pholidobolus montium*	0.03	0.02	0.03	0.03	0.02	0.02	0.02	0.02	0.04	0.03	0.03	0.04	0.04				
15	*Pholidobolus paramuno*	0.04	0.04	0.04	0.03	0.04	0.03	0.03	0.03	0.04	0.04	0.03	0.04	0.04	0.03			
17	*Pholidobolus prefrontalis*	0.03	0.03	0.03	0.03	0.03	0.02	0.03	0.03	0.03	0.03	0.03	0.04	0.04	0.03	0.03		
17	*Pholidobolus ulisesi*	0.05	0.05	0.05	0.05	0.05	0.05	0.06	0.06	0.05	0.05	0.05	0.06	0.04	0.05	0.05	0.05	
18	*Pholidobolus vertebralis*	0.05	0.04	0.04	0.04	0.05	0.04	0.04	0.04	0.05	0.04	0.05	0.05	0.05	0.04	0.04	0.04	0.06

Table 3. Pairwise genetic distances (uncorrected *p*) of 12S DNA sequences among species and clades of *Pholidobolus* included in this study. This analysis involved 65 nucleotide sequences and 339 positions.

	Taxon	1	2	3	4	5	6	7	8	9	10	11	12	13	14	15	16	17
1	*Pholidobolus condor* sp. nov.																	
2	*Pholidobolus samek* sp. nov.	0.01																
3	*Pholidobolus dolichoderes* sp. nov.	0.04	0.04															
4	*Pholidobolus fascinatus* sp. nov.	0.03	0.03	0.03														
5	Clade A	0.03	0.03	0.05	0.04													
6	Clade B	0.03	0.03	0.04	0.03	0.03												
7	Clade C	0.02	0.02	0.02	0.02	0.03	0.03											
8	Clade D	0.02	0.02	0.03	0.02	0.04	0.03	0.01										
9	Clade E	0.02	0.02	0.02	0.02	0.03	0.03	0.01	0.01									
10	Clade F	0.02	0.02	0.02	0.04	0.05	0.04	0.03	0.03	0.03								
11	*Pholidobolus affinis*	0.05	0.04	0.06	0.05	0.05	0.05	0.05	0.05	0.05	0.06							
12	*Pholidobolus dicrus*	0.07	0.07	0.08	0.07	0.07	0.07	0.07	0.08	0.07	0.08	0.08						
13	*Pholidobolus hillisi*	0.05	0.05	0.05	0.05	0.06	0.05	0.04	0.04	0.05	0.05	0.06	0.08					
14	*Pholidobolus montium*	0.03	0.04	0.05	0.05	0.06	0.04	0.04	0.04	0.04	0.05	0.02	0.07	0.05				
15	*Pholidobolus paramuno*	0.06	0.06	0.07	0.03	0.07	0.07	0.06	0.06	0.06	0.07	0.07	0.10	0.07	0.06			
16	*Pholidobolus prefrontalis*	0.02	0.02	0.04	0.04	0.03	0.03	0.02	0.03	0.03	0.05	0.03	0.05	0.04	0.02	0.06		
17	*Pholidobolus ulisesi*	0.04	0.04	0.04	0.04	0.04	0.04	0.03	0.04	0.03	0.04	0.04	0.07	0.04	0.04	0.06	0.03	
18	*Pholidobolus vertebralis*	0.08	0.08	0.09	0.08	0.08	0.07	0.08	0.08	0.08	0.09	0.08	0.06	0.10	0.08	0.10	0.06	0.08

Table 4. Pairwise genetic distances (uncorrected *p*) of ND4 DNA sequences among species and clades of *Pholidobolus* included in this study. This analysis involved 64 nucleotide sequences and 621 positions.

Taxon	1	2	3	4	5	6	7	8	9	10	11	12	13	14	15	16	17
1 *Pholidobolus condor* sp. nov.																	
2 *Pholidobolus samek* sp. nov.	0.08																
3 *Pholidobolus dolichoderes* sp. nov.	0.13	0.12															
4 *Pholidobolus fascinatus* sp. nov.	0.09	0.10	0.09														
5 Clade A	0.09	0.09	0.13	0.11													
6 Clade B	0.12	0.12	0.12	0.10	0.13												
7 Clade C	0.10	0.11	0.10	0.05	0.12	0.11											
8 Clade D	0.11	0.11	0.10	0.05	0.11	0.11	0.06										
9 Clade E	0.10	0.10	0.10	0.06	0.11	0.11	0.06	0.06									
10 Clade F	0.12	0.12	0.04	0.08	0.14	0.13	0.09	0.10	0.09								
11 *Pholidobolus affinis*	0.13	0.14	0.15	0.12	0.13	0.15	0.12	0.11	0.12	0.15							
12 *Pholidobolus dicrus*	0.15	0.15	0.15	0.15	0.17	0.15	0.15	0.16	0.16	0.15	0.16						
13 *Pholidobolus hillisi*	0.17	0.17	0.17	0.14	0.16	0.18	0.14	0.16	0.14	0.16	0.17	0.19					
14 *Pholidobolus montium*	0.13	0.14	0.15	0.12	0.12	0.17	0.13	0.13	0.13	0.14	0.11	0.17	0.17				
15 *Pholidobolus paramuno*	0.14	0.14	0.16	0.14	0.15	0.16	0.14	0.13	0.13	0.16	0.14	0.17	0.17	0.15			
16 *Pholidobolus prefrontalis*	0.12	0.12	0.14	0.11	0.12	0.14	0.13	0.13	0.12	0.14	0.13	0.16	0.17	0.13	0.13		
17 *Pholidobolus ulisesi*	0.15	0.15	0.15	0.16	0.15	0.16	0.14	0.15	0.14	0.15	0.15	0.17	0.16	0.16	0.17	0.16	
18 *Pholidobolus vertebralis*	0.17	0.17	0.17	0.17	0.17	0.17	0.15	0.16	0.15	0.17	0.16	0.19	0.18	0.18	0.16	0.17	0.17

Table 5. Character loadings, eigenvalues, and percentage of variance explained by Principal Components (PC) I and II. The analysis was based on 16 morphological characters of specimens of "*Pholidobolus macbrydei*", *Pholidobolus samek* sp. nov., *Pholidobolus condor* sp. nov., *Pholidobolus dolichoderes* sp. nov. and *P. fascinatus* sp. nov. Highest loadings are in bold.

Variable	PCA	
	PC I	PC II
NSO	0.13	-0.11
SUJ	**0.32**	-0.15
SLJ	0.30	-0.10
SGJ	0.29	-0.07
SGV	0.31	0.25
DEL	0.30	0.33
NTS	**0.32**	-0.20
SAB	0.26	**0.39**
SAT	0.18	**0.55**
SF3	0.18	-0.11
SF5	0.22	-0.31
ST3	0.24	0.04
ST4	0.20	-0.12
ST5	0.29	-0.02
LES	-0.05	0.20
SGC	-0.22	0.35
Eigenvalue	6.51	1.60
%	40.69	9.99

Morphological comparisons among species

Two components with eigenvalues > 1.0 were extracted from the PCA (Table 5). These components accounted for 50.7% of the total variation. The highest loadings corresponded to supratympanic temporals (NTS) and number of scales along margin of upper jaw (SUJ) for PC I, and number of scales around the tail (SAT) and number of scales around the body (SAB) for PC II (Table 5). In general, there is wide overlap in morphological space among species of the "*P. macbrydei*" complex (Fig. 2).

Comparative hemipenial morphology

Hemipenes of holotypes of the four new species described herein are approximately 4–5 mm and 5–7 subcaudal scales long. The organs are fully everted in specimens of *P. fascinatus*, *P. condor*, and *P. samek* and partially everted in *P. dolichoderes*; the hemipenes of the holotype of *P. fascinatus* and *P. condor* are fully expanded, whereas the organs of *P. dolichoderes* and *P. samek* are partially expanded (Fig. 3). All hemipenes have two small lobes detached from the hemipenial body when the organ is fully everted. The hemipenis of *P. condor* presents a distinctive capitular groove originating at the median hemipenial body and extending toward the lobes. The lobes of *P. fascinatus*, *P. condor*, and *P. samek* present folds on their tips, which are not visible in *P. dolichoderes* due to the partial eversion. The hemipenial body is
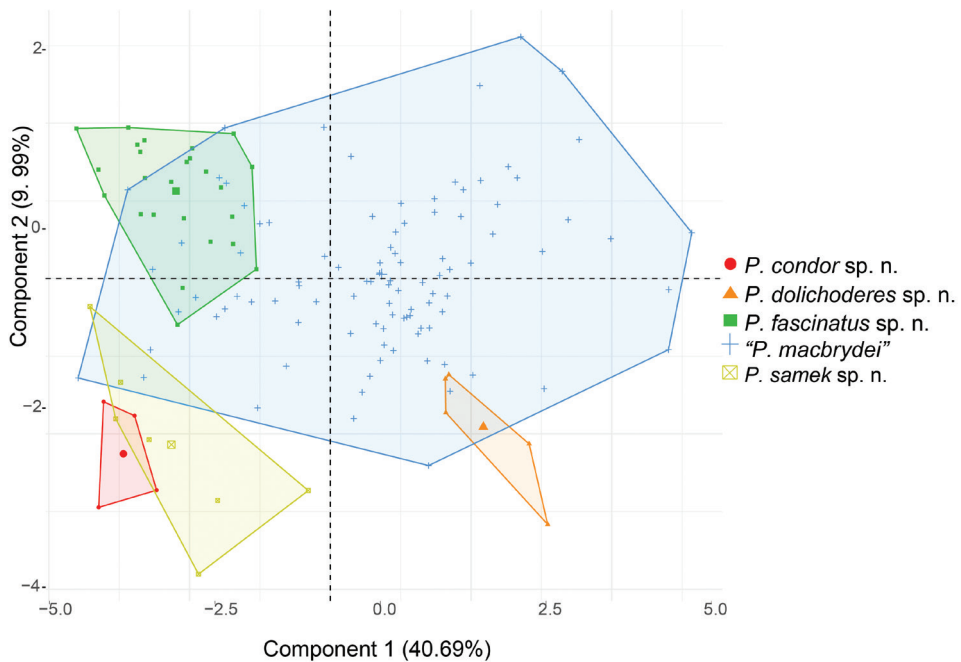
Figure 2. Principal components analysis of 16 morphological variables and 140 specimens of the "*Pholidobolus macbrydei*" species complex. See Table 5 for character loadings on each component.

cylindrical in *P. dolichoderes* and *P. condor*, whereas in *P. samek* and *P. fascinatus* the body is conical, with the basis distinctly thinner than the rest of the body. The sulcus spermaticus is broad in *P. fascinatus*, *P. dolichoderes*, and *P. samek*, narrower in *P. condor*; in *P. fascinatus* and *P. condor*, the sulcus spermaticus is deeper than in *P. dolichoderes* and *P. samek*. The sulcus originates medially at the base of the organ and extends in a straight line throughout the body towards the lobes in all species. However, unlike *P. dolichoderes* and *P. condor*, the sulcus originates between thick lips in *P. samek* and *P. fascinatus*. In all species, the sulcus spermaticus bifurcates at the lobular crotch, with each branch extending along the medial face of each lobe.

The sides and borders of the sulcate and asulcate faces are ornamented with a series of roughly equidistant and chevron-shaped flounces, with the chevron vertices aligned medially on each side and directed proximally. All flounces bear calcified comb-like series of spicules, distinctively stained in red with Alizarin. The number of flounces extending along the hemipenial body varies slightly among species: 21 in *P. condor* and *P. samek* and 22 in *P. dolichoderes* and *P. fascinatus*. The base of the asulcate face bears three medial flounces in *P. condor*, *P. dolichoderes*, and *P. samek*, and four in *P. fascinatus*. All species have a conspicuous unevenness forming a bulge along the margins of the asulcate face.
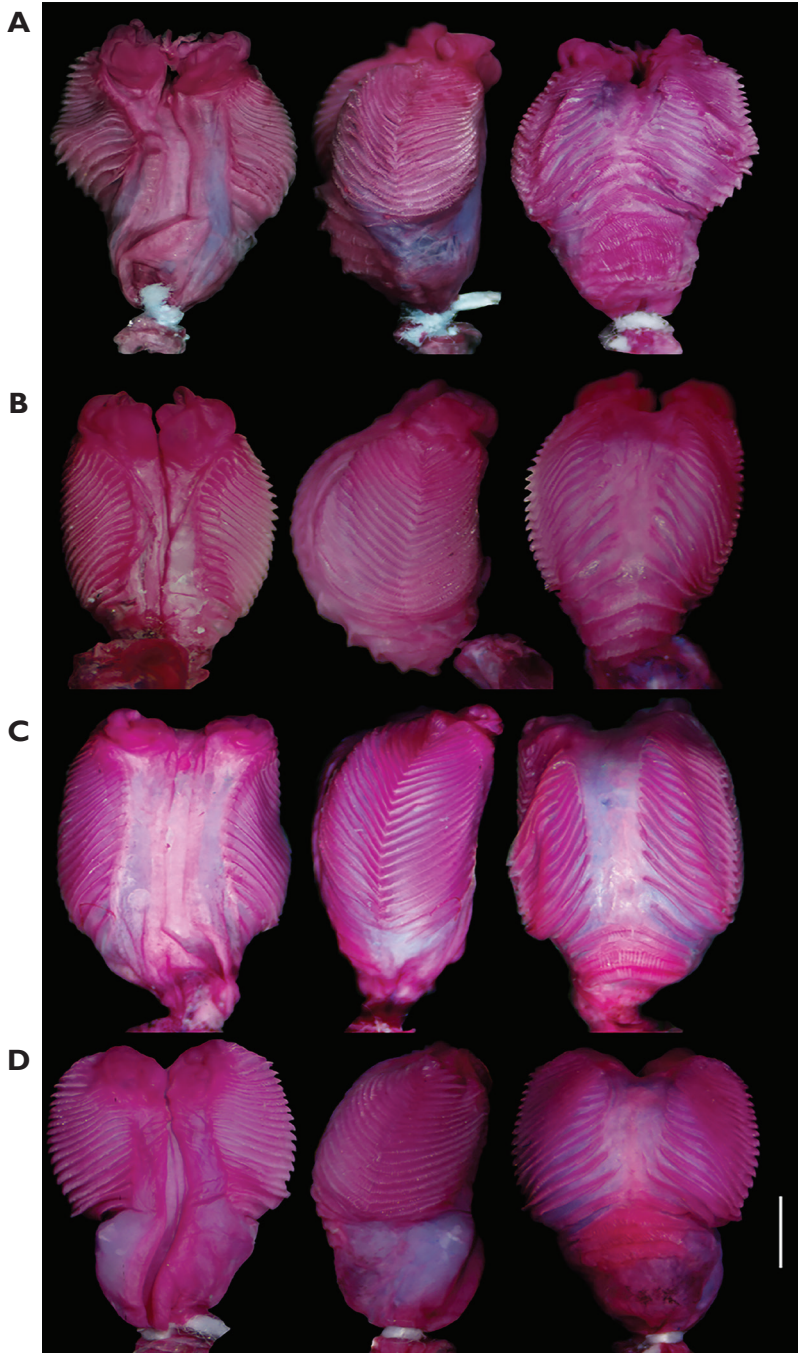
Figure 3. Comparative hemipenial morphology of *Pholidobolus*. Sulcate (left), lateral (center) and asulcate (right) views of: **A** *Pholidobolus samek* sp. nov. (QCAZ 14955) **B** *Pholidobolus condor* sp. nov. (QCAZ 15844) **C** *Pholidobolus dolichoderes* sp. nov. (QCAZ 16353) **D** *Pholidobolus fascinatus* sp. nov. (QCAZ 15120). Scale bar: 1 mm.

Systematic accounts

Pholidobolus samek sp. nov.

http://zoobank.org/431C8AD2-3164-4051-B7DC-1459C4949F51
Figures 4–6
Proposed standard English name: Green-striped cuilanes
Proposed standard Spanish name: Cuilanes de franjas verdes

Holotype. QCAZ 14955 (Figs 4, 5), adult male, Ecuador, Provincia Zamora-Chinchipe, Cerro Plateado Biological Reserve, Cerro Plateado plateau, 4.6159S, 78.7870W, WGS84, 2844 m, 23 September 2016, collected by Diego Almeida, Eloy Nusirquia, Fernando Ayala, Javier Pinto, Alex Achig and Malki Bustos.

Paratypes (6). Ecuador: Provincia Zamora-Chinchipe: QCAZ 14954 (adult female), same data as holotype; QCAZ 14956 (adult female), Cerro Plateado Biological Reserve, 4.6050S, 78.8167W, WGS84, 2320 m, 28 September 2016; QCAZ 14969–70, 14976–77(hatchlings) Cerro Plateado Biological Reserve, 4.6179S, 78.7838W, WGS84, 2873 m, 24 September 2016, same collectors as holotype.

Diagnosis. *Pholidobolus samek* is unique among its congeners, except *P. condor* sp. nov., in having green dorsolateral stripes on the head. However, adult males of *P. samek* differ from those of *P. condor* sp. nov. in having brighter dorsolateral head stripes and lacking a reddish venter. In addition, *P. affinis*, *P. prefrontalis*, *P. macbrydei*, *P. dolichoderes* sp. nov., and *P. montium* differ from *P. samek* (character states of *P. samek* in parentheses) in having a loreal scale frequently in contact with the supralabials (loreal scale not in contact with supralabials), and dorsal scales finely wrinkled (slightly keeled). *Pholidobolus ulisesi* and *P. hillisi* differ from *P. samek* in having a diagonal white bar along the rictal region (white rictal bar absent). *Pholidobolus samek* can be distinguished from *P. dicrus* by lacking a bifurcating vertebral stripe at midbody. *Pholidobolus affinis*, *P. prefrontalis*, *P. dicrus*, *P. hillisi*, and *P. vertebralis* further differ from *P. samek* in having well defined prefrontal scales (if present, prefrontal scales poorly differentiated). Additionally, *P. samek* has fewer dorsal scales (27–29) than *P. affinis* (45–55), *P. montium* (35–50), *P. prefrontalis* (37–46), *P. macbrydei* (31–43), *P. fascinatus* sp. nov. (32–37), and *P. dolichoderes* sp. nov. (35–40). *Pholidobolus samek* can be further distinguished from *P. fascinatus* by having widened medial scales on collar, and from *P. dolichoderes* sp. nov. by having fewer temporals (4–5 and 7–9, respectively), fewer ventrals (19–21 and 25–27), and fewer gulars (15–18 and 22–23).

Characterization. (1) Two (rarely three) supraoculars, anteriormost slightly larger than posterior one; (2) prefrontals present or absent; (3) femoral pores absent in both sexes; (4) four to five opaque lower eyelid scales; (5) scales on dorsal surface of neck striated, becoming slightly keeled from forelimbs to tail; (6) two or three rows of lateral granules at midbody; (7) 27–29 dorsal scales between occipital and posterior margin of hindlimb; (8) lateral body fold present; (9) keeled ventrolateral scales on each side absent; (10) dorsum grayish brown with a distinct golden gray middorsal stripe, slender at midbody, becoming pale gray towards tail; (11) labial stripe white or orange;

(12) flanks of body dark brown; (13) conical hemipenial body, with sulcus spermaticus originating between thick lips.

Description of holotype. Adult male (QCAZ 14955) (Figs 4, 5); SVL 46.7 mm; TL 80.9 mm; dorsal and lateral head scales juxtaposed, finely wrinkled; rostral hexagonal, 2.06 times as wide as high; frontonasal irregularly quadrangular, wider than long, laterally in contact with nasal, loreal and first superciliary, slightly bigger than frontal; prefrontal scales absent; frontal longer than wide, in contact with one supraocular on the left side, and two on the right side; frontoparietals pentagonal, longer than wide, slightly wider posteriorly, each in contact laterally with supraocular II; interparietal roughly heptagonal; parietals slightly bigger than interparietal, hexagonal, and positioned anterolaterally to interparietal, each in contact anteriorly with supraocular II (and supraocular III on right side) and dorsalmost postocular; postparietals three, medial scale smaller than laterals; seven supralabials, fourth one longest and below center of eye; six infralabials, fourth one shortest and below center of eye; temporals enlarged, irregularly hexagonal, juxtaposed, smooth; two large supratemporal scales, smooth; nasal slightly divided, irregularly pentagonal, longer than high, in contact with rostral anteriorly, first and second supralabials ventrally, frontonasal dorsally, loreal posterodorsally and frenocular posteroventrally; nostril on ventral aspect of nasal, directed lateroposteriorly; loreal rectangular, wider dorsally; frenocular higher than long, in contact with nasal, separating loreal from supralabials; two supraoculars on left side, three on right side (posteriormost much smaller), with the first one being the largest; four elongate superciliaries, first one enlarged, in contact with loreal; palpebral disc divided into four enlarged, pigmented scales; suboculars three (on the left side the medial subocular is fragmented), elongated and homogeneous in size; two postoculars, the dorsalmost wider than the other; ear opening vertically oval, without denticulate margins; tympanum recessed into a shallow auditory meatus; mental semicircular, wider than long; postmental pentagonal, slightly wider than long, followed posteriorly by three pairs of genials, the anterior two in contact medially and the posterior one separated by postgenials; all genials in contact with infralabials; gulars imbricate, smooth, posteriorly widened in two longitudinal rows; posterior row of gulars (collar) with six scales, the medial two widened.

Nuchal scales similar in size to dorsals, except for the anteriormost that are widened; scales on sides of neck small and granular; dorsal scales hexagonal, elongate, imbricate, arranged in transverse rows; scales on dorsal surface of neck striated, becoming progressively keeled from forelimbs to tail; number of dorsal scales between occipital and posterior margin of hindlimbs 27; dorsal scale rows in a transverse line at midbody 26; one longitudinal row of smooth, enlarged ventrolateral scales on each side; dorsals separated from ventrals by two rows of small scales at level of 13th row of ventrals; lateral body fold between fore and hindlimbs present; ventrals smooth, wider than long, arranged in 20 transverse rows between collar fold and preanals; six ventral scales in a transverse row at midbody; subcaudals smooth; axillary region with granular scales; scales on dorsal surface of forelimb striated, imbricate; scales on ventral surface of forelimb granular; two thick, smooth thenar scales; supradigitals (left/right)
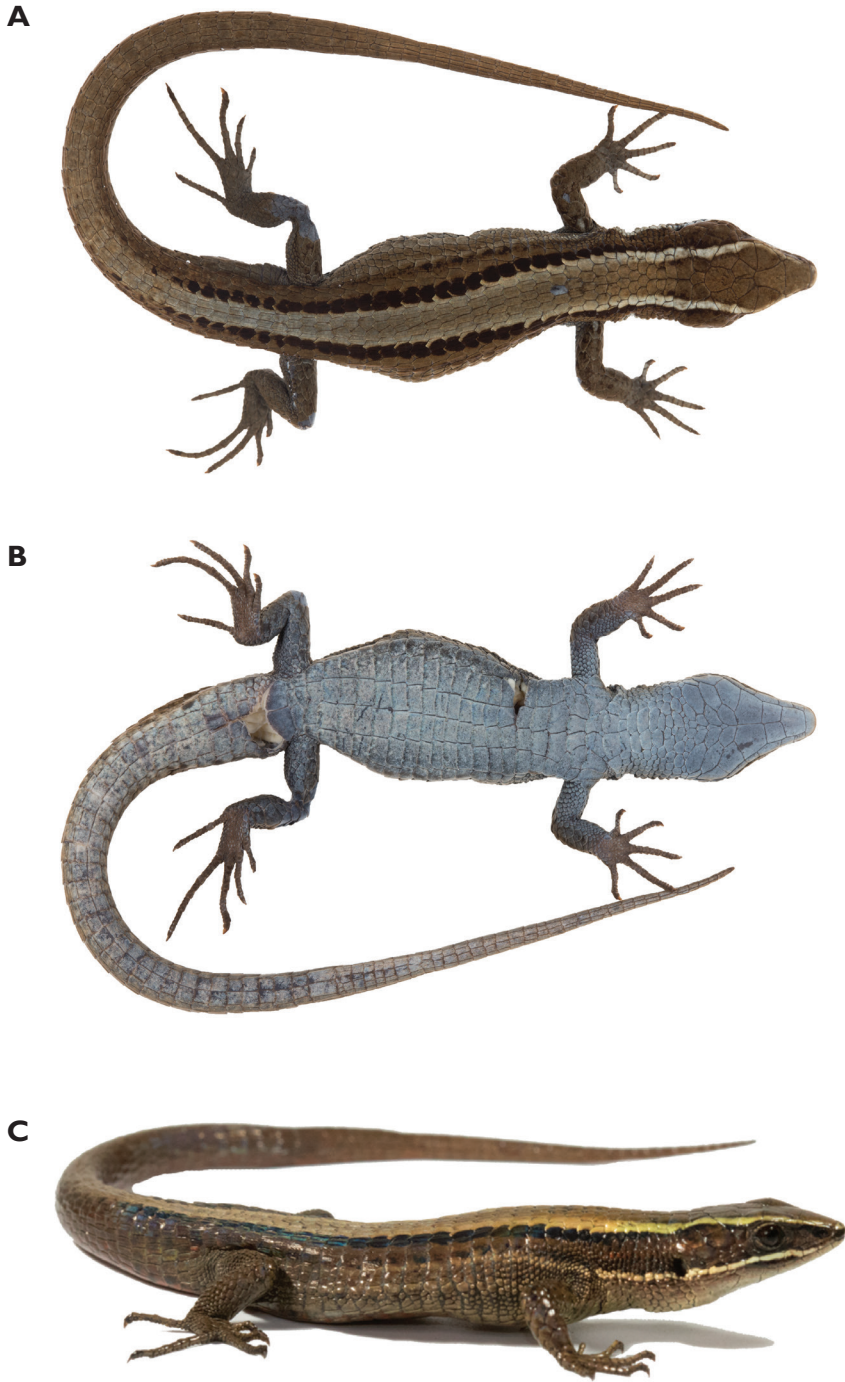
Figure 4. Holotype of *Pholidobolus samek* sp. nov. (QCAZ 14955) in dorsal (**A**), ventral (**B**), and lateral (**C**) views. Male, SVL = 46.7 mm. (A, B): preserved specimen; (C): live specimen. Photographs by Darwin Nuñez and Valeria Chasiluisa.

Figure 5. Head of holotype of *Pholidobolus samek* sp. nov. (QCAZ 14955) in lateral (**A**), dorsal (**B**), and ventral (**C**) views. Photographs by Valeria Chasiluisa. Scale bar: 5 mm.

3/3 on finger I, 6/7 on II, 8/8 on III, 9/9 on IV, 6/6 on V; supradigitals 3/4 on toe I, 6/6 on II, 10/9 on III, 11/12 on IV, 7/7 on V; subdigital lamellae of fingers I and II single, paired on III (except the four distalmost), paired at base on IV, on finger V all single; subdigital lamellae 5/5 on finger I, 11/12 on II, 15/16 on III, 17/16 on IV, 9/10 on V; subdigital lamellae on toes I and II single, on toe III, IV and V all paired, except for the three distalmost subdigitals; subdigital lamellae 6/6 on toe I, 11/10 on II, 16/15 on III, 21/21 on IV, 14/14 on V; groin region with small, imbricate scales; scales on dorsal surface of hindlimbs smooth and imbricate; scales on ventral surface of hindlimbs smooth; scales on posterior surface of hindlimbs granular; femoral pores absent; preanal pores absent; cloacal plate paired, bordered by four scales anteriorly, of which the two medialmost are enlarged.

Additional measurements (mm) and proportions of the holotype: HL 11.4; HW 7.4; ShL 7.0; AGD 23.9; TL/SVL 1.5; HL/SVL 0.2; HW/SVL 0.2; ShL/SVL 0.1; AGD/SVL 0.5.

Color of holotype in life. Dorsal background from head to base of tail grayish brown, with a golden light brown vertebral stripe extending from occiput to tail; bright green dorsolateral stripes on head; cream white longitudinal stripe extending from first supralabial to shoulder; sides of neck, flanks and limbs dark brown; reddish brown narrow stripe extending from tympanum to arm insertion; ventrolateral region of body grayish brown; throat cream; chest, belly and base of tail cream orange (Figs 4C, 6B).

Color of holotype in preservative. Dorsal background uniformly grayish brown, with a golden-gray vertebral stripe extending from occiput to tail; vertebral stripe wider anteriorly, becoming slightly slender at most posterior part of body; dorsal and lateral surfaces of head brown (rostral, frontonasal, frontal, frontoparietals, and supraoculars); bluish white longitudinal stripe extending from first supralabial to shoulder and fading on flanks; ventrolateral aspect of neck dark brown with a dorsolateral light brown stripe extending posteriorly along flanks to hindlimbs; forelimbs with scattered ocelli (black with white center); flanks grayish brown with two dorsolateral stripes on each side, the dorsal one dark brown and the most ventral one brown diffuse with dark brown spots; tail brown dorsally; ventral surface of head gray, chest and venter dark gray, ventral surface of tail slightly gray, with scattered dark brown marks.

Variations. Measurements and scale counts of *Pholidobolus samek* are presented in Table 6. Supralabials 8/7 (left/right) and temporals five in specimen QCAZ 14956; small and separated prefrontals on both sides in QCAZ 14954 and one prefrontal on right side in QCAZ 14956; little intrusive scales between parietal and postparietal in QCAZ 14954; frontal hexagonal in QCAZ 14956; roughly decagonal interparietal in QCAZ 14954. Usually two scales on posterior cloacal plate, four in QCAZ 14954 and 14956. Male is larger (SVL 46.7 mm, N = 1) than females (maximum SVL 45.4 mm, N = 2). Hatchlings (QCAZ 14969, 14970, 14976) with eight or seven (QCAZ 14976) posterior gular (collar) scales. Unlike the male holotype, females have an orange-brown longitudinal stripe extending from third supralabial to shoulder and fading on the flanks (Fig. 6).

Distribution and natural history. *Pholidobolus samek* inhabits cloud forests in Cordillera del Cóndor, southeastern Ecuador at elevations between 2324–2844 m (Fig. 7). The new species is known only from Zamora-Chinchipe province, on the

Figure 6. *Pholidobolus samek* sp. nov. in life. **A** Adult female, paratype (QCAZ 14954) **B** adult male, holotype (QCAZ 14955).

sandstone plateaus of Cerro Plateado Biological Reserve. The ground at the type locality is covered with mosses, roots, and bromeliads. Such ground cover is locally known as bamba. All specimens were found active at 11h30–17h00 under stones or terrestrial bromeliads (Fig. 8). Four eggs, collected under flat stones on 24-09-2016, were incubated in sphagnum and perlite in captivity for two months approximately. They were

Table 6. Summary of morphological characters and measurements (mm) of *Pholidobolus samek* sp. nov., *P. condor* sp. nov., *P. dolichoderes* sp. nov., and *P. fascinatus* sp. nov. Range (first line) and mean ± standard deviation (second line) are presented.

Character	*P. samek* sp. nov. N = 7 (adults = 3)	*P. condor* sp. nov. N = 4 (adults = 1)	*P. dolichoderes* sp. nov. N = 5 (adults = 3)	*P. fascinatus* sp. nov. N = 27 (adults = 4)
Scales along margin of upper jaw	7–10 (9.14 ± 1.07)	8–9 (8.75 ± 0.5)	9–11 (10.2 ± 0.84)	7–10 (8.36 ± 0.91)
Scales along margin of lower jaw	8–9 (8.25 ± 0.5)	5–10 (7.14 ± 2.67)	10–11 (10.2 ± 0.45)	4–10 (7.4 ± 1.58)
Gulars	15–18 (16.71 ± 1.11)	14–16 (15 ± 0.82)	22–23 (22.8 ± 0.48)	14–17 (15.72 ± 0.89)
Ventrals in transverse row at midbody	19–21 (20 ± 0.82)	18–20 (19 ± 1.15)	25–27 (25.8 ± 0.84)	21–25 (22.96 ± 1.21)
Dorsals from occiput to base of tail	27–29 (27.71 ± 0.76)	26–30 (27.75 ± 1.71)	35–40 (36.8 ± 2.05)	32–37 (34.64 ± 1.19)
Temporals	4–5 (4.14 ± 0.38)	4–5 (4.25 ± 0.5)	7–9 (8 ± 0.70)	3–5 (3.44 ± 0.65)
Scales around midbody	25–32 (27.71 ± 2.75)	27–30 (28 ± 1.41)	31–33 (32.2 ± 0.84)	28–34 (30.96 ± 1.79)
Scales around tail	14–16 (15 ± 0.81)	14–20 (17.86 ± 2.73)	18–19 (18.6 ± 0.55)	18–22 (20.32 ± 1.18)
Lower eyelid scales	4–5 (4.14 ± 0.38)	5	4–6 (4.8 ± 0.84)	4–6 (5.04 ± 0.61)
Gular (collar) scales	6–8 (7.14 ± 0.9)	6–9 (7.75 ± 1.26)	6–8 (6.4 ± 0.89)	9–12 (10.28 ± 0.73)
Head length in adults	9.9–11.4 (10.76 ± 0.77)	11	9.7–10.6 (10.05 ± 0.46)	8.9–12.3 (10.22 ± 1.80)
Head width in adults	6.5–7.4 (6.93 ± 0.48)	6.6	6.2–6.3 (6.26 ± 0.05)	6.6–9.2 (7.58 ± 1.45)
SVL in adults	41.6–49.3 (45.89 ± 3.89)	42.7	41.1–50.6 (45.75 ± 4.74)	42.6–52.5 (47.3 ± 4.98)

14.0–14.1 mm long, 8.0–8.5 mm wide, and weighted 0.4 g on average. Hatchlings (QCAZ 14969–70, 14976–77) weighted 0.3 g and were 24.7 mm in SVL on average.

Conservation status. *Pholidobolus samek* is only known from Cordillera del Cóndor. The population size for this species is unknown, but our sampling suggests low abundances. Because of the small known distribution, as well as habitat destruction through mining activities nearby (Van Teijlingen 2016), we suggest assigning *P. samek* to the Critically Endangered category under criteria B1a, b(iii); C1; D, according to IUCN (2012) guidelines.

Etymology. The specific epithet *samek* means green in the Shuar language, in allusion to the green dorsolateral head stripes distinguishing the new species from other congeners. The type locality of *Pholidobolus samek* lies within territory of Shuar indigenous people, who inhabit the Amazonian rainforest in Ecuador and Peru.

Remarks. *Pholidobolus samek* sp. nov. is very similar morphologically and genetically to *P. condor* sp. nov. These species can be easily distinguished from each other by coloration in adult males, although we recognize that our sample size is small (*N* = 7 and 4, respectively) and includes only one adult male per species. However,
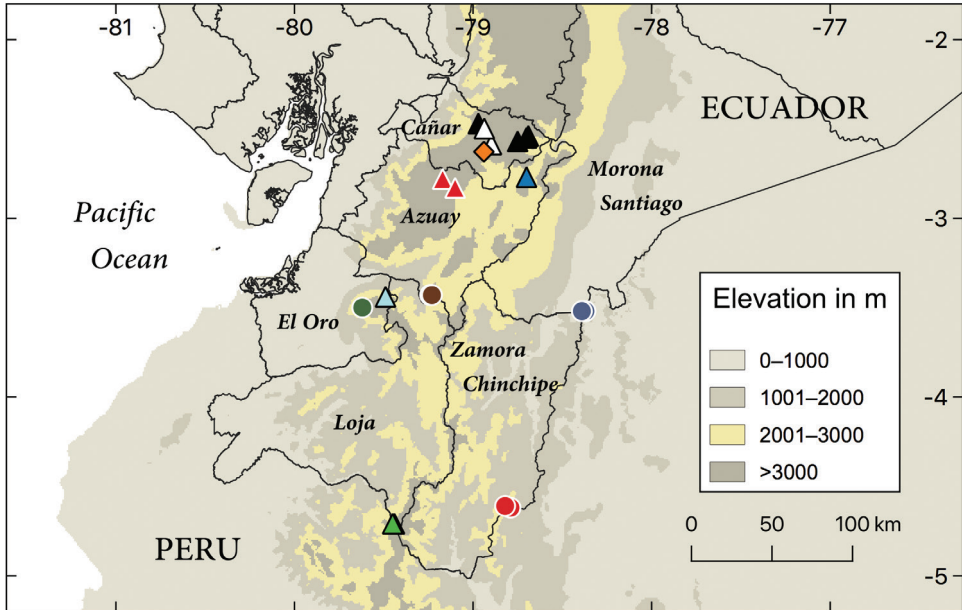
Figure 7. Distribution of samples of the "*Pholidobolus macbrydei*" species complex included in phylogenetic analyses. Circles correspond to four new species described in this paper: *P. samek* sp. nov. (red), *P. condor* sp. nov. (blue), *P. dolichoderes* sp. nov. (brown), and *P. fascinatus* sp. nov. (green). Triangles are "*Pholidobolus macbrydei*" clades as illustrated in the phylogenetic tree (Fig. 1): **A** (green) **B** (white) **C** (red) **D** (blue) **E** (black) **F** (turquoise). Orange diamond corresponds to type locality of *P. macbrydei*. This map was created in QGIS v3.10.

further evidence supports recognition of *P. samek* and *P. condor* as different species. First, they are reciprocally monophyletic and they are not sister taxa, with *P. samek* being sister to "*P. macbrydei*" Clade A (Fig. 1), which is very different in color patterns from either *P. samek* or *P. condor* (V. Parra and O. Torres-Carvajal, personal observation). Second, unlike the 12S gene (the less variable gene in this study), genetic distances between *P. samek* and *P. condor* for 16S and ND4 are not the lowest (Tables 2 and 4, respectively) within *Pholidobolus*. For example, the 16S distance between *P. samek* and *P. condor* (3%) is the same as the distance between the well-recognized species *P. paramuno* and *P. affinis*. In addition, genetic exchange among *P. samek*, *P. condor* and Clade A is very unlikely as they are isolated from each other on mountaintops above 2000 m (Fig. 7).

Pholidobolus condor sp. nov.
http://zoobank.org/BB38EC4E-634D-4728-BA30-412913E7D0E0
Figures 9, 10
Proposed standard English name: Condor cuilanes
Proposed standard Spanish name: Cuilanes del Cóndor
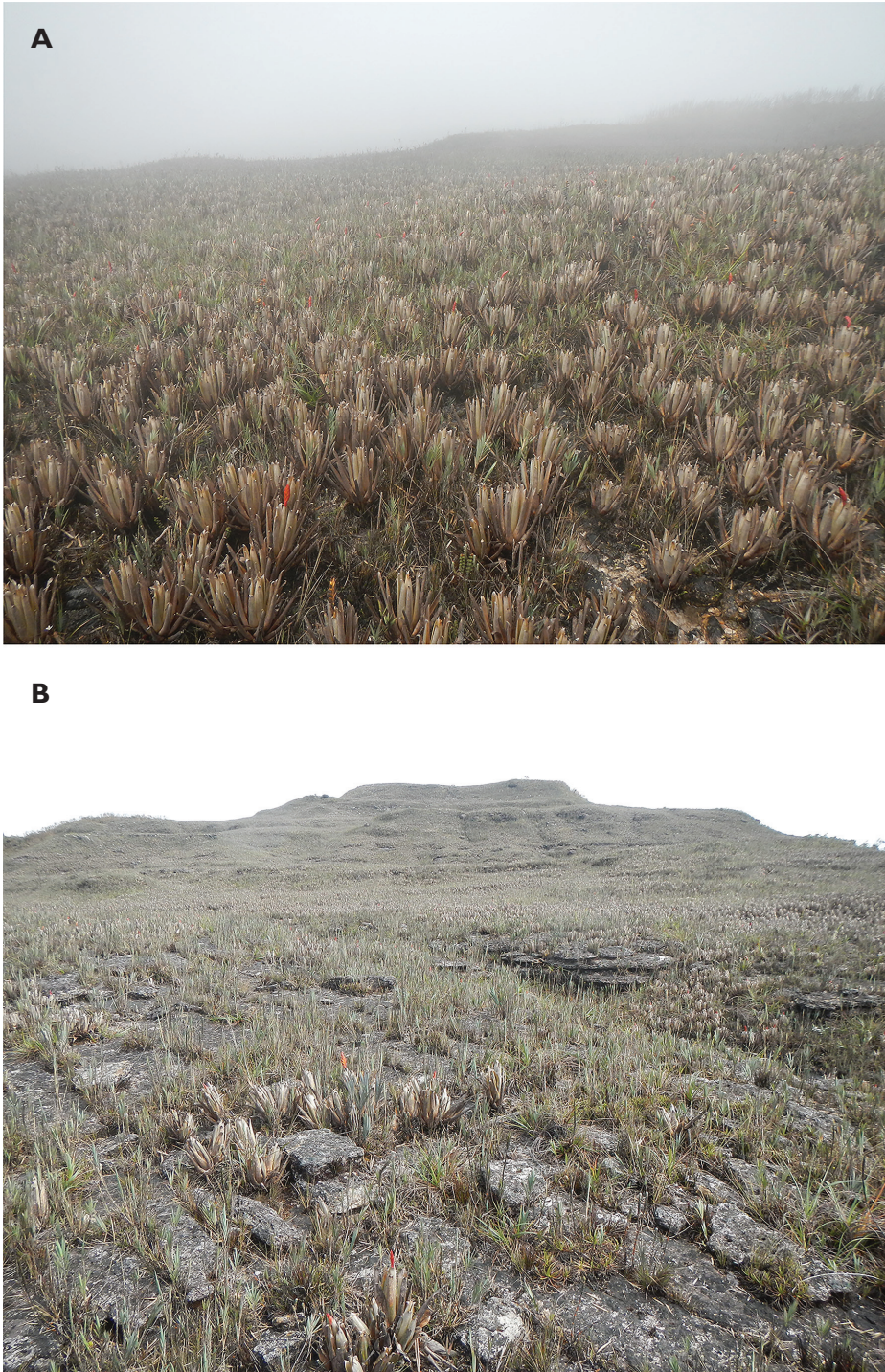
Figure 8. Habitat of *Pholidobolus samek* sp. nov. **A** Vegetation around type locality, Cerro Plateado Biological Reserve, Ecuador **B** habitat where holotype was found. Photographs by Álvaro Pérez.

Holotype. QCAZ 15844 (Figs 9, 10), adult male, Ecuador, Provincia Morona Santiago, buffer zone of El Quimi Biological Reserve, plateau on the eastern side of El Quimi river valley, 3.51892S, 78.3690W, WGS84, 2209 m, 11 July 2017, collected by Diego Almeida, Darwin Núñez, Eloy Nusirquia, Alex Achig and Ricardo Gavilanes.

Paratypes (3). Ecuador: Provincia Morona Santiago: QCAZ 16790 (hatchling), El Quimi Biological Reserve, base camp towards old heliport (high zone), 3.51894S, 78.36897W, WGS84, 2226 m, 17 April 2018; QCAZ 16788–89 (hatchlings), El Quimi Biological Reserve, near base camp, 3.5182S, 78.3913W, WGS84, 1994 m, 12 April 2018, collected by Diego Almeida, Darwin Núñez, Eloy Nusirquia, Alex Achig and María del Mar Moretta.

Diagnosis. *Pholidobolus condor* is unique among its congeners, except *P. samek* sp. nov., in having green dorsolateral stripes on the head. However, adult males of *P. condor* differ from those of *P. samek* sp. nov. in having lighter dorsolateral head stripes, and reddish flanks and venter. In addition, *P. ulisesi*, *P. dicrus*, *P. hillisi*, and *P. vertebralis* differ from *P. condor* (character states of *P. condor* in parentheses) in having a conspicuous light vertebral stripe (light vertebral stripe absent). *Pholidobolus affinis*, *P. prefrontalis*, *P. dicrus*, *P. hillisi*, and *P. vertebralis* further differ from *P. condor* in having prefrontal scales (prefrontal scales absent). Additionally, *P. condor* sp. nov. has fewer dorsal scales (26–30) than *P. affinis* (45–55), *P. montium* (35–50), *P. prefrontalis* (37–46), *P. macbrydei* (31–43), and *P. dolichoderes* sp. nov. (35–40). *Pholidobolus condor* can be further distinguished from *P. fascinatus* sp. nov. by having widened medial scales on collar, and from *P. dolichoderes* sp. nov. by having fewer temporals (7–9 and 4–5, respectively), fewer ventrals (18–20 and 25–27), and fewer gulars (14–16 and 22–23).

Characterization. (1) Two (rarely three) supraoculars, anteriormost larger than posterior one; (2) prefrontals absent; (3) femoral pores absent; (4) four opaque lower eyelid scales; (5) scales on dorsal surface of neck striated or smooth, progressively striated from forelimbs to tail; (6) two rows of lateral granules at midbody; (7) 27–31 dorsal scales between occipital and posterior margin of hindlimb; (8) lateral body fold present; (9) keeled ventrolateral scales on each side absent; (10) dorsum dark brown with a narrow, pale brown stripe; (11) labial stripe white; (12) flanks of body dark brown or gray; (13) hemipenial body cylindrical with distinctive capitular groove.

Description of holotype. Adult male (QCAZ 15844) (Figs 9, 10); SVL 42.7 mm; TL 74.8 mm; dorsal and lateral head scales juxtaposed, finely wrinkled; rostral hexagonal, 1.67 times as wide as high; frontonasal quadrangular, slightly bigger than frontal, laterally in contact with nasal, loreal and first superciliary; prefrontal scales absent; frontal pentagonal, longer than wide, wider anteriorly, in contact with first superciliary and supraocular; frontoparietals hexagonal, longer than wide, slightly wider in the middle, each in contact laterally with supraocular II; interparietal octagonal, with a short medial suture posteriorly, lateral borders nearly parallel to each other; parietals larger than interparietal, hexagonal and positioned anterolaterally to interparietal, each in contact laterally with supraocular II and dorsalmost postocular; postparietals three, medial scale smaller than lateral ones; eight supralabials, fourth one longest and below center of eye; six infralabials, fourth one below center of eye; temporals enlarged, irregularly hexagonal, smooth; two
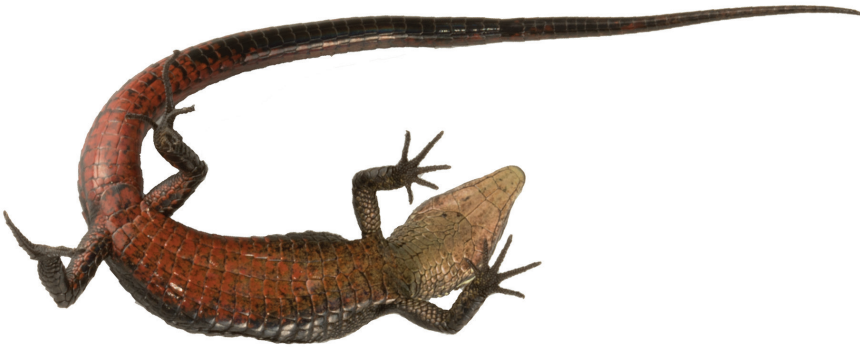
Figure 9. Holotype of *Pholidobolus condor* sp. nov. (QCAZ 15844) in dorsal (**A**), ventral (**B**), and lateral (**C**) views. Male, SVL = 42.7 mm. Preserved specimen (**A**); live specimen (**B, C**). Photographs by Malki Bustos.

Figure 10. Head of holotype of *Pholidobolus condor* sp. nov. (QCAZ 15844) in lateral (**A**), dorsal (**B**), and ventral (**C**) views. Photographs by Valeria Chasiluisa. Scale bar: 5 mm.

large and smooth supratemporals; nasal shield slightly divided above nostril, irregularly pentagonal, longer than high, in contact with rostral anteriorly, first and second supralabials ventrally, frontonasal dorsally, loreal posterodorsally and frenocular posteroventrally; nostril on ventral aspect of nasal, directed laterally; loreal quadrangular, slightly wider dorsally, not in contact with supralabials; frenocular higher than long, in contact with nasal; nasal separating loreal from supralabials; two supraoculars, anteriormost one the widest; four elongate superciliaries, anteriormost enlarged, in contact with loreal; palpebral disc divided into five pigmented scales; four suboculars, anteriormost three elongated and homogeneous in size, posteriormost widest; two postoculars, the dorsalmost wider than the other; ear opening vertically oval, without denticulate margins; tympanum recessed into a shallow auditory meatus; mental wider than long; postmental pentagonal, slightly wider than long, followed posteriorly by three pairs of genials, the anterior two pairs in contact medially and the third pair separated by postgenials; all genials in contact with infralabials; gulars imbricate, smooth, widened in two longitudinal rows; posterior row of gulars (collar) with nine scales, the medial three slightly widened.

Nuchal scales slightly smaller than dorsals, except for the anteriormost that are widened; scales on sides of neck small and granular; dorsal scales elongate, imbricate, arranged in transverse rows; scales on dorsal surface of neck striated, becoming progressively keeled from forelimbs to tail; dorsal scales between occipital and posterior margin of hindlimbs 27; dorsal scale rows in a transverse line at midbody 27; one longitudinal row of smooth, enlarged ventrolateral scales on each side; dorsals separated from ventrals by two rows of small scales at the level of 13th row of ventrals; lateral body fold between fore and hindlimbs present; ventrals smooth, wider than long, arranged in 20 transverse rows between collar fold and preanals; six ventral scales in a transverse row at midbody; subcaudals smooth; axillary region with granular scales; scales on dorsal surface of forelimb striated, imbricate; scales on ventral surface of forelimb granular; two thick, smooth thenar scales; supradigitals (left/right) 3/3 on finger I, 6/6 on II, 8/8 on III, 9/9 on IV, 6/6 on V; supradigitals 3/3 on toe I, 6/6 on II, 9/9 on III, 12/12 on IV, 7/7 on V; subdigital lamellae of finger I, II, III, and V single, on finger IV few scales in the middle paired; subdigital lamellae 6/6 on finger I, 11/11 on II, 15/15 on III, 17/16 on IV, 10/10 on V; subdigital lamellae on toes I and II single, on toes III, IV and V paired, except for two or three distalmost subdigitals; subdigital lamellae 7/6 on toe I, 12/12 on II, 15/16 on III, 22/22 on IV, 12/12 on V; groin region with small, juxtaposed scales; scales on dorsal surface of hindlimbs striated and imbricate; scales on ventral surface of hindlimbs smooth; scales on posterior surface of hindlimbs granular; femoral pores absent; preanal pores absent; cloacal plate paired, bordered by four scales anteriorly, of which the two medialmost are enlarged.

Additional measurements (mm) and proportions of the holotype: HL 11.0; HW 6.6; ShL 5.8; AGD 20.4; TL/SVL 1.7; HL/SVL 0.3; HW/SVL 0.2; ShL/SVL 0.1; AGD/SVL 0.5.

Color of holotype in life. Dorsal background from head to base of tail dark brown, with a golden brown vertebral stripe extending from occiput to tail; greenish cream dorsolateral stripes on head, becoming light brown on posterior part of body; white longitudinal stripe extending from first supralabial to shoulder; sides of neck, flanks

and limbs dark brown; chocolate brown narrow stripe extending from tympanum to arm insertion; ventrolateral region of body grayish brown; throat reddish cream; chest, belly, base of tail and lateral region of tail bright orange, with brown marks in some scales; ventral surface of hind limbs with orange diffuse marks (Fig. 9B,C).

Color of holotype in preservative. Dorsal background uniformly dark brown with a grayish brown middorsal stripe extending from occiput onto tail; dorsolateral stripe distinct, pale gray, extending from snout to near base of tail; head brown dorsally (rostral, frontonasal, frontal, frontoparietals and supraoculars) and dark brown laterally; white longitudinal stripe extending from first supralabial to forelimb; lateral aspect of neck dark brown with a dorsolateral light brown stripe extending posteriorly along flanks to hindlimbs; flanks grayish brown; tail dark brown dorsally and bronze laterally; ventral surface of head gray, with dirty cream genials and scattered black marks; chest, belly and ventral surface of tail light gray with light red spots; ventral surface of limbs dark gray (Fig. 9A).

Variations. Measurements and scale counts of *Pholidobolus condor* are presented in Table 6. Supraoculars three on left side in specimen QCAZ 16789; supralabials six in QCAZ 16789 and 16790, and seven in QCAZ 16788; two quadrangular frontonasals in QCAZ 16788; transverse rows of ventral scales between collar fold and preanals 18 in QCAZ 16788 and 19 in QCAZ 16790. Hatchlings with eight (QCAZ 16788–89) or six (QCAZ 16790) posterior gular (collar) scales. Unlike the adult male, hatchlings lack reddish color on tail.

Distribution and natural history. *Pholidobolus condor* occurs in Cordillera del Cóndor in southeastern Ecuador at elevations between 1994–2226 m. The new species is known from El Quimi Biological Reserve in Morona Santiago province (Fig. 7). The holotype was found active at 21h14 at the base of a bromeliad on a sandstone plateau of shrub vegetation (Fig. 11).

Several eggs were found within a bromeliad, suggesting that females of *P. condor* lay their eggs in communal nests. Four eggs that were found on the ground at the base of bromeliads and under a trunk were incubated in sphagnum and perlite in captivity for approximately three months. On average, hatchlings weighted 0.4 g and were 23.7 mm in SVL.

Conservation status. *Pholidobolus condor* is only known from Cordillera del Cóndor in southeastern Ecuador. This area is currently threatened by mining activities (Ron et al. 2018; Valencia et al. 2017; Van Teijlingen 2016). Habitat destruction and fragmentation is evident at a distance of ~11 km from the collection sites (Mazabanda et al. 2018). Because of the small known distribution and habitat disturbance, we suggest assigning *P. condor* to the Critically Endangered category under criteria B1a, b(iii); C1; D, according to IUCN (2012) guidelines.

Etymology. The specific epithet *condor* refers to Cordillera del Cóndor, where the new species was discovered. The Cordillera del Cóndor is an eastern outlier of the main Andean chain, where a significant number of species have been discovered in the last decade (Brito et al. 2017; Huamantupa-Chuquimaco and Neill 2018; Ron et al. 2018; Torres-Carvajal et al. 2009; Valencia et al. 2017).

Remarks. See remarks on *Pholidobolus samek* sp. nov. above.

Figure 11. Habitat of *Pholidobolus condor* sp. nov. at El Quimi Biological Reserve, Ecuador. Photographs by Álvaro Pérez.

Pholidobolus dolichoderes sp. nov.
http://zoobank.org/95D82201-D761-40F4-8395-4AAC38F24563
Figures 12–14
Proposed standard English name: Long-necked cuilanes
Proposed standard Spanish name: Cuilanes de cuello largo

Holotype. QCAZ 16353 (Figs 12, 13), adult male, Ecuador, Provincia Azuay, San Felipe de Oña, 3.4292S, 79.2364W, WGS84, 2672 m, 16 March 2018, collected by Diego Almeida, Darwin Núñez, Eloy Nusirquia, Alex Achig and Katherine Nicolalde.

Paratypes (4). Ecuador: Provincia Azuay: QCAZ 16349, 16352 (adult females), San Felipe de Oña, Susudel-Poetate road, 3.4322S, 79.2369W, WGS84, 2506 m, 16 March 2018; QCAZ 16350–51 (juveniles), San Felipe de Oña, 3.4275S, 79.2339W, WGS84, 2675 m, 16 March 2018, same collectors as holotype.

Diagnosis. *Pholidobolus dolichoderes* is unique among its congeners in having a long neck with granular scales between the posterior corner of the orbit and the anterior edge of the tympanum, as well as an inconspicuous ventrolateral fold between fore and hindlimbs. In addition, *P. ulisesi*, *P. dicrus*, *P. hillisi*, and *P. vertebralis* differ from *P. dolichoderes* in having a conspicuous light vertebral stripe. The new species further differs from *P. affinis* in lacking ocelli on flanks, and from *P. condor* sp. nov., *P. macbrydei*, and *P. montium* in having prefrontal scales. *Pholidobolus dolichoderes* has more dorsals

Figure 12. Holotype of *Pholidobolus dolichoderes* sp. nov. (QCAZ 16353) in life in dorsal (**A**), ventral (**B**), and lateral (**C**) views. Male, SVL = 41.1 mm. Photographs by Gustavo Pazmiño.

(35–40) and ventrals (25–27) than *P. samek* sp. nov. (27–29 and 19–21, respectively) and *P. condor* sp. nov. (26–30 and 18–20), and, unlike *P. fascinatus* sp. nov., it has widened medial scales on collar. In addition, *P. dolichoderes* has more temporals (7–9) and gulars (22–23) than *P. samek* sp. nov. (4–5 and 15–18, respectively), *P. condor* sp. nov. (4–5 and 14–16), and *P. fascinatus* sp. nov. (3–5 and 14–17).
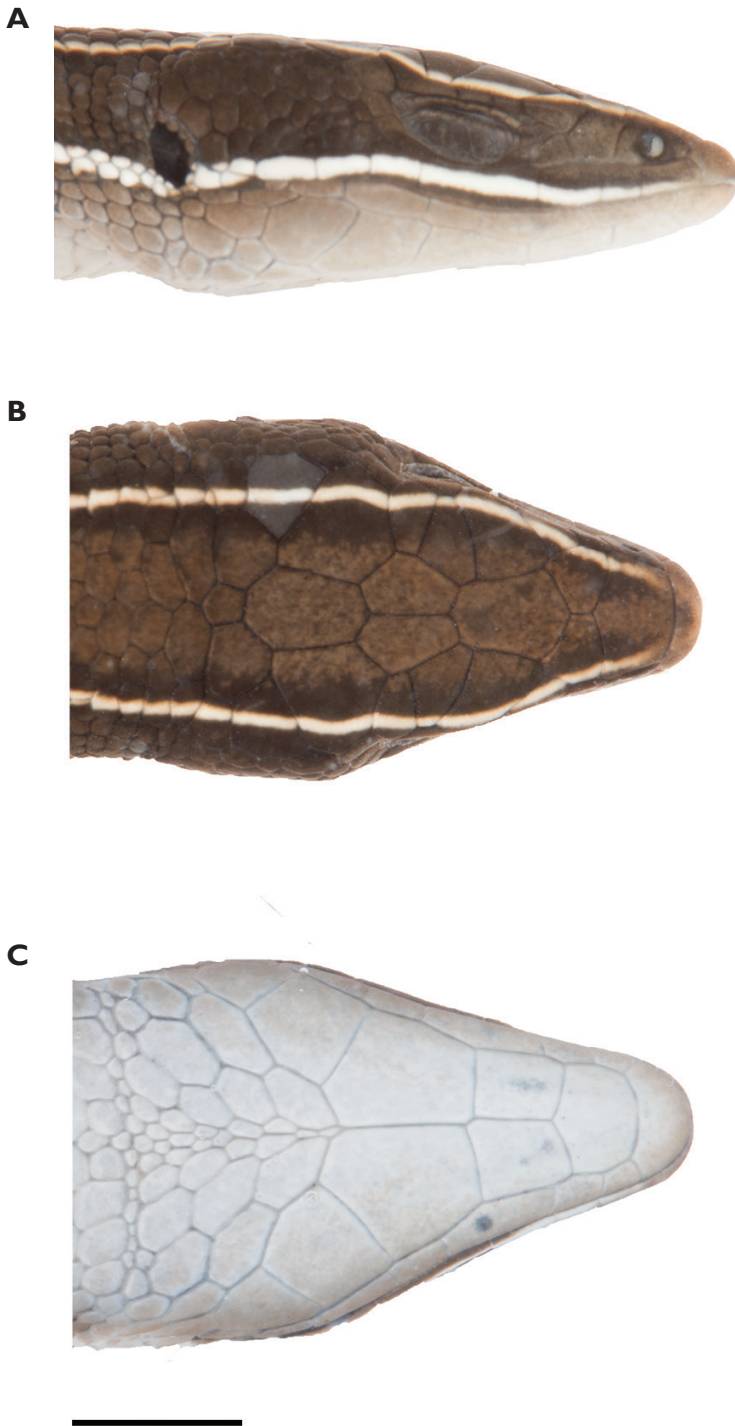
Figure 13. Head of holotype of *Pholidobolus dolichoderes* sp. nov. (QCAZ 16353) in lateral (**A**), dorsal (**B**), and ventral (**C**) views. Photographs by Valeria Chasiluisa. Scale bar: 5 mm.

Characterization. (1) Three supraoculars, anteriormost larger than posterior ones; (2) prefrontals present; (3) femoral pores present in both sexes; (4) four to six opaque lower eyelid scales; (5) scales on dorsal surface of neck smooth, becoming slightly keeled from forelimbs to tail; (6) two or three rows of lateral granules at midbody; (7) 35–20 dorsal scales between occipital and posterior margin of hindlimb; (8) lateral body fold present but inconspicuous; (9) keeled ventrolateral scales on each side absent; (10) dorsum dark brown with a diffuse pale brown vertebral stripe that becomes grayish brown towards tail; (11) labial stripe white; (12) flanks of body gray brown; (13) white stripe along forelimb present; (14) hemipenial body cylindrical, with sulcus spermaticus originating between thick lips.

Description of holotype. Adult male (QCAZ 16353) (Figs 12, 13); SVL 41.1 mm; TL 96.3 mm; dorsal and lateral head scales imbricated, smooth; rostral hexagonal, 1.75 times as wide as high; frontonasal heptagonal, slightly wider than long, laterally in contact with nasal, similar in size to frontal; prefrontals present, in wide contact medially, and in contact with loreal and first superciliary laterally; frontal hexagonal, longer than wide, wider anteriorly, in contact with first and second supraoculars; frontoparietals hexagonal, longer than wide, slightly wider posteriorly, each in contact with second and third supraoculars, parietals and interparietal; interparietal heptagonal, lateral borders nearly parallel to each other; parietals wider than interparietal, heptagonal, and positioned anterolaterally to interparietal, each in contact with third supraocular and dorsalmost postocular; postparietals three, medial scale smaller than lateral ones; seven supralabials, fourth one the longest and below center of eye; five infralabials, fourth one below center of eye; temporals small, irregularly, smooth; supratemporal scales not well differentiated, smooth; nasal shield divided above the nostril, longer than high, in contact with rostral anteriorly, first and second supralabials ventrally, frontonasal dorsally, loreal posteriorly; loreal pentagonal, slightly wider dorsally, in contact with second and third supralabials; frenocular longer than high, in contact with loreal; three supraoculars, with the first one being the widest; four elongate superciliaries, anteriormost one enlarged, in contact with loreal; palpebral disc oval, pigmented, divided into four scales; four suboculars, two elongated and similar in size, the anteriormost and posteriormost larger than the others; three postoculars, dorsalmost wider than the others; ear opening vertically oval, without denticulate margins; tympanum recessed into a shallow auditory meatus; mental wider than long; postmental pentagonal, slightly wider than long, followed posteriorly by three pairs of genials, the anterior two pairs in contact medially and the third pair separated by postgenials; all genials in contact with infralabials; gulars imbricate, smooth, widened in two longitudinal rows; gular fold complete, posterior row of gulars (collar) with six scales, the medial two distinctly widened.

Nuchal scales slightly smaller than dorsals, except for the anteriormost that are widened; scales on sides of neck small and granular; dorsal scales elongate, juxtaposed, arranged in transverse rows; scales on dorsal surface of neck striated, becoming slightly keeled from forelimbs to tail; dorsal scales between occipital and posterior margin of hindlimbs 35; dorsal scale rows in a transverse line at midbody 32; one longitudinal row of smooth, enlarged ventrolateral scales on each side; dorsals separated from ven-

trals by three rows of granular scales at level of 13th row of ventrals; lateral body fold between fore and hindlimbs poorly defined; ventrals smooth, arranged in 26 transverse rows between collar fold and preanals; six ventral scales in a transverse row at midbody; subcaudals smooth; axillary region with granular scales; scales on dorsal surface of forelimb smooth, imbricate; scales on ventral surface of forelimb granular; two thick, smooth thenar scales; supradigitals (left/right) 3/0 on finger I, 7/7 on II, 9/8 on III, 10/10 on IV, 5/5 on V; supradigitals 4/4 on toe I, 7/7 on II, 11/11 on III, 12/11 on IV, 9/8 on V; subdigital lamellae of fingers I and II mostly single, III and IV paired proximally, on finger V all single; subdigital lamellae 5 on left finger I (right finger missing), 10/10 on II, 14/14 on III, 14/14 on IV, 9/9 on V; subdigital lamellae on toe I single, on toe II paired at the middle, on toe III and IV paired along proximal half, and on toe V paired proximally; subdigital lamellae 5/5 on toe I, 10/10 on II, 14/14 on III, 18/19 on IV, 11/11 on V; groin region with small, imbricate scales; scales on dorsal surface of hindlimbs striated and imbricate; scales on ventral surface of hindlimbs smooth; scales on posterior surface of hindlimbs granular; femoral pores present, three on left leg and five on right leg; preanal pores absent; cloacal plate paired, bordered by four scales anteriorly, of which the two medialmost are enlarged.

Additional measurements (mm) and proportions of the holotype: HL 9.8; HW 6.2; ShL 5.4; AGD 20.7; TL/SVL 2.4; HL/SVL 0.2; HW/SVL 0.1; ShL/SVL 0.1; AGD/SVL 0.5.

Color of holotype in life. Dorsal background of head dark brown; diffuse pale brown vertebral stripe that becomes grayish brown towards tail; creamy white dorsolateral stripes on head extending posteriorly and fading away at midbody; white longitudinal stripe extending from first supralabial to shoulder; sides of neck brown; flanks grayish brown with diffuse dark brown marks; limbs brown; ventrolateral region of body grayish brown; throat and chest cream; belly grayish cream; base of tail gray with dark little spots (Figs 12, 14B).

Color of holotype in preservative. Dorsal background uniformly brown with a diffuse light brown vertebral stripe extending from occiput onto tail, but fading at posterior end of body; dorsal and ventral surface of head brown; flanks light brown, with scattered dark brown spots; head and neck with two distinct white longitudinal stripes, the ventral one extending from first supralabial to forelimb, and the dorsal one from canthus rostralis to scapular region, posterior to which if fades into a light brown stripe; lateral aspect of neck dark brown; tail grayish brown; gular, chest and venter regions pale gray; ventral surface of tail and limbs gray.

Variations. Measurements and scutellation data of *Pholidobolus dolichoderes* are presented in Table 6. Superciliaries 4/5 (left/right) in specimen QCAZ 16350; palpebral disc divided into 5/6 scales in QCAZ 16352 and 3/5 in QCAZ 16351; frontonasal pentagonal in QCAZ 16349–52; prefrontals pentagonal in QCAZ 16349, 16350 and 16352; two rows of lateral granules at midbody in QCAZ 16439, 16350 and 16351. Usually six gular (collar) scales, eight in QCAZ 16349. Male is smaller (SVL 41.1 mm, $N = 1$) than females (maximum SVL 48.1 mm, $N = 2$).

Figure 14. Close-up of head and neck of *Pholidobolus dolichoderes* sp. nov. in life. QCAZ 16349 (**A** adult female); QCAZ 16353 (**B** male holotype). Photographs by Gustavo Pazmiño.

Adult females differ from holotype in having a grayish brown vertebral stripe, fading away posteriorly, and grayish brown flanks (Fig. 14). Juvenile QCAZ 16350 differs from holotype in having grayish brown flanks, without scattered dark brown spots; juvenile QCAZ 16351 is unique in having white spots on flanks and over forelimbs.

Distribution and natural history. *Pholidobolus dolichoderes* is known to occur between 2506–2675 m in San Felipe de Oña, southwestern Azuay province (Fig. 7). This area is composed of many different landscapes including small valleys, desert areas and wet paramo. Most specimens were found active at day (10h26–15h30), mostly on the ground or near spiny ground bromeliads known as achupallas (*Puya* sp.).

Conservation status. *Pholidobolus dolichoderes* is only known from unprotected localities around Oña. The population size of this species is unknown, but our sampling suggests low abundances. Because of the small known distribution and lack of additional data, we suggest assigning *P. dolichoderes* to the Data Deficient category according to IUCN (2012) guidelines.

Etymology. The specific epithet *dolichoderes* derives from the Greek words *dolikhós*, meaning long, and *derē*, meaning neck, in allusion to the distinctively long neck of this species.

Pholidobolus fascinatus **sp. nov.**
http://zoobank.org/C5EC3F40-41DF-4A7D-A3AA-C2C8A6EF81C1
Figures 15–17
Proposed standard English name: Haunted cuilanes
Proposed standard Spanish name: Cuilanes encantados

Holotype. QCAZ 15120 (Figs 15, 16), adult male, Ecuador, Provincia El Oro, Lake Chillacocha, 3.4984S, 79.6188W, WGS84, 3382 m, 20 November 2016, collected by Diego Almeida, Darwin Núñez, Eloy Nusirquia, Santiago Guamán and Guadalupe Calle.

Paratypes (26). Ecuador: Provincia El Oro: QCAZ 15122 (adult male), QCAZ 15121 (adult female), QCAZ 15169–73, 15177–78, 15180, 15193, 15221, 15243–44, 15396–15405 (juveniles), same data as holotype; QCAZ 15118 (adult female), Lake Chillacocha, 3.4986S, 79.6187W, WGS84, 3348 m, 17 November 2016, same collectors as holotype.

Diagnosis. *Pholidobolus fascinatus* is unique among its congeners in lacking widened medial scales on collar (posterior row of gulars). In addition, *P. fascinatus* differs from *P. affinis*, *P. prefrontalis*, *P. macbrydei*, *P. dolichoderes* sp. nov., and *P. montium* in having a loreal scale frequently in contact with the supralabials (loreal scale, if present, not in contact with supralabials in the other species). *Pholidobolus ulisesi*, *P. dicrus*, *P. hillisi*, *P. paramuno*, and *P. vertebralis* differ from *P. fascinatus* in having a conspicuous light vertebral stripe. *Pholidobolus samek* sp. nov. and *P. condor* sp. nov. differ from *P. fascinatus* in having bright green dorsolateral stripes on the head. In addition, *P. fascinatus* has more dorsals (32–37) and ventrals (21–25) than *P. samek* sp. nov. (27–29 and 19–21, respectively) and *P. condor* sp. nov. (26–30 and 18–20); and it has fewer temporals (3–5) and gulars (14–17) than *P. dolichoderes* sp. nov. (7–9 and 22–23, respectively).

Characterization. (1) Two (rarely three) supraoculars, anteriormost larger than posterior one; (2) prefrontals present or absent; (3) femoral pores absent in both sexes; (4) four to six opaque lower eyelid scales; (5) scales on dorsal surface of neck smooth, becoming striated from forelimbs to tail; (6) one row of lateral granules at midbody; (7) 32–37 dorsal scales between occipital and posterior margin of hindlimb; (8) lateral body fold present; (9) dorsum brown with a diffused chocolate brown middorsal stripe that fades away towards tail; (11) labial stripe white or cream; (12) flanks of body brown; (13) conical hemipenial body, with sulcus spermaticus originating between distinctly thick lips; (14) 22 flounces extending along hemipenial body.

Description of holotype. Adult male (QCAZ 15120) (Figs 15, 16); SVL 52.5 mm; TL 37.6 mm; dorsal and lateral head scales juxtaposed, finely wrinkled; rostral hexagonal, 2.27 times as wide as high; frontonasal hexagonal, wider than long, in contact with nasal laterally, slightly larger than frontal; prefrontal scales irregularly pentagonal; frontal heptagonal, longer than wide, slightly wider anteriorly, in contact with prefrontals and frontonasal anteriorly, two supraoculars laterally, and frontoparietals posteriorly; frontoparietals pentagonal, longer than wide, slightly wider posteriorly, each in contact laterally with supraocular II; interparietal heptagonal, lateral borders nearly

parallel to each other; parietals hexagonal, each in contact laterally with supraocular II and dorsalmost postocular; postparietals four, with medial scales less than half the size of lateral ones; eight supralabials, fourth one the longest and below center of eye; eight infralabials, third and fourth one below center of eye; temporals enlarged, irregularly hexagonal, juxtaposed, smooth; two large, smooth supratemporal scales; nasal divided, irregularly pentagonal, longer than high, in contact with rostral anteriorly, first and second supralabials ventrally, frontonasal dorsally, loreal posterodorsally and frenocular posteroventrally; nostril in center of nasal, directed lateroposteriorly; loreal rectangular, wider ventrally; frenocular longer than high, higher anteriorly, in contact with nasal, separating loreal from supralabials; two supraoculars, homogeneous in size; four superciliaries, anteriormost enlarged and in contact with loreal; palpebral disc divided into five pigmented scales; suboculars elongated, four on right side and three on left side; two postoculars, dorsalmost wider than the other; ear opening vertically oval, without denticulate margins; tympanum recessed into a shallow auditory meatus; mental semicircular, longer than wide; postmental pentagonal, slightly longer than wide, followed posteriorly by three pairs of genials, the anterior two in contact medially and the posterior one separated by postgenials; all genials in contact with infralabials; gulars imbricate, smooth, widened in two longitudinal rows; posterior row of gulars (collar) with 11 scales that are similar in size.

Nuchal scales similar in size to dorsals, except for the anteriormost that are widened; scales on sides of neck small and slightly granular; dorsal scales hexagonal, elongate, imbricate, arranged in transverse rows; scales on dorsal surface of neck smooth, becoming progressively striated from forelimbs to tail; dorsal scales between occipital and posterior margin of hindlimbs 33; dorsal scale rows in a transverse line at midbody 25; dorsals separated from ventrals by one row of small scales at level of 13th row of ventrals; lateral body fold between fore and hindlimbs present; ventrals smooth, wider than long, arranged in 25 transverse rows between collar fold and preanals; six ventral scales in a transverse row at midbody; subcaudals smooth; axillary region with granular scales; scales on dorsal surface of forelimb striated, imbricate; scales on ventral surface of forelimb granular; two thick, smooth thenar scales; supradigitals (left/right) 3/3 on finger I, 7/6 on II, 8/8 on III, 10/10 on IV, 5/5 on V; supradigitals 3/3 on toe I, 6/6 on II, 8/9 on III, 11/11 on IV, 8/8 on V; subdigital lamellae of finger I single, on finger II all paired, except by the three distalmost, on finger III (proximal half) paired, on finger IV slightly paired at the middle, on finger V all single in right finger and three paired in left finger; subdigital lamellae 5/5 on finger I, 9/9 on II, 13/13 on III, 14/15 on IV, 9/9 on V; subdigital lamellae on toes I and II paired proximally and single distally, on toes III, IV and V paired, except for the three to five distalmost subdigitals; subdigital lamellae 5/5 on toe I, 10/10 on II, 14/13 on III, 18/18 on IV, 11/12 on V; groin region with small, imbricate scales; scales on dorsal surface of hindlimbs smooth and imbricate; scales on ventral surface of hindlimbs smooth; scales on posterior surface of hindlimbs granular; femoral pores absent; preanal pores absent; cloacal plate paired, bordered anteriorly by two enlarged scales.

A

B

C

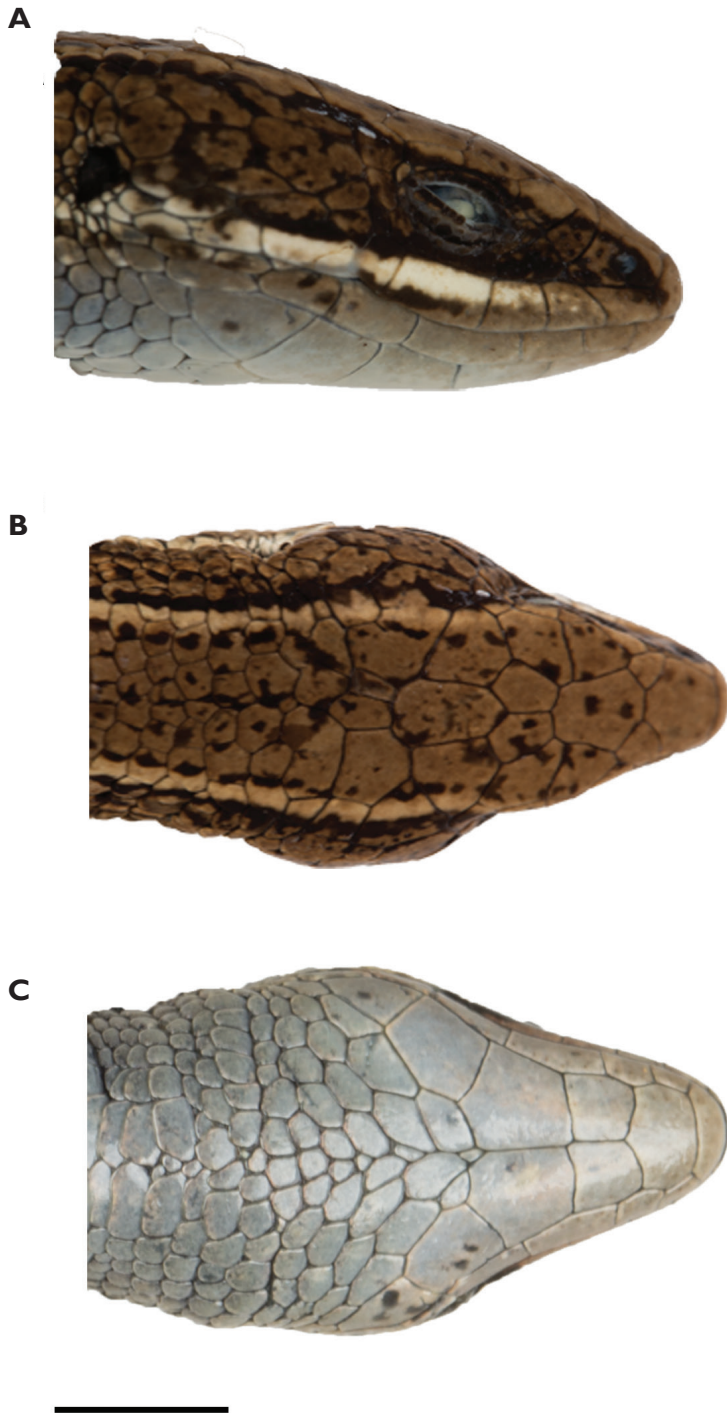**Figure 15.** Holotype of *Pholidobolus fascinatus* sp. nov. (QCAZ 15120) in life in dorsal (**A**), ventral (**B**), and lateral (**C**) views. Male, SVL = 52.5 mm. Photographs by Diego Quirola.

Additional measurements (mm) and proportions of the holotype: HL 12.3; HW 9.2; ShL 6.7; AGD 26.5; TL/SVL 0.7; HL/SVL 0.2; HW/SVL 0.2; ShL/SVL 0.1; AGD/SVL 0.5.

Color in life of the holotype. Dorsal background from head to base of tail brown, with a diffuse chocolate-brown middorsal stripe that fades away towards tail; light brown dorsolateral stripes on head extending posteriorly and fading away at midbody; white longitudinal stripe extending from third supralabial to shoulder; sides of neck, flanks, and limbs brown; reddish brown narrow stripe extending from tympanum to arm insertion; ventrolateral region of body grayish brown; throat and chest gray; belly background gray with conspicuous orange marks; tail orange anteriorly and laterally (Figs 15, 17A).

Figure 16. Head of holotype of *Pholidobolus fascinatus* sp. nov. (QCAZ 15120) in lateral (**A**), dorsal (**B**), and ventral (**C**) views. Photographs by Valeria Chasiluisa. Scale bar: 5 mm.

Color in preservative of the holotype. Dorsal background uniformly brown with a cream brown vertebral stripe extending from head onto tail; vertebral stripe slender anteriorly, becoming slightly wider posteriorly; head light brown with black dots dorsally (rostral, frontonasal, frontal, frontoparietals and supraoculars) and brown laterally; cream longitudinal stripe extending from third supralabial to shoulder; ventrolateral aspect of neck brown; forelimbs with scattered black dots; flanks brown; tail brown dorsally; ventral surface of head light gray, chest and venter dark gray, ventral surface of tail slightly brown, with scattered dark brown marks.

Variations. Measurements and scale counts of *Pholidobolus fascinatus* are presented in Table 6. Supralabials 9/9 (left/right) in specimens QCAZ 15118 and 15122, and supraoculars 3/3 in QCAZ 15118; loreal scale absent in QCAZ 15118; prefrontals absent in QCAZ 15122 and 15173; little intrusive scales between postparietal and frontoparietals in QCAZ 15118, 15121 and 15122; frontonasal quadrangular in QCAZ 15122; frontal nonagonal and pentagonal in QCAZ 15118 and 15173, respectively; interparietal hexagonal in QCAZ 15122; parietal pentagonal in QCAZ 15170. Four posterior cloacal scales in QCAZ 15118. Males are slightly smaller (SVL 47.6 mm, *N* = 2) than female (maximum SVL 48.2 mm, *N* = 2). Adult male QCAZ 15122 differs from holotype in having sides of tail and chest dark brown without gray spots. Adult female QCAZ 15118 differs from holotype in having a light gray chest, a dark gray ventral surface of tail, dark brown sides of tail, and in lacking orange or red brown color on sides of neck (Fig. 17).

Distribution and natural history. *Pholidobolus fascinatus* inhabits wet paramo in the western slopes of the Andes of southern Ecuador (Fig. 7). The new species is known only from El Oro province, at 3348–3382 m. All specimens were found active at 14h00–17h00 mostly under stones.

We found 41 eggs (17 as fragmented eggshells) in a communal nest next to male QCAZ 15120. We incubated the 24 unhatched eggs in soil and perlite in captivity. They were 11.9–13.2 mm long, 5.5–9.2 mm wide, and weighted 0.5 g on average. Hatchlings (*N* = 20) weighted 0.4 g and were 26.2 mm in SVL on average.

Conservation status. *Pholidobolus fascinatus* is only known from localities around Lake Chillacocha. The population size for this species is unknown, but our sampling suggests average abundances. Because of the small known distribution and lack of additional data, we suggest assigning *P. fascinatus* to the Data Deficient category, according to IUCN (2012) guidelines.

Etymology. The species epithet *fascinatus* is a Latin word meaning enchanted, in allusion to Lake Chillacocha, also known as the Enchanted Lake. According to local belief, this lake is enchanted and has healing powers.

Discussion

The systematics of *Pholidobolus* and its sister taxon *Macropholidus* have been controversial partly because morphological evidence has been misinterpreted. Nonetheless, the recent use of molecular phylogenies has reshaped the systematics and taxonomy

Figure 17. Color variation in live specimens of *Pholidobolus fascinatus* sp. nov. **A** male holotype (QCAZ 15120, SVL = 52.5 mm) **B** male paratype (QCAZ 15122, SVL = 42.6 mm) **C** female paratype (QCAZ 15118, SVL = 46.7 mm).

of this clade (Torres-Carvajal and Mafla-Endara 2013; Torres-Carvajal et al. 2015). In addition, recent collections in poorly explored areas along the Andes of Colombia, Ecuador, and Peru have led to the discovery and description of new species (Hurtado-Gómez et al. 2018; Torres-Carvajal et al. 2014; Venegas et al. 2016). In this paper we use morphological and molecular evidence to describe four new species of *Pholidobolus*, all except *P. dolichoderes* sp. nov. from remote highlands, based mostly on recent collections in southern Ecuador. Unexpectedly, allocating the new species described herein within the phylogenetic tree of *Pholidobolus* rendered *P. macbrydei* paraphyletic, suggesting that populations currently assigned to this taxon represent multiple species, some of which (e.g., Clades A and F) match the evolutionary significant units identified by Mafla-Endara (2011). Nonetheless, we refrain from describing any of these putative species (Clades A–F) in this paper as we believe that further sampling and analysis are necessary. According to our PCA results, three of the four new species are morphologically different from other "*Pholidobolus macbrydei*" (Fig. 2). Components I and II in the PCA, however, explain less than 50% of the variation within the "*P. macbrydei*" clade (Table 5). Thus, it is necessary to study additional morphological characters and increase sample size to better elucidate morphological differences.

Mafla-Endara (2011) also suggested hybridization between *P. macbrydei* from Cañar province and *P. prefrontalis* based on both the relatively great variation in morphology within the Cañar populations, and their morphological similarity to *P. prefrontalis*. Nevertheless, our nuclear phylogenetic tree does not suggest hybridization between *P. macbrydei* and *P. prefrontalis* (Appendix II).

Current evidence prevents us from assigning the name *P. macbrydei* to any of the recovered clades. However, we suspect that *P. macbrydei* belongs or is more closely related to Clades C, D, and E for two reasons (Fig. 1). First, adult males in these clades match closely the description of *P. macbrydei* (Montanucci 1973). Second, Clades C, D, and E lie nearby the type locality of *P. macbrydei*. It is noteworthy that Clade B also lies near the type locality of *P. macbrydei* (Fig. 7), although males in Clade B lack the red lateral stripes characteristic of *P. macbrydei*. DNA samples from the type locality should help clarify the taxonomy of this group.

The Cordillera del Cóndor is a sub-Andean mountain chain geologically similar to the Tepuis of the Guiana region. It is composed of marine and continental sediments (Neill 2005). This area is presently threatened by mining activities, despite discovery of a significant number of new species in the last ten years (Brito et al. 2017; Huamantupa-Chuquimaco and Neill 2018; Mashburn et al. 2020; Ron et al. 2018; Torres-Carvajal et al. 2009; Valencia et al. 2017) suggesting that Cordillera del Cóndor is a diversity hotspot. Our discovery of *P. samek* and *P. condor* further supports this idea. Therefore, we strongly advise authorities to improve conservation efforts for Cordillera del Cóndor.

The discovery of four new species and a paraphyletic *P. macbrydei* reveals high levels of unexpected diversity within *Pholidobolus* from southern Ecuador. This study supports the idea that Andean herpetofauna in this region is more diverse in species numbers than previously thought (Sánchez-Pacheco et al. 2012), especially for poorly explored areas like Cordillera del Cóndor. Collections in this area are usually scarce due to complex logistics. However, we recommend more intensive sampling efforts. Future studies should include larger samples and other types of evidence (e.g., genomic data, environmental variables) that might prove useful for species delimitation within *Pholidobolus* and other vertebrate taxa.

Acknowledgements

References

Betancourt R, Reyes-Puig C, Lobos SE, Yánez-Muñoz MH, Torres-Carvajal O (2018) Sistemática de los saurios *Anadia* Gray, 1845 (Squamata: Gymnophthalmidae) de Ecuador: límite de especies, distribución geográfica y descripción de una especie nueva. Neotropical Biodiversity 4: 83–102. https://doi.org/10.1080/23766808.2018.1487694

Brito JM, Tinoco N, Chávez D, Moreno-Cárdenas P, Batallas D, Ojala-Barbour R (2017) New species of arboreal rat of the genus *Rhipidomys* (Cricetidae, Sigmodontinae) from Sangay National Park, Ecuador. Neotropical Biodiversity 3:1, 65–79. https://doi.org/10.1080/23766808.2017.1292755

Castoe TA, Doan TM, Parkinson CL (2004) Data partitions and complex models in Bayesian analysis: The phylogeny of gymnophthalmid lizards. Systematic Biology 53: 448–469. https://doi.org/10.1080/10635150490445797

de Queiroz K (1998) The general lineage concept of species, species criteria, and the process of speciation. In: Howard DJ, Berlocher SH (Eds) Endless Forms: Species and Speciation. Oxford University Press, Oxford, 57–75.

de Queiroz K (2007) Species concepts and species delimitation. Systematic Biology 56: 879–886. https://doi.org/10.1080/10635150701701083

Dowling HG, Savage JM (1960) A guide to the snake hemipenis: a survey of basic structure and systematic characteristics. Zoologica 45: 17–28.

Harvey MB, Embert D (2008) Review of Bolivian *Dipsas* (Serpentes: Colubridae), with comments on other South American species. Herpetological Monographs 22: 54–105. https://doi.org/10.1655/07-023.1

Huamantupa-Chuquimaco I, Neill D (2018) *Vochysia condorensis* (Vochysiaceae), a new species from the Cordillera del Cóndor, Ecuador. Phytotaxa 340(1): 79–85. https://doi.org/10.11646/phytotaxa.340.1.6

Hurtado-Gómez J, Arredondo J, Nunes PMS, Daza JM (2018) A New Species of *Pholidobolus* (Squamata: Gymnophthalmidae) from the Paramo Ecosystem in the Northern Andes of Colombia. South American Journal of Herpetology 13(3): 271–286. https://doi.org/10.2994/SAJH-D-15-00014.1

IUCN (2012) IUCN Red List Categories and Criteria: Version 3.1. Second edition. IUCN, Gland, Switzerland and Cambridge, UK, iv + 32 pp.

Katoh K, Toh H (2010) Parallelization of the MAFFT multiple sequence alignment program. Bioinformatics 26: 1899–1900. https://doi.org/10.1093/bioinformatics/btq224

Kearse M, Moir R, Wilson A, Stones-Havas S, Cheung M, Sturrock S, Buxton S, Cooper A, Markowitz S, Duran C (2012) Geneious Basic: an integrated and extendable desktop software platform for the organization and analysis of sequence data. Bioinformatics 28: 1647–1649. https://doi.org/10.1093/bioinformatics/bts199

Kizirian DA (1996) A review of Ecuadorian *Proctoporus* (Squamata: Gymnophthalmidae) with descriptions of nine new species. Herpetological Monographs 10: 85–155. https://doi.org/10.2307/1466981

Kumar S, Stecher G, Tamura K (2016) MEGA7: molecular evolutionary genetics analysis version 7.0 for bigger datasets. Molecular biology and evolution 33(7): 1870–1874. https://doi.org/10.1093/molbev/msw054

Lanfear R, Calcott B, Ho SYW, Guindon S (2012) Partition-Finder: Combined selection of partitioning schemes and substitution models for phylogenetic analyses. Molecular Biology and Evolution 29: 1695–1701. https://doi.org/10.1093/molbev/mss020

Lehr E, Moravec J, Šmíd J, Lundberg M, Köhler G, Catenazzi A (2019) A new genus and species of arboreal lizard (Gymnophthalmidae: Cercosaurinae) from the eastern andes of Peru. Salamandra 55: 1–13.

Mafla-Endara P (2011) Filogeografía de las lagartijas andinas del género *Pholidobolus* (Squamata: Gymnophthalmidae) en Ecuador. Disertación previa a la obtención del título de Licenciada en Ciencias Biológicas. Pontificia Universidad Católica del Ecuador.

Manzani PR, Abe AS (1988) Sobre dois novos métodos de preparo do hemipênis de serpentes. Memorias do Instituto Butantan 50: 15–20.

Mashburn B, Pérez Á, Persson C, Zapata N, Cevallos D, Muchhala N (2020) *Burmeistera quimiensis* (Lobelioideae, Campanulaceae): A new species from the Cordillera del Cóndor range in southeast Ecuador. Phytotaxa 433: 67–74. https://doi.org/10.11646/phytotaxa.433.1

Mazabanda C, Kemper R, Thieme A, Hettler B, Finer M (2018) Impacts of Mining Project "Mirador" in the Ecuadorian Amazon. Monitoring Andean Amazon Project (MAAP). https://maaproject.org/mirador-ecuador

Miller MA, Pfeiffer W, Schwartz T (2010) Creating the CIPRES Science Gateway for inference of large phylogenetic trees. Proceedings of the Gateway Computing Environments Workshop (GCE), 14 Nov. 2010, New Orleans, LA, 1–8. https://doi.org/10.1145/2016741.2016785

Montanucci RR (1973) Systematics and evolution of the Andean lizard genus *Pholidobolus* (Sauria: Teiidae). Miscellaneous Publication. Museum of Natural History, University of Kansas 59: 1–52.

Moravec J, Šmíd J, Štundl J, Lehr E (2018) Systematics of Neotropical microteiid lizards (Gymnophthalmidae, Cercosaurinae), with the description of a new genus and species from the Andean montane forests. ZooKeys 774: 105–139. https://doi.org/10.3897/zookeys.774.25332

Neill DA (2005) Cordillera del Cóndor: Botanical treasures between the Andes and the Amazon. Plant Talk 41: 17–21.

Nunes PMS, Fouquet A, Curcio FF, Kok PJR, Rodrigues MT (2012) Cryptic species in *Iphisa elegans* Gray, 1851 (Squamata: Gymnophthalmidae) revealed by hemipenial morphology and molecular data. Zoological Journal of the Linnean Society 166: 361–376. https://doi.org/10.1111/j.1096-3642.2012.00846.x

Pellegrino KCM, Rodrigues MT, Yonenaga-Yassuda Y, Sites JW (2001) A molecular perspective on the evolution of microteiid lizards (Squamata, Gymnophthalmidae), and a new classification for the family. Biological Journal of the Linnean Society 74: 315–338. https://doi.org/10.1006/bijl.2001.0580

Pérez-Escobar O, Gottschling M, Chomicki G, Condamine F, Klitgård B, Pansarin E, Gerlach G (2017) Andean Mountain Building Did Not Preclude Dispersal of Lowland Epiphytic Orchids in the Neotropics. Scientific Reports 7: 4919. https://doi.org/10.1038/s41598-017-04261-z

Pesantes OS (1994) A Method for preparing the hemipenis of preserved snakes. Journal of Herpetology 28: 93–95. https://doi.org/10.2307/1564686

Peters AJ (1964) Dictionary of Herpetology. Hafner Publishing Company, New York, 392 pp.

R Core Team (2018) R: A Language and Environment for Statistical Computing. R Foundation for Statistical Computing, Vienna. https://www.R-project.org

Rambaut A (2014) FigTree version 1.4.2. http://tree.bio.ed.ac.uk/software/figtree/

Rambaut A, Drummond A (2007) Tracer v1.4. http://beast.bio.ed.ac.uk/Tracer

Ron SR, Caminer MA, Varela-Jaramillo A, Almeida-Reinoso D (2018) A new treefrog from Cordillera del Cóndor with comments on the biogeographic affinity between Cordillera del Cóndor and the Guianan Tepuis (Anura, Hylidae, *Hyloscirtus*). ZooKeys 809: 97–124. https://doi.org/10.3897/zookeys.809.25207

Ronquist F, Teslenko M, van der Mark P, Ayres DL, Darling A, H√∂hna S, Larget B, Liu L, Suchard MA, Huelsenbeck JP (2012) MrBayes 3.2: Efficient Bayesian phylogenetic inference and model choice across a large model space. Systematic Biology 61: 539–542. https://doi.org/10.1093/sysbio/sys029

Sánchez-Pacheco SJ, Aguirre-Peñafiel V, Torres-Carvajal O (2012) Lizards of the genus *Riama* (Squamata: Gymnophthalmidae): the diversity in southern Ecuador revisited. South American Journal of Herpetology 7: 259–275. https://doi.org/10.2994/057.007.0308

Sánchez-Pacheco SJ, Torres-Carvajal O, Aguirre-Peñafiel V, Nunes PMS, Verrastro L, Rivas GA, Rodrigues MT, Grant T, Murphy RW (2017) Phylogeny of *Riama* (Squamata: Gymnophthalmidae), impact of phenotypic evidence on molecular datasets, and the origin of the Sierra Nevada de Santa Marta endemic fauna. Cladistics 34: 260–291. https://doi.org/10.1111/cla.12203

Savage JM (1997) On terminology for the description of the hemipenis of squamate reptiles. Herpetological Journal 7: 23–25.

Stamatakis A (2014) RAxML Version 8: A tool for Phylogenetic Analysis and Post-Analysis of Large Phylogenies. Bioinformatics 30: 1312–1313. https://doi.org/10.1093/bioinformatics/btu033

Torres-Carvajal O, de Queiroz K, Etheridge R (2009) A new species of iguanid lizard (Hoplocercinae, *Enyalioides*) from southern Ecuador with a key to eastern Ecuadorian Enyalioides. Zookeys 27: 59–71. https://doi.org/10.3897/zookeys.27.273

Torres-Carvajal O, Lobos SE, Venegas PJ (2015) Phylogeny of Neotropical *Cercosaura* (Squamata: Gymnophthalmidae) lizards. Molecular Phylogenetics and Evolution 93: 281–288. https://doi.org/10.1016/j.ympev.2015.07.025

Torres-Carvajal O, Lobos SE, Venegas PJ, Chávez G, Aguirre-Peñafiel V, Zurita D, Echevarría LY (2016) Phylogeny and biogeography of the most diverse clade of South American gymnophthalmid lizards (Squamata, Gymnophthalmidae, Cercosaurinae). Molecular Phylogenetics and Evolution 99: 63–75. https://doi.org/10.1016/j.ympev.2016.03.006

Torres-Carvajal O, Mafla-Endara P (2013) Evolutionary history of Andean *Pholidobolus* and *Macropholidus* (Squamata: Gymnophthalmidae) lizards. Molecular Phylogenetics and Evolution 68: 212–217. https://doi.org/10.1016/j.ympev.2013.03.013

Torres-Carvajal O, Venegas PJ, Lobos SE, Mafla-Endara P, Nunes PMS (2014) A new species of *Pholidobolus* (Squamata: Gymnophthalmidae) from the Andes of southern Ecuador. Amphibian & Reptile Conservation 8: 76–88.

Townsend TM, Alegre RE, Kelley ST, Wiens JJ, Reeder TW (2008) Rapid development of multiple nuclear loci for phylogenetic analysis using genomic resources: An example from

squamate reptiles. Molecular Phylogenetics and Evolution 47: 129–142. https://doi.org/10.1016/j.ympev.2008.01.008

Uzzell T (1973) A revision of the genus *Prionodactylus* with a new genus for *P. leucostictus* and notes on the genus *Euspondylus* (Sauria, Teiidae). Postilla 159: 1–67. https://doi.org/10.5962/bhl.part.11535

Valencia JH, Dueñas MR, Székely P, Batallas D, Pulluquitín F, Ron SR (2017) A new species of direct-developing frog of the genus *Pristimantis* (Anura: Terrarana: Craugastoridae) from Cordillera del Cóndor, Ecuador, with comments on threats to the anuran fauna in the region. Zootaxa 4353: 447–466. https://doi.org/10.11646/zootaxa.4353.3.3

Van Teijlingen K (2016) The ´will to improve´ at the mining frontier: Neo-extractivism, development and governmentality in the Ecuadorian Amazon. Extractive Industries and Society 3: 902–911. https://doi.org/10.1016/j.exis.2016.10.009

Venegas PJ, Echeverría LY, Lobos SE, Nunes PMS, Torres-Carvajal O (2016) A new species of Andean microteiid lizard (Gymnophthalmidae: Cercosaurinae: *Pholidobolus*) from Peru, with comments on *P. vertebralis*. Amphibian & Reptile Conservation 10(1): 21–33.

Zaher H (1999) Hemipenial morphology of the South American xenodontine snakes, with a proposal for a monophyletic Xenodontinae and a reappraisal of colubroid hemipenes. Bulletin of the American Museum of Natural History 240: 1–168. http://hdl.handle.net/2246/1646

Appendix I

Additional specimens examined of *Pholidobolus macbrydei*. ECUADOR: **Provincia Azuay:** Cuenca-Azogues, 2.895222S, 78.95822W, 2486 m, QCAZ 6985; Cuenca-Chaucha, 2.861209S, 79.37869W, 2943 m, QCAZ 9668; Cuenca-Cochapamba, 2.797120S, 79.41562W, 3548 m, QCAZ 10133–10135; Cuenca-El Cajas, 2.77744S, 79.17001W, 3508 m, QCAZ 9932, 9936; 2.74105S, 79.23479W, 4092 m, QCAZ 8010; 2.776299S, 79.23743W, 4068 m, QCAZ 8011; 3.04155S, 79.21567W, 3766 m, QCAZ 8897, 8899–8903, 8906; Cuenca-Mazan Forest, 2.87522S, 79.12923W, 3189 m, QCAZ 8008, 8013; Cutchil, 3.133999S, 78.81300W, 2900 m, QCAZ 823; Guablid, 2.77488S, 78.69758W, 2453 m, QCAZ 9915, 9919–9920; Gualaceo, 2.909767S, 78.73436W, 2625 m, QCAZ 10875; Gualaceo-Limón; 2.948S, 78.71200W, 3110 m, QCAZ 819–20, 822; 2.964S, 78.70199W, 3140 m, QCAZ 825; Patacocha hill, 3.121109S, 79.065W, 3340 m, QCAZ 6144; Pucara, 3.21367S, 79.46739W, QCAZ 11038; Quinoas river, 3.087267S, 79.27762W, 3200 m, QCAZ 1564, 1566; Sigsig, 2.99900S, 78.80700W, 2890 m, QCAZ 1537; 3.129500S, 78.80400W, 2969 m, QCAZ 5605–5606, 5608; Sigsig-Gualaquiza, 3.106875S, 78.79558W, 2935 m, QCAZ 8646–8647; Tarqui, 3.015880S, 79.04447W, 2680 m, QCAZ 8512. **Provincia Cañar:** Cajas National Park, 2.70654S, 79.22765W, 3651 m, QCAZ 8946; Cañar, 2.560760S, 78.93077W, QCAZ 9947; Guallicanga river, 2.473189S, 78.97289W, 3048 m, QCAZ 10051–53; Gualaceo, 2.882159S, 78.77536W, 2298 m, QCAZ 9606; Juncal, 2.432109S, 78.90223W,

3960 m, QCAZ 10048; 2.473189S, 78.97289W, 3048 m, QCAZ 10050; Mazar, 2.54508S, 78.70078W, 2839 m, QCAZ 15811–13; 2.54649S, 78.69826W, 2924 m, QCAZ 15814–16; 2.57138S, 78.746W, 3442 m, QCAZ 15817–15823; 2.5708S, 78.74586W, 3451 m, QCAZ 15824; 2.545804S, 78.69611W, 2842 m, QCAZ 10970. **Provincia Chimborazo:** Frutatián lake, 2.21584S, 78.50136W, 3700 m, QCAZ 9217–9218; Magdalena lake, 2.187416S, 78.50686W, 3556 m, QCAZ 9214; Ozogoche, 2.368733S, 78.68871W, 4040 m, QCAZ 6006; Riobamba-Melán, 1.875020S, 78.54773W, 3564 m, QCAZ 9626–9628; Riobamba-Timbo, 1.929219S, 78.53718W, 3408 m, QCAZ 9616–9620; Shulata, 2.339309S, 78.84322W, 3228 m, QCAZ 5597–5598. **Provincia El Oro:** Guanazán, 3.440034S, 79.48695W, 2638 m, QCAZ 7894. **Provincia Loja:** Fierro Hurco, 3.710421S, 79.30498W, 3439 m, QCAZ 6949–6950; Jimbura-Jimbura lake, 4.708868S, 79.44657W, 3036 m, QCAZ 6947–6948; Jimbura- path to Jimbura lake, 4.709469S, 79.43558W, 3348 m, QCAZ 10054–10055, 10057–10062; Jimbura-Lagunillos, 4.628244S, 79.46353W, 3450 m, QCAZ 6146–6147; 4.817000S, 79.36199W, 3600 m, QCAZ 3785; San Lucas, 3.731853S, 79.26059W, 2470 m, QCAZ 2861; Saraguro, 3.62025S, 79.23581W, 3100 m, QCAZ 3606; 3.679457S, 79.23769W, 3190 m, QCAZ 3673–3674; Tarqui, QCAZ 5545. **Provincia Morona Santiago:** Sangay National Park, 1.960939S, 78.43198W, 3345 m, QCAZ 9612. **Provincia Tungurahua:** Patate-El Corral, 1.2725S, 78.46805W, 3468 m, QCAZ 9995–9996. **Provincia Zamora Chinchipe:** Podocarpus National Park, 4.484149S, 79.14875W, 1800 m, QCAZ 3743.

Appendix II

Phylogeny of *Pholidobolus*. ML phylogram derived from the analysis of 411 bp of nuclear DNA. Bootstrap values are shown above branches and Bayesian posterior probabilities below branches (≤ 50% not shown). Asterisks indicate maximum values. The outgroup taxon (*Anadia rhombifera*) is not shown. Species names followed by voucher numbers are shown.